Facultad de Ciencias
Departamento de Química Orgánica

Anion Receptors Based on Ion Pairing and Hydrogen Bonding: from Nitrate to Naproxen

Director:
Dr. Javier de Mendoza Sans
Co-directora:
Dra. Pilar Prados Hernando

Memoria que presenta
Pascal Blondeau
Para optar el grado de Doctor en Ciencias Químicas

Madrid, Mayo de 2007

“[…] Every night and every morn
Some to misery are born,
Every morn and every night
Some are born to sweet delight.

Some are born to sweet delight,
Some are born to endless night.”

William Blake, *Auguries of Innocence*

Agradecimientos

Ahora hace más de cuatro años que llegué a España para empezar este trabajo en el grupo. En primer lugar me gustaría agradecer a toda la gente del grupo así como a mi amigo Santiago por haberme acogido y ayudado puesto que yo no entendía mucho lo que me intentaban decir en español (¡Recordaré siempre aquel primer momento en el que bajamos al laboratorio y Javier empezó a hablar en español!). Hubo muchos momentos de desilusión con el trabajo pero siempre se recuerdan los mejores (cuando cristalizan los productillos…). Aprendí mucho durante estos cuatros años y quiero aprovechar la ocasión para agradecer particularmente a algunas personas.

En primer lugar al profesor Javier de Mendoza por darme la oportunidad de trabajar en su grupo de investigación y contagiarme su entusiasmo por la química supramolecular, por poder hablar tanto de ciencia como de muchos otros temas y sobre todo por dejar mucha libertad e independencia a sus alumnos para que el aprendizaje sea más interesante.

Aunque sólo coincidí un año y medio con Pilar Prados, quiero agradecerle muy atentamente su apoyo constante, paciencia y su gran saber científico. Pilar sabe establecer una excelente relación de confianza aconsejándote siempre lo mejor para ti. Por estas cualidades y por mucho más, se te echa mucho de menos aquí, en Tarragona.

Se me ha brindado la oportunidad de estar en la red europea “Chiral recognition of carboxylic acid derivatives” y aprovecho para agradecer todas esas personas por los consejos, discusiones científicas y buenos momentos compartidos. En primer lugar, a Joe Hayes y Martin Smiesko por los cálculos así como por las respuestas a mis preguntas con respeto a un campo de la química que me queda muy lejano. En segundo lugar Prof. Johannes G. de Vries y a Dr. Andy Hallet en DSM de Holanda y Prof. Christian Roussel, Federico Andreoli y Nicolas Vanthuyne de la Universidad de Marsella por las prácticas realizadas en sus respectivos centros.

En el Institut Catala de Investigació Química, tenemos una infraestructura muy bien desarrollada. Quiero primero agradecer a Jordi Benet-Buchholz y Eduardo Escudero por el análisis por difracción de radio X. A Susana Delgado y Enrique Cequier por el análisis por HPLC y su disponibilidad para contestar a las preguntas analíticas. A Jonathan Barr y Joan Salles por el LC-MS y por la identificación de los “beads” por masas. Al Dr. Pau Ballester por haberme enseñado el manejo de la calorimetría y por las discusiones sobre termodinámica. Además, quiero agradecer a la Dra. Sandrine Perroche por toda la parte de química combinatoria, el desarrollo de un

Naproxeno fluorescente y por compartir mucho tiempo de trabajo juntos “dans la joie et la bonne humeur”. A Alex Fragoso por haberme permitido utilizar el microscopio en la Universidad Rovira y Virgili.

Quería también dar las gracias a todos los del grupo de investigación allí en Madrid y aquí en Tarragona. En particular a Ruth con quien aprendí mucho en el laboratorio, por su gran saber, su humildad, su amistad y por ser “mi coach” en muchas ocasiones. A Eric “le comique-troupier du groupe” pour son training sur la cristalisation, sa générosité et son amitié très importante surtout ces derniers mois. Quiero también agradecer a toda la gente del laboratorio por haber hecho la vida en el laboratorio menos rutinaria, con un buen intercambio cultural y químico: a “Monsieur Cinema” Jesus, “Reggae” Fred, “el artista” Julian, “Pilar y Vera”, “Mass Master” Gerald, Enrique, Aritz, Elisa, Hitos, Jose, “los sabios” Curra y Gunther y Roger. Además a Margot por los drafts, settings, correcciones y bibliografía.

Muy especialmente quisiera agradecer a mi familia su continuo apoyo, a mis amigos por dejarme mantener una vida social normal y seguir aceptándome sin tener en cuenta mi bruixismo: Dr. Chi, Yaya, Boris, “Niko, Nono y Batiste”, Fabrice, Santiago, Go-Go Oliver, TTC, Azrotator, Guns of Brixton, M. Manhattan, Antoine Doisnel, Henri Husson, “Elvis & John” y sobre todo a Cristina por mantenerme los pies en la tierra en los momentos menos entretenidos y apoyarme en los más entretenidos.

Esta tesis ha sido realizada gracias a la financiación del proyecto europeo “Enantioselective separation” (TMR) así como al ICIQ.

List of Abbreviations

Ar: aromatic
Bn: benzyl
Boc: *tert*-butoxycarbonyl
BzO: benzoate
t-Bu: *tert*-butyl
CDI: *N*,*N´*-carbonyldiimidazole
COX-2: cyclooxygenase-2
DCL: Dynamic Combinatorial Library
DIPEA: diisopropylethylamine
DMF: *N*,*N´*-dimethylformamide
DMSO: dimethylsulfoxide
EtOAc: ethyl acetate
FDA: food and drug administration
Fmoc: 9*H*-fluoren-9-ylmethoxycarbonyl
Guan: guanidinium
HOBt: 1-hydroxybenzotriazole
MD: molecular modeling
M.p.: melting point
Ms: methanesulfonyl or mesyl
NMM: *N*-methylmorpholine
Nap: naproxenate
Naph: naphthoyl
NSAID: Non-Steroidal Anti-inflammatory Drug
ORTEP: Oak Ridge Thermal Ellipsoid Plot Program
Ph: phenyl
PyBOP: 1-*H*-benzotriazol-1-yloxy-tris(pyrrolidino)phosphonium hexafluorophosphate
SLM: supported liquid membrane
TBDMS: *tert*-butyldimethylsilyl
TBDPS: *tert*-butyldiphenylsilyl
TFA: trifluoroacetic acid
THF: tetrahydrofuran
Techniques
ESI-MS: electrospray ionisation mass spectrometry

FAB/LSIMS: fast atom bombardment/liquid secondary ion mass spectroscopy
HPLC: high performance liquid chromatography
ITC: isothermal calorimetry
LC-MS: liquid chromatography-mass spectroscopy
NMR: nuclear magnetic resonance

Amino Acids

Ala (A): alanine
Arg (R): arginine
Asn (N): asparagine
Asp (D): aspartate
Cys (C): cysteine
Glu (E): glutamate
Gln (Q): glutamine
Gly (G): glycine
His (H): hystidine
Ile (I): isoleucine
Leu (L): Leucine
Lys (K): lysine
Met (M): methionine
Phe (F): phenylalanine
Pro (P): praline
Ser (S): serine
Thr (T): threonine
Trp (W): tryptophan
Tyr (Y): tyrosine
Val (V): valine

Chapter 1
General Introduction

1.1 Molecular Recognition of Oxoanions Based on Guanidinium Receptors 1
1.1.1 Introduction 1
1.1.2 Guanidinium-based Artificial Receptors for Oxoanions 2
1.1.3 Chiral Guanidines for the Enantioselective Recognition of Carboxylate 8
1.1.4 Phosphate and Sulfate Recognition 13
1.1.4.1 Phosphate Recognition 13
1.1.4.2 Sulfate Recognition 16
1.2 Objectives 19
1.2.1 Nitrate Recognition 19
1.2.2 Naproxen Enantiorecognition 20

Chapter 2
Nitrate Recognition

2.1 Introduction 25
2.1.1 Abiotic Receptors for Small Anions 25
2.1.2 Design of Guanidinium-based Receptors for Nitrate Recognition 29
2.2 Guanidinium Receptors Synthesis 32
2.3 Binding Study 35
2.3.1 ^{1}H-NMR and ITC Titrations with Nitrate 35
2.3.2 I.T.C. Binding Titrations and Selectivity 39
2.3.3 I.T.C. Titrations Binding with TBA Fluoride 44
2.3.4 Influence of Stereochemistry of Guanidinium Scaffold on Anion Association 47
2.3.5 Liquid-liquid Extractions: CH-π Interactions 49
2.4 X-ray Solid State Structures 52
2.5 Conclusions 63
2.6 Experimental Section 64
2.6.1 General Procedures 64
2.6.2. Synthesis 65
2.6.3 X-ray Data 74

Chapter 3
Naproxen Enantiorecognition

3.1 Introduction 79
3.1.1 Naproxen Overview 79
3.1.2 Naproxen Synthesis 80
3.1.3 Racemates Resolution 83
3.1.4 Current Strategies 86
3.1.5 Synthetic Receptors for Naproxen Recognition 86
3.2 Rational Design Approach 90
3.2.1 Additional Steric Hindrance 91
3.2.2 Pincer-like Receptor 94
3.2.2.1 Spacer Influence 95
3.2.2.2 π-Interactions Evaluation 100
3.2.2.3 Additional Chirality 103
3.2.3 Pre-Organized Receptors 104
3.2.3.1 Introduction 104
3.2.3.1 Lysine Derivative Macrocycle 106
3.2.3.2 Nobin Macrocycles 110
3.3 Combinatorial Approach 114
3.3.1 Introduction 114
3.3.1.1 General Principles 114
3.3.1.2 Combinatorial Approach based on Guanidinium Receptors 117
3.3.1.3 Combinatorial Approach for Enantioselective Substrate 120
3.3.2 Combinatorial Approach to (*S*)-Naproxen Enantiorecognition 123
3.3.2.1 Previous Work 123
3.3.2.2 New Approach 124
3.3.2.3 Synthesis of Guanidinium Receptors Libraries 126
3.3.2.4 Synthesis of a Fluorescent Naproxen 129
3.3.2.5 Screening Experiments 134
3.4 Conclusions 137
3.5 Experimental Section 138
3.5.1 General Procedures 138
3.5.2 Synthesis 138
3.5.3 Libraries Synthesis and Screening 167

Contents

Summary 173
Introducción General y Conclusiones 175

Explanation notes:

Literature references as well as compounds number have been treated independently in each chapter (repetitions indeed occur in some necessary case).

1.1 Molecular Recognition of Oxoanions Based on Guanidinium Receptors

1.1.1 Introduction

Nature frequently uses the guanidinium group to coordinate anions. Present in the side chain of the amino acid arginine, the guanidinium group forms strong ion-pairs with oxoanions such as carboxylates or phosphates of enzymes and antibodies, and also contributes to the stabilization of protein tertiary structures *via* internal salt bridges, mainly carboxylates.[1] Not surprisingly, guanidinium-based compounds are found in many drugs and have been extensively used in molecular recognition studies, leading to the design and synthesis of various receptors for anions.[2]

The capacity of the guanidinium group to bind oxoanions is due to its geometrical Y-shaped, planar orientation, which directs the hydrogen bonding, and to its high pK_a value (around 12-13),[3] which ensures protonation over a wide pH range. The positive charge is delocalized over the three nitrogen atoms, and four out of the five hydrogen bond donors present in the guanidinium group of arginine can complement bidentate oxoanion acceptors, along the two edges available (Fig 1). This accounts for the geometrical versatility of the binding modes. From the energy point of view, binding to oxoanions results from both ion-pairing and hydrogen bonding, and this turns out to be a difficult challenge in highly polar solvents or in water. In fact, the binding energy arises from the difference of the energy released by the host-guest interactions and the energy penalty necessary to remove the solvation shell around the host, which is quite high in water.

[1] Schug, K. A.; Lindner. W. *Chem. Rev.* **2005**, *105*, 67-113.

[2] Best, M. D.; Tobey, S. L.; Anslyn, E. V. *Coord. Chem. Rev.* **2003**, *240*, 3-15.

[3] The pK_a value of the guanidinium moiety may vary depending on adjacent group effects; in general it is lowered by acyl ≥ phenyl ≥ alkyl direct substitution (see ref. 1).

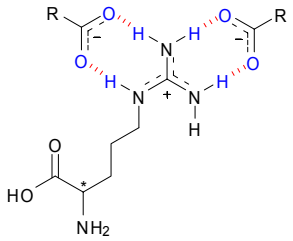

Fig 1. The guanidinium group of arginine and its two possible binding modes with carboxylates.

In proteins, the guanidinium-oxoanion interaction usually occurs inside hydrophobic pockets or in areas of low dielectric constant. On the contrary, in artificial synthetic systems designed to work in water or polar solvents, complexation has to take place in an environment more exposed to solvation effects which compete with the donor and acceptor sites, causing a substantial decrease in binding. This is usually overcome by increasing the number of charges or hydrogen bond donors or by designing more sophisticated receptors where the access to the solvent is restricted. In this introductory review, several examples on how this has been achieved in artificial guanidinium receptors will be provided.

1.1.2. Guanidinium-based Artificial Receptors for Oxoanions

Lehn and co-workers first reported in the late 1970's guanidinium-containing macrocycles for the recognition of phosphate PO_4^{3-} in water.[4] The weak association constants (K_a = 50 (**I**), 158 (**II**) and 251 (**III**) M^{-1}, (Fig 2), pH-metric titrations) as compared with the corresponding analogues could be explained in terms of the more delocalized charge of guanidinium over ammonium and accounts for the electrostatic prevailing interaction.

[4] Dietrich, B.; Fyles, T. M.; Lehn, J.-M.; Pease, L. G.; Fyles, D. L. *J. Chem. Soc. Chem. Commun.* **1978**, 934-936.

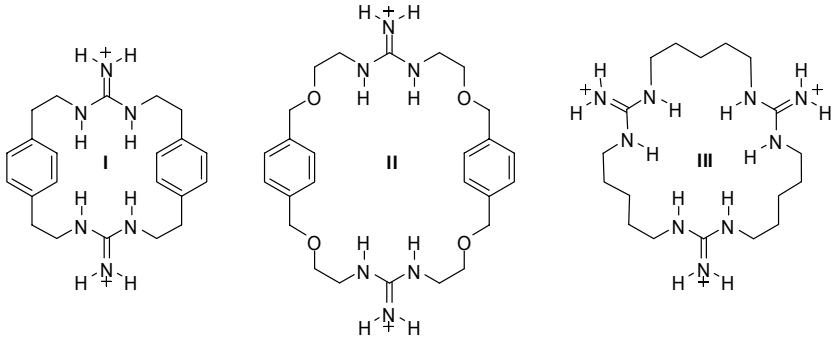

Fig 2. Guanidinium macrocycles for phosphate recognition.

The guanidinium can be incorporated into a bicyclic framework (Fig 3a) in order to improve its solubility in apolar solvents, where the hydrogen bonds are stronger, and to avoid the *anti* conformation, not suitable for hydrogen-bonding to oxoanions (Fig 3b). As a result, the hydration of the cation is reduced and the conformational freedom restricted. Inserted into a decaline framework, the guanidinium cation becomes therefore an almost ideal complement for oxoanions, since both NH protons are docking sites for the two *syn* lone pairs of the oxoanion. The resulting ionic DD-AA (donor-donor-acceptor-acceptor) hydrogen-bonded complex is particularly stable and geometrically well defined. Due to the large pK_a difference between guanidinium and carboxylic acids (*ca*. 9 pK_a units in water) a trans-protonation from the NH to the carboxylate oxygen that would destroy the salt bridge and give a less robust AD-DA hydrogen bond interaction (Fig 3c) [5] is unlikely, although it could occur in non-polar solvents, where the differences in pK_a are substantially reduced. Finally, chirality (C_2 symmetric or pseudo-symmetric structures) can be introduced into the molecule by means of two stereogenic centers located at the vicinal atoms, allowing chiral recognition of the oxoanion guest. Such a chiral bicyclic guanidinium binding subunit has been efficiently prepared in our group in multigram quantities in nine steps from chiral amino acids (asparagine and

[5] The secondary interactions between the H-donor and the neighbouring acceptor atoms are attractive in a DD-AA scaffold, but repulsive in a DA-AD one: W. L. Jorgensen, W. L.; Pranata, J. *J. Am. Chem. Soc.* **1990**, *112*, 2008-2010.

methionine), in an optimized sequence following the synthesis reported by Schmidtchen.[6]

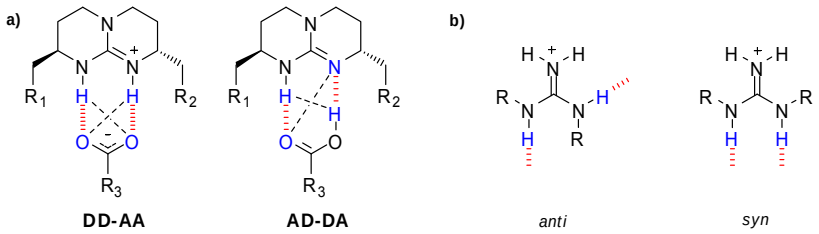

Fig 3. a) Chiral bicyclic guanidinium receptor. b) Anti and syn conformations of guanidinium group.

The association constant between bicyclic guanidinium derivatives and carboxylates are quite high in chloroform or apolar solvents. Thus, UV titrations between **IV** (tetraphenylborate salt) and tetrabutylammonium (TBA) *p*-nitrobenzoate gave $K_a = 7 \times 10^6$ M^{-1}.[7] The crystal structure of an acetate salt confirmed the formation of two strong symmetric hydrogen bonds between the host and the guest (N···O 2.850 Å). This first binding study confirmed the linear arrangement of the guanidinium-carboxylate hydrogen-bonded ion pair, like in most arginine-aspartate or arginine-glutamate contacts in proteins.

We developed receptor **V** (with chloride as the counterion) for aromatic carboxylates, but the stability constant with TBA *p*-nitrobenzoate was much lower than in the previous example with tetraphenylborate as counterion ($K_a = 1.6 \times 10^3$ M^{-1}, ^{1}H NMR titrations in $CDCl_3$).[8] This example illustrates the competition with the initial counterion and the importance of the counterion in binding strength: the tetraphenylborate counterion results in a significantly stronger binding than chloride. Thus, poorly coordinating counterions such as hexafluorophosphate or tetraphenylborate are necessary if strong binding constants are desired.

[6] a) Echavarren, A. M.; Galán, A.; de Mendoza, J.; Salmerón A.; Lehn, J.-M. *Helv. Chim. Acta* **1988**, *71*, 685-692. b) Kurzmeier, H.; Schmidtchen, F. P.; *J. Org. Chem.* **1990**, *55*, 3749-3755.

[7] Müller, G.; Riede, J.; Schmidtchen, F. P. *Angew. Chem. Int. Ed. Engl.* **1988**, *27*, 1516-1518.

[8] Echavarren, A.; Galán, A.; Lehn, J.-M.; de Mendoza, J. *J. Am. Chem. Soc.* **1989**, *111*, 4994-4995.

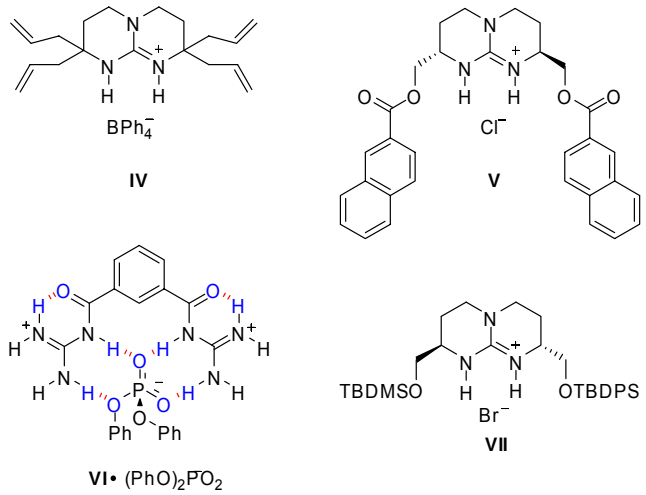

*Fig 4. Bicyclic guanidinium receptors for carboxylate recognition (**IV**, **V** and **VII**) and phosphodiester recognition (**VI**).*

The strong deshielding of the NH signals in the ^{1}H NMR spectrum of **V**•*p*-nitrobenzoate indicates the presence of hydrogen bonds. Moreover, stacking interactions between the naphthoyl side arms and the *p*-nitrophenyl moiety are evidenced by the shifting of the aromatic signals. Despite their ionic character, hosts **IV** and **V** are insoluble in water but easily dissolved in chlorinated solvents. Consequently, single liquid-liquid extractions of water solutions of carboxylate salts give quantitatively the ion pair in the organic solvent, free from any competing ion, which remains in the water phase.

Hamilton and co-workers reported that the bis-acylguanidinium salt **VI** was a receptor for phosphodiesters. The binding constant with TBA diphenylphosphate (K_a = 4.6 × 10^4 M^{-1}, measured by UV in CH_3CN), was one order of magnitude higher than with a simpler benzoylguanidinium tetraphenylborate.[9] The adjacent carbonyl groups contribute to the binding in two ways: they increase the acidity of the guanidinium NHs (but not to such an extent that trans-protonation can occur) and they pre-organize the host by intramolecular hydrogen bonds (chelation effect). The combination of these two factors allows strong complexation in more polar solvents, such as acetonitrile.

[9] Dixon, R. P.; Geib, S. J.; Hamilton, A. D. *J. Am. Chem. Soc.* **1992**, *114*, 365-366.

Schmidtchen studied guanidinium-carboxylate interactions by isothermal titration calorimetry (ITC).[10] The isotherm binding curve from the titration between **VII** (bromide) and tetraethylammonium acetate in acetonitrile (K_a = 2.0 × 10^5 M^{-1}) revealed that the process was both entropically and enthalpically favorable for a 1:1 complex. Although thermodynamic parameters could be determined in both CH_3CN and DMSO, the reaction in MeOH produced too little heat to allow quantification of the association constant. This result shows that the stabilization of the guanidinium-carboxylate is not only due to the strong electrostatic interactions (ΔH^o) but also to a favorable release of solvent molecules (ΔS^o), which strongly emphasizes the importance of solvation in host-guest interactions, a factor often neglected in receptor design.

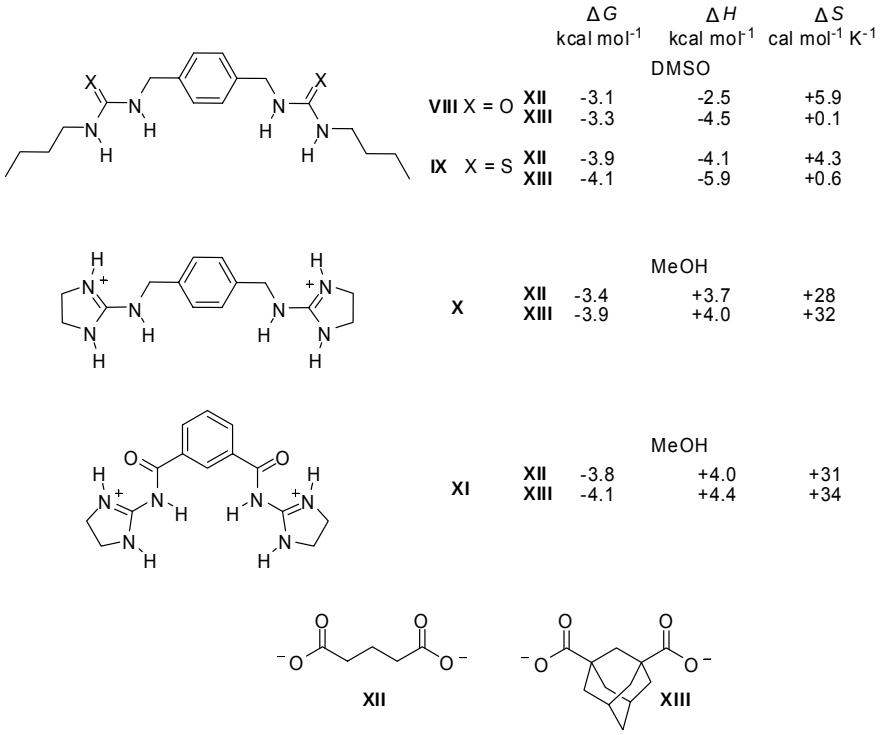

*Fig 5. Urea- (**VIII**), thiourea- (**IX**) and guanidinium-based (**X**-**XI**) receptors and association data for dicarboxylates **XII** and **XIII** by isothermal titration calorimetry.*

[10] Berger, M.; Schmidtchen, F. P. *J. Am. Chem. Soc.* **1999**, *121*, 9986-9993.

The thermodynamic aspects of dicarboxylate recognition by artificial receptors with increasingly acidic hydrogen bond donor groups such as two ureas (**VIII**), thioureas (**IX**), or guanidiniums (**X** and **XI**) in polar solvents (from DMSO to water) were studied by Hamilton (Fig 5).[11]

As expected, association constants with carboxylates (**XII** and **XIII**) increase with hydrogen acidity but are decreased in more polar solvents. While guanidinium-carboxylate association in DMSO is enthalpically driven, in more polar solvents such as methanol or water the association becomes an entropically driven process due to the liberation of solvent molecules upon binding.

Anslyn and co-workers developed receptor **XIV**, with three guanidinium moieties attached to a 1,3,5-triethyl-2,4,6-trimethylbenzene pre-organized tripodal platform,[12] showing selective binding towards citrate **XV** in pure water ($K_a = 6.9 \times 10^3$ M^{-1}, ^1H NMR titrations). The host was able to complex citrate even from a crude extract of orange juice, which highlights its selectivity towards other carboxylates. This receptor shows how the solvent competition can be overcome by accumulation of hydrogen bond donors (three guanidinium subunits) in a suitable fashion.

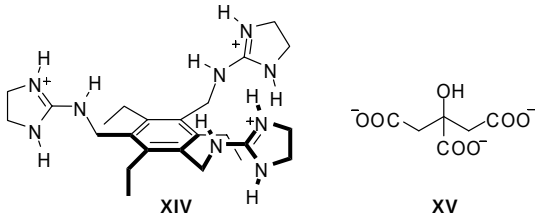

XIV **XV**

*Fig 6. Guanidinium receptor (**XIV**) for selective citrate (**XI**) selection.*

The same principles inspired Schmuck's 2-(guanidiniocarbonyl)-1*H*-pyrroles (Fig 7), designed to complex carboxylate groups in highly competitive media, even in water.[13] Whereas the simple guanidinium cation **XVI** ($pK_a = 13$) does not show any sign of complexation with carboxylates in aqueous DMSO, the increased acidity of the

[11] Linton, B. R.; Goodman, M. S.; Fan, E.; van Arman, S. A.; Hamilton, A. D. *J. Org. Chem.* **2001**, *66*, 7313-7319.

[12] Metzger, A.; Lynch, V. M.; Anslyn, E. V. *Angew. Chem. Int. Ed. Engl.* **1997**, *36*, 862-864.

[13] Schmuck, C. *Chem. Eur. J.* **2000**, *6*, 709-718.

acylguanidinium **XVII** (pK_a = 7-8), rises the binding affinity (K_a = 50 M^{-1}). An additional hydrogen bond from the pyrrole NH (as in **XVIII**) increases the association significantly (K_a = 130 M^{-1}) and the additional amide group (**XIX**) adds a further hydrogen donor, reasonably well oriented to reach the *anti* oxygen lone pair (K_a = 770 M^{-1}). The predicted geometries have been confirmed by X-ray crystal structures. Even dipeptides are bound efficiently in water by a receptor such as **XX** (K_a = 54300 M^{-1} for Val-Val).[14] A similar scaffold has been used in a combinatorial approach showing the importance of additional interactions caused by the side arm to improve selectivity.

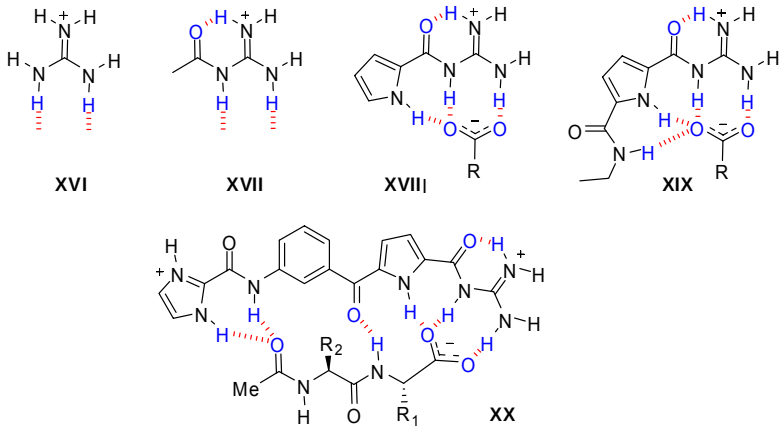

*Fig 7. Guanidinium cations **XVI-XX** and their carboxylate complexes.*

1.1.3. Chiral Guanidines for the Enantioselective Recognition of Carboxylates

Chiral discrimination of anions based on abiotic receptors is still an underdeveloped area of supramolecular chemistry. Enantiomerically pure compounds are usually obtained by asymmetric synthesis, crystallization of diastereomeric salts, kinetic resolution of racemic mixtures or chiral chromatography. An interesting alternative to these methods is the separation of enantiomers based on the complementarity of a receptor. Those processes based on the translocation of a guest between immiscible phases (chromatography, extraction, membrane transport) are particularly attractive. If the receptor is chiral, one of the enantiomers can be

[14] Schmuck; C.; Geiger, L. *J. Am. Chem. Soc.* **2004**, *126*, 8898-8899.

complexed preferentially and a kinetic resolution could be achieved. Moreover, the process needs only a catalytic amount of receptor since it can transfer several substrate molecules across the phases, without being removed from its own (stationary or liquid) phase.

In this context, a useful concept, developed for chiral chromatography, is the *three-point binding rule*, which states that a minimum of three simultaneous interactions between the chiral stationary phase and for instance one of the enantiomers are necessary to achieve enantioselection, with at least one of these interactions being stereochemically dependent.[15] For anions, receptors containing ammonium groups, amides, ureas, thioureas and guanidinium subunits, as well as porphyrins, saphyrins, or metal-containing ligands have been employed. Only chiral guanidines aimed at the discrimination of the enantiomers of amino acids will be reviewed here.

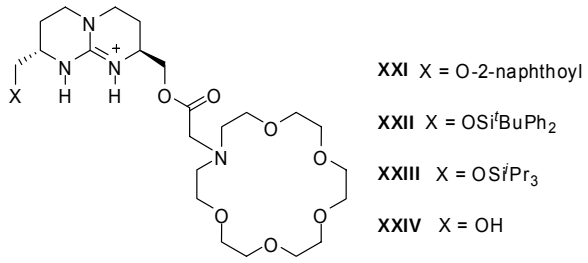

Fig 8. Guanidinium receptors for enantiorecognition of Trp and Phe.

The first example of chiral recognition of a carboxylate by a guanidinium-based receptor was reported by de Mendoza in 1989. Indeed, compound **V** was shown to extract enantiomeric salts of *N*-protected amino acids, such as tryptophan, with modest selectivities (up to 17% excess of *N*-Ac-L-Trp or *N*-Boc-L-Trp were extracted by (*S,S*)-**V** from water into chloroform). ^{1}H NMR titrations of the triethylammonium salts of *N*-acetyltryptophan in $CDCl_3$ gave K_a = 1000 and 500 M^{-1} for the L- and D-enantiomers, respectively. For the non protected, strongly solvated zwitterionic amino

[15] Pirkle; W. H.; Pochapsky, T. C. *Chem. Rev.* **1989**, *89*, 347-362.

acids, receptor (*S*,*S*)-**XXI** was designed (Fig 8).[16] The compound features non self-complementary binding sites for carboxylate (the guanidinium function) and ammonium (namely a crown ether), preventing the receptor from internal collapse. An aromatic planar surface (a naphthalene ring) was attached as a third point for additional stacking interactions (Fig. 5a). Up to 40% of racemic tryptophan or phenylalanine were extracted by (*S*,*S*)-**XXI** from saturated aqueous neutral solutions into dichloromethane, with a *ca.* 80% content of the L-enantiomer. Reciprocally, chiral host (*R*, *R*)-**XXI** extracted mainly D-Trp.

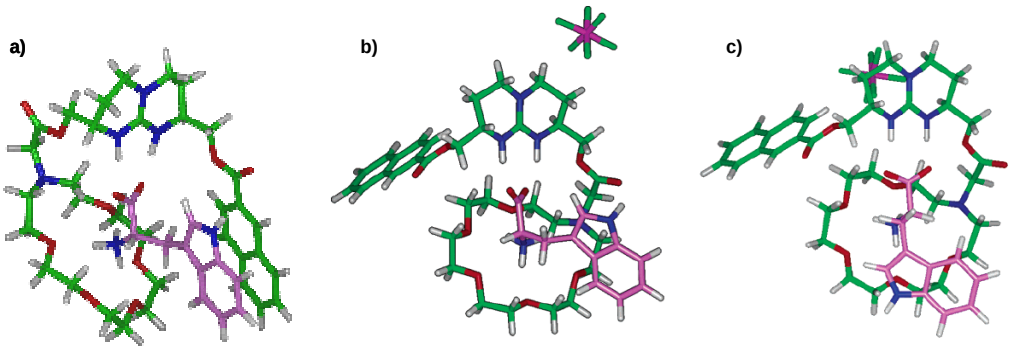

*Fig 9. a) Three-point binding mode for receptor (S,S)-**XXI** and L-Trp.[16b] b) Two-point binding mode for L-Trp. c) Two-point binding mode for D-Trp.*

Further guanidinium receptors were synthesized later by the same research group in order to optimize the binding and extraction properties, and were tested as membrane carriers (U-tube tests with dichloromethane between two water phases).[17] Interestingly, both single liquid-liquid extractions and U-tube transport experiments revealed that **XXII** and **XXIII** transported Trp with comparable degrees of selectivity as **XXI**. This suggests that the aromatic naphthoyl group does not play a significant role in the discrimination process. Even compound **XXIV**, lacking the potential π-π

[16] a) Galán, A.; Andreu, D.; Echavarren, A. M.; Prados, P.; de Mendoza, J. *J. Am. Chem. Soc.* **1992**, *114*, 1511-1512. b) de Mendoza, J.; Gago, F. *Computational Approaches in Supramolecular Chemistry*, NATO ASI Ser., Series C, **1994**, *426*, 79-99.

[17] Breccia, P.; Van Gool, M.; Pérez-Fernández, R.; Martín-Santamaría, S.; Gago, F.; Prados, P.; de Mendoza, J. *J. Am. Chem. Soc.* **2003**, *125*, 8270-8284.

interaction, was enantioselective, although to a lesser extent. Another binding mode was then proposed, without participation of the naphthoyl arm, as the outcome of molecular dynamics calculations with explicit solvent molecules. In this model, binding of D-Trp exposes a highly polar area of the receptor (around the crown ether nitrogen) to the apolar solvent, causing the overall energy to increase (Fig 9b,c).[17]

A series of receptors for *N*-protected amino acids, bearing guanidinium and carbamate moieties anchored to the curved and lipophilic surface of cholic acid (compounds **XXV**-**XXVII**, Fig 10) have been reported by Davies and co-workers.[18] The chirality is provided by the steroidal framework, the guanidinium as well as the carbamate groups establishing the ion pair and hydrogen bonds with the substrate. All these hosts efficiently extract (52-87%) *N*-acyl α-amino acids from an aqueous phosphate buffer solution (pH 7.4) into chloroform. Compound **XXV** showed high enantioselectivity (up to 7:1, ^{1}H NMR measurements) for several *N*-acyl α-amino acids although this selectivity decreased dramatically for the more hindered *N*-Boc derivatives. On the contrary, chiral discrimination increased (9:1) with derivatives **XXVI** and **XXVII**, carrying the more acidic carbamoyl groups.

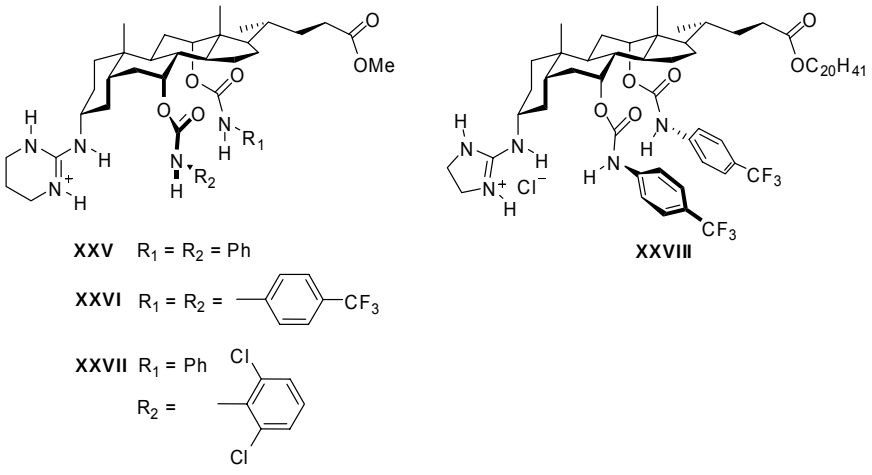

Fig 10. Guanidinium receptors for N-acyl α-amino acids recognition.

[18] Lawless, L. J.; Blackburn, A. G.; Ayling, A. J.; Pérez-Payán, M. N.; Davis, A. P. *J. Chem. Soc., Perkin Trans. 1* **2001**, *11*, 1329-1341.

The highly lipophilic receptor **XXVIII** was then synthesized in gram amounts for transport studies with *N*-acetylphenylalanine either in U-tube bulk liquid membranes (dichloromethane) or with hollow-fiber membrane contactors (2.5% octanol in hexane).[19] High enantioselectivity and transport rates were observed in the U-tubes (27% of *N*-Ac-Phe transported in 24 h with 56% e.e.), as well as with the large scale hollow fiber system (*ca.* 70 equivalents of substrate transported after 48 hours) although in this case the initial selectivity (*ca.* 30%) decreased over time.

Guanidiniocarbonyl pyrrole systems have also been tested for enantioselection. Schmuck reported host **XXIX** which was able to bind strongly carboxylates in water (Fig 11). Despite its flexible structure and the fact that it bears only one chiral centre, this receptor showed enantioselectivity towards *N*-acetylalanine (K_a = 1610 and 910 M^{-1} for *N*-Ac-L-Ala and *N*-Ac-D-Ala, respectively), a remarkable result considering the small size of alanine's side chain. Curiously, other amino acids with bulkier side chains (such as *N*-acetylphenylalanine or *N*-acetyltryptophan) showed only slight differences in binding for both enantiomers.

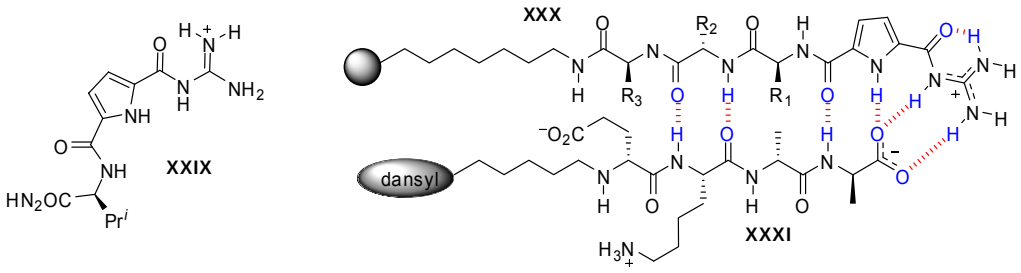

Fig 11. Guanidiniocarbonyl pyrrole receptors for enantioselection.

More recently, tris-cationic receptors based on the guanidiniocarbonyl pyrrole scaffold were developed by combinatorial chemistry. One compound (**XXX**, R_1 = R_2 = Lys; R_3 = Phe) showed efficient binding to the sequence D-Glu-L-Lys-D-Ala-D-Ala-OH (**XXXI**) with $K_a > 10^4$ M^{-1} in buffered water.[20] This peptide sequence is related to

[19] Baragana, B.; Blackburn, A. G.; Breccia, P.; Davis, A. P.; de Mendoza, J.; Padrón-Carrillo, J. M.; Prados, P.; Riedner, J.; de Vries, J. G. *Chem. Eur. J.* **2002**, *8*, 2931-2936.

[20] a) Schmuck; C.; Wich, P. *Angew. Chem. Int. Ed.* **2006**, *45*, 4277-4281. b) Schmuck, C.; Heil, M. *Chem. Eur. J.* **2006**, *12*, 1339-1348.

the bacterial peptidoglycan that is recognized by the vancomycin family of antibiotics, preventing formation of the cell wall.

1.1.4. Phosphate and Sulfate Recognition

In addition to carboxylates or phosphodiesters, other oxoanions such as phosphate, sulfate and nitrate are biologically relevant[21] and chemically challenging to recognize, due to their weak basicity. At neutral pH, phosphate (as HPO_4^{2-}) and sulfate present a tetrahedral binding mode with two negative charges, although nitrate has a trigonal planar binding motif with just one negative charge. Thus, for a neutral complex, two guanidines are required for phosphate and sulfate whereas only one is needed for nitrate, in addition to other hydrogen bond donor atoms. The design of suitable linkers between the hydrogen donors with optimal orientation and maximum participation of host's lone pairs represents a major issue in the field.

1.1.4.1. Phosphates

Anslyn and co-workers showed that metallo-receptor **XXXII** displayed a selective binding for monoprotonated phosphate (HPO_4^{2-}) and arsenate ($HAsO_4^{2-}$) over other anions (such as AcO^-, NO_3^-, HCO_3^- or Cl^-) at biological pH ($K_a = 10^4$ M^{-1} in 98:2 water/methanol, UV/vis and ITC titrations).[22] Hosts bearing only the Cu(II) centre were less effective ($K_a = 10^2$ M^{-1}), highlighting the role of the cavity and the presence of the guanidinium groups. Thermodynamic data showed that association of HPO_4^{2-} with guanidinium derivative **XXXII** was both enthalpically and entropically driven, whereas complexation with an ammonium analogue was mainly governed by entropy. The different mode of binding was rationalized in terms of the different solvation energies of both binding groups.

[21] a) Jacobson, B. L.; Quiocho, F. A. *J. Mol. Biol.* **1988**, *204*, 783-787. b) Luecke, H.; Quiocho, F. A. *Nature* **1990**, *347*, 402-406.

[22] Tobey; S. L.; Anslyn, E. V. *J. Am. Chem. Soc.* **2003**, *125*, 14807-14815.

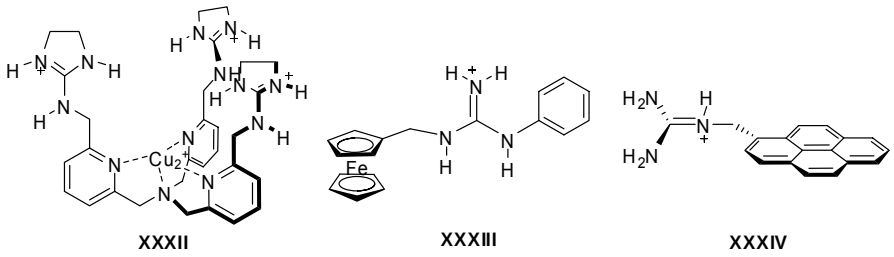

Fig 12. Guanidinium receptors for phosphate recognition.

Ferrocenyl-based receptor **XXXIII** gives moderately strong complexes with pyrophosphate $P_2O_7^{4-}$ (K_a = 4600 M^{-2}, 50% methanol-water) showing a 2:1 host-guest stoichiometry.[23] The presence of a redox active subunit (the ferrocene) allows its use as an electrochemical sensor for this biologically relevant anion. Another receptor binding pyrophosphate in a 2:1 fashion (K_a = 1.2 × 10^8 M^{-2} and 1.0 × 10^4 M^{-1} for 2:1 and 1:1 complexes, respectively) is guanidinium **XXXIV**, containing a fluorescent pyrene antenna, which appeared to be highly selective for $P_2O_7^{4-}$ over a variety of anions.[24] Moreover, ^{1}H NMR suggests that the two hosts in the 2:1 complex are self-assembled through pyrene-pyrene stacking interactions.

Polyanionic messenger inositol-1,4,5-triphosphate (**XXXVI**, Fig 13) was recognized by receptor **XXXV** bearing up to six guanidinium subunits on top of a pre-organized 2,4,6-triethylbenzene platform.[25] Steric gearing causes the guanidinium groups to converge toward the cavity. As a result, a cleft-like cavity is formed. Since **XXXV** has no chromophore, the binding constant (K_a = 2.2 × 10^4 M^{-1} in a buffered solution, 1.0 × 10^8 M^{-1} in MeOH) was measured by competition with a fluorescent guest (5-carboxyfluorescein), which is released in the presence of the selected guest **XXXVI**.

[23] Beer, P. D.; Drew, M. G. B.; Smith, D. K. *J. Organomet. Chem.* **1997**, *543*, 259-261.

[24] Nishizawa, S.; Kato, Y.; Teramae, N. *J. Am. Chem. Soc.* **1999**, *121,* 9463-9464.

[25] Niikura, K.; Metzger, A.; Anslyn, E. V. *J. Am. Chem. Soc.* **1998**, *120*, 8533-8534.

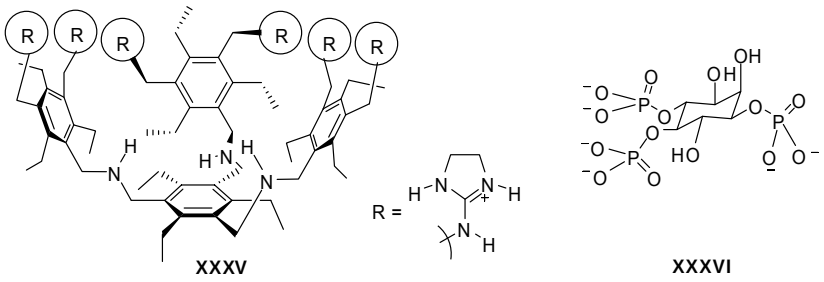

Fig 13. Guanidinium receptors for triphosphate recognition.

Schmidtchen designed a urethane-linked bis-guanidinium receptor **XXXVII** for the binding of ditopic tetrahedral anions.[26] A binding constant of 10^6 M^{-1} in water for *p*-nitrophenyl phosphate and cytidine-5'-phosphate was determined by ^{1}H NMR. Such a high value in a polar solvent was explained by the simultaneous complexation of both guanidinium groups to the tetrahedral guest.

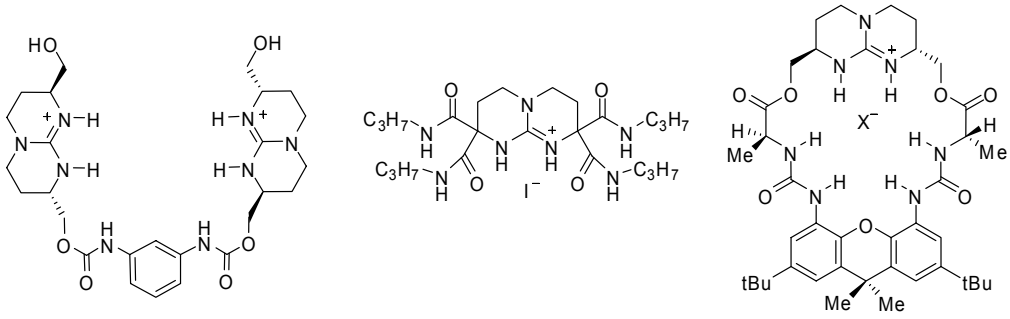

Fig 14. Bicyclic guanidinium receptor for phosphate recognition.

Recently, binding studies between **XXXVIII** and **IV** and phosphates of different sizes were measured by both ^{1}H NMR and ITC in acetonitrile.[27] For **XXXVIII**, ^{1}H NMR gave a curve fitting for a 1:1 stoichiometry whereas ITC predicted a 1:2 host-guest binding model and revealed that the binding was not caused by a large enthalpic contribution but to a strong entropic factor instead. In this regard, calorimetry prevents

[26] Schmidtchen, F. P. *Tetrahedron Lett.* **1989**, *30*, 4493-4496.

[27] Jadhav, V. D.; Schmidtchen, F. P. *Org. Lett.* **2005**, *7*, 3311-3314.

misleading conclusions from NMR in cases where rapidly interconverting species are in equilibrium. Thus, introduction of several hydrogen bond donors in the receptor scaffold counteracts rather than enhances the enthalpic stabilization of the host-guest complex.

Macrocycle **XXXIX**, based on the chiral bicyclic guanidinium subunit, has been designed by de Mendoza and co-workers to afford six strong hydrogen bonds oriented inwards its cavity to facilitate wrapping around tetrahedral oxoanions.[28] Although diphenylphosphate was readily extracted from water, the binding constant could not be measured from the tetraphenylborate salt ($K_a > 10^5$ M^{-1}) by NMR in $CDCl_3$. However, from the chloride salt the constant was 10^3 M^{-1}, which indicates that the receptor is selective for diphenylphosphate over chloride. Contrary to the expectation that the guest would be threaded across the cavity, splitting of most signals at low temperature indicated the rapid counterion scrambling between both sides of the macrocycle. Consequently, attempts to make a rotaxane by using the bulkier 3,5-di-*tert*-butyldiphenylphosphate as a template during the cyclization (clipping) were unsuccessful.

1.1.4.2. Sulfates

Sulfate recognition by guanidinium receptors has been much less explored than carboxylate or phosphate binding. Therefore, no detailed comparative binding studies for sulfates and other anions are available. However, despite phosphate and sulfate are tetrahedral, the latter is less basic, thus the affinity for guanidinium receptors is shifted towards phosphate.

In 1996 de Mendoza and co-workers reported on chiral bicyclic bis-guanidinium (**XXXX** and **XXXXI**) and tetrakis-guanidinium (**XXXXII**) salts whose sulfate counterions, unlike the corresponding chloride salts, required hydrogen donors from two different molecules to balance the charges and to fully wrap around the anion, since the selected spacer CH_2SCH_2 was designed in such a way that it was simply too short to use guanidines from the same chain (Fig 15).[29] Therefore, two subunits are

[28] Alcázar, V.; Segura, M.; Prados, P.; de Mendoza, J. *Tetrahedron Lett.* **1998**, *39*, 1033-1036.

[29] Sánchez-Quesada, J.; Seel, C.; Prados, P.; de Mendoza, J. *J. Am. Chem. Soc.* **1996**, *118*, 277-278.

forced to self-assemble orthogonally around the tetrahedral anion in a double-helical structure (sulfate helicates). ^{1}H NMR spectra showed large downfield shifts of guanidinium NH's as dimers or tetramers complexed sulfate anion. Moreover, ROESY spectra confirmed intermolecular contacts due to the folded conformation.

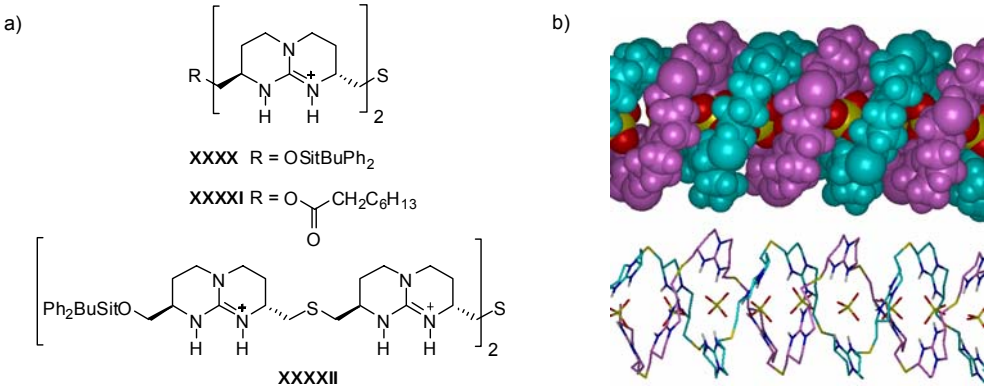

*Fig 15. a) Chiral bicyclic bis-guanidinium salts **XXXX** and **XXXXI** and tetrakis-guanidinium salt **XXXXII**. b) Optimized model of a sulfate helicate from a strand of (S,S)-guanidines.*

A recent computational study concludes that for simple sulphate-guanidinium interactions several minima of similar energies could be found.[30] For more complex guanidines, such as the closely related ligands **XXXXIII** and **XXXXIV**, the crystal structure shows 1:1 sulfate complexes, with a good docking of the anion into the cavity of **XXXXIV**, but this was not the case for **XXXXIII** (Fig 16).[31] Interestingly, the pyridine nitrogen of **XXXXIII** induces pre-organization by intramolecular hydrogen bonding but causes repulsion of the anion due to the increased charge density in the pocket around the heteroatoms.

[30] Rozas, I.; Kruger, P. K. *J. Chem. Theory Comput.* **2005**, *1*, 1055-1062.

[31] Grossel, M. C.; Merckel, D. A. S.; Hutchings, M. G. *Cryst. Eng. Comm.* **2003**, *5*, 77-81.

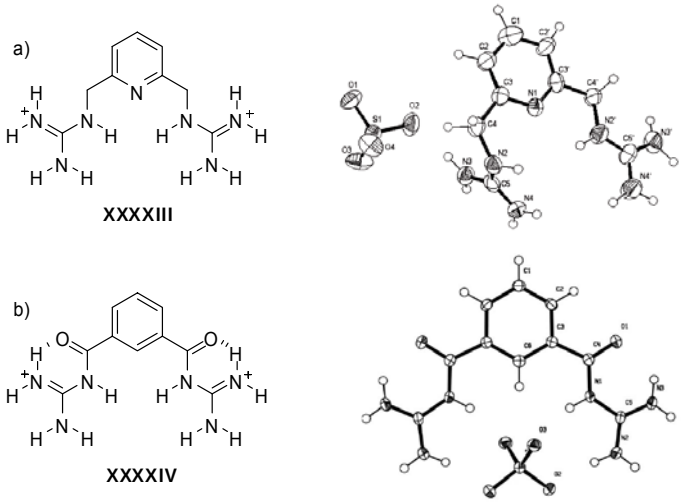

Fig 16. Crystal structure of ***XXXXIII*** *•H_2SO_4 (a) and of* ***XXXXIV*** *•H_2SO_4 (b).*

The energetics of the guanidinium-sulfate system have been analyzed by Schmidtchen using two bicyclic guanidinium subunits linked through a suitable spacer, such as **XXXXV** (Fig 17).[32] ITC measurements revealed that guest complexation was strongly endothermic with entropy as the driving force. The interactions are strong enough in methanol (K_a = 6.8 × 10^6 M^{-1}) to overcome the positive enthalpy change. Assuming that free host and free guest are more highly solvated than the complex, the positive enthalpy reflects the reorganization of the solvent shell upon complexation. A comparison between receptors which combine two guanidinium groups (such as **XXXXV**) and monotopic bicyclic guanidinium ones, which showed little or no interaction with sulfate in methanol, accounts for the importance of the bridging spacer between both cationic subunits.

[32] Berger, M.; Schmidtchen, F. P. *Angew. Chem. Int. Ed.* **1998**, *37*, 2694-2696.

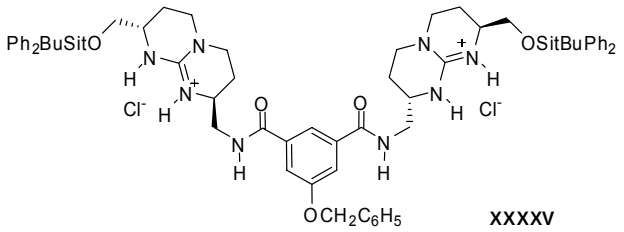

Fig 17. Bicyclic guanidinium receptor for sulfate recognion.

2.2 Objectives

2.2.1 Nitrate recognition

The second chapter of this Thesis reports on the synthesis of new chiral bicyclic guanidinium receptors to study host-guest interactions with small anions.[33] Besides the good hydrogen bond donor ability of the guanidinium function, two urea groups have been incorporated in the scaffold of the receptors to enhance the affinity towards weak coordinative nitrate.[34] Therefore, several receptors (either open or macrocyclic) with six hydrogen bond donors have been synthesized as well as some macrocycles of different cavity sizes (Fig 18).

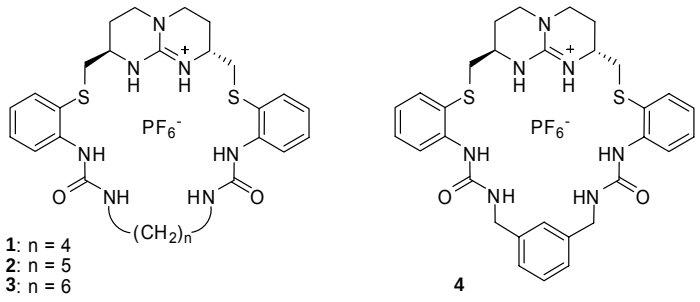

Fig 18. Bicyclic guanidinium receptors for nitrate recognition.

[33] a) Schmidtchen, F. P.; Berger, M. *Chem. Rev.* **1997**, *97*, 1609-1646. b) Beer P. D., Gale, P. A. *Angew. Chem. Int. Ed.* **2001**, *40*, 486-516.

[34] Hay, B. P.; Gutowski, M; Dixon, D. A.; Garza, J.; Vargas, R.; Moyer, B. A. *J. Am. Chem. Soc.* **2004,** *126*, 7925-7934.

In summary, ^{1}H-NMR and isothermal calorimetric (ITC) techniques were used to quantify the association between hosts and guests and to determine thermodynamic parameters. Small anions such as nitrate, acetate, chloride and bromide were investigated as well as larger one such as benzoate. Selectivity was established for the different anions under study. Solid state X-ray crystal structures have been resolved for several complexes, showing the inclusion of nitrate, acetate or chloride anions inside the cavity of the macrocyclic guanidinium receptors, and shedding light on the structural parameters governing the binding.

2.2.2 Naproxen Enantiorecognition

The third chapter deals with the challenging problem of the chiral recognition of the NSAID (Non-Steroidal Anti-inflammatory Drug) Naproxen.[35] To do so, two different strategies have been employed: on the first hand, the rational design for a step to step host-guest interactions assay, on the second hand, the combinatorial approach with the synthesis of amino acid libraries to be screened with a fluorescent Naproxen derivative.

Since multiple hydrogen bond donor hosts synthesized in the second chapter revealed as being good receptors for carboxylate, we first checked open-chain, symmetric guanidinium receptors for our target Naproxen. Therefore, chiral receptors with six hydrogen bond donors and bearing bulky group as adamantyl, 2-*tert*-butyl-6-methylphenyl or diphenylmethyl were synthesized in order to discriminate one enantiomer from the other (Fig 19).

[35] Giordano, C.; Villa, M.; Panossian, S. *Naproxen: Chirality in Industry*, Wiley (New York), **1992**.

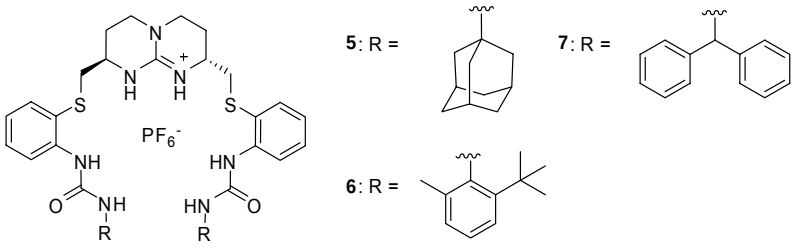

Fig 19. Symmetric chiral guanidinium receptors bearing bulky.

Moreover, several symmetric hosts bearing butyl or phenyl as well as benzyl or phenylethyl groups have been prepared as a preliminary step in the synthesis of pincer-like receptors. Additional π-π stacking interactions were then investigated with Naproxen (bearing an electronically enriched ring). We also introduced additional chirality in both arms of the host in a view of leading the enantioselective recognition of (*S*)-Naproxen. Besides, this study was run for both chiral (*R*, *R*) and achiral *meso* (*R*, *S*) guanidinium scaffolds in an attempt to select the best pre-organized pocket.

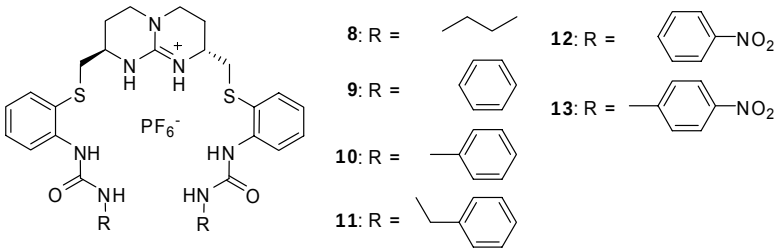

Fig 20. Symmetric receptors for pincer-like binding assays.

A more rigid and pre-organized macrocycle **14**, incorporating a lysine derivative with both additional hydrogen bond and an electronically poor aromatic ring, as a chiral linker between the two urea groups, was also designed and synthesized.

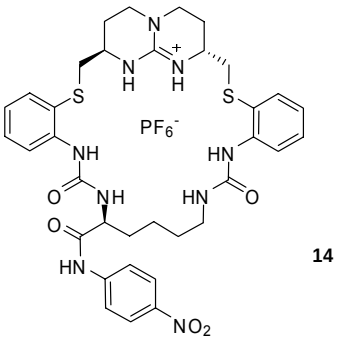

14

*Fig 21. Lysine-containing macrocycle **14**.*

In an effort to introduce a new and strong chiral barrier into the receptor scaffold, we designed two guanidinium-based macrocycles employing NOBIN, a catalysis ligand as spacer.[36] A short (4 carbon atoms, **15**) or a rigid (xylylene, **16**) linker was then introduced between the two urea moieties in order to restrict host conformational degree (Fig 22).

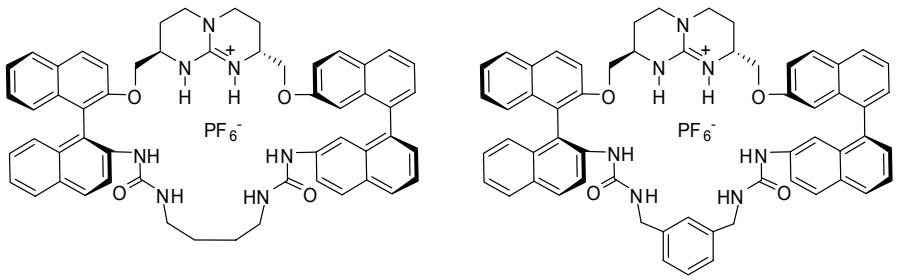

15 **16**

*Fig 22. Nobin macrocycles **15** and **16**.*

Apart from rational design, combinatorial chemistry[37] comes as a second approach for the chiral recognition of (*S*)-Naproxen. A fluorescent probe (Naproxen derivative **17**, Fig 23) was then used to screen libraries of receptors susceptible of

[36] a) Smrčina, M.; Lorenc, M.; Hanuš, V.; Sedmera, P.; Kočovskỳ, P. *J. Org. Chem.* **1992**, *57*, 1917-1920.

[37] Lowe, G. *Chem. Soc. Rev.* **1995**, *24*, 309-317.

showing enantioselection. The fluorescent dansyl group was then attached to both Naproxen enantiomers.

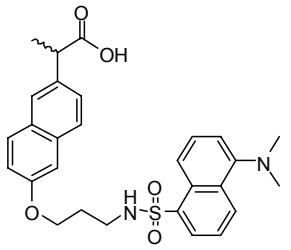

(*R*)-**17**
(*S*)-**17**

*Fig 23. Fluorescent Naproxen derivative (S) and (R)-**17**.*

A peptide library was then synthesized and subsequently attached by alkylation to two guanidinium scaffolds: **18,** with a protected guanidinium arm, and **19,** with a better binding pocket with two additional hydrogen bond donor groups for the carboxylate function of the guest.

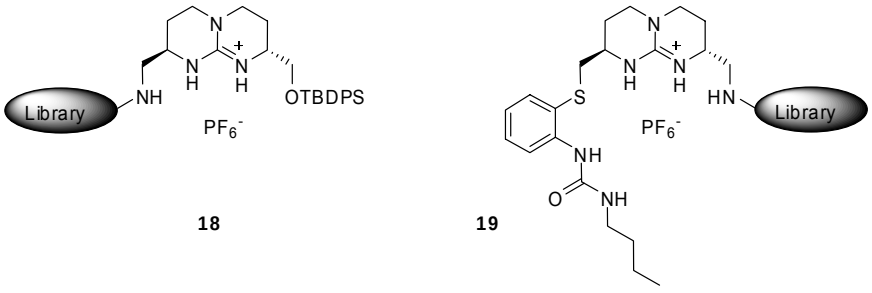

18 **19**

*Fig 24. Guanidinium receptor libraries **18** and **19**.*

2 Nitrate Recognition

2.1 Introduction

2.1.1 Abiotic Receptors for Small Anions

Molecular recognition of anions is a current important area of supramolecular chemistry with an increasing interest every year.[1] Considering anion characteristics, synthesizing a host able to selectively distinguish it from its size, shape and basicity is still challenging.[2] To do so, hydrogen bonds, electrostatic interactions, hydrophobic effect as well as metal or Lewis acid coordination have been employed in order to reach the ultimate goal of developing sensors.[3] Taking into account supramolecular interactions, a rational design may thus lead to new receptors for a specific anion.

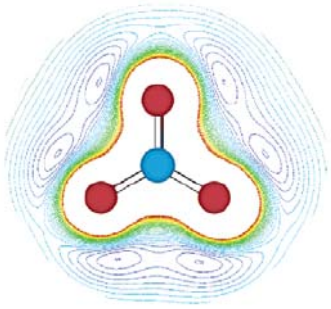

Fig 1. Contour map of the electrostatic potential surface for a positive point charge in the plane of nitrate.[4]

Nitrate is a weak basic anion with a highly symmetric trigonal planar binding mode (Fig 1), so selective binding to suitable hosts through multiple hydrogen bonds

[1] a) Gale, P. A. *Coord. Chem. Rev*. **2006**, *250*, 2917. b) Gale, P. A.; Quesada, R. *Coord. Chem. Rev.* **2006**, *250*, 3219-3244.

[2] Schmidtchen, F. P.; Berger, M. *Chem. Rev*. **1997**, *97*, 1609-1646.

[3] Beer, P. D.; Gale, P. A. *Angew. Chem. Int. Ed.* **2001**, *40*, 486-516.

[4] Hay, B. P.; Gutowski, M.; Dixon, D. A.; Garza, J.; Vargas, R.; Moyer, B. A. *J. Am. Chem. Soc.* **2004**, *126*, 7925-7934.

is demanding. Even though nitrate is a biologically relevant substrate and plays a very important role in environmental pollution,[5] comparatively little attention has been given to this target by supramolecular chemists relative to other anions, such as halides or acetate. Nitrate in groundwater originates primarily from fertilizers and excessive levels in drinking water may cause serious illness due to conversion into nitrite by reduction into the body. Anion exchange, reverse osmosis, electrodialysis and distillation have been approved for removing nitrates/nitrites.[6] The health standard for nitrate is 50 mg/L in the European Community countries.[7] We propose herein a supramolecular approach for removing nitrate from water by liquid-liquid extraction. However, its little tendency to establish robust hydrogen-bonded frameworks in solution makes it indeed difficult to compete with other anions such as chloride or carboxylates for the hydrogen donor sites of the receptors (Table 1).

Anions	Ionic size	pK_a of corresponding acid	Binding mode
NO_3^-	179	-1.3	Trigonal planar
F^-	133	+3	Spherical
Cl^-	181	-7	Spherical
Br^-	196	-9	Spherical
I^-	220	-10	Spherical
$HCOO^-$	156	+3.75	Bidentate planar

Table 1. Ionic size (pm), pK_a of HA and binding mode of selected anions A^-.

Anslyn et *al.* designed a bicyclic cyclophane **I** (Fig 2) to recognize anions through NH-π hydrogen bonds (hydrogen bond donation through the π-system of the oxoanion rather than the oxygen lone pairs) resulting in an enhancement of nitrate

[5] Mason, C. F. *Biology of Freshwater Pollution, 2nd ed., Longman:Harlow, U. K., 2nd ed.* **1991**.

[6] http://www.nesc.wvu.edu/ndwc/pdf/OT/TB/TB4_IonExchange.pdf.

[7] European Communities *Off. J. Eur. Commun.* **1998**, *L330*, 32.

complexation over other anions tested (K_a = 300 M^{-1} in CD_2Cl_2/CD_3CN 1:3).[8] This amide-based receptor is one of the few that has a higher affinity for nitrate than chloride (K_a = 40 M^{-1}) although acetate binds better (K_a = 770 M^{-1}). Besides, this receptor was employed in an optical sensing assay with colorimetric dyes confirming its selectivity over Br^- and ClO_4^-.[9] Moreover, this receptor was tested as a new optical absorption-based disposable sensor for the analysis of nitrate in water.[10]

Herges et *al.* synthesized macrocycles of different rigidity bearing three urea or thiourea subunits and did calculate binding constants with tetrabutylammonium nitrate in polar media by ^{1}H-NMR titrations, revealing however no selectivity towards this guest (for **II**, K_a = 17.1 M^{-1} in DMSO-d_6).[11]

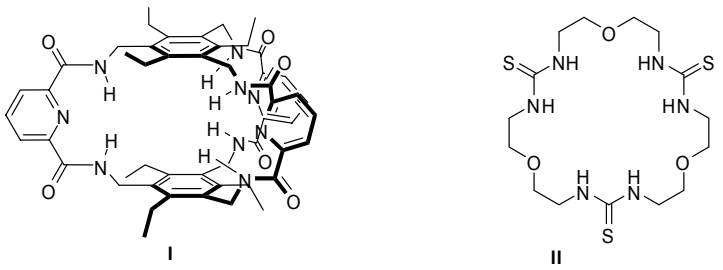

I II

*Fig 2. Anion receptors by Anslyn (**I**) and Herges (**II**).*

Hamilton et *al*. described a rigid amide-based macrocycle **III** able to selectively bind sulfate and phosphate oxoanions and reported one of the largest K_a observed for nitrate (K_a = 4.6 x 10^5 M^{-1} in 2% DMSO-d_6/$CDCl_3$, Fig 3).[12]

[8] Bisson, A. P.; Lynch, V. M.; Monahan, M. K.; Anslyn, E. V. *Angew. Chem. Int. Ed. Engl.* **1997**, *36*, 2340-2343.

[9] Niikura, K.; Bisson, A. P.; Anslyn, E. V. *J. Chem. Soc., Perkin Trans. 2* **1999**, 1111-1114.

[10] Capitán-Vallvey, L. F.; Arroyo-Guerrero, E.; Fernández-Ramos, M. D.; Santoyo-Gonzalez, F. *Anal. Chem.* **2005**, *77*, 4459-4466.

[11] Herges, R.; Dikmans, A.; Jana, U.; Köhler, F.; Jones, P. G.; Dix, I.; Fricke, T.; König, B. *Eur. J. Org. Chem.* **2002**, *17*, 3004-3014.

[12] Choi, K.; Hamilton, A. D. *J. Am. Chem. Soc.* **2003**, *125*, 10241-10249.

Jeong et *al.* have recently developed an indole-based macrocycle **IV** that acts as a chemosensor and is able to strongly bind anions through hydrogen bonds (K_a = 3.9 x 10^5 M^{-1} in CH_3CN).[13]

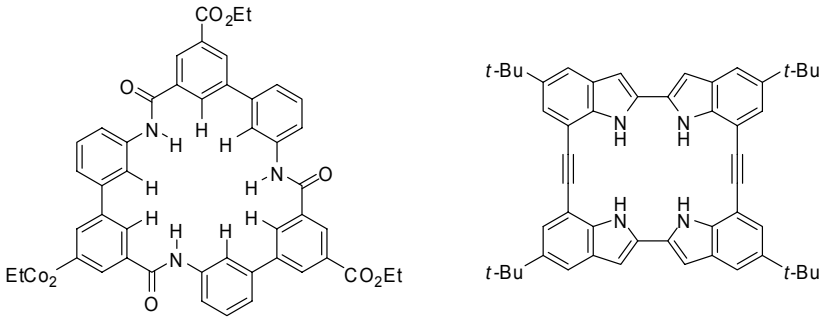

*Fig 3. Anion receptors from Hamilton (**III**) and Jeong (**IV**).*

Various anions receptors have been designed and shown nitrate complexation through hosts containing metal entities,[14] metal complexation,[15] ion-pair formation,[16] and mainly hydrogen bonding as pyrrole,[17] ammonium,[18] amide,[19] and urea[20] as

[13] Chang, K. -J.; Moon, D.; Soo Lah, M.; Jeong, K.-S. *Angew. Chem. Int. Ed.* **2005**, *48*, 7926-7929.

[14] Schnebeck, R.-D.; Freisinger, E.; Lippert, B. *Angew. Chem. Int. Ed.* **1999**, *38*, 168-171.

[15] Drew, M. G. B.; Guillaneux, D.; Hudson, M. J.; Iveson, P. B.; Madic, C. *Inorg. Chem. Commun.* **2001**, *4*, 462-466.

[16] Mahoney, J. M.; Stucker, K. A.; Jiang, H.; Carmichael, I.; Brinkmann, N. R.; Beatty, A. M.; Noll, B. C.; Smith, B. D. *J. Am. Chem. Soc.* **2005**, *127*, 2922-2928.

[17] Sessler, J. L.; An, D.; Cho, W.-S.; Lynch, V.; Marquez, M. *Chem. Eur. J.* **2005**, *11*, 2001-2011.

[18] Motekaitis, R. J.; Martell, A. E.; Lehn, J.-M.; Watanabe, E.-I. *Inorg. Chem.* **1982**, *21*, 4253-4251.

[19] Bondy, C. R.; Gale, P. G.; Loeb, S. J. *Chem. Commun*. **2001**, 729-730.

[20] a) Jagessar, R. C.; Burns, D. H. *Chem. Commun*. **1997**, 1685-1686. b) Albrecht, M.; Zauner, J.; Burgert, R.; Rottele, H.; Frohlich, R. *Materials Science and Engineering* **2001**, 185-190. c) Turner, D. R.; Paterson, M. J.; Steed, J. W. *J. Org. Chem.* **2006**, *71*, 1598-1608. d) Russell, J.

hydrogen bond donors. These synthetic anion receptors revealed an increase of its association even in polar media, although selectivity for nitrate remained difficult to achieve. For instance, similar sized Cl^- often gives a better association with the host because of its spherical shape mode and higher basicity. Most remarkably, Beer and co-workers succeeded in inverting the chloride *vs* nitrate selectivity by using a solvation effect. In a 9:1 (CH_2Cl_2/MeOH) mixture, the ruthenium(II) tris(5,5´-diamide-2,2´-bipyridine) receptor is indeed selective towards chloride whereas in 1:1 (CH_2Cl_2/MeOH) mixture, this order is inversed.[21]

2.1.2 Design of Guanidinium-based Receptors for Nitrate Recognition

Although guanidinium-based systems have been widely used to recognize oxoanions such as carboxylates and phosphates,[22] its use for nitrate binding has not been reported so far.[23] From a recent theoretical study, the combination of both guanidinium and urea moieties should provide an almost ideal complement to the guest (Fig 4a).[4,24] An important feature of the receptor design is therefore the orientation of the nitrate inside the cavity. Each oxygen atom should share its lone pairs either with a single NH donor from different functions (Fig 4b), or alternatively from the same function, by means of bifurcated hydrogen bonds (Fig 4c). So far, evidence from reported X-ray structural data indicates that nitrate binds to one or two urea functions in a linear fashion giving rise to linear hydrogen bonds with the host.[20c,d,25] Those results are in good agreement with energy data from theoretical

M.; Parker, A. D. M.; Radosavljevic-Evans, I.; Howard, J. A. K.; Steed, J. W. *Chem. Commun*. **2006**, 269-271.

[21] Uppadine, L. H.; Drew. M. G. B.; Beer, P. D. *Chem. Commun*. **2001**, 291-292.

[22] a) Houk, R. J. T.; Tobey, S.L.; Anslyn, E.V. *Top. Curr. Chem.* **2005**, *255*, 199-230. b) Blondeau, P.; Segura, M.; Pérez-Fernández, R.; de Mendoza, J. *Chem. Soc. Rev.* **2007**, *36*, 198-210.

[23] For a X-ray structure of a nitrate-guanidinium salt, see: Gleich, A.; Schmidtchen, F. P.; Mikulcik, P.; Müller, G. *J. Chem. Soc*., *Chem Commun.* **1990**, *1*, 55-57.

[24] Hay, B. P.; Firman, T. K.; Moyer, B. A. *J. Am. Chem. Soc.* **2005**, *127*, 1810-1820.

[25] a) Custelcean, R.; Moyer, B. A.; Bryantsev, V. S.; Hay, B. P. *Cryst. Growth Des*. **2006**, *6*, 555-563. b) Aakeroy, C. B.; Beffert, K.; Desper, J.; Elisabeth, E. *Cryst. Growth Des*. **2003**, *3*, 837-846.

calculations, which revealed that forcing urea to bind a single oxygen atom in a bifurcated fashion yields complexes that are less stable (more than a 10% difference) than those involving hydrogen bonds with two oxygen atoms.[24] Considering the hydrogen bond donor strength[26] and the electrostatic interactions, the hydrogen donor atoms should be along the edge of the polyhedron defined by the oxygen atoms (Fig 4b). Higher stability of linear hydrogen bonds should indeed prevent formation of a second complex based on significant geometrically unfavorable bonds (Fig 4c).

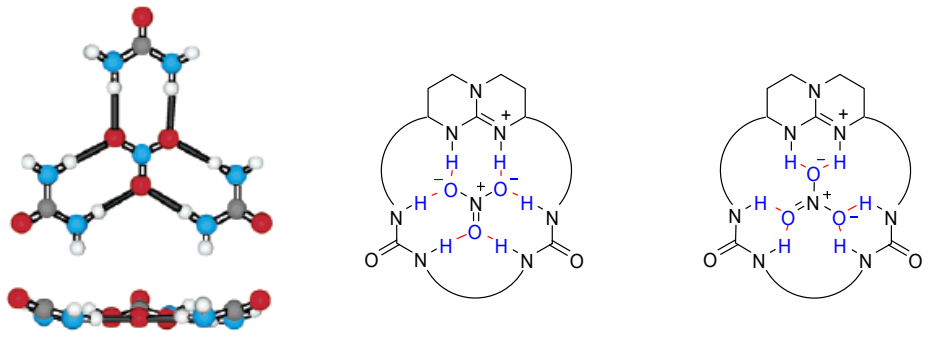

a) b) c)

Fig 4. Top and side views of optimized geometries (B3LYP) for representative examples of (a) 3:1 urea: NO_3^- complexes[24] and (b) & (c) binding mode for nitrate inclusion.

The nitrate anion offers six optimal sites for proton location according to the number and orientation of the lone pair orbitals, but so far no structural evidence on an example fulfilling this feature has been reported. This represents in fact a key point in host design because spacing between hydrogen bond donors is different for linear and non-linear host-guest bonds. We present herein a nitrate recognition example for the first binding mode.

We have prepared a number of hosts endowed with multiple hydrogen bond donors. Common to these designs is a bicyclic guanidinium scaffold and two ureas attached through an *ortho*-aminothiophenylene aromatic spacer in such a way that the distance between the nitrogen atoms of ureas and guanidines is ideal (five atoms apart)

[26] Linton, B. R.; Goodman, M. S.; Fan, E.; van Arman, S. A.; Hamilton, A. D. *J. Org. Chem.* **2001**, *66*, 7313-7319.

for the hydrogen donors to complement both the *syn* and *anti* lone pairs of each oxygen.[27] Moreover, the aromatic ring increases the acidity of the urea and brings pre-organization to the overall structure (Fig 5). Also, the sulfur atoms should contribute to shape the host by chelation while not introducing a too electronegative atom that would cause electronic repulsion with the guest.[28] The second urea NH's, located seven atoms away from guanidinium NH, would interact with each lone pair of the third oxygen atom guest. Besides, among the receptors reported so far, use of macrocycles take the advantage of affording a pre-organized scaffold with convergent binding groups to include the guest by size and shape complementarities.[29] Macrocycles of different cavity sizes (four, five and six carbon atoms spacers) and rigidities (xylylene based host) have been synthesized for nitrate inclusion. Regarding the linker between the ureas in the macrocycles, a five carbon chain should be again the best choice for nitrate encapsulation.

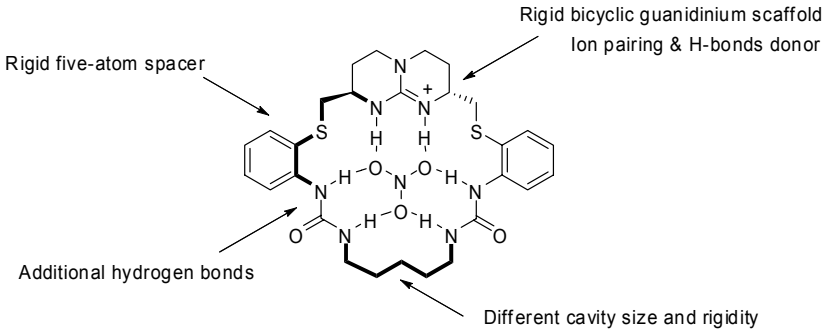

Fig 5. Design of guanidinium receptors for nitrate recognition.

[27] González, S.; Peláez, R.; Sanz, F.; Jiménez, M. B.; Morán, J. R.; Caballero, M. C. *Org. Lett.* **2006**, *21*, 4679-4683.

[28] Kavallieratos, K.; Bertao, C. M.; Crabtree, R. H. *J. Org. Chem.* **1999**, **64**, 1675-1683.

[29] Choi, K.; Hamilton, A. D. *Coord. Chem. Rev.* **2003**, *240*, 101-110.

2.2 Guanidinium Receptors Synthesis

The synthesis of all receptors was performed starting from the chiral bicyclic guanidinium salt **1**, obtained on a multi-gram scale following the methodology described by Schmidtchen and improved in our group. **1** was obtained bearing two different protecting groups in 9 steps with a 46% overall yield. Chirality comes from the two starting amino acids: thus, D-Asn and D-Met produce the (*R*,*R*) enantiomer. In chapter 2 and 3, *meso* (*R*,*S*) guanidinium salt was also used (produced from D-Asn and L-Met).[30]

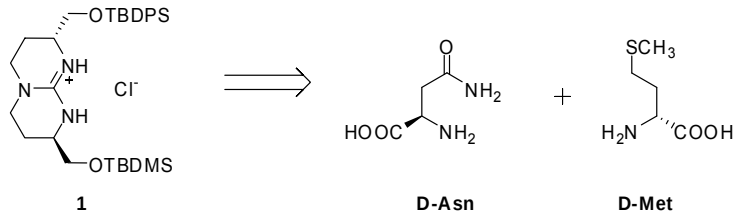

1 **D-Asn** **D-Met**

Scheme 1. Chiral bicyclic guanidinium precursors.

The synthesis of the guanidinium-based receptors is described in Scheme 2. First, deprotection of both silyl groups (OTBDPS and OTBDMS) was easily achieved with HCl to give **2** in 97% yield. Then, guanidinium dichloride **3** was obtained by reaction with thionyl chloride in a 95% yield. Compound **3** was then transformed into diamine **4** (hexafluorophosphate salt) with 2-aminothiophenol in a 60% yield. Hexafluorophosphate, as a less competitive anion than chloride, was selected as the counterion for all receptors. Linear amide receptor **5** was obtained with good yield (70%) using PyBOP as the coupling reagent. For compounds **6**, **7**, **9** and **10**, the appropriate isocyanate or diisocyanate reagents were employed. Thus, butylisocyanate reacted with **4** in a sealed vessel in CH_2Cl_2 to form **6** in 85% yield, whereas hosts **7**, **9** and **10** resulted in 40% and 15% respectively, under more dilute conditions, using 1,4-diisocyanatobutane, 1,6-diisocyanatohexane and *m*-xylylene diisocyanate respectively. For the synthesis of macrocycle **8** a different procedure was followed, since 1,5-diisocyanatopentane is not commercially available. We used a bis-imidazolide

[30] Synthesis of (*R*,*S*)-**1** was performed by Delphine Guichard.

intermediate (**11**, 95% yield), prepared from 1,5-diaminopentane and 1,1'-carbonyldiimidazole (CDI) which was reacted afterwards with **4** in dry MeOH to obtain **8** though in a modest 8% yield.

Aromatic receptor **10** was obtained also in a rather modest yield (15%) as compared to alkyl analogues **7** and **9** using the same procedure. We then studied the cyclization of receptor **10** from **4** with PF_6^-, Cl^- or AcO^- as counterions. *In situ* macrocyclization was followed with analytical HPLC during 24 hours but did not show any templating effect. Since HPLC monitoring did not show substantial amounts of impurities, the rather low yield was attributed to the purification process (column chromatography).

Receptors **5-10** were soluble in solvents like CH_2Cl_2, CH_3CN or MeOH. For NMR and ITC determinations, aprotic CH_3CN of medium polarity seemed thus appropriate to avoid solvent interferences.

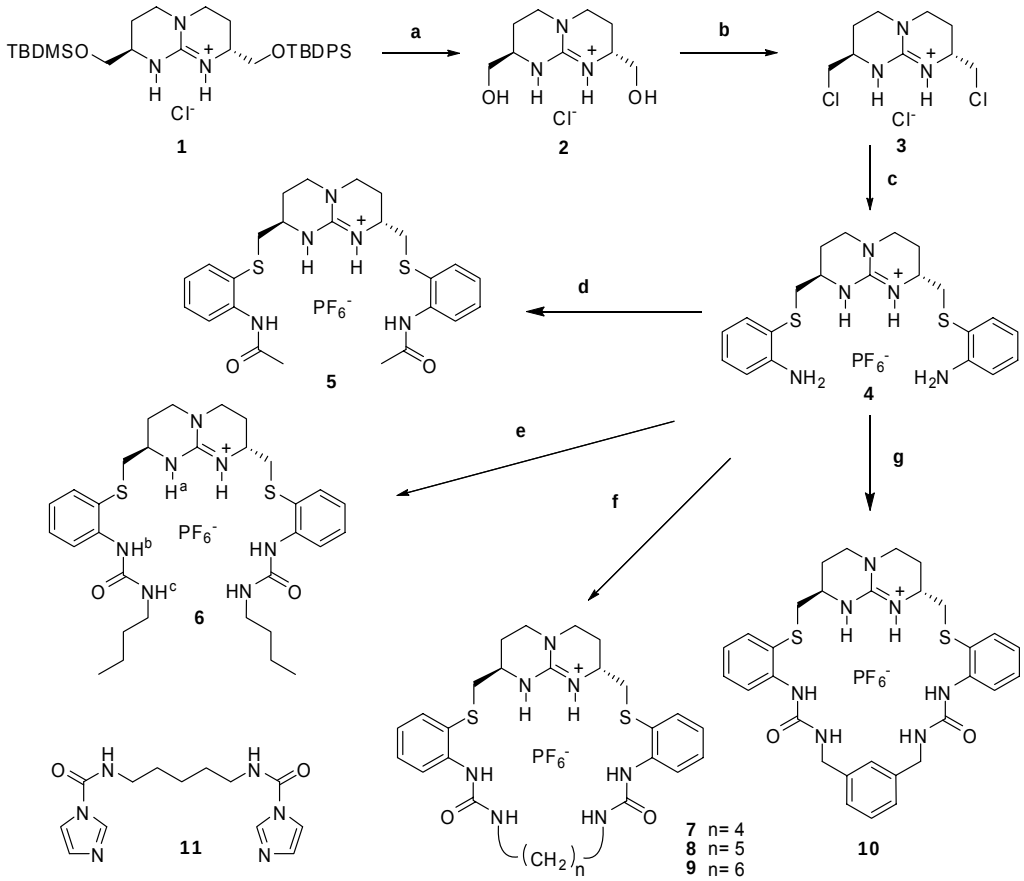

Reagents and conditions: **a**) 3N HCl-CH_3CN (1:2), 2 days (97%). **b**) $SOCl_2$, reflux, 4 h (95%). **c**) 2-aminothiophenol, NaI, KO*t*Bu, acetone, room temperature, 4 h, then 0.1M NH_4PF_6 (60%). **d**) Acetic acid, NMM, PyBOP, HOBt, CH_2Cl_2, 1 day (75%). **e**) butylisocyanate, dry CH_2Cl_2, 45ºC, overnight, then 0.1M NH_4PF_6 (85%). **f**) butyl diisocyanate (for **7** and **9**), CH_2Cl_2, 45 ºC, overnight, then 0.1M NH_4PF_6 and Dowex ion-exchange resin (PF_6^-) (40%) or 1,5-diaminopentane (for **8**), CDI, 80 ºC, 2 days, then Dowex ion-exchange resin (PF_6^-) (8%). **g**) m-xylylene diisocyanate, dry CH_2Cl_2, 45 ºC, overnight, then 0.1M NH_4PF_6 and Dowex ion-exchange resin (PF_6^-) (15%).

Scheme 2. Synthesis of receptors ***5-10****.*

2.3 Binding Study

2.3.1 ^{1}H-NMR and ITC Titrations with Nitrate

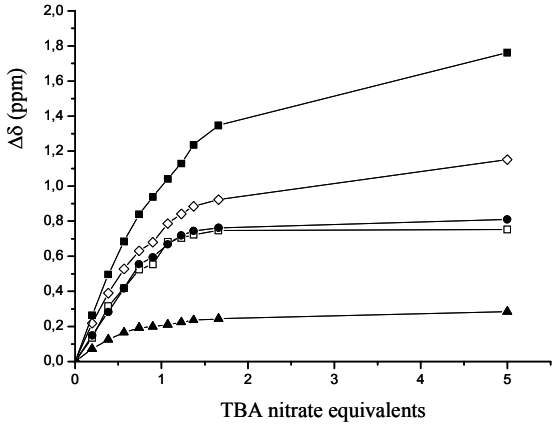

*Fig 6. ^{1}H-NMR titration curves of receptors **1** and **4-7** with TBA nitrate in CD_3CN at 25ºC; **1** (■), **4** (◊), **5** (▲), **6** (□) and **7** (●), (Δδ of guanidinium NH).*

^{1}H-NMR titrations with tetrabutylammonium (TBA) nitrate and hosts **1** and **4-10** were performed in CD_3CN. As the amount of guest added increased, guanidinium NH chemical shifts suffer a downfield shift for all receptors ($\Delta\delta$ = 1.80 ppm for **1**, 1.05 ppm for **4**, 0.80 ppm for both **6** and **7**, 0.25 ppm for **5**, Fig 6). Saturation was observed for hosts **5**, **6** and **7** after addition of 1,5 equivalents of nitrate, whereas a control with starting compound **1** and diamine **4** did not show saturation even after addition of 10 equivalents, accounting for the importance of additional hydrogen bonds (ureas) to stabilize the complex. Indeed, K_a values increased almost by two orders of magnitude from 373 M^{-1} for **1** to 9.94 × 10^3 M^{-1} for **7** (Table 2). Different binding modes or complementarities are thus involved depending on the number of H-bonds provided by the receptor (amine, amide and urea). In all cases, the amine and guanidinium NH protons, the amide and guanidinium NH protons, or the urea and guanidinium NH protons involved in hydrogen bonding, showed strong downfield shifts upon addition of guest (see Fig 7 for a titration between **7** and TBA nitrate). Diamine receptor **4** gave an association constant higher than the starting material **1**

due to the better pre-organization of the system as well as to the participation of two additional weak hydrogen bond (amine NH_2). In amide host **5** the association was enhanced by the presence of two strong hydrogen bonds. However **6** showed a K_a twice higher, revealing that the urea receptor allows a full hydrogen bonding to all oxygen lone pairs of the guest. Even if the overall binding value was not that highly shifted from amide to urea receptor (revealing once again that amide hydrogen bonds are strong enough to reach saturation), urea receptors are more suitable due to their array of hydrogen bonds. Macrocyclic effect was evidenced by the twice bigger binding constant for **7** than for the linear analogue **6**. Guest inclusion inside the cavity of **7** could not be detected by ^{1}H-NMR, as no significant chemical shifts of the protons of the four carbon atom spacer were observed, revealing no significant rearrangement of the macrocycle scaffold to complex nitrate.

The titrations corresponds to a widely studied[31] anion exchange process of the type:

$$\text{Host}\,(PF_6^-) + TBA^+\,(NO_3^-) \rightleftharpoons \text{Host}\,(NO_3^-) + TBA^+\,(PF_6^-)$$

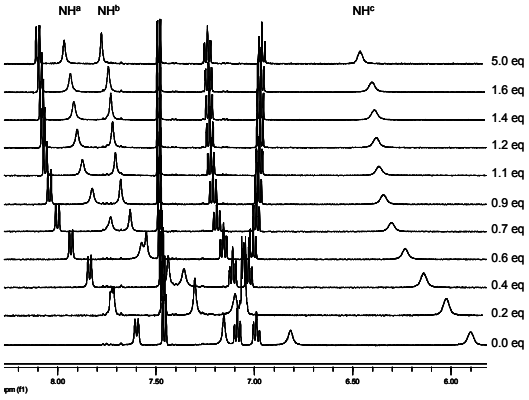

*Fig 7. ^{1}H-NMR titration between **7** and TBA nitrate in CD_3CN.*

Single liquid-liquid extraction experiments between **6** (in CH_2Cl_2) and $NaNO_3$ (in a saturated water solution) confirmed the strong host-guest interaction, since one

[31] a) Berger, M.; Schmidtchen, F. P. *J. Am. Chem. Soc.*, **1999**, *121*, 9986-9993. b) Haj-Zaroubi, M.; Mitzel, N. W.; Schmidtchen, F. P. *Angew. Chem. Int. Ed.*, **2002**, *41*, 104-107.

full equivalent of nitrate was extracted and a 1:1 stoichiometry was observed in the organic layer.[32] An important characteristic of lipophilic bicyclic guanidinium receptors is thus the property of extracting anions from aqueous media to organic phases through single liquid-liquid extraction or membrane transport such anions from a feeding to a receiving phase.[33]

No accurate NMR binding data could be obtained for **8**, **9** and **10** due to *in situ* crystallization at the concentrations required by the titrations. To overcome this problem, we used isothermal titration calorimetry (ITC) as an alternative tool for measuring binding constants and thermodynamic parameters at much lower concentrations.[34] The binding isotherms are characteristic of exothermic 1:1 complexes and values for K_a are in good agreement with those previously obtained by ^{1}H-NMR (Table 2).

Increase of cavity size results in a binding affinity enhancement between the macrcocycle and nitrate. Hence, macrocycle **9** showed an increase of two orders of magnitude respect to **4** and presents one of the highest K_a values reported so far for nitrate. Increase of cavity rigidity afforded however a weaker association between the host and the guest. Indeed, macrocycle **10** afforded the lowest K_a among all macrocycles synthezised and even lower than linear receptor **6**. Likely, the aromatic xylylene proton pointing inward the cavity prevents the guest to get inside and difficults the correct orientation of the urea NHs towards the nitrate oxygen atoms.

---

[32] Single liquid-liquid extractions were performed by shaking for 5 min a 1 mg ml^{-1} host solution in CH_2Cl_2 and a saturated $NaNO_3$ solution in water. The organic phase was isolated after centrifugation, the solvent removed (without addition of any drying agent) and the ^{1}H-NMR spectrum was recorded. As for other related guanidinium receptors and carriers,[33] spectra of both aqueous and organic phases confirmed the complete partition of the host into the organic phase in a 1:1 host-guest stoichiometry.

[33] Breccia, P.; Van Gool, M.; Pérez-Fernández, R.; Martín-Santamaría, S.; Gago, F.; Prados, P.; de Mendoza, J. *J. Am. Chem. Soc.* **2003**, *125*, 8270-8284.

[34] a) Ladbury, J. E.; Chowdhry, B. Z. *Chem. Biol.* **1996**, *3*, 791-801. b) Wadsö, I. *Chem. Soc. Rev.* **1997**, 79-86.

	1	**4**	**5**	**6**	**7**	**8**	**9**	**10**
$K_a(10^3)^a$	0.37	0.99	2.26	5.50	9.94	*c*	*c*	*c*
$K_a(10^3)^b$	0.19	0.35	1.14	5.83	7.26	15.2	73.7	3.90
ΔH	-1.90	-2.00	-8.25	-3.74	-1.07	-3.02	-3.48	-0.97
ΔS	4.14	5.06	-12.8	4.72	14.2	9.16	10.8	13.2
ΔG	-3.15	-3.53	-4.37	-5.17	-5.37	-5.79	-6.76	-4.97

[a] Determined by ^{1}H-NMR titrations in CD_3CN at 298 K. [b] Determined by ITC titrations in CH_3CN at 303 K. [c] Not determined because of *in situ* crystallization. ΔH and ΔG in kcal mol^{-1}, ΔS in cal mol^{-1} K^{-1}.

*Table 2. Association constants (M^{-1}) and thermodynamic parameters for the binding of **1** and **4-10** with TBA nitrate.*

The binding isotherms reveal that binding of nitrate with **7** and **10** is governed mainly by entropy (Fig 8, see also Table 2), whereas for the other receptors, especially the macrocycles, both enthalpic and entropic contributions play a significant role. As the cavity size of the macrocycle increases, the enthalpy is enhanced whereas entropy diminishes. The strong negative enthalpy values indicate that hydrogen bonding with the oxygen acceptors of the guest is almost optimal, the entropic contribution being likely due to solvent release from the cavity upon guest inclusion, and increases as the conformational freedom of the macrocycle is reduced. In macrocycles **7** and **10** the cavity is too small for optimal inclusion. Indeed, the hydrogen bonding is weaker, and the smaller enthalpy change is compensated by a stronger entropy contribution.

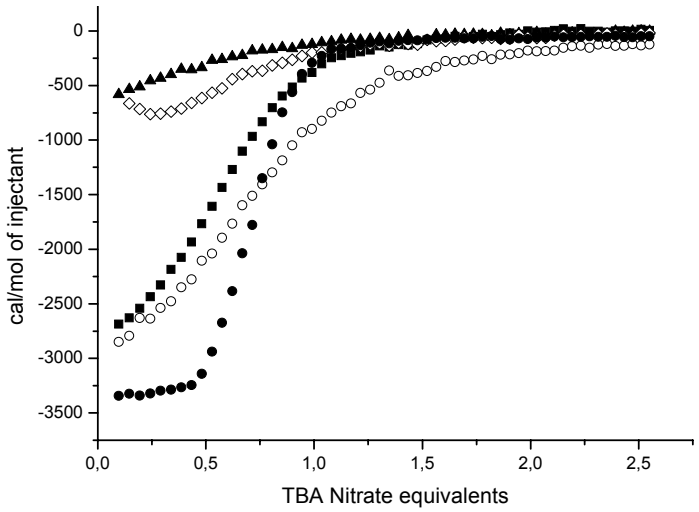

*Fig 8. ITC titration curves of receptors **6-10** with TBA nitrate in CD_3CN at 303K; **6** (○), **7** (◊), **8** (■), **9** (●) and **10** (▲).*

2.3.2 ITC Binding Titrations and Selectivity

In view of the good binding properties shown by the receptors towards nitrate, we then determined by ITC their selectivity with respect to spherical anions of different size and basicity such as bromide or chloride, as well as to carboxylates like the small acetate and aromatic benzoate. Starting compound **1** and the guanidinium diamine salt **4** are strongly selective towards carboxylates (NO_3^- < Br^- < Cl^- < AcO^- ≃ BzO^-, Table 3). For host **4** the increase is one order of magnitude relative to **1** for spherical guests Br^- and Cl^-. The presence of weak additional amine H-bonds causes the enthalpic contribution to multiply by a factor of two. Similarly, in the presence of additional urea H-bonds, receptor **6** shows an increase of one order of magnitude of binding in both cases and the association becomes both enthalpically and entropically driven. Interestingly, receptor **6** prefers Cl^- to AcO^- (NO_3^- < Br^- < AcO^- < Cl^- ≃ BzO^-, Table 3). From **1** to **6**, additional stabilization by H-bonds causes enthalpy enhancement and entropy diminishment for all anions tested although overall carboxylate binding stays almost similar ($K_a \approx 10^5$ M^{-1}). The K_a obtained for **1** with benzoate salt is consistent with the previously reported result measured by Schmidtchen with a similar diprotected bicyclic guanidinium salt.[31b] Authors

emphasize on the risk of discussing binding exclusively in terms of free energy when similar values for different hosts with additional interaction sites are observed. For instance, an ITC titration between **6** and acetate shows a complexation mainly enthalpically driven whereas both thermodynamic factors play a significant role in association between **1** and the guest.

For Br^- and Cl^-, the binding constants with macrocycles **7**, **8** and **9** are similar and one order of magnitude higher than for the linear urea receptor **6**. The macrocyclic effect is significant for the spherical anions resulting in a change in selectivity order ($NO_3^- < Br^- \simeq AcO^- < BzO^- \simeq Cl^-$). As pointed out for additional H-bonds, increasing the cavity size by changing the bridge between the ureas from 4 to 6 carbon atoms has a similar influence for Br^- and Cl^-. Enthalpy indeed increases (flexibility allows a better adjustment to optimize the host-guest interactions) whereas entropy decreases due to a larger cavity and higher conformational freedom. Among the compounds tested, receptor **9** is indeed the best macrocycle for anion complexation and the first guanidinium-based receptor reported so far that is selective toward Cl^- over AcO^-. Assuming a strong entropic contribution with benzoate, receptor **9** behaves as with chloride ($K_a \approx 10^6$ M^{-1} with similar enthalpy and entropy contributions).

ITC titrations between macrocycle **10** and anion salts gave an association one order of magnitude lower than macrocycles **7**, **8** and **9** (as pointed out previously, the aromatic hydrogen atom pointing inwards the cavity may contribute to diminish guest association). Unlike **7-9**, spherical anions present a strong entropically driven binding. As guest size increases from Cl^- to Br^-, entropy increases but enthalpy decreases accounting for the better accommodation of a smaller guest in the small cavity of the more rigid macrocycle. With acetate, receptor **10** shows the smallest association whereas for benzoate the binding is similar to receptors **1** and **4**. A strong entropic contribution allows benzoate to keep macrocycles selective towards aromatic carboxylates over smaller acetate.

	1	**4**	**6**	**7**	**8**	**9**	**10**
Br^-							
$K_a(10^3)^a$	0.63	3.40	55.9	118	156	238	37.8
ΔH	-0.59	-1.05	-3.32	-1.72	-2.41	-3.85	-0.47
ΔS	10.8	12.7	10.8	17.2	15.8	11.9	19.4
ΔG	-3.86	-4.89	-6.59	-6.93	-7.20	-7.45	-6.35
Cl^-							
$K_a(10^3)^a$	5.85	14.7	781	2240	1040	2090	305
ΔH	-0.84	-2.20	-4.92	-4.05	-4.96	-5.38	-2.09
ΔS	14.4	11.8	10.7	15.7	11.2	11.2	18.2
ΔG	-5.21	-5.77	-8.16	-8.81	-8.35	-8.77	-7.60
AcO^-							
$K_a(10^3)^a$	128	268	306	147	222	322	30.5
ΔH	-3.97	-4.33	-6.97	-4.89	-3.49	-6.95	-5.47
ΔS	10.2	10.5	2.06	7.49	12.9	2.25	2.46
ΔG	-7.06	-7.51	-7.59	-7.16	-7.39	-7.63	-6.22
BzO^-							
$K_a(10^3)^a$	202	176	895	1970	1340	1360	122
ΔH	-3.92	-4.78	-5.99	-5.40	-5.40	-5.65	-5.27
ΔS	11.3	8.21	7.43	10.9	10.2	9.39	6.00
ΔG	-7.35	-7.27	-8.24	-8.70	-8.49	-8.49	-7.04

[a] Determined by ITC titrations in CH_3CN. ΔH and ΔG in kcal mol^{-1}, ΔS in cal mol^{-1} K^{-1}.

*Table 3. Thermodynamic parameters evaluated by ITC of TBA bromide, chloride, acetate and benzoate complexes of **1**, **4** and **6-10**.*

Comparing receptors, the binding order is as follows: **1** < **4** < **10** < **6** < **7** ≃ **8** ≃ **9**. The thermodynamic factors variation between **7**, **8** and **9** is not as important as for NO_3^- and does not allow prediction of guest inclusion. Spherically shaped chloride accommodates well in all the macrocycles series but seems to be penalized in the most rigid scaffolds where rearrangement of the macrocycle structure is more difficult. Bromide displays association with macrocycles with binding constants one order of

magnitude lower than chloride due to its larger size. Acetate association is constant for all receptors ($K_a = 10^5$ M^{-1}) whereas benzoate is favored in the case of macrocycle ($K_a = 10^6$ M^{-1}). For acetate, linear host **6** gives an enthalpically favored complexation as for host **9** (as the cavity size increases, the macrocycle structure recovers enough flexibility to behave like the linear receptor).

Selectivity was calculated for receptors **1**, **4**, **6-10** by the ratios ($\Delta G X^-/\Delta G X'^-$) (Table 4). For all anions, (ΔG $X^-/\Delta G$ NO_3^-) decreases from starting material **1** to the best receptor **9** accounting for the weak coordinative abilities of this anion (Fig 9). Additional H-bonds, pre-organized scaffolds as well as appropriate cavity sizes suit indeed better for NO_3^- than for the other anions. Receptor **9** gives the most favorable ratio for nitrate, and this ratio dramatically decreases from **1** to **9** for carboxylate anions [(i.e. ΔG $AcO^-/\Delta G$ NO_3^-) from 2.24 to 1.13 and (ΔG $BzO^-/\Delta G$ NO_3^-) from 2.36 to 1.26]. Selectivity between spherical anions Br^- and Cl^- stays almost similar for every receptor (from 1.35 down to 1.16) whereas for acetate ((ΔG $Cl^-/\Delta G$ AcO^-) is inverted from 0.73 up to 1.15). Protected bicyclic guanidinium salt **1** is selective for acetate whereas macrocycle **9** is chloride-selective. This selectivity is less significant with benzoate since this guest is favored by a strongest entropic contribution. Therefore, among small anions macrocycle **9** is chloride-selective and among carboxylate anions it is benzoate-selective.

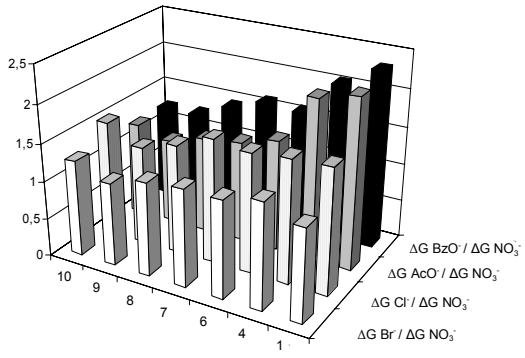

*Fig 9. Nitrate selectivity compared to Br^-, Cl^-, AcO^- and BzO^- for receptors **1**, **4**, **6-10**.*

	1	**4**	**6**	**7**	**8**	**9**	**10**
Cl^-/NO_3^-	1.65	1.63	1.58	1.64	1.44	1.30	1.52
Br^-/ NO_3^-	1.22	1.39	1.28	1.29	1.24	1.10	1.27
AcO^-/ NO_3^-	2.24	2.12	1.47	1.33	1.27	1.13	1.25
BzO^-/ NO_3^-	2.33	2.06	1.59	1.62	1.46	1.26	1.41
Cl^-/ Br^-	1.35	1.18	1.24	1.27	1.16	1.18	1.20
Cl^-/ AcO^-	0.73	0.77	1.07	1.23	1.13	1.15	1.22
Cl^-/ BzO^-	0.71	0.79	0.99	1.01	0.98	1.03	1.08
Br^-/ AcO^-	0.55	0.65	0.87	0.97	0.97	0.98	1.02
Br^-/ BzO^-	0.53	0.67	0.80	0.80	0.85	0.88	0.90
AcO^-/ BzO^-	0.96	1.04	0.92	0.82	0.87	0.90	0.88

*Table 4. Selectivity ratios for receptors **1**, **4** and **6-10** ($\Delta G\, X^-/\Delta G\, X'^-$).*

Receptor **1** is strongly carboxylate-selective due to the large pK_a difference between the guanidinium function and carboxylic acids. Macrocycle **9** presents a totally different association in which spherical binding mode is favored over p*K*a difference (Fig 10). As some additional hydrogen bonds through urea groups and pre-organization are incorporated in the host structure, the association is thus not governed by pK_a differences anymore. Anions of suitable shape and size complementarities with the host overcome their weak binding affinity compared to carboxylate anion with guanidinium-based receptors.

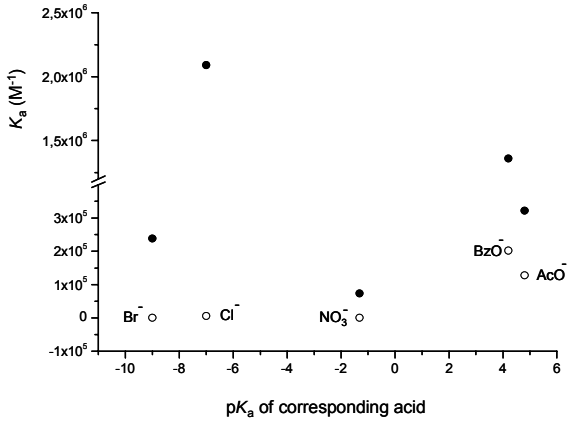

*Fig 10. Binding constants K_a of TBA salts with **1** (○) and **9** (●) versus pK_a of the corresponding acid.*

2.3.3 ITC titrations with TBA Fluoride

Macrocycle **9** is selective toward Cl^- over Br^- with association constants differing by one order of magnitude. This prompted us to measure the binding with smaller anion F^-. Fluoride is a much smaller anion but much more basic (Table 1). So far, few data have been reported about guanidinium-fluoride interactions.[35]

ITC titration between **9** and TBAF was performed and the binding isotherm presents a different stoichiometry than for chloride (Fig 11). Indeed, the titration curve fits well for a 1:3 complex: 3 F^- atoms are complexed by one receptor molecule through six hydrogen bonds. A first fast exothermic complexation is observed until one equivalent of guest is added, then a second one until two equivalents, followed by a last slow endothermic interaction.

A control ITC titration was achieved between linear receptor **6** and TBAF in order to evaluate the influence of the macrocycle in the observed host-guest stoichiometry (Fig 11). A similar binding isotherm was however obtained as for **9** accounting for a 1:3 stoichiometry. The urea functions of macrocycle **9** could easily fold to bind one F^- atom each, in addition to a guanidinium-fluoride interaction, whereas the flexibility of the open chain receptor **6** should allow it to wrap around

[35] Bonner, O. D. *J. Phys. Chem.* **1977**, *81*, 2247-2249.

only one anion. Guest sizes might be responsible for such different binding mode with the receptors and halides, as it has been previously reported for receptors bearing two urea moieties.[36]

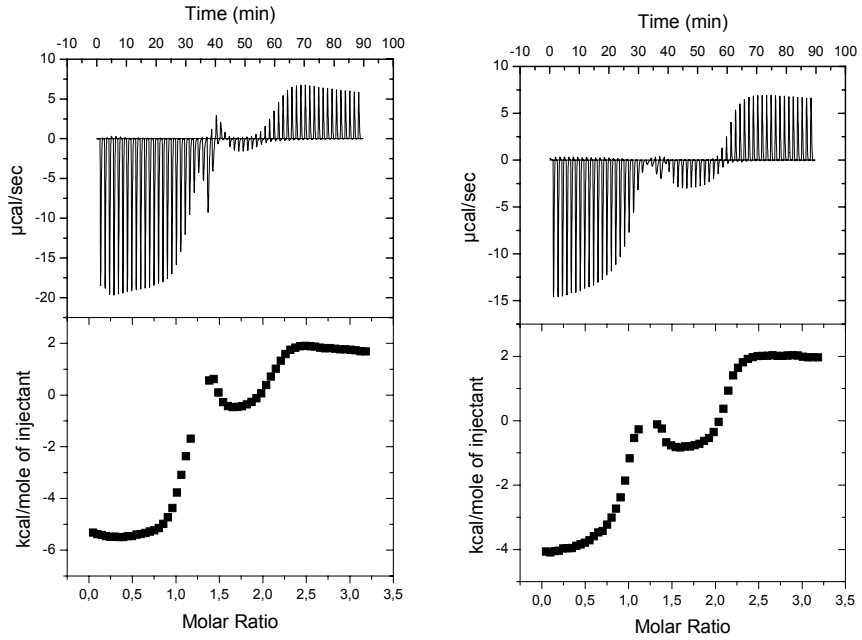

a) b)

Fig 11. ITC titrations between TBAF and receptor a) ***6*** *& b)* ***9*** *in CH_3CN at 303 K.*

Thermodynamic parameters from ITC titrations between TBAF and **6** or **9** are comparable (Table 5). The first association is both enthalpically and entropically driven giving rise to the first guanidinium-fluoride complex because of the ion pair and the superior binding strength of the guanidinium moiety over urea (Fig 12).

The entropic factor is higher for the macrocycle than for the open structure due to the release of solvent molecule. The second interaction is mainly entropically driven resulting from the formation of one urea-fluoride association. Among the several different possible equilibria two are depicted in Fig 12. Binding mode (a) is quite difficult to achieve without severe repulsions with both guest anions. As this complexation is mainly entropically driven, due to strong release of solvent molecules

[36] Kim, K. S.; Kim, H.-S. *Tetrahedron* **2005**, *61*, 12366-12370.

and much less influenced by electrostatic interactions, model (b) would better fit to this complexation (strong rearrangement of the receptor scaffold in order to bind a new guest). Eventually, the last complexation is the result of folding the second arm of the receptor (again mainly entropically driven and even enthalpically disfavored).

Because of the different stoichiometries data cannot be compared with Cl^- and establish selectivity.

	1:1	1:2	1:3
6			
K_a [a]	2.52 x 10^5	2.35 x 10^5	106
ΔH	-5.44	-0.60	80.47
ΔS	6.75	22.6	289
ΔG	-7.48	-7.45	-2.82
9			
K_a [a]	4.93 x 10^5	1.76 x 10^7	1.93 x 10^4
ΔH	-4.24	-0.84	2.20
ΔS	12.0	30.4	26.9
ΔG	-7.88	-10.05	-5.95

[a] K_a in M^{-1}, ΔH and ΔG in kcal mol^{-1}, ΔS in cal mol^{-1} K^{-1}.

*Table 5. Thermodynamic parameters between TBAF and **6** and **9** evaluated by ITC.*

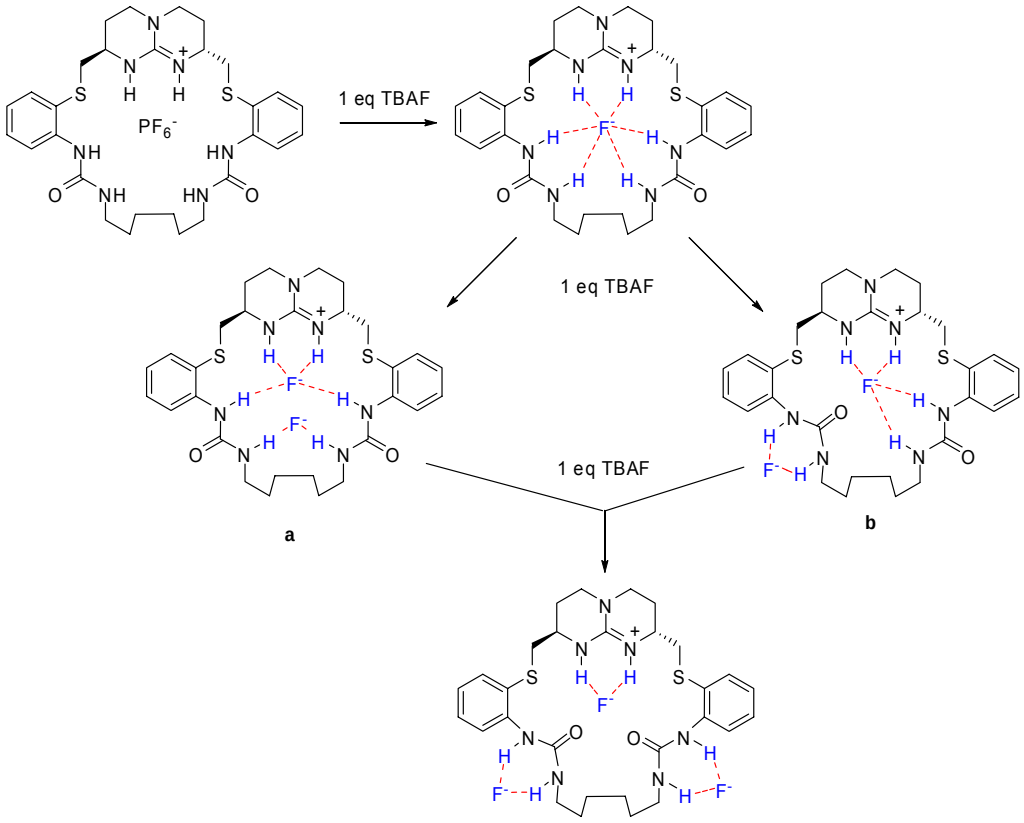

Fig 12. Binding steps for a 1:3 complex of ***9*** *$(F^-)_3$.*

2.3.4 Influence of Stereochemistry of the Guanidinium Scaffold on Anion Association

Measuring the influence of the guanidinium scaffold stereochemistry under the molecular recognition of anions appears to be relevant in a rational design approach to improve the receptor for nitrate. In achiral (*R*,*S*) guanidinium receptors both arms are oriented towards the same side of the bicyclic main plane, which might favor the binding of planar anions such as nitrate (Fig 4a, side view of optimized geometry representing a planar arrangement of the 3:1 urea:nitrate complex). The best receptor for nitrate **9** and macrocycle **10** with a rigid aromatic xylylene spacer were thus proposed as optimal candidates in this respect (Chart 1). (*R*,*S*)-**9** and (*R*,*S*)-**10** were

synthesized similarly as their (*R*,*R*) analogue with similar yields, and ITC titrations were performed (K_a and thermodynamic parameters are shown in Table 6).

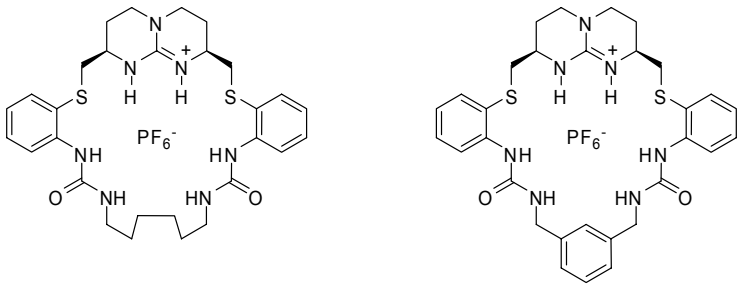

(*R*,*S*)-**9** (*R*,*S*)-**10**

*Chart 1. Achiral receptor (R,S)-**9** and (R,S)-**10**.*

Binding constants are similar for spherical anions Cl^- and Br^- and also for the sterically unhindered carboxylate AcO^- whereas the association diminishes for aromatic benzoate. Nitrate behaves different with a K_a decreasing for (*R*,*S*)-**9** and increasing for (*R*,*S*)-**10**. A common trend is an enthalpy increase and an entropy decrease when going from the (*R*,*R*) to the (*R*,*S*) series. There is a general compensation between both contributions governing the overall association. The enhancement of enthalpy may be due to a better orientation of the NH towards the guest leading therefore to a better match between complexing partners. Electrostatic interactions are thus favored for the *meso* form (*R*,*S*) with respect to the chiral (*R*,*R*) one. Consequently, the release of solvent molecules participates less as the pre-organization of the receptor is more effective. The well balanced association between enthalpy and entropy observed for (*R*,*R*)-**9** translates into a mainly enthalpy driven process for (*R*,*S*)-**9**. This remark is not that obvious for (*R*,*S*)-**10** as the binding is strongly entropic for NO_3^-, Cl^- and Br^-.

(*R*,*S*)-**9** is selective toward Cl^- (one order of magnitude higher than Br^-, AcO^- and BzO^- and two orders of magnitude higher than NO_3^-) whereas (*R*,*S*)-**10** does not differentiate so strongly between these anions ($12.1 < K_a < 232 \times 10^3\ M^{-1}$).

	NO_3^-	Cl^-	Br^-	AcO^-	BzO^-
(*R*,*S*)-**9**					
$K_a(10^3)^a$	17.4	2040	176	371	201
ΔH	- 3.43	- 7.89	-4.15	- 7.23	-7.75
ΔS	8.08	2.83	10.3	1.62	-1.39
ΔG	-5.88	- 8.75	-7.27	- 7.71	-7.33
(*R*,*S*)-**10**					
$K_a(10^3)^a$	12.1	232	98.7	69.7	42.7
ΔH	- 1.89	- 3.32	-1.69	- 5.47	-6.33
ΔS	12.4	13.6	17.3	4.07	0.31
ΔG	-5.65	- 7.44	-6.94	- 6.71	-6.42

[a] K_a in M^{-1}, ΔH and ΔG in kcal mol^{-1}, ΔS in cal mol^{-1} K^{-1}.

*Table 6. Thermodynamic parameters evaluated by ITC titrations of TBA salts complexation by (R,S)-**9** and (R,S)-**10**.*

(*R*,*S*)-**10** affords one of the best binding constants so far measured for NO_3^- with the urea receptors (**10** < **6** < **7** < (*R*, *S*)-**10** ≈ **8** ≈ (*R*, *S*)-**9** < **9**). Nevertheless the association remains strongly entropically driven. Predictably, nitrate inclusion will take place when the association is both enthalpically and entropically driven, and even when the enthalpic factor is much higher, such as for (*R*,*S*)-**10**, it seems that the cavity is still too tight to allow the guest properly fitting inside.

2.3.5 Liquid-Liquid Extractions: CH-π Interactions

Among macrocycles, **10** presents the weakest binding although it possesses the advantage of an aromatic surface linking the two urea functions. Aromatic host-guest interactions would afford a new stabilization for carboxylates. Single liquid-liquid extraction between **10** (in CH_2Cl_2) and sodium benzoate (NaBzO, saturated water solution) allows formation of the 1:1 complex. However, control experiments with the **6** (BzO^-) and **10** (AcO^-) did not show any significant shift of the aromatic protons of both host and guest. Indeed, a NOESY experiment confirmed the absence of contact between the aromatic protons of host and guest. Nevertheless, the guest methyl group

of **10** (AcO^-) was shifted upfield up to 1.56 ppm. Control experiments between **8** (with a five carbon atoms spacer instead of a xylylene) or **6** (linear host) and NaAcO did not show any shift of the acetate methyl group (δ (CH_3) = 2.05 ppm for **8** and **6**, Fig 13). This significant 0.5 ppm upfield shift accounts for CH-π interactions between the acetate methyl group and the aromatic ring of the xylylene spacer **10** (Fig 14). A similar shift was obtained for (*R*,*S*)-**10** in ^{1}H-NMR.

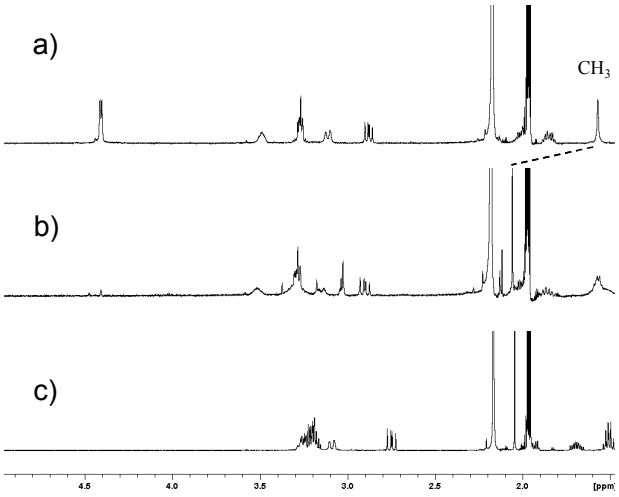

*Fig 13. ^{1}H-NMR spectra of the organic phase after liquid-liquid extractions between aqueous NaAcO and an organic solution of a) **10**, b) **8** and c) **6**.*

Although CH-π interactions can be considered as weak hydrogen bonds, various examples in chemistry and biology have been reported, using experimental methods such as X-Ray, NMR and IR.[37] However, the enthalpic contribution of one CH-π interaction is rather small compared to other H-bonds (about 1 kcal mol^{-1}).[38] From ITC titration, acetate gives the lowest binding with receptor **10**. These interactions are indeed not detectable in a quantitative manner compared to the strong interaction between the carboxylate and the NHs of the host.

[37] Castellano, R. K.; Diederich, F.; Meyer, E. A. *Angew. Chem. Int. Ed.* **2003**, *42*, 1210-1250.

[38] Nishio, M.; Umezawa, Y.; Hirota, M.; Takeushi, Y *Tetrahedron* **1995**, *51*, 8665-8701.

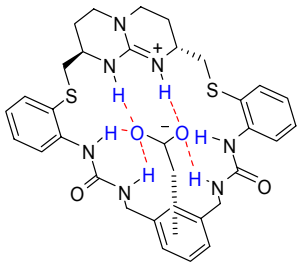

Fig 14. CH-π interactions between the acetate CH_3 and the xylylene spacer.

In order to further study these CH-π interactions, single extractions with NaC_2H_5COO and NaC_3H_7COO have been performed. Figure 15 shows again an upfield shift for CH_2 and CH_3 of the guest when complexed with **10** (0.43 ppm upfield shift of δ (CH_2) and 0.25 ppm upfield shift of δ (CH_3)). This interaction diminishes from acetate to propionate but still remains significant. Besides, the shift is higher for CH_2 than for CH_3 because of the closer environment and lower flexibility.

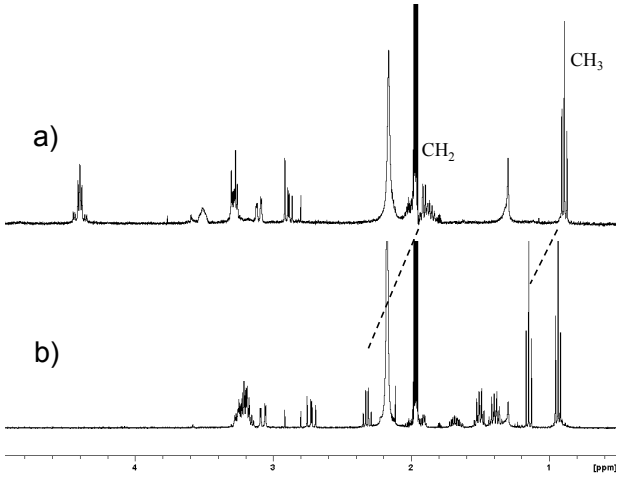

*Fig 15. ^{1}H-NMR spectra of the organic phase after liquid-liquid extractions between aqueous NaC_2H_5COO ($0.1M^{-1}$) and an organic solution of a) **10** and b) **6**.*

Extractions with butyrate gave a similar pattern (0.28 ppm upfield shift of δ (CH_2), 0.17 ppm upfield shift of δ (CH_2) and 0.10 ppm upfield shift of δ (CH_3), Fig

16). Therefore, as the carbon chain of the carboxylate increases, the magnitude of the shift decreases (accounting for the higher flexibility of the guest).

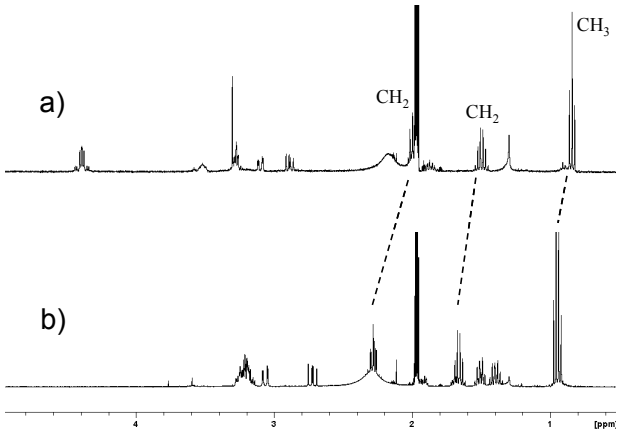

Fig 16. ^{1}H-NMR spectra of the organic phase after liquid-liquid extractions between aqueous NaC_3H_7COO ($0.1M^{-1}$) and an organic solution of a) ***10*** *and b)* ***6****.*

2.4 X-Ray Solid State Structures

7 (NO_3^-) was able to crystallize in CH_3CN and its X-ray solid state structure was resolved (an ORTEP plot is shown in Fig 17). The asymmetric unit contains three independent molecules partially disordered (molecules A/B/C). The NO_3^- anion and the NHs of the hydrogen bond donor functions are not affected by this disorder (atoms C2, C3, C4 and C25, C26, C27 involved). The three refined independent molecules differ broadly in their conformations, but have a similar arrangement of the NO_3^- in the center of the molecule. In all cases, NO_3^- is bound to both NH_{guan} and to one of the NH_{urea} of only one of the urea functions (distances in Table 8). The second urea is pointing away from the macrocycle cavity forming intermolecular hydrogen bonds with another urea (NH···O=C hydrogen bonding network). As a result, the macrocycle is strongly folded with the guest pointing to the centre of the molecule with only two of the oxygen atoms located in this central area. The third oxygen is pointing to neighboring molecules achieving additional intermolecular contacts. Besides, for

molecule B, the distance between one oxygen atom of the urea group and a sulfur atom is shorter than the sum of their Van der Waals radii (S2B···O2B: 3.07 Å).

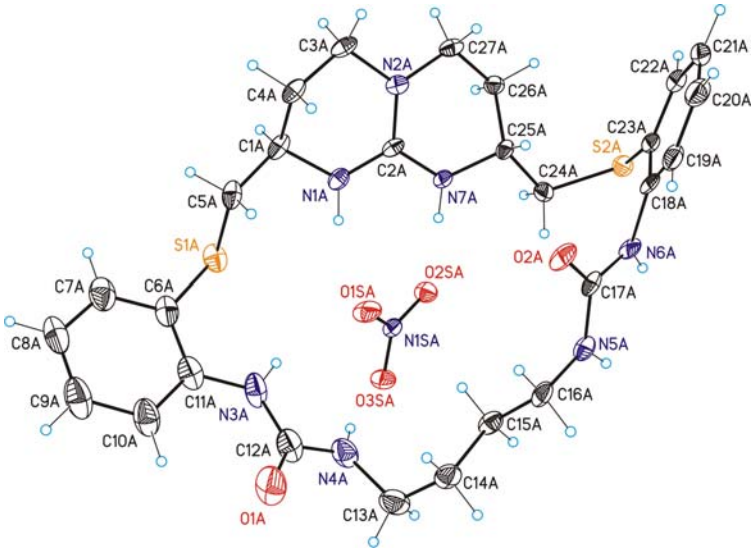

Fig 17. ORTEP plot of the X-ray structure of ***7*** *(NO_3^-).*

8 (NO_3^-) single crystals were obtained in CH_2Cl_2 and the crystal cell contains two independent molecules (A/B) (A is shown as an ORTEP plot in Fig 18). In both cases the guest forms hydrogen bonds with the two NH_{guan} and the four NH_{urea} (see distances in Table 8). Considering the plane formed by the nitrogen atoms of the bicyclic guanidinium scaffold, the guest is not exactly oriented in a planar arrangement to it. Indeed, nitrate forms a dihedral angle of 24.0º/9.7º (A/B) with respect to this latter. The pentane chain in between the urea moieties is folded out of the defined plane, and one of the guest oxygen atoms (O3S) is thus pointing outside the ring. On the other hand, there is a dihedral angle formed between planes (N1, N2, N7) and urea groups in opposite directions (21º/27º (A) and 12º/35º (B)). Again, distances between one of the oxygen atoms of the anion and one of the sulfur atoms, is shorter than the sum of their Van der Waals radii (S2···O2: 3.221/3.218 Å). Moreover, no relevant intermolecular interactions can be observed in this structure.

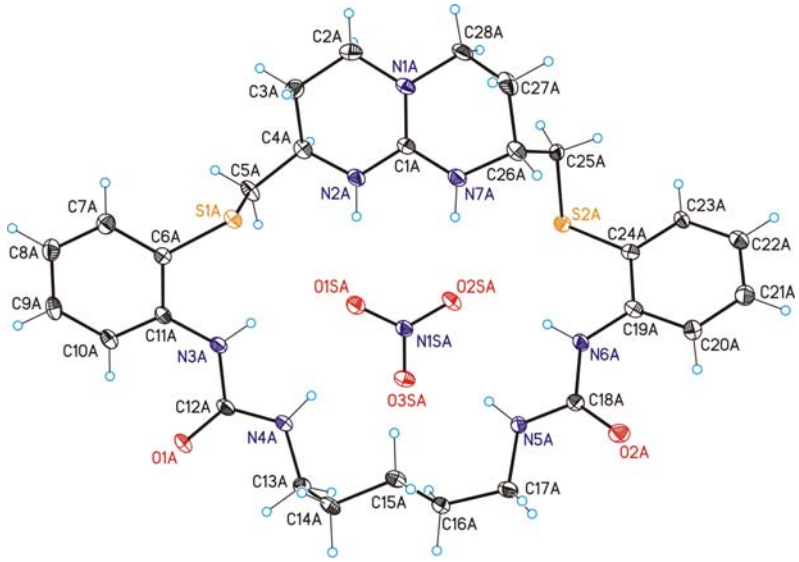

*Fig 18. ORTEP plot of the X-ray structure of **8** (NO_3^-).*

9 (NO_3^-) crystallizes in DMF and only one independent molecule was observed for the hexylene chain between the urea functions (C13-C18), although disordered in two orientations (Fig 19). The nitrate is not located at the same plane as the guanidinium (defined by the N1, N2, and N7 atoms), so NH_{guan} are not pointing to the centre of the macrocyclic ring. A dihedral angle of 49.2º is indeed formed between the (N1, N2, N7) plane and the guest. In contrast, the planes of the aromatic rings form a dihedral angle of only 17.4º. Despite the observed angle between (N1, N2, N7) and the nitrate, NH_{guan} are forming hydrogen bonds with two oxygen atoms of the anion (distances in Table 8). Both NH_{urea} bind also to the guest's oxygen atoms with O3S located between N4 and N5. Due to the different orientation of the bicyclic guanidinium fragment compared to the two previous molecules, the measured dihedral angles between the urea groups and the (N1, N2, N7) plane are not comparable (64.3º/26.2º). Therefore, the dihedral angles formed between the urea plane and the nitrate were considered (24.9º/34.2º). Again, the distances between the sulfur atoms and respectively one of the oxygen atoms of the anion, are shorter than the sum of their Van der Waals radii (S2···O2: 3.220/3.305 Å).

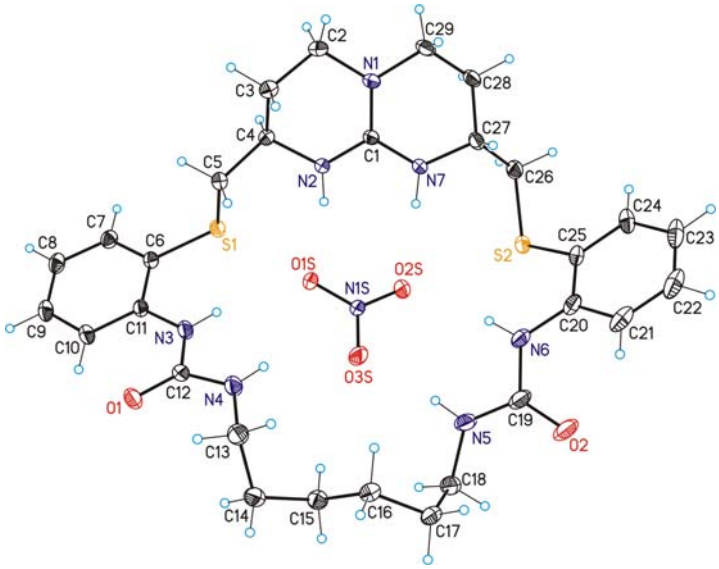

Fig 19. ORTEP plot of the X-ray structure of **9** *(NO_3^-).*

(*R*,*S*)-**9** (NO_3^-) structure was also resolved by single crystal X-ray diffraction (Fig 20). The macrocycle shows a more pronounced folding arrangement than in the case of (*R*,*R*)-**9** (NO_3^-). The guest presents a more distorted arrangement with two oxygen atoms (O2S, O3S) pointing towards one urea group (N6, N5) and the third oxygen atom (O1S) pointing away from the ring. The shortest hydrogen bonds are between (O2S) and (N7) and (N6) (Table 8). The dihedral angle between (N1, N2, N7) and the nitrate is 45.7º [similar to the (*R*,*R*)-**9** (NO_3^-) one]. However, the angle is more pronounced due to an axial rotation of the anion with O1S out of the macrocycle. The dihedral angles (26.5º, 15.0º) between (N1, N2, N7) and the urea groups are lower than for (*R*,*R*)-**9** (NO_3^-). Interestingly, the sulfur atoms do not show any relevant interactions with the nitrate oxygens.

The comparison of the long range contacts in (*R*,*S*)-**9** gives shorter distances (NO_3^-) between the sulfur atoms and between N3 and N6. The distance between N4 and N5 is slightly longer (Table 7).

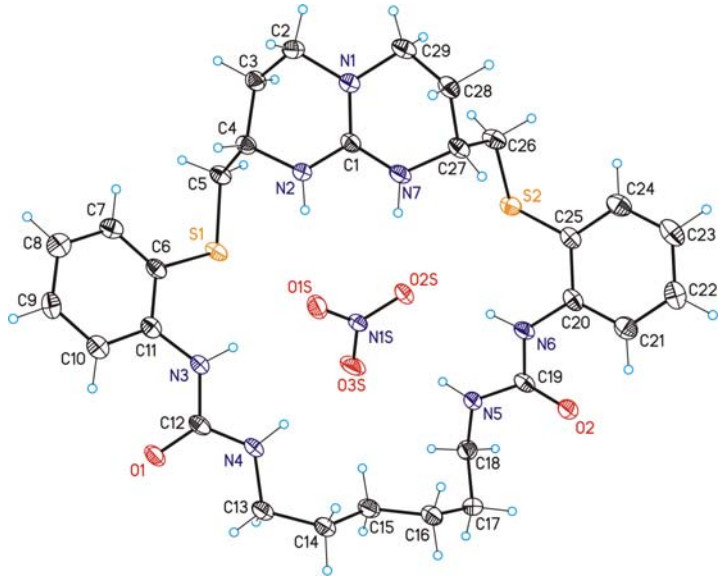

*Fig 20. ORTEP plot of the X-ray structure of (R,S)-**9** (NO_3^-).*

Distances (Å)	(*R*,*R*)-**9** (NO_3^-).	(*R*,*S*)-**9** (NO_3^-).
S1···S2	7.37	7.06
N3···N6	7.73	7.59
N4···N5	5.39	5.46

*Table 7. Long range contacts in (R,R)-**9** (NO_3^-) and (R,S)-**9** (NO_3^-).*

Most remarkably, in the solid state, all four nitrate salts behave as predicted and anticipated from the studies in solution. Salt **7** displays a distorted structure, with one urea twisted away from the cavity (hydrogen-bonded to an urea from another macrocycle) and only three well identified hydrogen bonds with the nitrate. On the contrary, in **8,** (*R*,*R*)-**9** and (*R*,*S*)-**9** the nitrate nicely fits inside the cavity surrounded by six NH donors. Moreover, the X-ray structure shows that the guest oxygen atoms form two hydrogen bonds with the host in such a way that each oxygen shares its lone pairs with single NH donors from different functions (ureas or guanidinium). This orientation

(Fig. 4b) is preferred in the solid state over the alternative one where the oxygen lone pairs bind to NH donors from the same function (Fig. 4c). These results are thus in good agreement with energy data from the computational study by Hay *et al.*[24] Optimized geometry of a 3:1 urea:NO_3^- complex shows a planar arrangement (Fig 4a) whereas none of the 3:1 guanidinium/urea: NO_3^- complexes reported in the literature display a planar arrangement (Fig 21).

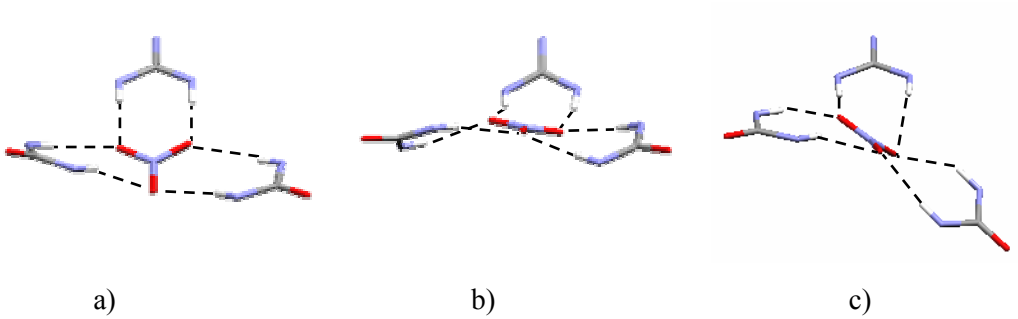

a) b) c)

Fig 21. Binding motifs from the X-ray structures of a) ***8*** *(NO_3^-) b) (R,R)-****9*** *(NO_3^-) and c) (R,S)-****9*** *(NO_3^-).*

It is tempting to compare association constants in solution to structures in the solid state, so hydrogen bonds distances were therefore evaluated (Table 8). The weakest K_a is given by macrocycle **7** which has only three well identified H-bonds with the nitrate. **8** and (*R*,*S*)-**9** give a similar association constant with nitrate whereas for (*R*,*R*)-**9** this value is multiplied by a factor of 5. **8** possesses two strong H-bonds between the guanidinium moiety and the oxygen guest (2.03 and 2.04 Å) but the four other ones from the two urea moieties (> 2.20 Å) are much weaker. In contrast, (*R*,*R*)-**9** provides five strong H-bonds (< 2.20 Å) and only one weak one (2.32 Å). Eventually, (*R*,*S*)-**9** gives three strong and three weak H-bonds. In all cases, the H-bonds between the NH_{guan} and the oxygens guest are strong (< 2.10 Å), with the exception of one in (*R*,*S*)-**9** (2.31 Å) due to the orientation of one oxygen guest away from the cavity (Fig 21). Even though the orientation is not optimal in all cases (no planar arrangements), the hydrogen bond distances in the solid state provide interesting details on the different binding properties of each receptor.

Distance in Å[a]	**7**	**8**	**9**	*(R,S)-**9***
O1S···N2 (O1S···H2)	2.887 (2.04)	2.864 (2.04)	2.842 (2.02)	3.135 (2.31)
O2S···N7 (O2S···H7)	2.884 (2.03)	2.883 (2.03)	2.951 (2.10)	2.917 (2.07)
O1S···N3 (O1S···H3)	2.904 (2.05)	3.205 (2.39)	3.114 (2.32)	3.089 (2.35)
O3S···N4 (O3S···H4)	3.082 (2.30)	3.036 (2.28)	2.932 (2.18)	3.047 (2.17)
O3S···N5 (O3S···H5)		3.067 (2.23)	2.903 (2.07)	3.095 (2.26)
O2S···N6 (O2S···H6)		3.074 (2.23)	3.048 (2.19)	2.961 (2.10)

[a] The observed distances to hydrogen atoms are uncorrected.

*Table 8. Intramolecular contacts of **7**, **8**, **9** and (R,S)-**9** with NO_3^-.*

4 (Cl^-) crystallizes in an ideal C_2 symmetry with two independent half molecules (A/B) in the crystal packing (Fig 22). The independent molecules differ in the orientation of the aromatic rings and the conformation of the central bicyclic guanidinium. The guest is located on the C_2-axis centered between the hydrogen atoms of N2 forming hydrogen bonds (Table 9). On the other hand, the guest is stabilized by one of the hydrogen atoms of each N3. Moreover, chloride has intermolecular contacts to different hydrogen atoms of neighboring molecules: the shortest one is with the N3-atoms (Cl1A···N3B2: 3.705, Cl1A···H3BE 2.83 Å, uncorrected). Considering the plane (C1, N1, N2) and the plane formed by N3 and the hydrogen atoms linked to it a dihedral angle of 41.8º/49.1º (A/B) results. This dihedral angle indicates that one hydrogen atom of N3 is pointing to the central Cl^- whereas the second one is pointing to the guest of a neighboring molecule.

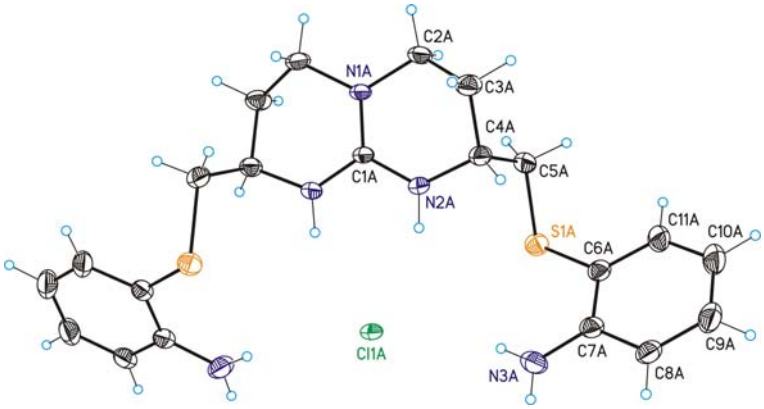

*Fig 22. ORTEP plot of the X-ray structure of **4** (Cl^-).*

The X-ray solid structure of **9** (Cl^-) also shows an ideal C_2 axis of symmetry with a half molecule in the crystal packing (Fig 23). As for **4** (Cl^-), the guest is located on the C_2-axis, centered between the six NHs and forming hydrogen bonds with all of them (Table 9). It can be observed that the atoms N1, C1, N2, Cl2, C15 and their symmetry equivalents are located on a same plane with the C_2-axis crossing at the center of the bond formed by C15/C15' and on the atoms C1 and N1. In contrast, the urea group formed by the nitrogen atoms N3 and N4 is out of the described plane, pointing to the guest rotated to each side. Considering the described plane and the plane formed by one of the ureas, a dihedral angle of 41.14º can be measured. In agreement with the ideal C_2 symmetry observed, the identical urea groups at the same molecule are rotated to opposite directions. Only weak intermolecular interactions can be observed.

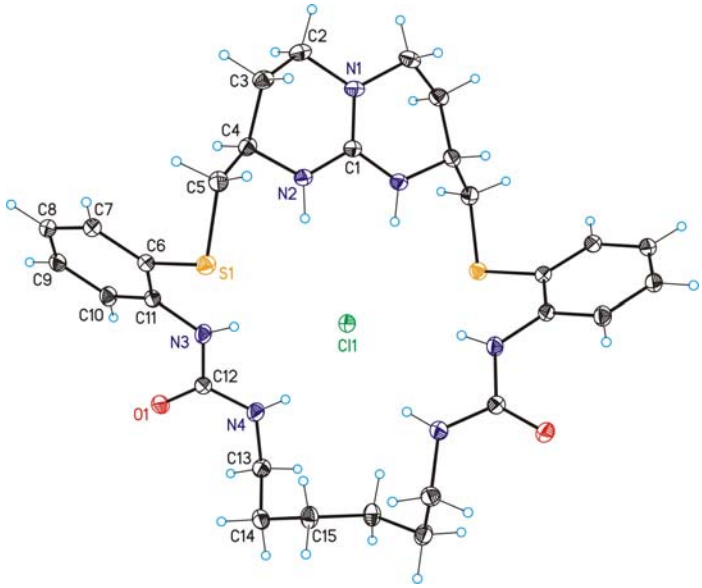

Fig 23. ORTEP plot of the X-ray structure of ***9*** *(Cl^-).*

Distance in Å	**4**	**9**
Cl1···N2 (Cl1···H2)	3.220 (2.40)	3.405 (2.54)
Cl1···N3 (Cl1···H3)	3.495 (2.73)	3.344 (2.57)
Cl1···N4 (Cl1···H4)		3.301 (2.51)

[a] The observed distances to hydrogen atoms are uncorrected.

Table 9. Intramolecular contacts of ***4*** *and* ***9*** *with Cl^-.*

8 (AcO^-) crystallizes in two independent molecules (A/B) (Fig 24). Both macrocycles crystallize with the two anion oxygen atoms pointing to the center of the molecules and the methyl group having a weak intermolecular interaction with the carbonyl function of neighboring urea groups (C···N: 3.137/3.231 Å). The NH_{guan} protons point to the acetate oxygen atoms forming well oriented hydrogen bonds (Table 10). The H-bonds are slightly shorter than the one previously reported from a

bicyclic guanidinium-based receptor acetate complex (2.850 Å).[39] Moreover, the NH_{urea} point to one of the oxygen atoms of the anion. Considering the plane (N1, N2, N7) and the one formed by the urea groups, dihedral angles of 17.5º/23.4º (molecule A) and 3.2º/29.2º (molecule B) in opposite directions are observed. Particularly interesting is the orientation of the hydrogen bonds O2···N5 and O1···N4 (Fig 25). Whereas the NH_{guan} and the NH_{urea} (located five atoms away) are forming hydrogen bonds with the lone pairs of the oxygen guest, N4 and N5 contact to the π-system of the acetate guest. These NH-π H-bonds have been previously reported by Anslyn et *al.*[8,40] These additional hydrogen bonds enhance stabilization of the complex (this is consistent with the enthalpic factor increase observed by ITC).

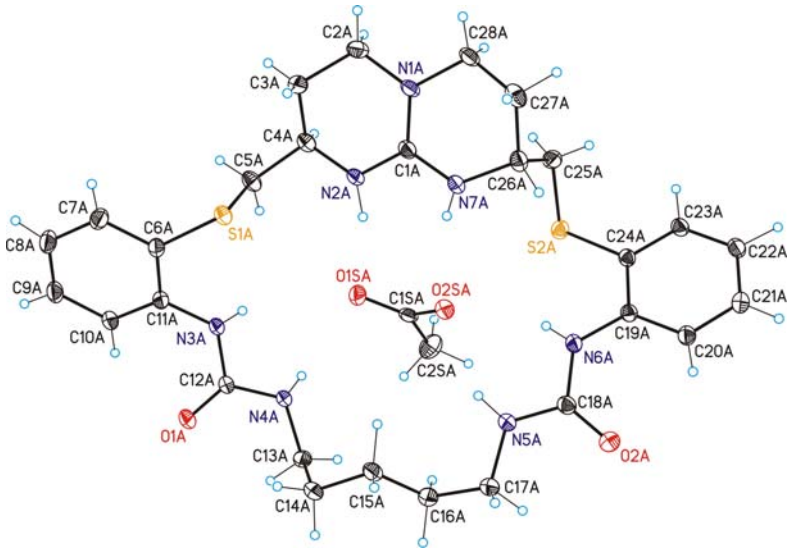

Fig 24. ORTEP plot of the X-ray structure of ***8*** *(AcO^-).*

[39] Müller, G.; Riede, J.; Schmidtchen, F. P. *Angew. Chem. Int. Ed. Engl.* **1988**, *27*, 1516-1518.
[40] Snowden, T. S.; Bisson, A. P.; Anslyn, E. V. *J. Am. Chem. Soc.* **1999**, *121,* 6324-6325.

Distance in Å[a]	**8**
O1S···N2 (O1S···H2)	2.812 (1.93)
O2S···N7 (O2S···H7)	2.806 (2.10)
O1S···N3 (O1S···H3)	3.273 (2.65)
O1S···N4 (O1S···H4)	2.928 (2.24)
O2S···N5 (O2S···H5)	2.858 (2.06)
O2S···N6 (O2S···H6)	2.947 (2.28)

[a] The observed distances to hydrogen atoms are uncorrected.

*Table 10. Intramolecular contacts of **8** with AcO^-.*

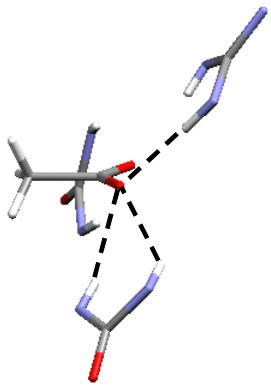

*Fig 25. Binding motif from the X-ray structure of **8** (AcO^-) (only three H-bonds are shown for clarity).*

Comparison of these X-ray structures revealed that the guanidinium-based receptors are flexible enough to adapt themselves to the guest structures. Spherical anions of suitable size (such as Cl^-) fit nicely inside the macrocycle cavity of **9** with six strong hydrogen bonds wrapping around the anion. The structural results in the solid state are in good agreement with those obtained in solution (ITC titrations) and by the theoretical model studies by Hay et *al*. (Fig 26).

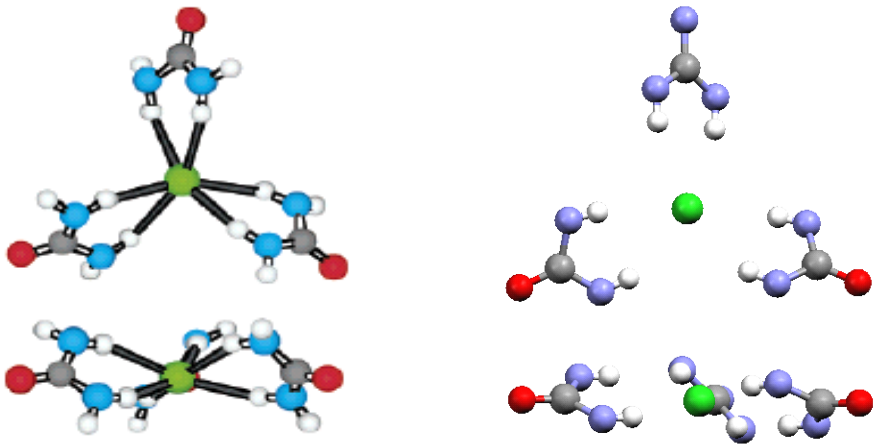

a) b)

*Fig 26. a) Top and side views of B3LYP optimized geometries for representative examples of 3:1 urea: Cl^- complexes[24] and b)binding motif from the X-ray structure of (R,R)-**9** (Cl^-).*

2.5 Conclusions

In this chapter, guanidinium-based macrocycles have been synthesized and their binding ability measured. **8**, **9** and (*R*,*S*)-**9** shown an enthalpy driven nitrate complexation with all six lone pairs of the guest complemented by well oriented hydrogen bond donors from the guanidinium and urea moieties. All complexes show a 1:1 stoichiometry apart from small and strongly basic F^- which comes up with a 1:3 complex. Selective complexation towards a spherical guest of suitable size (Cl^-) was shown in solution. Additionally, macrocycle **10** with an aromatic moiety displays CH-π interactions towards different carboxylate anions. Solid state X-ray crystal structures have been resolved for several complexes showing the inclusion of nitrate, chloride and acetate inside the cavity of the macrocyclic guanidinium receptors, and shedding light on the structural parameters governing the binding.

2.6 Experimental section

2.6.1 General Procedures

Synthesis. All commercially available reagents (Aldrich, Fluka, Acros, NovaBiochem, Panreac) were used without any further purification. The solvents were dried and distilled as described in the literature.[41] Unless specified, all reactions were performed under nitrogen.

Chromatography. Thin layer chromatography (TLC) was performed on aluminum supported Alugram Sil G/UV254 (Macherey-Nagel). Column chromatography was done using silica gel by SDS (chromagel 60 ACC, 40-60 mm) following the procedure described by W. C. Still.[42] HPLC chromatograms were recorded on an Agilent Technologies Serie 1100, with UV-diode array, fluorescence and light scattering detectors. The template synthesis experiments was followed by analytical HPLC (column: Synergi Max-RP 4 μm, 4.6 x 250 mm, UV-detector with λ = 254 nm). The mobile phase consisted of (ACN (0.1% TFA) / H_2O (0.1% TFA), gradient: 35-100% ACN (0.1%TFA) in 15 minutes. The solvents were provided by Scharlau (HPLC gradient grade).

Analysis. Melting points were measured with a Büchi B-540 apparatus. The optical rotations $[\alpha]^{25}_{D}$ were determined on a Perkin-Elmer 241 MC polarimeter using a cell (1 dm) at 20°C (Na_D 589 nm). ^{1}H-NMR and ^{13}C-NMR spectra were recorded on a Bruker Avance 500 Ultrashield NMR spectrometer (^{1}H: 500 MHz; ^{13}C: 125 MHz) using the residual solvent peak as internal standard. Mass spectra were recorded on a Waters LCT Premier spectrometer using ESI technique or on a Bruker Autoflex MALDI-TOF instrument. Elemental analyses were performed on Perkin-Elmer 2400 CHN and 2400 CHNS apparatus.

ITC titrations. ITC titrations were performed using an isothermal titration Microcal VP-ITC microcalorimeter. All measurements were performed at 303K. The host solution was filled into the cell of the ITC instrument and guest solutions were added with the syringe. In each case control experiments with dilution of guest in the

[41] Perrin, D. D.; Perrin, D. R.; Amarego, W. L. F. *Purification of Laboratory Chemicals, 2nd Edition*, Pergamon Press Ltd, Oxford, **1980**.

[42] Still, W. C.; Kahn, M.; Mitra, A. *J. Org. Chem.* **1978**, *43*, 2923-2925.

solvent were performed and were found to be negligible. Concentration of host (PF_6^-) (c = 1 mM in acetonitrile) and concentration of guest, tetrabutylammonium salts (c = 14 mM in acetonitrile) were similar for all titrations. The volume of injection was 5 μL and the stirring speed was 300 rpm. The solvent was previously degassed by sonication during 15 minutes. Titrations were made 3 times in order to be reproducible. Analysis and curve fitting was done using the software Origin 7. Samples were weighted with a microbalance Mettler Toledo MX5. Tetrabutylammonium salts of acetate, benzoate and chloride were weighted in a dry box.

^{1}H NMR titrations. Two standard solutions were prepared in acetonitrile, one for the receptor ($[R]_0$ = 0.005 M) and the other one for the substrate and receptor together ([S] = 0.05M and $[R]_0$ = 0.005M). All titrations were performed using an initial amount of 0.5 mL of receptor solution. To this solution was added an increasing amount of standard solution of the substrate (0.4 mL, 0 up to 5 equivalents). After each addition, the ^{1}H NMR spectra was registered and the variation in the chemical shifts of the protons affected were plotted against guest concentration. Association constants were obtained by using a non-linear square curve fitting program.[43]

2.6.2 Synthesis

(2*R*,8*R*)-2,8-Bis-(hydroxymethyl)-3,4,6,7,8,9-hexahydro-2*H*-pyrimido-[1,2-*a*]-pyrimidin-1-ium chloride (2).

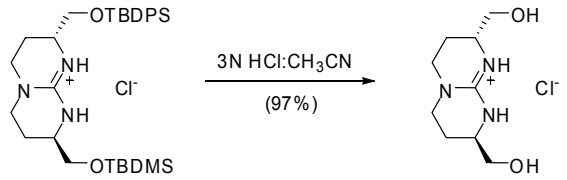

1 2

Procedure

A solution of **1** (3 g, 5.10 mmol) in 3 N HCl/CH_3CN (1:2, 75 mL) was stirred at room temperature for 2 days. The solvent was removed and the resulting crude dissolved in H_2O (50 mL) and washed with CH_2Cl_2 (4 × 50 mL). The aqueous phase was

[43] http://www.shef.ac.uk/uni/projects/smc/software.html

evaporated under reduced pressure affording **2** (1.16 mg, 97%) as a white solid. Mp 178-180°C. $[\alpha]^{25}_{D}$ -64 (*c* = 0.5, H_2O). **^{1}H-NMR** (200 MHz, D_2O) δ 3.46 (m, 2H, CH_2O), 3.35 (m, 2H, CH_2O), 3.32 (m, 2H, CH_α), 3.26-3.13 (m, 4H, $CH_{2\gamma}$), 1.86-1.66 (m, 4H, $CH_{2\beta}$). **^{13}C-NMR** (50 MHz, D_2O) δ 151.2 (C_{guan}), 64.3 (CH_2O), 48.8 (CH_α), 45.0 ($CH_{2\gamma}$), 22.7 ($CH_{2\beta}$). **FAB/LSIMS** *m/z* 200.13 $[(M - Cl^-)^+$, 100%].

(2*R*,8*R*)-2,8-Bis-(chloromethyl)-3,4,6,7,8,9-hexahydro-2*H*-pyrimido-[1,2-*a*]-pyrimidin-1-ium chloride (3).

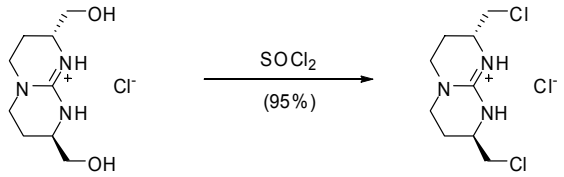

2 **3**

Procedure

A solution of compound **2** (350 mg, 1.48 mmol) in $SOCl_2$ (12 mL) was stirred at reflux for 4 h. The solvent was removed and the crude was purified by silica gel column chromatography eluting with a solvent mixture (CH_2Cl_2/MeOH, 96:4) afforded **3** (379 mg, 95%) as a light yellow solid. Mp 76-79°C. $[\alpha]^{25}_{D}$ -16 (*c* = 0.5, $CHCl_3$). **^{1}H-NMR** (500 MHz, $CDCl_3$) δ 8.57 (s, 2H, NH), 3.57-3.53 (m, 2H, CH_2Cl), 3.50-3.40 (m, 4H, CH_2Cl, CH_α), 3.28-3.25 (m, 4H, $CH_{2\gamma}$), 2.02-1.96 (m, 2H, $CH_{2\beta}$), 1.86-1.80 (m, 2H, $CH_{2\beta}$). **^{13}C-NMR** (125 MHz, $CDCl_3$) δ 151.3 (C_{guan}), 49.4 (CH_2Cl), 44.2 (CH_α), 45.6 ($CH_{2\gamma}$), 23.5 ($CH_{2\beta}$). **ESI-MS** *m/z* 236.1 $(M - Cl^-)^+$.

(2*R*,8*R*)-2,8-Bis-((2-aminophenylthio)methyl)-3,4,6,7,8,9-hexahydro-2*H*-pyrimido[1,2-*a*]pyrimidin-1-ium hexafluorophosphate (4).

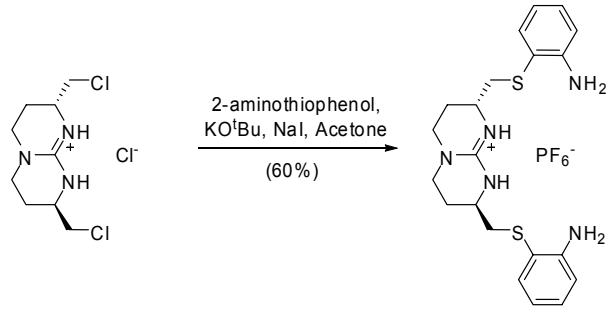

3 **4**

Procedure

To a solution of guanidinium salt **3** (200 mg, 0.73 mmol) in acetone (20 mL) were added NaI (440 mg, 2.93 mmol), potassium *tert*-butoxide (400 mg, 3.52 mmol) and 2-aminothiophenol (0.39 mL, 3.66 mmol). The mixture was then stirred for 4 hours. After evaporation of the solvent, the resulting solid was dissolved in CH_2Cl_2, washed with a 0.1N NH_4PF_6 solution and dried under Na_2SO_4. The organic layer was filtered over cotton and concentrated *in vacuo*. Purification by silica gel column chromatography (CH_2Cl_2/MeOH, 97:3) afforded **4** (190 mg, 60%) as a yellow pale solid. Mp 162-164ºC. $[\alpha]_D^{25}$ -105.76 (*c* = 0.5, $CHCl_3$). **^{1}H-NMR** (500 MHz, CD_3CN) δ 7.35 (dd, *J* = 1.5, 7.7 Hz, 2H, CH_{Ar}), 7.09 (td, *J* = 1.4, 7.5 Hz, 2H, CH_{Ar}), 6.81 (s, 2H, NH_{guan}), 6.67 (dd, *J* = 1.2, 7.9 Hz, 2H, CH_{Ar}), 6.61 (td, *J* = 1.1, 7.4 Hz, 2H, CH_{Ar}), 3.40 (m, 2H, CH_α), 3.24 (m, 10H, $CH_{2\gamma}$, CH_2S, NH_2), 2.80 (dd, *J* = 1.1, 7.4 Hz, 2H, CH_2S), 2.16-1.75 (m, 4H, $CH_{2\beta}$). **^{13}C-NMR** (CD_3CN, 125 MHz) δ 150.8 (C_{guan}), 148.8 (CN), 136.1, 130.3, 118.3, 115.6, 115.2 (CH_{Ar}, C_{Ar}), 47.9 (CH_α), 45.4 (CH_2S), 39.5 ($CH_{2\gamma}$), 25.6 ($CH_{2\beta}$). **ESI-MS** *m/z* 414.2 $(M\text{-}PF_6^-)^+$.

(2*R*,8*R*)-2,8-bis((2-acetamidophenylthio)methyl)-3,4,6,7,8,9-hexahydro-2*H*-pyrimido[1,2-*a*]pyrimidin-1-ium hexafluorophosphate (5).

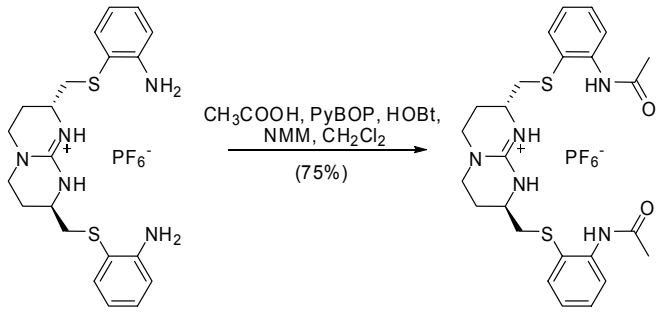

4 **5**

Procedure

To a solution of acetic acid (0.006 mL, 0.10 mmol) in CH_2Cl_2, were added *N*-methylmorpholine (NMM) (0.012 mL, 0.10 mmol), PyBOP (0.054 g, 0.10 mmol) and HOBt (catalityc amount) After stirring for 15 minutes, guanidinium salt **4** (0.03 g, 0.05 mmol) was added and the mixture was stirred overnight. After evaporation of the solvent, the resulting solid was dissolved in CH_2Cl_2, washed with a 0.1N NH_4PF_6 solution and dried under Na_2SO_4. The organic layer was filtered over cotton and concentrated *in vacuo*. Purification by silica gel column chromatography (CH_2Cl_2/MeOH, 98:2) afforded **5** (23 mg, 70%) as a yellow pale solid. Mp 167-169ºC. $[\alpha]_D^{25}$ -50.65 (*c* = 1, $CHCl_3$). **^{1}H-NMR** (500 MHz, CD_3CN) δ 8.42 (s, 2H, NH_{guan}), 7.74 (d, *J* = 7.3 Hz, 2H, CH_{Ar}), 7.51 (d, *J* = 7.8 Hz, 2H, CH_{Ar}), 7.28 (t, *J* = 7.1 Hz, 2H, CH_{Ar}), 7.19 (t, *J* = 7.0 Hz, 2H, CH_{Ar}), 7.02 (s, 2H, NH_{Amide}), 3.24-2.84 (m, 8H, $CH_{2\gamma}$, CH_α, CH_2S), 2.71 (dd, *J* = 1.2, 7.5 Hz, 2H, CH_2S), 1.92-1.78 (m, 4H, $CH_{2\beta}$), 1.77 (m, 6H, CH_3).**^{13}C-NMR** (CD_3CN, 125 MHz) δ 168.9 (CO), 149.8 (C_{guan}), 140.4, 130.2, 129.5, 124.1, 123.9, 116.2 (CH_{Ar}, C_{Ar}), 46.5 (CH_α), 45.3 (CH_2S), 39.2 ($CH_{2\gamma}$), 25.7 ($CH_{2\beta}$), 25.6 (CH_3). **ESI-MS** *m/z* 498.2 $(M\text{-}PF_6^-)^+$.

(2*R*,8*R*)-2,8-Bis-((2-(3-butylureido)phenylthio)methyl)-3,4,6,7,8,9-hexahydro-2*H*-pyrimido[1,2-*a*]pyrimidin-1-ium hexafluorophosphate (6).

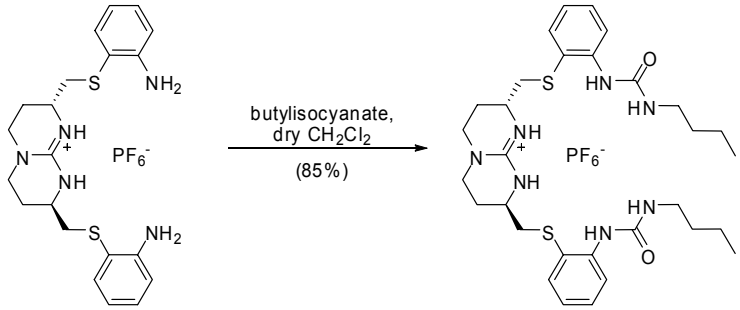

4 6

Procedure

To a solution of guanidinium salt **4** (100 mg, 0.18 mmol) in dry CH_2Cl_2 (2 mL) in a sealed tube was added butylisocyanate (45 μL, 0.39 mmol) under nitrogen atmosphere and the mixture was stirred overnight at 45ºC. After evaporation of the solvent, the resulting solid was dissolved in CH_2Cl_2, washed with a 0.1N NH_4PF_6 solution and dried under Na_2SO_4. The organic layer was filtered over cotton and concentrated *in vacuo*. Purification by silica gel column chromatography (CH_2Cl_2/MeOH, 98:2) afforded **6** (110 mg, 80%) as a yellow pale solid. Mp 169-171ºC. $[\alpha]_D^{25}$ -175.76 (*c* = 0.5, $CHCl_3$). **^{1}H-NMR** (500 MHz, CD_3CN) δ 8.34 (d, *J* = 7.3 Hz, 2H, CH_{Ar}), 7.50 (d, *J* = 7.8 Hz, 2H, CH_{Ar}), 7.37 (s, 2H, NH_{guan}), 7.26 (t, *J* = 7.1 Hz, 2H, CH_{Ar}), 7.12 (t, *J* = 7.41 Hz, 2H, CH_{Ar}), 7.09 (s, 2H, NH_{urea}), 5.91 (s, 2H, NH_{urea}), 3.24-2.84 (m, 10H, $CH_{2\gamma}$, CH_α, CH_2), 3.14 (dd, *J* = 1.1, 7.4 Hz, 2H, CH_2S), 2.71 (dd, *J* = 1.0, 7.5 Hz, 2H, CH_2S), 1.92-1.78 (m, 4H, $CH_{2\beta}$), 1.58 (m, 4H, CH_2), 1.39 (m, 4H, CH_2), 0.89 (t, *J* = 7.6 Hz, 6H, CH_3). **^{13}C-NMR** (CD_3CN, 125 MHz) δ 155.6 (CO), 150.0 (C_{guan}), 138.4, 134.2, 129.5, 122.1, 119.9, 118.5 (CH_{Ar}, C_{Ar}), 47.9 (CH_α), 45.4 (CH_2S), 40.1 (CH_2), 39.5 ($CH_{2\gamma}$), 32.2 (CH_2), 25.6 ($CH_{2\beta}$), 19.7 (CH_2), 14.5 (CH_3). **ESI-MS** *m/z* 612.4 $(M\text{-}PF_6^-)^+$.

(2*R*,8*R*) bicyclic guanidinium macrocycle (7).

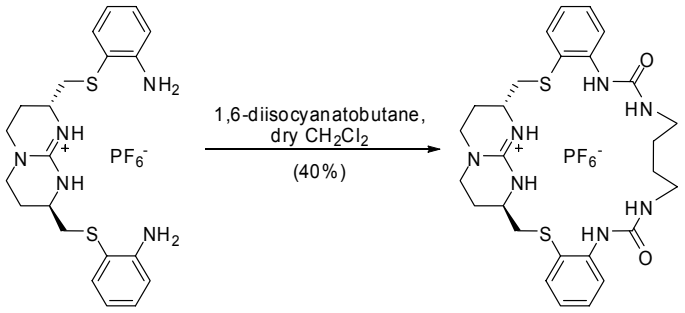

4 **7**

Procedure

To a solution of guanidinium salt **4** (30 mg, 0.06 mmol) in dry CH_2Cl_2 (2 mL), in a sealed tube was added 1,4-diisocyanatobutane (0.01 mL, 0.06 mmol) under nitrogen atmosphere and the mixture was stirred overnight at 45ºC. After evaporation of the solvent, the resulting solid was dissolved in CH_2Cl_2, washed with a 0.1N NH_4PF_6 solution and dried under Na_2SO_4. The organic layer was filtered over cotton and concentrated *in vacuo*. Purification by silica gel column chromatography ($MeOH/CH_2Cl_2$ 100:0 to 98:2) afforded **7** as a pure yellow pale solid. The solid was then dissolved in acetonitrile and eluted in a Dowex resin (PF_6^-) column to obtained **7** (PF_6^-) (15 mg, 40 %). Mp 123-125ºC. $[\alpha]_D^{25}$ -76.24 (*c* = 0.25, $CHCl_3$). **^{1}H-NMR** (500 MHz, CD_3CN) δ 7.61 (d, *J* = 8.3 Hz, 2H, CH_{Ar}), 7.48 (d, *J* = 7.8 Hz, 2H, CH_{Ar}), 7.15 (s, 2H, NH_{guan}), 7.09 (t, *J* = 7.6 Hz, 2H, CH_{Ar}), 6.98 (t, *J* = 11.0 Hz, 2H, CH_{Ar}), 6.82 (s, 2H, NH_{urea}), 5.92 (s, 2H, NH_{urea}), 3.24-3.06 (m, 10H, $CH_{2\gamma}$, CH_α, CH_2S), 2.89 (m, 4H, CH_2), 2.01-1.71 (m, 4H, $CH_{2\beta}$), 1.51 (m, 4H, CH_2). **^{13}C-NMR** (CD_3CN, 125 MHz) δ 165.5 (C_{urea}), 150.6 (C_{guan}), 140.9, 133.5, 128.5, 121.8, 120.1, 119.6 (CH_{Ar}, C_{Ar}), 46.9 (CH_α), 44.4 (CH_2S), 41.9 ($CH_{2\gamma}$), 28.7 ($CH_{2\beta}$), 25.9 (CH_2), 25.0 (CH_2). **ESI-MS** *m/z* 554.2493 $(M\text{-}PF_6^-)^+$.

(2*R*,8*R*) bicyclic guanidinium macrocycle (8).

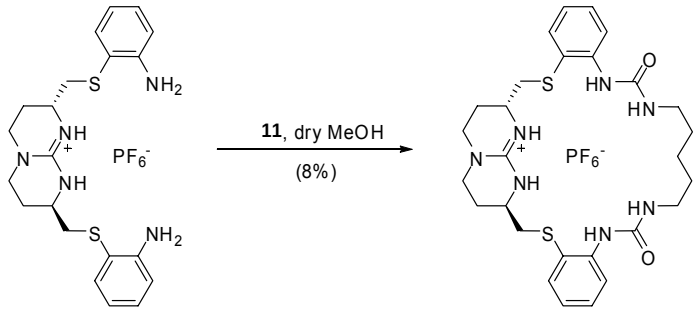

4 8

Procedure

To a solution of guanidinium salt **4** (Cl^-) (100 mg, 2.26 mmol) in dry MeOH (6 mL), in a sealed tube was added 11 (0.64 mg, 2.26 mmol) under a nitrogen atmosphere and the mixture was stirred for two days at 80ºC. After removing the solvent, the resulting solid was purified by column chromatography ($MeOH/CH_2Cl_2$ 100:0 to 98:2) and then precipitated in acetonitrile to afford compound **8** (Cl^-) as a white pure solid. The solid was then dissolved in MeOH and eluted in a Dowex resin (PF_6^-) column to obtained **8** (PF_6^-) (20 mg, 8 %). Mp 136-138ºC. $[\alpha]_D^{25}$ -26.24 (*c* = 0.25, CH_3CN). **^{1}H-NMR** (500 MHz, CD_3CN) δ 7.62 (d, *J* = 7.9 Hz, 2H, CH_{Ar}), 7.48 (d, *J* = 7.8 Hz, 2H, CH_{Ar}), 7.23 (s, 2H, NH_{guan}), 7.05 (t, *J* = 7.5 Hz, 2H, CH_{Ar}), 6.97 (t, *J* = 7.1 Hz, 2H, CH_{Ar}), 6.85 (s, 2H, NH_{urea}), 5.89 (s, 2H, NH_{urea}), 3.45-2.90 (m, 10H, $CH_{2\gamma}$, CH_α, CH_2S), 2.89 (m, 4H, CH_2), 2.21-1.81 (m, 4H, $CH_{2\beta}$), 1.62 (m, 6H, CH_2). **^{13}C-NMR** (CD_3CN, 125 MHz) δ 165.5 (C_{urea}), 150.6 (C_{guan}), 140.9, 133.5, 128.5, 121.8, 120.1, 119.6 (CH_{Ar}, C_{Ar}), 46.9 (CH_α), 44.4 (CH_2S), 41.9 ($CH_{2\gamma}$), 28.7 ($CH_{2\beta}$), 26.2 (CH_2), 25.9 (CH_2), 25.0 (CH_2). **ESI-MS** *m/z* 568.3 $(M\text{-}PF_6^-)^+$.

(2*R*,8*R*) bicyclic guanidinium macrocycle (9).

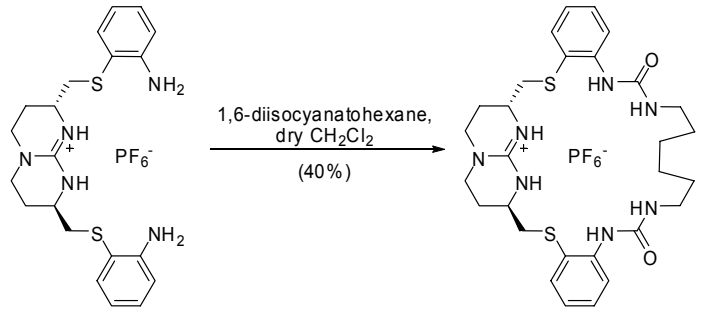

4 **9**

Procedure

To a solution of guanidinium salt **4** (30 mg, 0.06 mmol) in dry CH_2Cl_2 (2 mL), in a sealed tube was added 1,6-diisocyanahexane (0.01 mL, 0.06 mmol) under nitrogen atmosphere and the mixture was stirred overnight at 45ºC. After evaporation of the solvent, the resulting solid was dissolved in CH_2Cl_2, washed with a 0.1N NH_4PF_6 solution and dried under Na_2SO_4. The organic layer was filtered over cotton and concentrated *in vacuo*. Purification by silica gel column chromatography ($MeOH/CH_2Cl_2$ 100:0 to 98:2) afforded **9** as a pure yellow pale solid. The solid was then dissolved in acetonitrile and eluted in a Dowex resin (PF_6^-) column to obtained **9** (PF_6^-) (15 mg, 40 %). Mp 151-153ºC. $[\alpha]_D^{25}$ -17.20 (*c* 0.25, CH_3CN). **^{1}H-NMR** (500 MHz, CD_3CN) δ 7.70 (d, J = 8.1 Hz, 2H, CH_{Ar}), 7.48 (d, J = 7.7 Hz, 2H, CH_{Ar}), 7.35 (s, 2H, NH_{guan}), 7.05 (m, 4H, CH_{Ar}), 6.90 (s, 2H, NH_{urea}), 5.82 (s, 2H, NH_{urea}), 3.40(m, 2H, CH_2S), 3.24-2.84 (m, 12H, $CH_{2\gamma}$, CH_α, CH_2S, CH_2), 2.01-1.74 (m, 4H, $CH_{2\beta}$), 1.39-1.25 (m, 4H, CH_2). **^{13}C-NMR** (CD_3CN, 125 MHz) δ 164.9 (C_{urea}), 151.1 (C_{guan}), 140.7, 132.8, 128.9, 122.3, 120.2, 119.9 (CH_{Ar}, C_{Ar}), 47.1 (CH_α), 44.1 (CH_2S), 41.9 ($CH_{2\gamma}$), 28.7 ($CH_{2\beta}$), 25.8 (CH_2), 25.1 (CH_2), 24.8 (CH_2). **ESI-MS** *m/z* 582.3 $(M\text{-}PF_6^-)^+$.

(2*R*,8*R*) bicyclic guanidinium macrocycle (10).

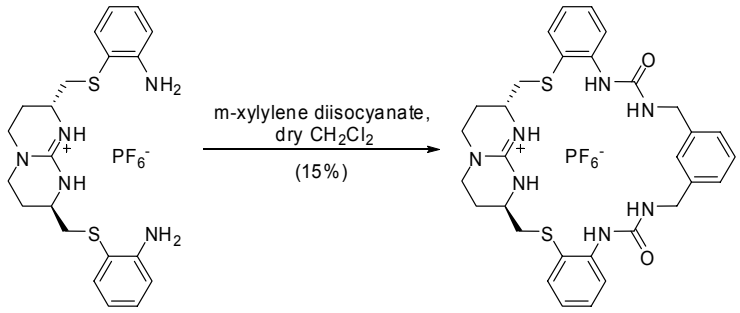

4 **10**

Procedure

To a solution of guanidinium salt 4 (60 mg, 0.10 mmol) in dry CH_2Cl_2 (4 mL), in a sealed tube was added *m*-xylylene diisocyanate (0.17 mL, 0.10 mmol) under a nitrogen atmosphere and the mixture was stirred overnight at 45ºC. After evaporation of the solvent, the resulting solid was dissolved in CH_2Cl_2, washed with a 0.1N NH_4PF_6 solution and dried under Na_2SO_4. The organic layer was filtered over cotton and concentrated *in vacuo*. Purification by silica gel column chromatography ($MeOH/CH_2Cl_2$ 100:0 to 98:2) afforded **10** as a pure yellow pale solid. The solid was then dissolved in acetonitrile and eluted in a Dowex resin (PF_6^-) column to obtained **10** (PF_6^-) (13 mg, 15 %). Mp 170-172ºC. $[\alpha]_D^{25}$ -24.36 (*c* = 0.5, CH_3CN). **^{1}H-NMR** (500 MHz, CD_3CN) δ 7.57 (d, *J* = 8.0 Hz, 2H, CH_{Ar}), 7.44 (d, *J* = 7.9 Hz, 2H, CH_{Ar}), 7.37 (s, 2H, NH_{guan}), 7.31 (m, 6H, CH_{Ar}), 7.15 (d, *J* = 7.9 Hz, 2H, CH_{Ar}), 7.04 (t, *J* = 6.2 Hz, 2H, CH_{Ar}), 6.74 (m, 4H, NH_{urea}, CH_{Ar}), 6.23 (s, 2H, NH_{urea}), 4.79 (dd, *J* = 8.4, 16.7 Hz, 2H, NCH_2), 4.09 (d, *J* = 17.8 Hz, 2H, NCH_2), 3.22-2.77 (m, 10H, $CH_{2\gamma}$, CH_α, CH_2S,), 2.19-1.65 (m, 4H, $CH_{2\beta}$). **^{13}C-NMR** (CD_3CN, 100 MHz) δ 156.9 (C_{urea}), 150.4 (C_{guan}), 140.7, 139.2, 133.2, 128.5, 128.3, 125.8, 125.2, 124.9, 124.5 (CH_{Ar}, C_{Ar}), 47.6 (CH_α), 44.4 (CH_2N), 43.1 (CH_2S), 37.9 ($CH_{2\gamma}$), 24.1 ($CH_{2\beta}$). **ESI-MS** *m/z* 602.5 $(M\text{-}PF_6^-)^+$.

***N,N'*-(pentane-1,5-diyl)bis(1*H*-imidazole-1-carboxamide) (11).**

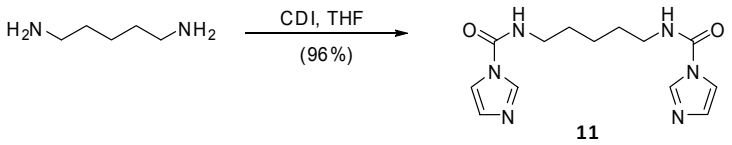

11

Procedure

To a solution of CDI (0.476 g, 2.978 mmol) in THF, 1,5-diaminopentane (0.114 mL, 0.978 mmol) was added dropwise. After 30 minutes, the solvent was removed and the pure product precipitated as a white solid (280 mg, 96%) in ethyl acetate. M.p. 89-91°C. **^{1}H-NMR** (500 MHz, CD_3OD) δ 8.24 (s, 2H, CH), 7.60 (s, 2H, CH), 7.01 (s, 2H, CH), 3.35 (t, J = 7.1 Hz, 4H, CH_2), 1.79 (q, J = 7.7 Hz, 4H, CH_2), 1.67 (m, 2H, CH_2). **^{13}C-NMR** (125 MHz, CD_3OD) δ 150.8 (CO), 137.4, 130.1, 130.0 (C_{Ar}), 41.6 (CH_2), 29.9 (CH_2), 25.0 (CH_2).

2.6.3 X-ray Data

For crystal growth, a solution of **8** (NO_3^-) or **8** (AcO^-), (3 mg) in CH_2Cl_2 (1 mL) were prepared and then left to evaporate in a saturated atmosphere of hexane for 2 days. To a solution of **4** (Cl^-) in $CHCl_3$ (3 mg, 05 mL) was added dropwise diethyl ether (0.5 mL) and the mixture was left to air-evaporate for one day. For **7** (NO_3^-) and **9** (Cl^-), a solution in CH_3CN (3 mg, 0.5 mL) was left to air-evaporate for three days. For **9** (NO_3^-), (*R,S*)-**9** (NO_3^-), a solution in DMF (3 mg, 0.5 mL) was left to air-evaporate for 5 days at 80 ºC in a fume hood. The selected crystals were prepared under inert conditions immersed in perfluoropolyether as protecting oil for manipulation. All ORTEP plots are shown with ellipsoids drawn at the 50% probability level.

Data were collected on a Bruker-Nonius diffractometer equipped with a APPEX 2 4K CCD area detector, a FR591 rotating anode with $Mo_{K\alpha}$ radiation, Montel mirrors as monochromator and a Kryoflex low temperature device (T = -173 ^{o}C). Full-sphere data collection was used with ω and φ scans. Programs used: Data collection Apex2 V. 1.0-22 (Bruker-Nonius 2004), data reduction Saint + Version 6.22 (Bruker-Nonius

2001) and absorption correction SADABS V. 2.10 (2003). Structure Solution and Refinement: SHELXTL Version 6.10 (Sheldrick, 2000) were used.[44]

The structure of **7** (NO_3^-) can be solved and refined in the higher symmetric orthorhombic chiral space group $P2_12_12_1$ or in the lower symmetric monoclinic chiral space group $P2_1$ as a monoclinic twin which emulates a higher symmetric orthorhombic crystal with a β angle close to 90º. In the higher symmetric space group the three independent refined structures are partly disordered and the obtained R-values are higher [R1 = 0.0752 (Fo > 4σFo)]. In the lower symmetric space group which refines with better R-values applying a twin matrix (1 0 0 0 -1 0 0 0 -1, basf 0.43), six different independent molecules without disorder can be refined [R1 = 0.0654 (Fo > 4σFo)]. In this case the six independent molecules are showing correlation effects. In order to discuss the crystal packing and the arrangement of the NO_3^- anions the higher symmetrical and partly disordered structure solution was selected.

The different data obtained for compound **8** (NO_3^-) corresponded always to the overlap of the reflections of more than one crystal. The best R_1-value (Fo > 4σFo) reached was not lower than 11%. Using the program Gemini[45] the overlapped data of two crystals could be first separated for integration and later refined as one data set taking in account the overlapping reflections. If only the reflections with not overlap were considered the R_1-value (Fo > 4σFo) reached for 6182 independent reflections was 6.86%. If a factor was included for reflections overlapping more than 50% a R_1-value (Fo > 4σFo) 8.12% (20146 reflections) was reached. If different factors were applied in correlation with the different degrees of overlapping of the reflections a R_1-value (Fo > 4σFo) 9.31% (35238 reflections) could be reached. For the structure description the refinement model with one overlapping factor was used. Additionally to the described overlapping of crystals pseudosymmetry from *P*1 to *P*-1 was detected, being, for a chiral structure, the correct space group *P*1.

[44] G. M. Sheldrick (1998) *SHELXTL Crystallographic System Ver. 5.10*, Bruker AXS, Inc.: Madison, Wisconsin.

[45] Gemini, Autoindexing Program for Twinned Crystals, Vers. 10.02 Release 5/2000; Bruker AXS Inc., Madison, Wisconsin (USA).

*Table 11. Crystal data for **4** (Cl^-), **9** (Cl^-), and **7** (NO_3^-).*

Compound	**4**	**9**	**7**
Formula	$C_{21}H_{28}Cl_1N_5S_2$	$C_{29}H_{40}Cl_1N_7O_2S_2$	$C_{27}H_{36}N_8O_5S_2$
Solvent detected	---	---	¼ H_2O for 3 molecules of **7**
Formula weight	450.05	618.25	618.09
Crystal size (mm^3)	0.40 x 0.40 x 0.40	0.20 x 0.10 x 0.05	0.10 x 0.02 x 0.01
Crystal color	colorless	colorless	colorless
Temp (K)	100	100	100
Crystal system	Orthorhombic	Tetragonal	Orthorhombic
Space group	$P2_12_12_1$	$P4_12_12$	$P2_12_12_1$
A (Å)	9.7597(4)	10.31310(10)	9.1246(10)
B (Å)	24.4855(9)	10.31310(10)	20.319(2)
C (Å)	9.2271(4)	27.9314(7)	47.951(5)
α (deg)	90	90	90
β (deg)	90	90	90
γ (deg)	90	90	90
V ($Å^3$)	2205.01(15)	2970.78(8)	8890.1(16)
Z	4	4	12
ρ (g/cm^3)	1.356	1.382	1.385
μ (mm^{-1})	0.381	0.310	0.232
θ_{max} (°)	38.56	39.69	25.39
Reflec. measured	44207	61564	78274
Unique reflections	11879 [R_{int}=0.0371]	8870 [R_{int}=0.0267]	15128 [R_{int}=0.0952]
Obs. Reflec. Fo>4σ(Fo)	10548	8467	11345
Absorption correction	SADABS (Bruker)	SADABS (Bruker)	SADABS (Bruker)
Trans. min/max	0.68259/1.00000	0.87131/1.00000	0.71015/1.00000
Parameters	265	216	1193
R1/wR2 [I>2σ(I)]	0.0534/0.1384	0.0265/0.0735	0.0748/0.1620
R1/wR2 [all data]	0.0607/0.1440	0.0285/0.0747	0.1046/0.1761
Goodness-of-fit (F^2)	1.061	1.114	1.094
Flack (Std Dev.)	-0.14(5)	0.01(2)	-0.05(9)
Peak/hole ($e/Å^3$)	1.174/-0.384	0.478/-0.247	1.285/-0.481

*Table 12. Crystal data for compounds **8** (NO_3^-), **9** (NO_3^-) and **8** (AcO^-).*

Compound	***8*** *(NO_3^-)*	***9*** *(NO_3^-)*	***8*** *(AcO^-)*
Formula	$C_{28}H_{38}Cl_1N_8O_5S_2$	$C_{29}H_{40}N_8O_5S_2$	$C_{30}H_{41}N_7O_4S_2$
Solvent detected	---	---	---
Formula weight	630.78	644.81	627.82
Crystal size (mm^3)	0.08 x 0.05 x 0.05	0.20 x 0.10 x 0.02	0.20 x 0.20 x 0.10
Crystal color	colorless	colorless	colorless
Temp (K)	100	100	100
Crystal system	Triclinic	Monoclinic	Triclinic
Space group	*P*1	$P2_1$	*P*1
A (Å)	10.8570(15)	12.8416(10)	10.8173(10)
B (Å)	12.4706(16)	8.7033(7)	12.7233(12)
C (Å)	12.9263(16)	13.7476(11)	12.9472(12)
α (deg)	98.088(3)	90	71.619(2)
β (deg)	112.786(3)	96.649(2)	66.523(2)
γ (deg)	107.966(3)	90	71.889(2)
V ($Å^3$)	1465.8(3)	1526.2(2)	1515.5(2)
Z	2	2	2
ρ (g/cm^3)	1.429	1.403	1.376
μ (mm^{-1})	0.236	0.228	0.225
θ_{max} (°)	39.44	39.51	38.84
Reflec. measured	22507 Twin Gemini	30934	29169
Unique reflections	17936 [R_{int}=0.0345]	14681 [R_{int}=0.0406]	18391 [R_{int}=0.0169]
Obs. Reflec. Fo>4σ(Fo)	20146 Twin Gemini	14085	17135
Absorption correction	SADABS (Bruker)	SADABS (Bruker)	SADABS (Bruker)
Trans. min/max	0.89235/1.00000	0.73350/1.00000	0.78172/1.00000
Parameters	776	467	1081
R1/wR2 [I>2σ(I)]	0.0812/0.2163	0.0329/0.0881	0.0379/0.1011
R1/wR2 [all data]	0.0863/0.2213	0.0346/0.0897	0.0422/0.1053
Goodness-of-fit (F^2)	1.026	1.032	1.038
Flack (Std Dev.)	-0.07(4)	0.01(2)	0.04(3)
Peak/hole (e/$Å^3$)	0.437/-0.408	0.558/-0.499	0.926/-0.462

*Table 13. Crystal data for compound (R,S)-**9** (NO_3^-).*

Compound	*(R,S)-**9** (NO_3^-).*
Formula	$C_{29}H_{40}N_8O_5S_2$
Solvent detected	---
Formula weight	644.81
Crystal size (mm^3)	0.06 x 0.06 x 0.01
Crystal color	colorless
Temp (K)	100
Crystal system	Triclinic
Space group	$P\bar{1}$
A (Å)	8.487(6)
B (Å)	13.831(9)
C (Å)	13.855(9)
α (deg)	101.602(16)
β (deg)	98.297(19)
γ (deg)	93.981(18)
V ($Å^3$)	1568.2(18)
Z	2
ρ (g/cm^3)	1.366
μ (mm^{-1})	0.222
θ_{max} (°)	27.53
Reflec. measured	17707
Unique reflections	8980 [R_{int}=0.1113]
Obs. Reflec. Fo>4σ(Fo)	4307
Absorption correction	SADABS (Bruker)
Trans. min/max	0.77887/1.00000
Parameters	397
R1/wR2 [I>2σ(I)]	0.0788/0.1671
R1/wR2 [all data]	0.1794/0.2139
Goodness-of-fit (F^2)	1.005
Flack (Std Dev.)	---
Peak/hole (e/$Å^3$)	0.588/-0.603

3.1 Introduction

3.1.1 Naproxen Overview

Naproxen is the international non-proprietary name for (+)-(*S*)-2-(6-methoxynaphthalen-2-yl)propanoic acid, a Non-Steroidal Anti-inflammatory Drug (NSAID).[1] Naproxen was first sold by Synthex[2] as a prescription drug under the trade name Naprosyn in 1976 and Naproxen sodium as Anaprox in 1980. The U. S. Food and Drug Administration (FDA) approved its use as an over-the-counter drug in 1991.

In 2003 Roche was the biggest seller in the small sub sector of Naproxen painkillers. Although Naproxen sales are relatively small, combined Bayer-Roche sales amount to $1.3 billion (€970 million) making it the best-selling NSAIDs in the U.S.A..

Naproxen is a member of the 2-arylpropionic acid (profen) family of NSAIDs, as Ibuprofen, Flurbiprofen and Ketoprofen (Fig 1). These drugs are used for the management of mild to moderate pain, fever, and inflammation. They work by reducing the levels of prostaglandins, chemicals that are responsible for those symptoms. Naproxen blocks the enzyme cyclooxygenase-2 (COX-2) that produces prostaglandins, resulting in lower concentrations of these compounds and, as a consequence, reducing inflammation, pain and fever.

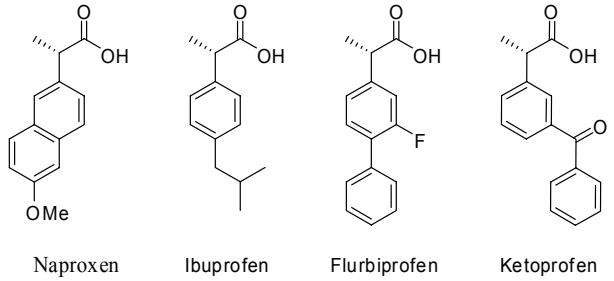

Fig 1. Examples of non-steroidal anti-inflammatory drugs.

[1] Giordano, C.; Villa, M.; Panossian, S. *Naproxen: Chirality in Industry*, Wiley (New York), **1992**.

[2] Harrington, P. J.; Lodewijk, E. *Organic Process Research & Development* **1997**, *1*, 72-76.

In the late 1970s, due to the large activity range of the steroidal anti-inflammatory drugs, many laboratories tried to synthesize NSAIDs. Studies showed that arylacetic acid derivatives had the basic structure suitable for this biological activity, so a large amount (more than 100 compounds per year) of these derivatives was prepared. At the beginning, the indoleacetic acid structure (such as Indomethacin), seemed to be the best, but the strong side effects made it come down. Methylphenylacetic acid derivatives looked like a good alternative as their activity range was smaller. Further studies confirmed the importance of the α-methyl group. Two enantiomers indeed exist with the potential for different biological effects and metabolism for each one. Only the *S*-enantiomers of arylpropionic acid NSAIDS can potently inhibit COX-2, whereas the *R*-enantiomers exert almost no COX-2 activity. Regarding Naproxen, the *S*-configuration appears to be essential for its pharmacological action.[3] In fact, the *S*-enantiomer is 28 times more effective than the *R* one. Although, Ibuprofen and Ketoprofen are now available in single, active enantiomer preparations (Dexibuprofen and Dexketoprofen), Naproxen has always been the only NSAID marketed as a pure single active enantiomer.

3.1.2 Naproxen Synthesis

The Naproxen patent expired in December 1993 leading to a search for new asymmetric technology. In fact, (*S*)-Naproxen ranked fourth in sales of optically pure pharmaceuticals in 1991.

Several methods have been described for the synthesis of chiral 2-arylpropionic acids.[4] After two large scale synthesis processes, Synthex developed a synthetic route diminishing the undesirable features and wastes (Scheme 1). Researchers focused on two steps, the naphthol alkylation and the racemate resolution. In fact production yields increased from 50% in 1984 to more than 90% in early 1995. The *N*-

[3] Harrison, I. T.; Lewis, B.; Nelson, P.; Rooks, W.; Roszkowski, A.; Tomolonis, A.; Fried, J. H. *J. Med. Chem.* **1970**, *13*, 203-211.

[4] a) Rieu, J. M.; Boucherle, A.; Cousse, H.; Mouzin, G. *Tetrahedron* **1986**, *42*, 4095-4131. b) Sonawane, H. R.; Bellur, N. S.; Ahuja, J. R.; Kulkarni, D. G. *Tetrahedron: Asymmetry* **1992**, *3*, 163-192.

alkylglucamine[5] was preferred to cinchonidine keeping the resolution efficient (> 95%) with lower cost and greater availability (from reductive amination of D-glucose).[6]

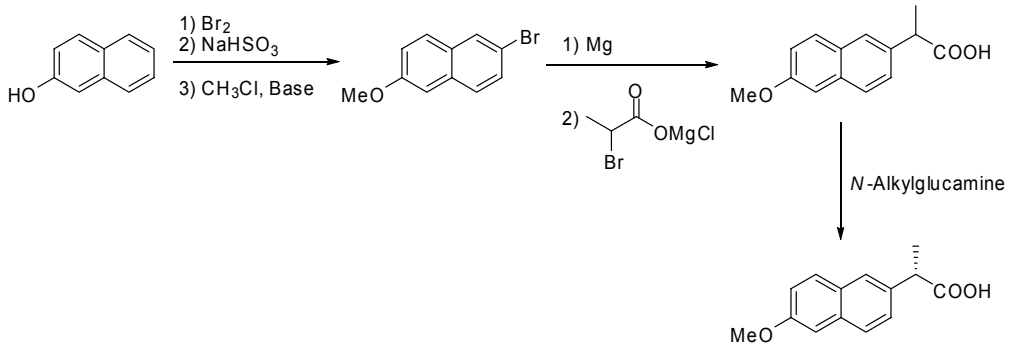

Scheme 1. Large-scale manufacturing process of Naproxen.

Two-thirds of the total production cost was attributed to the resolution-racemization process whereas one third was in the production of the racemic acid. Therefore, research for the production of the desired enantiomer was undertaken.

Several asymmetric technologies were designed for Naproxen production (Scheme 2). The Zambon[7] process affords the (*S*)-enantiomer (e.e. > 98%) using (*R*, *R*)-tartaric acid as chiral auxiliary, bromination of the activated methylene and ester hydrolysis but was somehow considered as too complicated by Synthex to be processed. A catalytic asymmetric hydrogenation of a naphthacrylic acid using a ruthenium (*S*)-BINAP catalyst gives (*S*)-Naproxen (e.e. > 98%).[8] Again Synthex judged this method too expensive to be settled. A catalytic hydroformylation of 2-methoxy-6-vinylnaphthalene using a rhodium catalyst with BINAPHOS ligand

[5] Holton, P. G.; U.S. Pat. 4, 515, 811, May 7, **1985**.

[6] a) Wilth, P.; Dannenberg, G. E. M.; Schmied-kowarzik, V.; Weinhold, P.; Gudel, D Ger. Pat. 2 319 245, **1973**. b) Felder, E.; Pitre, H.; Zutter, M.M. U.K. Pat. GB 2 025 968A, **1980**.

[7] Giordano, C.; Castaldi, G.; Cavicchioli, S.; Villa, M. *Tetrahedron* **1989**, *45*, 4243-4252.

[8] a) Wan, K. T.; Davis, M. E. *Nature* **1994**, *370*, 449-450. b) Ohta, T.; Takaya, H.; Kitamura, M.; Nagai, K.; Noyori, R. *J. Org. Chem.* **1987**, *52*, 3174-3176.

produces an optically active aldehyde which on oxidation yields (*S*)-Naproxen.[9] This approach was also refused due to cost and product availability issues.

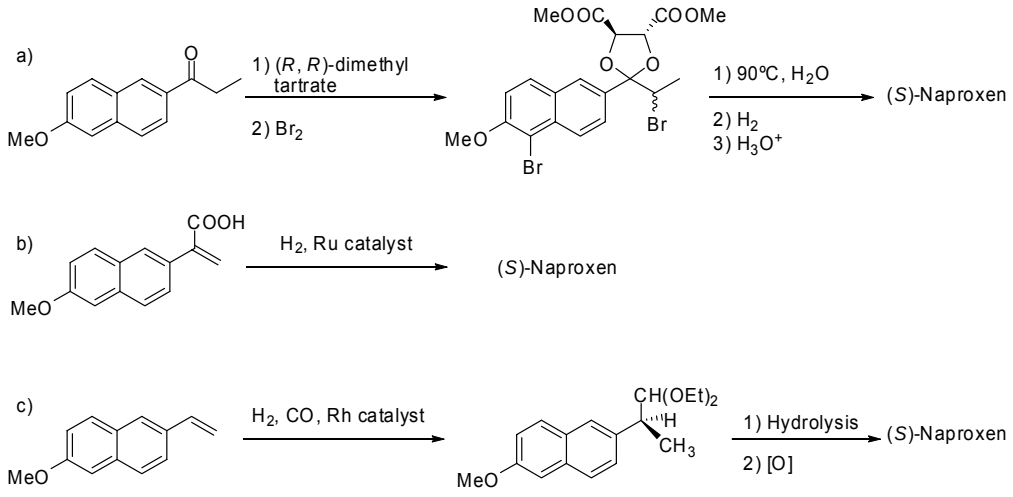

Scheme 2. a) Naproxen synthesis by Zanbon ,b) asymmetric hydrogenation and c) asymmetric hydroformylation .

One example of Naproxen production by the chiral pool approach was developed at Synthex in 1982 (Scheme 3). (*S*)-Ethyl lactate is converted to a mesylate, then ester hydrolysis and conversion to the acid chloride provides a chiral acylating agent. Acrylation, ketalization with 2,2-dimethyl-1,3-propanediol followed by rearrangement and ester hydrolysis yields (*S*)-Naproxen.

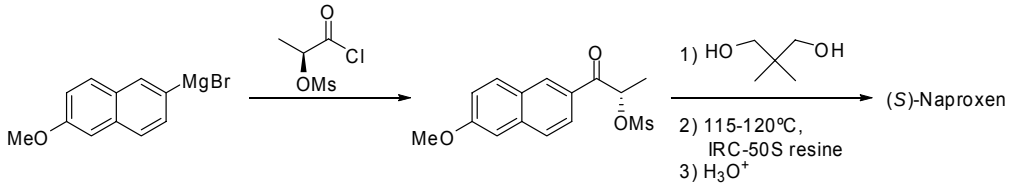

Scheme 3. Naproxen synthesis using the chiral pool approach.

[9] a) Stille, J. K.; Su, H.; Brechot, P.; Parinello, G.; Hegedus, L. S. *Organometallics* **1991**, *10*, 1183-1189. b) Babin, J. E.; Whiteker, G. T. WO 93 03,839, March 4, **1993**.

As Naproxen catches so much attention and interest in research area, many other synthetic pathways have been described[10] but for cost reasons or environmental concerns, the racemic synthesis by Synthex is still processed nowadays.

3.1.3 Racemates Resolution

Worldwide sales of chiral drugs in single-enantiomer dosage forms continued growing at a more than 13% annual rate to $133 billion in 2000 (Table 1).[11] At a future growth rate, the figure could hit $200 billion in 2008. Among chiral drugs approved by the FDA in 2003 more than 80% were single enantiomers.[12] The efficient and economical production of enantiomerically pure compounds is thus one of the major challenges facing the modern chemical industry. Moreover, a need for developing new technologies to produce optically pure drugs is primary. Although considerable advances in synthesis, analysis and separation have been achieved, production of enantiopure chemicals from resolution of racemates is still significant.[13] Although resolution only gives 50% yield, in combination with racemization may become a 100% yield concept (dynamic kinetic resolution).[14]

[10] a) Gu, Q.; Chen, C.; Sih, C. J. *Tetrahedron Lett.* **1986**, *27*, 1763-1766. b) García, M.; del Campo, C.; Llama, E. F.; Sánchez-Montero, J.; Sinisterra, J. V. *Tetrahedron* **1993**, *49*, 8433-8440. c) Vedejs, E.; Kruger, A. W. *J. Org. Chem.* **1998**, *63*, 2792-2793. d) Vedejs, E.; Lee, N.; Sakata, S. T. *J. Am. Chem. Soc.* **1994**, *116*, 2175-2176. e) Rajanbabu, T. V.; Casalnuovo, A. L.; Ayers, T. A.; Warren, T. H. *J. Am. Chem. Soc.* **1994**, *116*, 9869-9882. f) Effenberger, F.; Graef, B. W.; Osswald, S. *Tetrahedron: Asymmetry* **1997**, *8*, 2749-2755. g) Brunner, H.; Schmidt, P. *Eur. J. Org. Chem.* **2000**, 2119-2133.

[11] http://www.technology-catalysts.com/

[12] http://pubs.acs.org/cen/coverstory/7940/7940chiral.html

[13] a) *Chiral Separation Techniques*, Subramanian, G., Ed., Wiley-VCH, **2001**. b) Rouhi, A. M. *Chem. Eng. News* **2002**, *80*, 23, 51-57.

[14] a) Kroutil, W.; Faber, K. *Tetrahedron: Asymmetry* **1998**, *9*, 2901-2913. b) Shi, Y. J.; Wells, K. M.; Pye, P. J.; Choi, W. B.; Churchill, H. R. O.; Lynch, J. E.; Maliakal, A.; Sager, J. W.; Rossen, K.; Volante, R. P.; Reider, P. J. *Tetrahedron* **1999**, *55*, 909-918.

	ALL DRUGS		SINGLE-ENANTIOMER DRUGS		
$ MILLIONS	**1999**	**2000**	**1999**	**2000**	**2005**
Analgesics	$21,500	$23,000	$1,173	$1,291	$1,395
Antibiotic/antifungals	29,300	31,700	24,918	26,140	29,747
Antiviral	17,700	19,100	6,717	8,820	12,201
Cancer	13,700	15,600	8,891	10,690	13,605
Cardiovascular	42,700	46,600	24,895	27,650	34,627
Central nervous system	47,700	53,900	8,439	9,094	14,700
Dermatology	17,900	18,400	16,202	1,272	1,540
Gastrointestinal	43,900	47,200	1,970	4,033	6,590
Hematology	16,500	15,400	7,405	8,879	11,295
Hormone/endocrinology	20,000	22,000	14,510	15,384	19,790
Ophthalmics	7,100	7,400	1,270	2,265	2,705
Respiratory	36,500	40,500	5,696	6,615	9,620
Vaccines	6,500	7,300	2,503	3,349	4,320
Other	39,000	41,900	6,248	7,032	9,730
TOTAL	$360,000	$390,000	$117,763	$132,514	$171,865
NOTE: Figures are for dosage formulations. SOURCE: Technology Catalysts International					

Table 1. Worldwide sales of single-enantiomer drugs.

The "classical method of resolution" using crystallization of diastereomeric salts is widely used on industry because of the easy scale up and rapid screening of resolving agents possible.[15] Through often the best method available, this technology suffers from drawbacks like the use of a stoichiometric quantity of resolving agents. Resolution via hydrolytic enzymes gives a high enantioselectivity for fairly wide range of products as esters, amides, acids, alcohols and amines. Nevertheless, the availability of only one enantiomer presents a major limitation to this technique.

Physical separations represent still an attractive area for producing optical pure compounds. These methods require a chiral phase that induces the enantiomers separation (a need for chiral phases for multiple products application is primary). Solid-liquid based separations still have important disadvantages, chiral

[15] Fogassy, E.; Nógrádi, M.; Kozma, D.; Egri, G.; Pálovics, E.; Kiss, V. *Org. Biomol. Chem.* **2006**, *4*, 3011-3030.

chromatography suffer from low capacity and chiral simulated moving bed (SMB)[16] from high investment. In contrast, liquid-liquid separation is considered as a very effective way of producing enantiopure products, as it largely avoids solids handling and can be a very rapid process. This technology requires transfer from one liquid phase to another, the use of chiral transferring agent with preferentially transport one enantiomer with sufficient selectivity and a high concentration of racemates. Still, the technology is not mature enough due to lack of wide range of readily cheap selectors as well as solubility problems in one of the two liquid phases.

Despite its limited application in industrial scale, supported liquid membrane (SLM)[17] continues to attract large academic interest. Goto and co-workers have reported a highly enantioselective separation of the NSAID Ibuprofen using this technology (Fig 2).[18] Combining the use of SLM with enzymes (enantioselective catalysts of hydrolysis or esterification of drugs and amino acids) affords indeed elevated resolution of both Ibuprofen and phenylalanine. The surfactant-lipase (from *Candida rugosa*) complex was encapsulating in the SLM and another lipase (from porcine pancreas) was dissolved in the receiving phase. An enantiomeric excess of 91% and 99% was achieved after 48 hours for (*S*)-Ibuprofen and L-phenylalanine respectively.

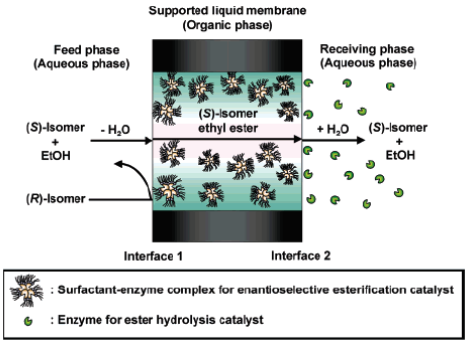

Fig 2. Concept of enantioselective separation of racemic mixtures through the SLM encapsulating the surfactant-enzyme complex.

[16] Wei, F.; Shen, B.; Chen, M. *Ind. Eng. Chem. Res.* **2006**, *45*, 1420-1425.

[17] a) Jönsson, J. Å.; Mathiasson, L. *Trends Anal. Chem*. **1999**, *18*, 318-325. b) de Gyves, J.; de Miguel, E. R. *Ind. Eng. Chem. Res*. **1999**, *38*, 2182-2202.

[18] a) Miyako, E.; Maruyama, T.; Kamiya, N.; Goto, M. *Chem. Commun*. **2003**, 2926-2927. b) Miyako, E.; Maruyama, T.; Kamiya, N.; Goto, M. *J. Am. Chem. Soc.*, **2004**, *126*, 8622-8623.

3.1.4 Current Strategy

The recent developments in supramolecular chemistry suggest an alternative approach to the traditional resolution of racemates. Certain synthetic receptors are able to bind their substrates with sufficient power to extract them from an aqueous medium into an organic solvent. Therefore the transport is facilitated between separated phases (such as an aqueous–organic–aqueous system). If the receptor is enantioselective,[19] one enantiomer of racemic substrate will be transported preferentially and resolution could be achieved.[20] Moreover, since the process is catalytic in the amount of receptor; one receptor molecule can indeed transfer many molecules of substrate between the two phases.[21] The selector would stay in the organic phase and could be reused without difficulty.

The importance of the development of an efficient method for the resolution of the racemate of Naproxen is double. On the one hand the academic interest of being able to design a receptor so subtle that it could discriminate between a methyl group and a hydrogen atom, and on the other hand the industrial interest. Chiral recognition of Naproxen is therefore a challenging goal in supramolecular chemistry.

3.1.5 Synthetic Receptors for Naproxen Recognition

The enantiomers of Naproxen differ only in the orientation of one methyl group. It is therefore a quite demanding target substrate for recognition and there are indeed few receptors described in the literature regarding the resolution of this compound.

Diederich and co-workers reported an optically active cyclophane **I** able to bind Naproxen derivatives.[22] By complexation studies in ^{1}H-NMR, (*S*)-Naproxen

[19] a) Webb, T.H.; Wilcox, C. S. *Chem. Soc. Rev.* **1993**, *2*, 383-395. b) Martín, M.; Raposo, C.; Almaraz, M.; Crego, M.; Caballero, C.; Grande, M.; Morán, J. M. *Angew. Chem. Int. Ed. Engl.* **1996**, *35*, 2386-2389. c) Zhang, X. X.; Bradshaw, J. S.; Izatt, R. M. *Chem. Rev.* **1997**, *97*, 3313-3361. d) Ragusa, A.; Rossi, S.; Hayes, J. M.; Stein, M.; Kilburn, J. D. *Chem. Eur. J.* **2005**, *11*, 5674-5688.

[20] Afonso, C. A. M.; Crespo, J. G. *Angew. Chem. Int. Ed*. **2004**, *43*, 5293-5295.

[21] Pirkle, W. H.; Doherty, E. M. *J. Am. Chem. Soc.* **1989**, *111*, 4113-4114.

[22] a) Dharanipragada, R.; Diederich, F. *Tetrahedron Lett.* **1987**, *28*, 2443-2446. b) Dharanipragada, R.; Ferguson, S.; Diederich, F. *J. Am. Chem. Soc.* **1988**, *110*, 1679-1690. c)

derivatives form different 1:1 diastereomeric complexes with (*R*)- and (*S*)-**I**. Enantiomeric ratios were nevertheless quite modest (from $\Delta(\Delta G^{o}) = 0.15$ up to 0.33 kcal mol^{-1}, for Naproxen $\Delta(\Delta G^{o}) = 0.16$ kcal mol^{-1} in D_2O/MeOH-d_4 (60:40)).

In our group, an optically abiotic receptor **II** containing the chiral bicyclic guanidinium binding subunit was evaluated in the late 80's for chiral recognition of aromatic carboxylates.[23] Although extraction experiments of sodium (*S*)-mandelate and (*S*)-Naproxenate with both (*R*,*R*)- and (*S*,*S*)-**II** afforded diastereomeric salts with different NMR spectra, no enantiodiscrimination was reported.

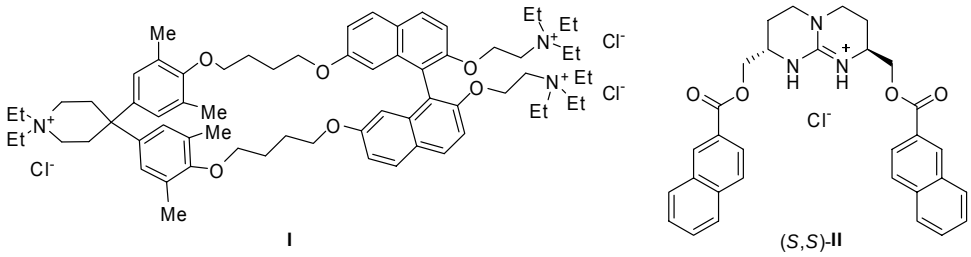

*Fig 3. Receptors by Diederich (**I**) and de Mendoza [(S,S)-**II**].*

Pirkle and co-workers employed a chromatographic approach to design, synthesize and evaluate new chiral selectors for Naproxen.[24] They employed the principle of reciprocity in chiral recognition, which means that if a single molecule of a chiral selector has different affinities for the enantiomers of another substance, then a single enantiomer of the latter will have different affinities for the enantiomers of the initial selector. Two chiral stationary phases (CSPs) derived from (*S*)-Naproxen were therefore produced and HPLC techniques were used to screen Naproxen receptors. A third (*R*,*R*) CSP **III** (Fig 4) was then produced from the best candidate displaying a high level of enantiodiscrimination not only for Naproxen ($\alpha = 2.25$) but also towards most of NSAIDs (for profen, $\alpha = 1.09$ up to 1.71).

Castro, P. P.; Georgiadis, T. M.; Diederich, F. *J. Org. Chem.* **1989**, *54*, 5835-5838. d) Georgiadis, T. M.; Georgiadis, M. M.; Diederich, F. *J. Org. Chem.* **1991**, *32*, 6277-6280.

[23] Echavarren, A.; Galán, A.; Lehn, J.-M.; de Mendoza, J. *J. Am. Chem. Soc.*, **1989**, *111*, 4994-4995.

[24] Pirkle, H. W.; Welch, J. C.; Lamm, B. *J. Org. Chem.* **1992**, *57*, 3854-3860.

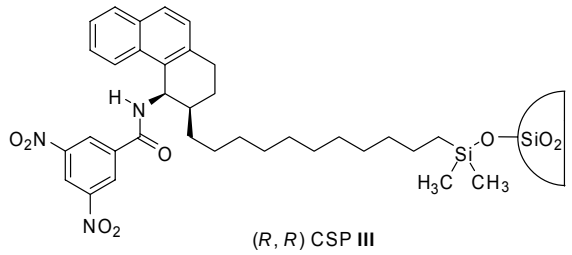

(*R*, *R*) CSP **III**

Fig 4. Chiral stationary phase by Pirkle's (*R*,*R*) CSP **III**.

A neutral host **IV** (Fig 5) based on a rigid xanthene scaffold was developed by Rebek and co-workers.[25] ^{1}H-NMR titrations in CD_3OD show a slight enantioselection [for (*S*)-Naproxenate, K_a = 160 M^{-1} and 110 M^{-1} with (*R*,*R*)-**IV** and (*S*,*S*)-**IV** respectively].

Davis and co-workers synthesized a hindered bicyclic chiral guanidine **V** and performed ^{1}H-NMR experiments with both Naproxen enantiomers.[26] Nevertheless, no discrimination was reported toward this target.

In 2001, Kilburn and co-workers published an acyclic thiourea receptor **VI** showing moderate enantioselectivity for a range of amino acid derivatives.[27] Binding constants measured by ^{1}H-NMR titrations in $CDCl_3$ show only modest differentiation for Naproxen enantiomers [K_a = 1570 M^{-1} and 1870 M^{-1} for (*R*) and (*S*) form respectively].

[25] Hamann, B. C.; Branda, N. R.; Rebek, J., Jr. *Tetrahedron Lett.* **1993**, *34*, 6837-6840.

[26] a) Davis, A. P.; Dempsey, K. J. *Tetrahedron: Asymmetry* **1995**, *6*, 2829-2840. b) Boyle, P. H.; Davis, A. P.; Dempsey, K. J.; Hosken, G. D. *J. Chem. Soc., Chem. Commun*. **1994**, 1875-1876.

[27] Kyne, G. M.; Light, M. E.; Hursthouse, M. B.; de Mendoza, J.; Kilburn, J. D. *J. Chem. Soc., Perkin Trans. 1* **2001**, 1258-1263.

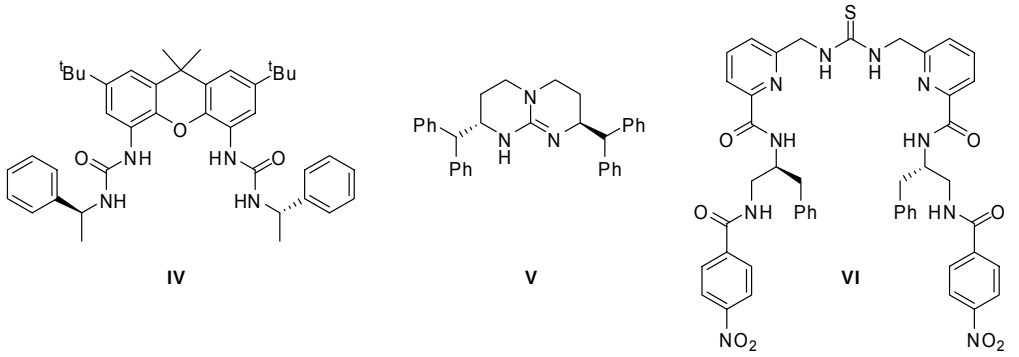

*Fig 5. Receptors by Rebek (**IV**), Davis (**V**) and Kilburn (**VI**).*

In 2001, a steroidal guanidine **VII** was synthesized as an enantioselective receptor for *N*-acyl α-amino acids.[28] Modest but significant selectivity was found with Naproxen in extraction experiments (1.5:1).

Recently, Morán and co-workers have synthesized a racemic macrocyclic receptor **VIII** based on bischromenylurea that provides a C_2 chiral cavity and hydrogen bond donor groups (Fig 6).[29] Competitive experiments between racemic **VIII** and a (*S*)-Naproxen salt gives the highest enantiomeric ratio published so far (7.2:1). Molecular mechanics calculations give an energy difference range from 0.5 kcal/mol to 3 kcal/mol using two different forcefields (MM2 and MMFF). The rigid and hindered cavity where host-guest association occurs gives rise to this high selectivity (steric repulsion is believed to be decisive for enantiodiscrimination).

[28] Lawless, L. J.; Blackburn, A. G.; Ayling, A. J.; Perez-Payan, M. N.; Davis, A. P. *J. Chem. Soc., Perkin Trans. 1* **2001**, 1329-1341.

[29] González, S.; Peláez, R.; Sanz, F.; Jiménez, M. B.; Morán, R. J.; Caballero, M.C. *Org. Lett.* **2006**, *8*, 4679-4682.

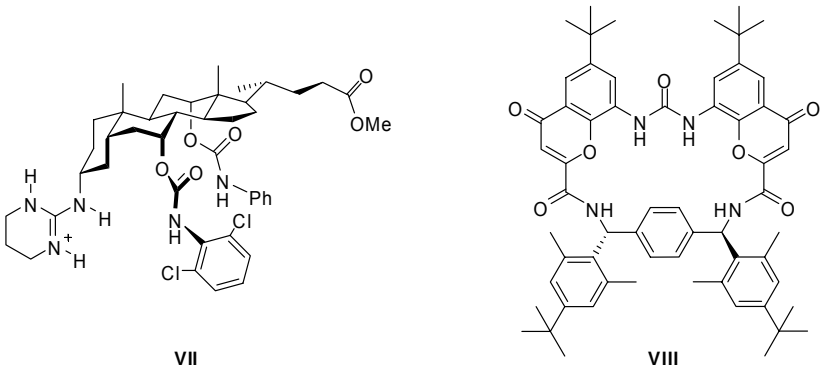

VII **VIII**

*Fig 6. Receptors by Davis (**VII**) and Morán (**VIII**).*

So far, no receptors capable of selectively extracting (*S*)-Naproxen from its racemic mixture in aqueous media have been reported.

In this chapter, we aimed at designing and synthesizing a receptor for Naproxen which could be employed in a liquid-liquid separation technique such as a U-tube set up, membranes or extraction systems. As pointed out in the introduction, we will employ the bicyclic guanidinium scaffold allowing extraction of carboxylate anions through hydrogen bonds and ion-pair interactions. Thus, we propose two different approaches to reach this goal: first, a rational, *de novo* design and second, a combinatorial chemistry approach.

3.2 Rational Design Approach

In the preceding Chapter, we have described guanidine receptors bearing urea functions in order to improve the binding pocket for oxoanions with four additional hydrogen bonds (Fig 7a). ITC titrations of the simpler amide derivatives (two additional hydrogen bonds) with acetate salts revealed a 1:2 complex binding mode.[30] The host indeed affords four hydrogen bonds but its conformational freedom allows a rearrangement of each arm allowing it to bind two guest molecules. On the contrary, symmetric receptors using urea groups as additional hydrogen bond donors present a

[30] Blondeau, P. DEA, Universidad Autónoma de Madrid, **2005**.

1:1 complex binding mode with acetate (affording up to six strong hydrogen bonds to the guest) (Fig 7b). Although association constants are similar to a simpler guanidinium receptor lacking the additional donors at the side arms ($K_a \approx 10^5$ M^{-1}), the enthalpic contribution enhancement constitutes an improvement of the binding pocket for oxoanions. As it was previously reported by Schmidtchen and co-workers, it then provides a strong argument to take enthalpy instead of the almost exclusively used free energy as a design criterion.[31] On the other hand, the increased receptor rigidity (aromatic ring) and the two additional hydrogen bonds present a considerable benefit in order to bring closer the chiral guest center to the host scaffold. In this chapter, we will develop guanidinium-urea receptors as multiple hydrogen bond donor hosts introducing various groups as bulk, aromatic surfaces and additional chiral barriers (R groups).

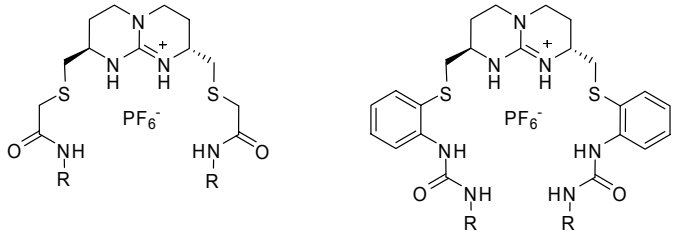

a) b)

Fig 7. Symmetric guanidinium receptors with different additional hydrogen bond donors: a) amide and b) urea.

3.2.1 Additional Steric Hindrance

A first approach suggested by molecular modeling is the incorporation of bulky groups directly connected to the second urea NH (Fig 8). By introduction of such groups, the configuration of the guanidinium scaffold (*R*,*R*) would lead the enantioselection of the guest. Even though the host chiral centers are located far away from the guest's one, the large array of hydrogen bonds should maintain the guest close to the host backbone.

[31] Haj-Zaroubi, M.; Mitzel, N. W.; Schmidtchen, F. P. *Angew. Chem. Int. Ed*. **2002**, *41*, 104-107.

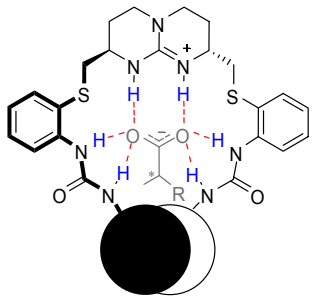

Fig 8. Host-guest interactions between a bulky chiral guanidinium receptor and a chiral α-methyl carboxylate anion.

Molecular modeling was performed for receptors **1**-**4** with both enantiomers of Naproxen using the two different forcefields MMFFs and OPLS-AA (Table 2).[32] Free energy difference goes from 0.1 up to 2.0 kcal mol^{-1} and enthalpy difference from 0.2 up to 1.8 kcal mol^{-1}. Both forcefields are in good agreement and according to these calculations, receptors **2**-**4** should afford considerable enantioselectivity.

Figure 9 shows host-guest interactions between receptor **2** and each enantiomer. Both cases reported the well formation of the binding pocket (six H-bonds). The environment provided by the bulk 2-tert-butyl-6-methylphenyl groups gives a significant stability difference between both complexes. (*R*)-Naproxen appears to have the most stable complex with the (*R*,*R*) configuration of the chiral bicyclic guanidinium scaffold.

[32] Modeling studies were performed by Joe Hayes at Anterio Consult & Research Gmbh, Mannheim, Germany.

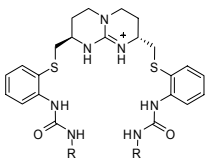

Receptor	MMFFs Forcefield $\Delta\Delta G_{R\text{-}S}$ ($\Delta\Delta H_{R\text{-}S}$)	OPLS-AA Forcefield $\Delta\Delta G_{R\text{-}S}$ ($\Delta\Delta H_{R\text{-}S}$)
1: R = 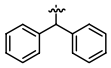	-0.4 (-0.9)	-0.1 (-0.2)
2: R = 	-1.1 (-1.3)	-1.6 (-1.8)
3: R = 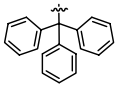	-1.5 (-1.5)	-1.1 (-1.5)
4: R = 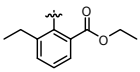	-2.0 (-1.6)	-1.5 (-1.6)

Table 2. Molecular modeling using two different forcefields (MMFFs and OPLS-AA) in a continuum solvent GB/SA ($CHCl_3$), $\Delta\,\Delta G_{R\text{-}S}$ and $\Delta\,\Delta H_{R\text{-}S}$ represent the ΔG and ΔH difference between the enantiomers of Naproxen respectively (kcal mol^{-1}).

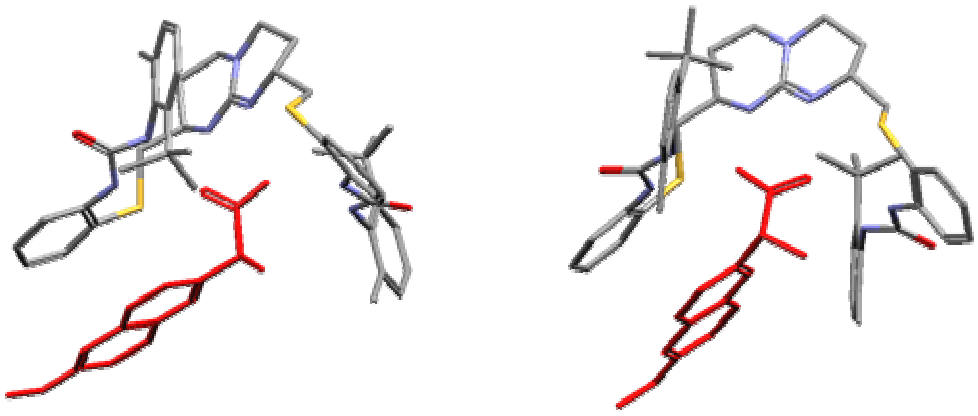

a) b)

*Fig 9. Optimized models of **2** with a) (S)-Naproxenate and b) (R)-Naproxenate (hydrogen atoms are omitted and Naproxen is colored in red).*

Receptors **1** and **2** were therefore synthesized as well as an adamantyl analogue **6** (Scheme 4). Addition of the corresponding isocyanate to the guanidinium diamine salt gave the expected product in good yield (73-86%).

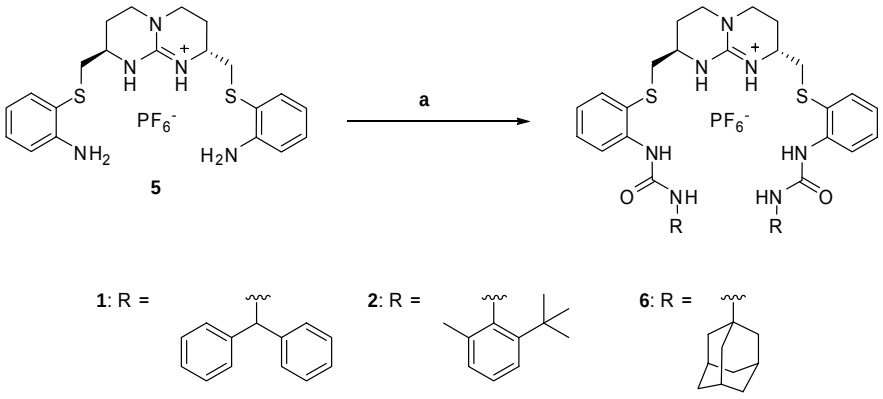

Reagents and conditions: **a**) Isocyanate, dry CH_2Cl_2, sealed tube, 24 h (73-86%).

*Scheme 4. Synthesis of compounds **1**, **2** and **6**.*

Liquid-liquid extraction between an organic solution of receptor (PF_6^-) dissolved in CH_2Cl_2 (1 mg/mL) and a sodium Naproxenate aqueous solution (0.08 M) was then performed. The organic phase was then isolated and the solvent removed. The resulted solid was dissolved in MeOH and analyzed by HPLC using a chiral column [(*S*,*S*) WHELK-01]. Each enantiomer extracted was then quantified but no discrimination was observed for any of these three hosts.

Computer modeling predicted a substantial stability difference according to calculations made for each enantiomer separately. Competitive experiments revealed no differences between both complexes and pointed again to slight differences in energy upon opposite orientations of the α-methyl group of the guest. Restricting complex conformational freedom is therefore essential for chiral selection of Naproxen. Introducing other kind of interactions as well as rigidifying the receptor scaffold should also contribute to this goal.

3.2.2 Pincer-like Receptor

A key feature in the design of a Naproxen host is to bring closer the chiral center of the guest to the host's backbone to allow discrimination between the methyl group and the α proton of the carboxylate. As Naproxen possesses an electronically enriched ring (methoxynaphthyl), π stacking interactions with a receptor bearing withdrawing groups in their aromatic rings would represent an important step for further

stabilization of the complex (in green in Fig 10). Moreover, introduction of a new chiral center (by a R substituent) near the guest's one could afford the desired selectivity.

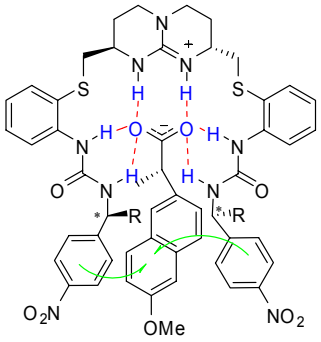

Fig 10. General design of guanidinium receptors with π-π interactions (green) with (S)-Naproxen and additional chiral centers.

In the following sections, both (*R*,*R*) and (*R*,*S*) guanidinium scaffolds will be used to improve the host-guest interactions by the orientation of the arms. We decided to study step by step the design of the receptor so that each variation of the scaffold could be evaluated. By both ^{1}H-NMR an ITC techniques, we will first measure the importance of the spacer between the aromatic surface and the urea function, then introduce a withdrawing group into it and eventually add a chiral center.

3.2.2.1 Spacer Influence

a) (*R*,*R*) Guanidinium Scaffold

As π interactions are necessary in order to design pincer-like receptors, we first suggested studying the binding pocket formation according to the rigidity and nature of the spacer between the urea moiety and the aromatic surface. Therefore, several symmetric receptors with six hydrogen bond donors and bearing butyl or phenyl as well as benzyl or phenethyl group have been synthesized (Scheme 5). ^{1}H-NMR and isothermal calorimetry were used to measure the association between hosts (**7**-**10**) and guests [TBA AcO and TEA (*S*)-Nap]. ^{1}H-NMR titration is used as a qualitative tool for controlling which proton is affected by host-guest interactions and ITC as a

quantitative tool for accurate determination of binding constants and thermodynamic parameters.

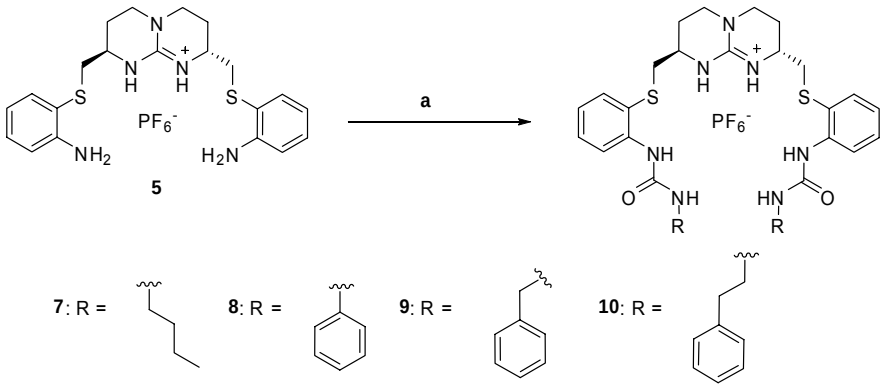

Reagents and conditions: **a**) Isocyanate, dry CH_2Cl_2, sealed tube, 24 h (75-90%).

*Scheme 5. Synthesis of receptors **7**, **8**, **9** and **10**.*

^{1}H-NMR titrations between receptors **7**-**10** and both TBA AcO and TEA (*S*)-Nap show a strong downfield shift of guanidinium and urea NHs. The formation of a good pre-organized pocket in which the carboxylate part of the guest is forming six strong H-bonds with the host is therefore confirmed. Interestingly, **8** has a different behavior: protons a, b, c and d suffer indeed a moderate to strong upfield shift as the amount of guest is increased [with TEA (*S*)-Nap, $\Delta\delta$ from 0.15 up to 0.7 ppm, Fig 11]. In receptor **9** the protons are much less affected [with TEA (*S*)-Nap, $\Delta\delta \approx 0.1$ ppm], as well as **10** which has a similar behavior as **7** (operating as a control experiment). As the rigidity of the link between the urea and the aromatic surface increases, the scaffold needs to rearrange itself in order to permit formation of the binding pocket. In addition to highlighting host-guest interactions, NMR strongly evidences the influence of the spacer used between the urea and aromatic surface.

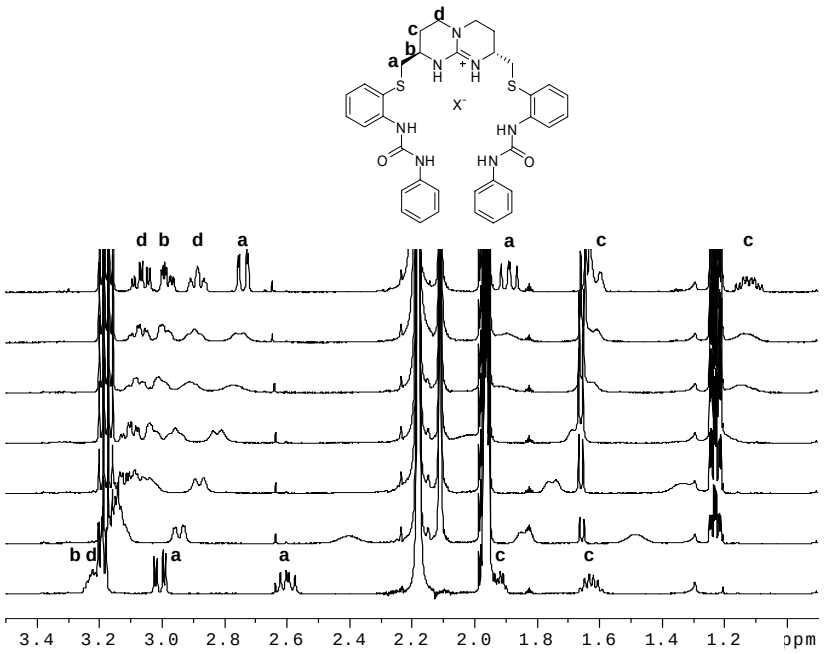

*Fig 11. ^{1}H-NMR titration between (R,R)-**8** and TEA (S)-Nap in CD_3CN at 298K [from bottom to top: 0 to 1.1 equivalents TEA (S)-Nap].*

K_a's between **8** and both carboxylate salts are one order of magnitude lower than for **7**, **9** and **10** (K_a from 10^4 up to 10^5 M^{-1}, Table 3). For TBA AcO and TEA (*S*)-Nap, the more pronounced negative entropic contribution is the important difference between these four hosts. The association for **8** is indeed entropically disfavored and contributes to a lower free energy ΔG. Receptors **7**, **9** and **10** display a similar binding behavior mainly enthalpically driven (K_a from 3.06 x 10^5 up to 5.41 x 10^5 M^{-1}). This significant enthalpic factor is due to electrostatic interactions whereas the entropic one comes from the release of solvent molecules. **8** suffers from an unfavorable spatial arrangement to complete complex formation.

Therefore, both ^{1}H-NMR and ITC techniques are in good agreement to evaluate the spacer influence on binding. **8** is thus too rigid to achieve optimal association but as the host scaffold is recovering flexibility (by addition of CH_2 groups to the linker); the stability of the complex is again higher.

	(*R*,*R*)-**7**	(*R*,*R*)-**8**	(*R*,*R*)-**9**	(*R*,*R*)-**10**
TBA AcO				
K_a	3.06 x 10^5	2.57 x 10^4	1.02 x 10^5	5.41 x 10^5
ΔH	-6.97	-8.55	-7.32	-8.05
ΔS	2.06	-8.05	2.14	-0.33
ΔG	-7.60	-6.11	-7.97	-7.50
TEA (*S*)-Nap				
K_a	3.98 x 10^5	2.65 x 10^4	1.76 x 10^5	2.59 x 10^5
ΔH	-7.78	-7.36	-7.74	-7.98
ΔS	0.01	-4.07	-1.57	-1.57
ΔG	-7.78	-6.13	-7.27	-7.27

*Table 3. Thermodynamic parameters from ITC titrations in acetonitrile at 303K between receptors (R,R)-**7**-**10** and TBA AcO and TEA (S)-Nap (K_a in M^{-1}, ΔH and ΔG in kcal mol^{-1}, ΔS in cal mol^{-1} K^{-1}).*

b) (*R*,*S*) Guanidinium Scaffold

Synthesis of (*R*,*S*) **7**-**10** was performed like those described in scheme 5 (starting from (*R*,*S*)-**5**). (*R*,*S*)-**9** precipitates *in situ* and was then filtered off whereas column chromatography was the common purification process for all other compounds.

^{1}H-NMR titrations proved again the formation of a nicely pre-organized pocket but no upfield shifts were detected for (*R*,*S*)-**8** as in the case of (*R*,*R*)-**8** reported previously. The absence of chirality in the bicyclic guanidinium scaffold strongly influences the arms' orientation and therefore the system conformation.

Addition of a chiral carboxylate salt [TEA (*S*)-Nap] leads to the splitting of all receptor's proton signals due to the loss of the symmetry axis (Fig 12). NOESY were performed for each complex formed but no contacts were detected between the aromatic ring of the host and the naphthyl ring of the guest.

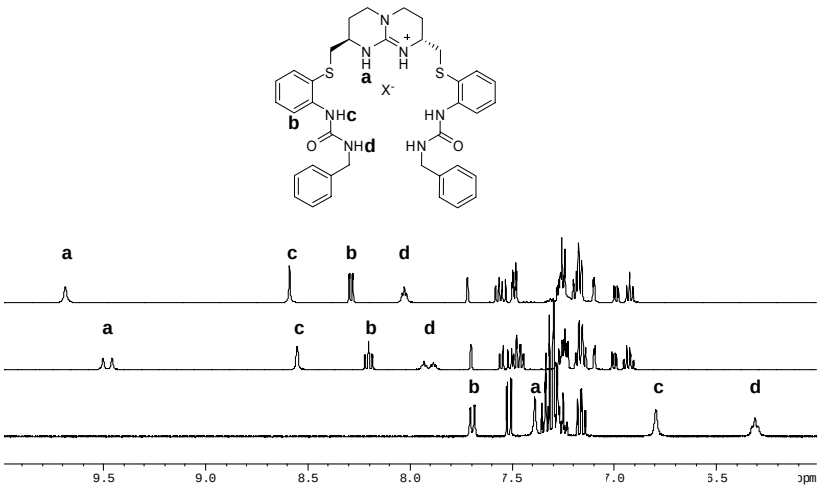

*Fig 12. ^{1}H-NMR spectrum of (R,R)-**9** (PF_6^-), (R,S)-**9** [(S)-Nap$^-$], and (R,R)-**9** [(S)-Nap$^-$] in CD_3CN at 298K (from bottom to top).*

ITC gives a similar enthalpically driven association for both (*R*,*S*) and (*R*,*R*)**-7** (Table 4). As revealed by ^{1}H-NMR experiments, (*R*,*S*)**-8** is not as much affected as (*R*,*R*)**-8** and its behavior is comparable to (*R*,*S*)**-7** and **10**. Moreover, receptor **9** presents the best binding so far reported with both carboxylate salts [K_a = 2.07 x 10^7 M^{-1} with TBA AcO and K_a = 1.23 x 10^6 M^{-1} with TEA (*S*)-Nap]. Indeed, a favorable positive entropic contribution enhances host-guest interactions. The overall binding is therefore both enthalpically and entropically driven for this receptor. It is in fact important to highlight the role played by entropy in the association behavior. Entropy is somewhat more difficult to control than enthalpy in designing receptors, but receptor **9** proves that a considerable association increase can be achieved by a proper balance between both thermodynamic parameters.

In conclusion, first comparison between (*R*,*R*) and (*R*,*S*) guanidinium scaffold shows the better scaffold organization for (*R*,*S*) receptors in order to form the binding pocket for carboxylate guests.

TBA AcO	(*R*,*S*)-**7**	(*R*,*S*)-**8**	(*R*,*S*)-**9**	(*R*,*S*)-**10**
K_a	5.63 x 10^5	2.05 x 10^5	2.07 x 10^7	9.73 x 10^5
ΔH	-6.88	-7.01	-6.29	-7.31
ΔS	3.58	1.20	12.7	3.27
ΔG	-7.97	-7.37	-10.13	-8.30
TEA (S)-Nap				
K_a	3.39 x 10^5	1.54 x 10^5	1.23 x 10^6	6.56 x 10^5
ΔH	-8.00	-7.54	-7.23	-7.63
ΔS	-1.14	-1.14	3.99	1.43
ΔG	-7.66	-7.19	-8.43	-8.06

*Table 4. Thermodynamic parameters from ITC titrations in CH_3CN at 303K between receptors (R,S)-**7**-**10** and TBA AcO and TEA (S)-Nap (K_a in M^{-1}, ΔH and ΔG in kcal mol^{-1}, ΔS in cal mol^{-1} K^{-1}).*

3.2.2.2 π Interactions Evaluation

In order to study π-stacking interaction between Naproxen and an aromatic moiety, different (*R*,*R*) and (*R*,*S*) receptors were synthesized (Scheme 6). A major factor in aromatic interactions is the nature of the substituents of the aromatic ring. π-clouds with partial charges of opposite sign will stack stronger than the ones of the same sign. As Naproxen possesses an electronically enriched ring (methoxynaphthyl), we decided to use a *p*-nitroaryl derivative as withdrawing group.[33] Receptor **12** was obtained by previous activation of *p*-nitrobenzylamine by CDI in order to get imidazolide **13**. Yields by either direct addition of isocyanate or imidazolide are similar (70%).

[33] Cockroft, S. L.; Hunter, C. A.; Lawson, K. R.; Perkins, J.; Urch, C. J. *J. Am. Chem. Soc.* **2005**, *127*, 8594-8595.

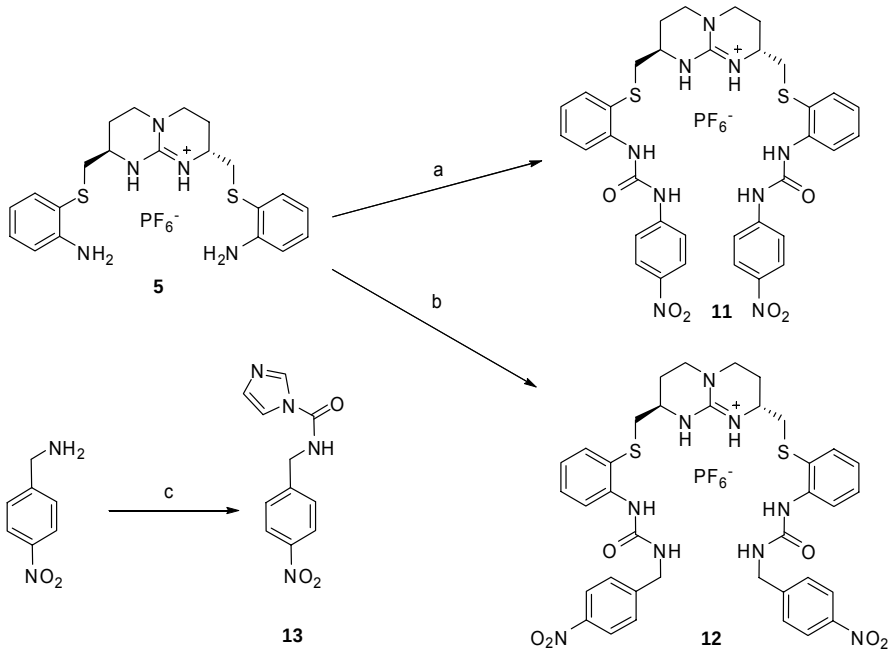

Reagents and conditions: **a**) *p*-nitrophenyl isocyanate, dry CH_2Cl_2, sealed tube, reflux 24 h (70%). **b**) 13, dry MeOH, sealed tube, reflux, 24 h (70%). **c**) *p*-nitrobenzylamine, CDI, THF, 30 min (70%).

*Scheme 6. Synthesis of receptors **11** and **12**.*

^{1}H-NMR titrations were performed between both (*R*,*R*) and (*R*,*S*)-**11** and **12** and TBA AcO and TEA (*S*)-Nap in CD_3CN. A special attention was given to the CH_2 between the urea group and the phenyl ring upon addition of the (*S*)-Nap salt (**a**, Fig 13). Protons **a** are only shifted slightly upfield ($\Delta\delta$ = 0.1 ppm). Comparing these data with those from (*R*,*R*) and (*R*,*S*)-**9** (which do not have any withdrawing group) confirm the absence of relevant new interactions. The upfield shift is rather small and cannot be explained as a rigidification of the system due to π-stacking interactions. Moreover, NOESY were performed and confirm the absence of contacts between the aromatic ring of the host and naphthyl ring of the guest. On the other hand, protons **a** appear as a doublet with AcO^- as counterion (due to coupling with the urea NH) whereas the CH_2 is converted into a doublet of doublets with PF_6^- or (*S*)-Nap^- (due to different environment for each proton).

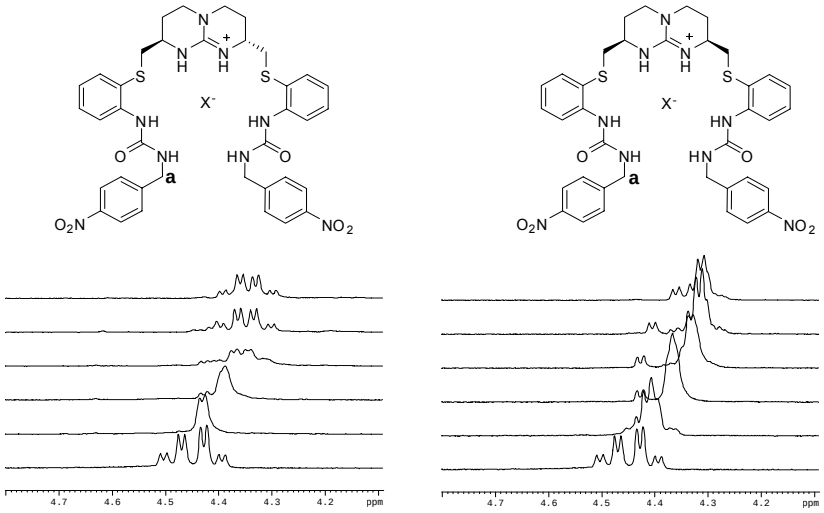

*Fig 13. ^{1}H-NMR titrations between (R,R)-**12** (right) (R,S)-**12** (left) and TEA (S)-Nap in CD_3CN at 298K [from bottom to top: 0 to 1.1 equivalents TEA (S)-Nap].*

ITC titrations were also performed for those receptors (Table 5). K_a are affected moderately (from 6.75 x 10^4 up to 4.25 x 10^5 for (*R*,*R*)-**12** and (*R*,*S*)-**12** respectively). Introducing a nitro group in *para* position of the phenyl results in an enhancement of the binding only for (*R*,*R*)-**11** due to a less negative entropic factor [for (*R*,*S*)-**11**, K_a stays unaffected]. The electronically poor aromatic ring in each leg has such an influence on the organization of the host conformation that it allows a better carboxylate complexation (stacking between each arm as well as repulsion could take place).[34] However, incorporation of the nitro group in the benzyl ring decreases the association constant, considerably for (*R*,*S*)-**12** [two orders of magnitude with TBA AcO and one with TEA (*S*)-Nap] and moderately for (*R*,*R*)-**12** (the entropic contribution is decreasing). More than affecting enthalpy, introduction of a withdrawing group translates into entropy alteration. Thermodynamic parameters measured by ITC are in good agreement with ^{1}H-NMR results and confirm the absence of π-stacking interactions between Naproxen and aromatic surfaces of the host.

[34] Meyer, E. A.; Castellano, R. K.; Diederich, F. *Angew. Chem. Int. Ed*. **2003**, *42*, 1210-1250.

TBA AcO	(*R*,*R*)-**11**	(*R*,*R*)-**12**	(*R*,*S*)-**11**	(*R*,*S*)-**12**
K_a	1.65 x 10^5	6.75 x 10^4	1.02 x 10^5	4.25 x 10^5
ΔH	-7.66	-7.32	-4.07	-6.82
ΔS	-1.17	-2.07	9.46	3.22
ΔG	-7.25	-6.69	-6.94	-7.80
TEA (*S*)-Nap				
K_a	1.24 x 10^5	6.92 x 10^4	9.53 x 10^4	3.90 x 10^5
ΔH	-8.35	-7.74	-5.82	-7.40
ΔS	-4.25	-3.41	3.57	1.15
ΔG	-7.06	-6.71	-6.90	-7.75

*Table 5. Thermodynamic parameters from ITC titrations in acetonitrile at 303K between receptors (R,R) and (R,S)-**11** & **12** and TBA AcO and TEA (S)-Nap (K_a in M^{-1}, ΔH and ΔG in kcal mol^{-1}, ΔS in cal mol^{-1} K^{-1}).*

3.2.2.3 Additional Chirality

Despite the absence of π-stacking interactions between receptors **8-12** and Naproxen, we decided to synthesize receptors (*R*,*R*) and (*R*,*S*) **14-17** containing both an aromatic surface and a stereogenic center in α position of the urea NH (Scheme 7).

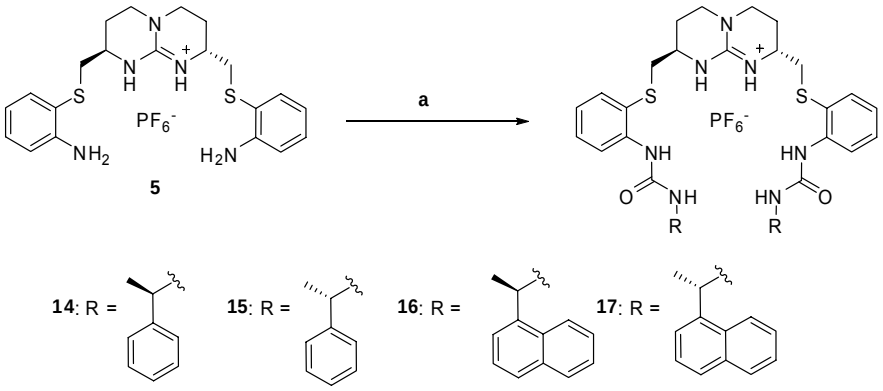

Reagents and conditions: **a**) Isocyanate, dry CH_2Cl_2, sealed tube, reflux 24 h (85-90%).

*Scheme 7. Synthesis of compound **14-17**.*

Single liquid-liquid extractions between **14**-**17** (dissolved in CH_2Cl_2, 1 mg/mL) and aqueous sodium Naproxenate solution (0.08 M) were performed. No discrimination was observed for (*R*,*R*) and (*R*,*S*)-**14**-**17**. As it was previously demonstrated, those receptors do not work as pincer-like receptors and therefore only interact through hydrogen bonds with the carboxylate part of the guest. Naproxen chiral center is therefore free to rotate and discrimination between the enantiomers cannot be achieved. The aromatic surface is not electronically poor enough and the chiral barrier too small to reach the goal.

3.2.3 Pre-Organized Receptors

3.2.3.1 Introduction

As it was stated previously, the too high flexibility of the receptors synthesized so far did not lead to selection. To face this problem, we decided to use guanidinium based macrocycles endowed with a more rigid scaffold and convergent binding groups.

As a preliminary experiment, we decided to study the binding of Naproxen by receptor **18**, previously synthesized for nitrate binding. ^{1}H-NMR titrations with TEA (*S*)-Nap confirm the formation of six H-bonds (Fig 14). No rearrangement of the scaffold was detected (as pointed out in figure 11 for (*R*,*R*)-**8** with protons a, b, c and d).

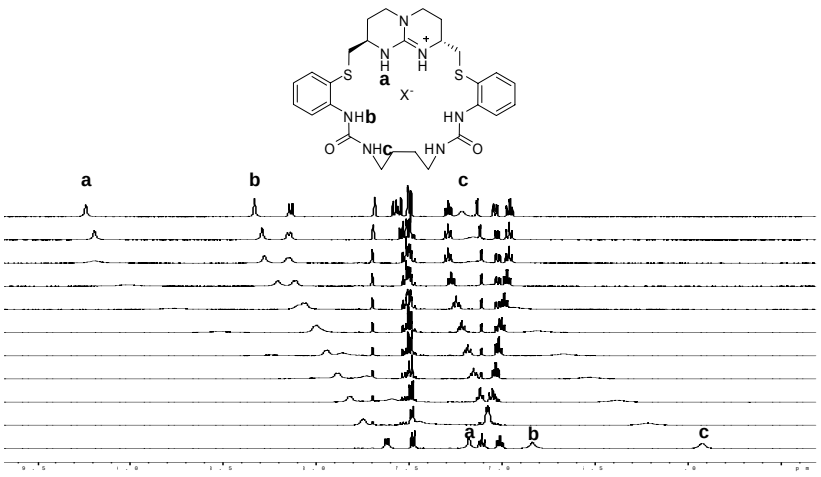

*Fig 14. ^{1}H-NMR titrations between **18** and TEA (S)-Nap in CD_3CN at 298K [from bottom to top: 0 to 1.1 TEA (S)-Nap equivalents].*

Whereas association with AcO is both enthalpically and entropically driven, with both Naproxen enantiomers the binding is mainly entropically driven (due to a higher solvent release for the bigger guest). The large desolvation of host and guest gives rise to a K_a one order of magnitude higher (from 1.47 x 10^5 to 2.16 x 10^6 M^{-1}, Table 6). No discrimination was observed by this macrocycle, probably because the stereogenic centers of the chiral bicyclic guanidinium are too far away from the guest chiral center. Moreover, a single liquid-liquid extraction confirmed this result.

Even if this host-guest complex only shows a subtle entropy gap ($T\Delta\Delta S$ = 1.57 kJ mol^{-1}) which is annihilated by the enthalpy-entropy compensation,[35] it points out the previous remark by Schmidtchen about the association entropy as an indicator of enantiorecognition.[36] Observing an entropy gap considerably higher ($T\Delta\Delta S$ = 7.6 kJ mol^{-1}) with tartrate enantiomers, Schmidtchen reports that the complex of better geometrical fit (lower entropy) displays weaker affinity than the disordered counterpart. By extension, he claims that maximizing host-guest affinity is not the suitable way to reach enantiorecognition. Similar behavior was previously mentioned

[35] a) Dunitz, J. D. *Chem. Biol.* **1995**, *2*, 709-712. b) Exner, O. *Chem. Commun*. **2000**, 1655-1656.

[36] Jadhav, V. D.; Schmidtchen, F. P. *Org. Lett.* **2006**, *8*, 2329-2332.

by Kilburn and co-workers with a thiourea based receptor for the enantiorecognition of glutamate and aspartate.[19d]

	TBA AcO	TEA (*R*)-Nap	TEA (*S*)-Nap
K_a	1.47 x 10^5	1.98 x 10^6	2.16 x 10^6
ΔH	-4.89	-3.77	-2.25
ΔS	7.49	16.3	21.5
ΔG	-7.16	-8.71	-8.76

Table 6. Thermodynamic parameters from ITC titrations in acetonitrile at 303K between receptors ***18*** *and TBA AcO and TEA (R) & (S)-Nap (K_a in M^{-1}, ΔH and ΔG in kcal mol^{-1}, ΔS in cal mol^{-1} K^{-1}).*

3.2.3.2 Lysine Derivative Macrocycle

Introducing new stereogenic centers was considered essential to reach enantioselection. An approach is to induce the chirality in between the two urea moieties. This requires some important characteristics, such as a readily available chiral molecule (diamine or diisocyanate) capable of affording new interaction(s) with the guest. However, few compounds fulfill these requirements. Amino acid derivatives present the right features but only lysine provides a diamine function. Lysine, with its five carbon atom spacer, is indeed a suitable spacer for the formation of the macrocycle. L-lysine *p*-nitroanilide dihydrobromide possesses an electronically poor ring (with a nitro group in *para* position) for π-interactions, a new stereogenic center as well as an additional H-bond donor (amide NH). Macrocycle **19** represents therefore a possible chiral receptor for Naproxen (Fig 15).

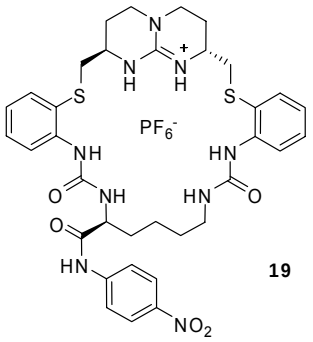

19

*Fig 15. Lysine derivative macrocycle **19**.*

Molecular modeling was performed and showed different interactions for each enantiomer (Fig 16).[37] There is π stacking between the nitrophenyl group of the receptor and the methoxynaphthyl of (*R*)-Naproxenate (Figure 16, (a)). Moreover, the side chain is stabilized by a hydrogen bond between the amide NH and one of the urea's oxygen atoms. For the (*S*)-enantiomer, the global minimum is completely different with carboxylate binding to the center of the ring by 5 hydrogen bonds including the one from the side chain (amide NH) (Figure 16, (b)). Molecular modeling showed indeed an important distinction concerning the guanidinium-carboxylate binding:

- (*R*)-Naproxenate: linear hydrogen bonds
- (*S*)-Naproxenate: non linear hydrogen bonds.

The enthalpy difference between the two complexes is however rather small, only $\Delta\Delta H_{R\text{-}S}$ = 1.2 kcal mol^{-1}, which does not fully account for the quite different geometries predicted for both complexes. The receptor was nevertheless synthesized for binding assays with the target.

[37] Model studies were performed by Martin Smiesko at Anterio Consult & research GmbH, Mannheim (Germany).

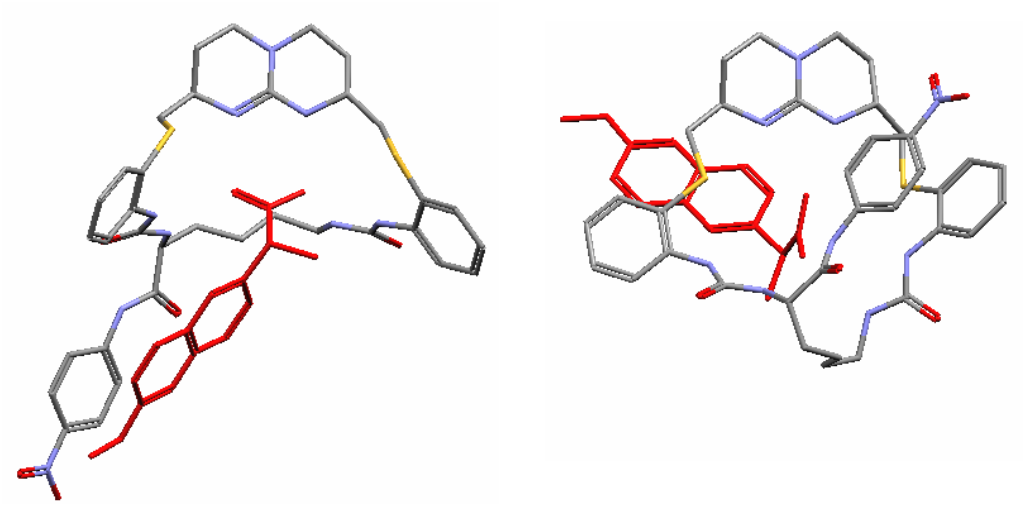

a) b)

*Fig 16. Molecular modeling of **19** with a) (R)-Naproxenate and b) (S)-Naproxenate (hydrogen atoms are omitted and Naproxen is colored in red).*

Bisimidazolide intermediate **20** was synthesized from L-lysine *p*-nitroanilide dihydrobromide in good yield (Scheme 8). The formation of receptor **19** was achieved but purification process did not afford the pure compound. The desired product was indeed detected by LCMS after a first purification by column chromatography. A method in semi-preparative HPLC was therefore developed for purification (Column: SunFire C18 5 µm, 4.6 x 100 mm, FM: CH_3CN (0.1% TFA) / H_2O (0.1% TFA), Gradient: 10-100% CH_3CN (0.1% TFA) in 30 min, Flow: 1 mL/min, ambient Tº). The crude obtained from the column chromatography was thus purified by HPLC and afford the pure product in a modest 8% yield (Fig 17).

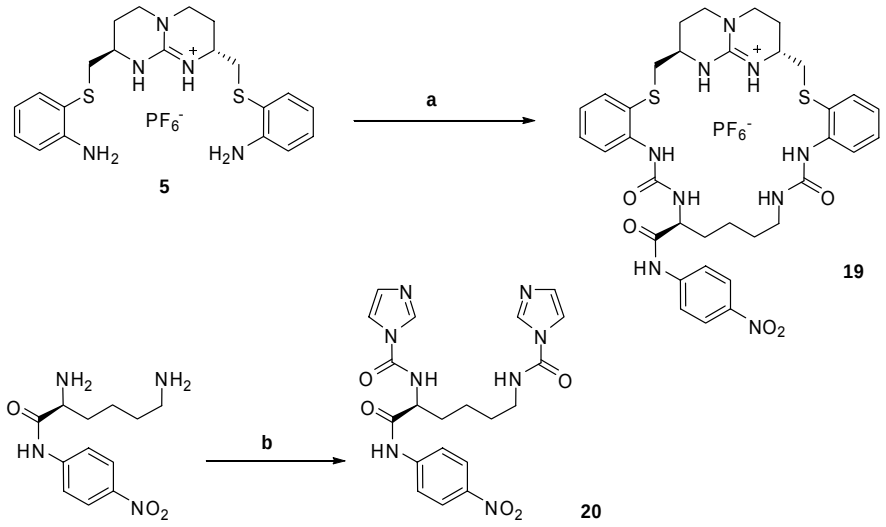

Reagents and conditions: **a**) **20**, dry MeOH, sealed tube, reflux 48 h (8%). **b**) L-lysine *p*-nitroanilide, CDI, THF (95%).

*Scheme 8. Synthesis of macrocycle **19**.*

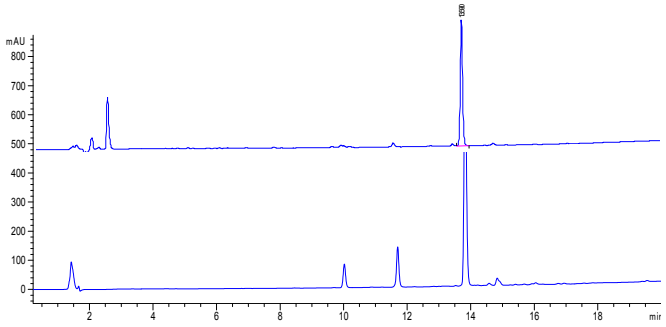

*Fig 17. HPLC spectrum of compound **19** before (bottom) and after (top) purification by semi-preparative HPLC.*

A liquid-liquid extraction between **19** and rac Nap$^-$ Na$^+$ was then performed but no discrimination was observed. This negative result agrees with the theoretical prediction that the energy difference between both complexes is not too high.

3.2.3.3 NOBIN Macrocycles

Attempts of designing an enantioselective receptor for (*S*)-Naproxen were unsuccessful so far. Differentiating the orientation of the methyl group is indeed too demanding for receptors with too high conformational freedom. One step forward is the use of conformationally constrained macrocycles with convergent binding groups (Fig 18). Receptor **19** presents these characteristics but the too flexible chiral barrier did not translate into selectivity. A CPK model revealed indeed that introducing a rigid chiral barrier between the two urea functions would not afford the expected interactions without an efficient control of entropy. However, introduction of such a chiral barrier between the bicyclic guanidinium scaffold and the urea groups might lead to the desired interactions.

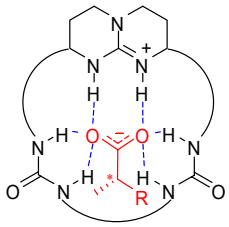

Fig 18. Host-guest interactions between a guanidinium-based macrocycle and an α-methyl carboxylate.

One option is the incorporation of an easily available chiral scaffold. Binaphthol and derivatives have been widely used in asymmetric catalysis. Cram also reported its use for chiral recognition of α-phenylethylamine.[38] However, synthesis of a binaphthol derivative with both accessible thiol SH and amine NH_2 functions remains difficult to achieve.[39] An alternative is use of NOBIN,[40] a ligand bearing an alcohol function

[38] Kyba, E. B,; Koga, K.; Sousa, L. R.; Siegel, M. G.; Cram, D. J. *J. Am. Chem. Soc.* **1973**, *95*, 2692-2693.

[39] Smrčina, M.; Vyskočil, S.; Polívková, J.; Poláková, J.; Sejbal, J.; Hanuš, V.; Polášek, M.; Verrier, H.; Kočovskỳ, P. *Tetrahedron: Asymmetry* **1997**, *8*, 537-546.

[40] a) Smrčina, M.; Lorenc, M.; Hanuš, V.; Sedmera, P.; Kočovskỳ, P. *J. Org. Chem.* **1992**, *57*, 1917-1920. b) Belokon, Y. N.; Bespalova, N. B.; Churkina, T. D.; Císařová, I.; Ezernitskaya,

instead of a thiol that would likely introduce little changes into the binding pocket. On the other hand, the suitable five atoms spacer would be maintained between the NH_{guan} and the first NH_{urea} (the binaphthyl acts as a simple benzene ring in term of distance). Therefore the second H-bond donor located seven atoms away from a guanidinium NH would provide a perfect complement for the otherwise unexploited carboxylate *anti* lone pair.

In an attempt of reducing receptor conformational degree, a short (butyl) or rigid aromatic (xylylene) spacer present the desired characteristics for target selection (Fig 19). In addition, **22** may provide further stabilization by CH-π interactions with the xylylene aromatic ring. Assuming formation of the six H-bonds, CPK models gave some evidence of a difference in stability between the complexes with each enantiomer of Naproxen.

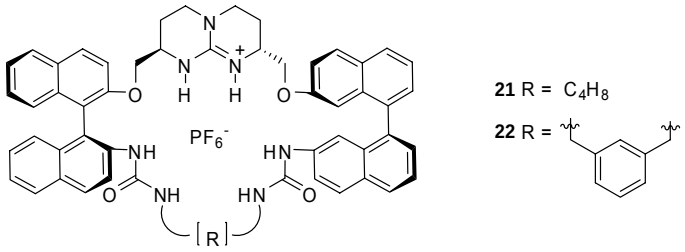

*Fig 19. Guanidinium-based macrocycles **21** and **22**.*

First, deprotection of both silyl groups (OTBDPS and OTBDMS) of guanidinium salt **23** was achieved with HCl in 97% yield (Scheme 9). Then, the guanidinium dichloride product **25** was obtained by reaction with thionyl chloride (95%). As the amine function of (*S*)-NOBIN is more nucleophilic than the alcohol one, a previous BOC protection was performed to afford **28** in a 94% yield.[41b] The guanidinium dichloride salt **25** was then transformed into the diprotected amine **26** with K_2CO_3 in a 65% overall yield. Deprotection by 4N HCl in 1,4-dioxane gives **27**

M.G.; Harutyunyan, S. R.; Hrdina, R.; Kagan, H. B.; Kočovskỳ, P.; Kochetkov, A.; Larionov, O. V.; Lyssenko, K. A.; North, M.; Polášek, M.; Peregudov, A. S.; prisyazhnyuk, V. V.; Vyskočil, S. *J. Am. Chem. Soc.* **2003**, *125*, 12860-12871.

(PF_6^-) in a 98% yield. Reaction with the appropriate diisocyanate in a sealed tube afforded the final products **21** and **22** in 57 and 55% yield, respectively.

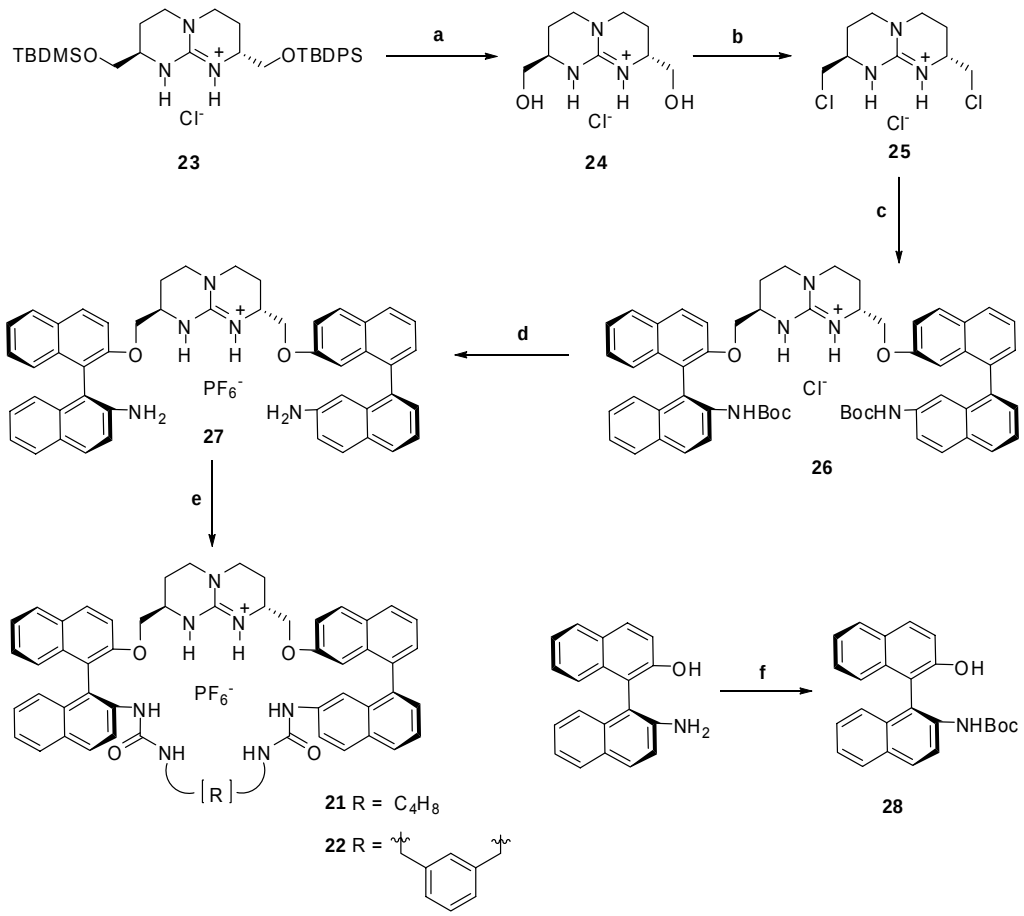

Reagents and conditions: **a**) 3N HCl/CH_3CN (1:2) (97%). **b**) $SOCl_2$, reflux (95%). **c**) **28**, K_2CO_3, acetone (50%). **d**) 4N HCl, 1,4-dioxane, 0,1N NH_4PF_6 (98%). **e**) **21**: 1,4-diisocyanatobutane, dry CH_2Cl_2, sealed tube, 24 h (57%); **22**: *m*-xylylene diisocyanate, dry CH_2Cl_2, sealed tube, 24 h (55%). **f**) (*S*)-NOBIN, $(BOC)_2O$, toluene (94%).

*Scheme 9. Synthesis of macrocycles **21** and **22**.*

21 (Cl^-) was able to be recrystallized in CH_3CN and a solid state X-ray structure was resolved (Fig 20), revealing an unpredicted structure for the complex. The host-guest ion pair is indeed not formed with the guanidinium salt as widely described so

far in our group and in the literature. One oxygen atom from a urea function is thus hydrogen bonded to the guanidinium (N···O 2.863 and 2.789 Å, respectively) whereas the chloride counter-ion is only bound by the two NHs from the second urea (N···Cl 3.088 and 3.247 Å). The orientation of the (*S*)-NOBIN induced each arm to fold apart in order to give the NH_{urea} pointing away from the cavity instead of wrapping around the spherical guest. In addition, each urea function is stabilized by additional intermolecular hydrogen bonds with an urea from another receptor molecule: the NH_{urea} from the function complexed by the guanidinium as well as the oxygen atom from the one bound to the chloride (N···O 2.785 and 2.755 Å). All attempts to obtain a single crystal of a complex with a carboxylate guest for X-ray analysis failed.

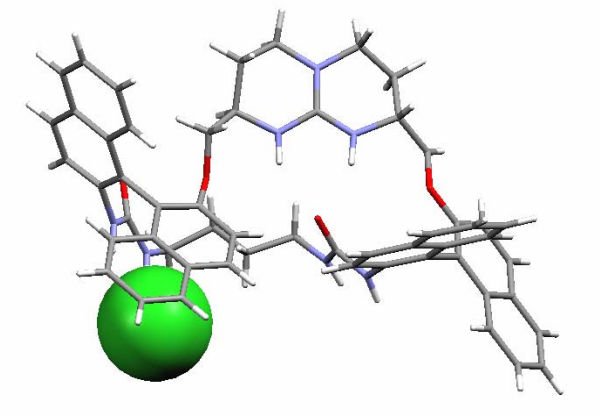

Fig 20. X-ray solid state structure of guanidinium-based macrocycles ***21****(Cl^-).*

At NMR concentration in CH_3CN, **21** crystallized with Cl^- as counter-ion whereas it precipitates in situ with AcO^-. Increasing the temperature to 375K, **21** dissolved again with both counter-ions. With Cl^-, NH_{gua} and NH_{urea} suffered a downfield shift (0.45 up to 0.65 ppm) whereas with AcO^- the NH signals were not detected because of fast equilibrium. ^{1}H-NMR could not afford any additional data on the binding mode of **21** with regard to the counter-ion employed.

Thus, single liquid-liquid extractions were run with receptors **21**, **22** and **26**. The NHBoc groups of **26** are probably also involved in the binding pocket so **26** should therefore be considered also as a potential receptor for enantiorecognition (by ^{1}H-NMR downfield shift of 0.7 ppm from PF_6^- to AcO^- for NHBoc, 1 ppm for NH_{gua}).

The e.e. determined by chiral HPLC was however modest: 10 % for **26**, 20% for **21** and 22% for **22** (Table 7). The (*R*/*S*) ratio is enhanced from **26** to **21**-**22** proving again the advantage of a conformationally restrained macrocyclic structure over a more flexible open one. Nevertheless, from this experiment, the discrimination is quite weak considering the very low selectivity measured (1.5:1).

	26	**21**	**22**
Naproxen	10 % (55/45)	20 % (60/40)	22 % (61/39)

*Table 7. Enantiomeric excess determined by HPLC from liquid-liquid extraction between receptor **26**, **21** and **22** and Naproxenate sodium salt. (R/S ratio is indicated in parenthesis)*

3.3 Combinatorial Approach

3.3.1 Introduction

3.3.1.1 General principles

Designing a host for a concrete guest is one of the current challenging goals of supramolecular chemistry. To do so, two different approaches have so far been developed: the rational design and the "irrational design"[41]. Designing receptors with predictable association and selectivity towards small to medium-sized molecules has reached a good degree of success.[42] Nevertheless, the main drawback of this approach is that the goodness of the design is only validated at the end of the study, after receptor synthesis and binding properties evaluation. The precedent chapter provides a number of typical examples. Besides, as the target is becoming trickier to be selectively recognized, in particular for enantiomers, the host design turns out to be a less certain method. Alternatively, efforts have been employed to use a more "biomimetic approach". Combinatorial chemistry proposes indeed to generate a large

[41] Brenner, S.; Lerner, R. A. *Proc. Nati. Acad. Sci.* **1992**, *89*, 5381-5383.

[42] Lavigne, J. J.; Anslyn, E.V. *Angew. Chem. Int. Ed.* **2001**, *40*, 3118-3130.

number of compounds capable of binding a target. Selection of the most suitable one for its desired property is though achieved by rapid screening of the library. Synthetic expenditure is reduced while the possibilities of generating an effective receptor are enhanced highlighting this approach as very attracting.

The combinatorial chemistry concept was first reported in 1988[43] and published in 1991.[44] Since then, this approach has been widely employed and successfully reported. One reason of this fast growth is the rapid generation of compounds and screening of biological activity.[45] Combinatorial chemistry first played a significant role in chemical biology and currently extends to almost all fields of chemistry such as host-guest chemistry.[46] The combinatorial approach to the identification of selective peptide receptors was pioneered by Still in the 1990's.[47] Afterwards, another approach for receptor discovery appears by the use of dynamic combinatorial libraries (DCL) pioneered by the research group of Sanders and Lehn.[48]

Considering the field of supramolecular chemistry, combinatorial receptor design is the first step toward the generation of a library. "Tweezers" or "two-armed" receptors have been then widely developed.[49] Such receptors possess a scaffold or "head group" which pre-organizes the substrate binding arms as well as containing the binding functionality. Attachment of this scaffold to a solid support is necessary for solid phase synthesis of the library. Parallel synthesis of the arms by means of Split

[43] Furka, A.; Sebestyen, F.; Asgedom, M.; Dibo, G. *Abstr. 14th Int. Congre. Biochem., Prague, Czechoslovakia,* **1988**, Budapest, Hungary, 288.

[44] a) Furka, A.; Sebestyen, F.; Asgedom, M.; Dibo, G. *Int. J. Pept. Protein Res.* **1991**, *37*, 487-493. b) Houghten, R. A.; Pinilla, C.; Blondelle, S. E.; Appel, J. R.; Dooley, C. T.; Cuervo, J. H. *Nature* **1991**, *354*, 84-86. c) Lam, K.; Salmon, S.; Herch, E.; Hruby, V.; Kazmierski, W.; Knapp, R. *Nature,* **1991**, *354*, 82-84.

[45] Lowe, G. *Chem. Soc. Rev.* **1995**, 309-317.

[46] Linton, B.; Hamilton, A. D. *Curr. Opin. Chem. Biol.* **1999**, *3*, 307-312.

[47] Still, W. C. *Acc. Chem. Res.* **1996**, *29*, 155-163.

[48] a) Huc, I.; Lehn, J. M. *Proc. Natl. Acad. Sci. U.S.A.* **1997**, 94, 2106-2110. b) Otto, S.; Burlan, R. L. E.; Sanders, J. K. M. *Curr. Opin. Chem. Biol.* **2002**, *6*, 321-327. c) Rowan, S. J.; Cantrill, S. J.; Cousins, G. R. L.; Sanders, J. K. M.; Stoddart, J. F. *Angew. Chem. Int. Ed.* **2002**, *41*, 898-952.

[49] Srinivasan, N.; Kilburn, J. D. *Curr. Opin. Chem. Biol.* **2004**, *8*, 305-310.

and Mix method is then achieved using different monomer units (Fig 22). Higher order or multi-armed receptors have also been reported.

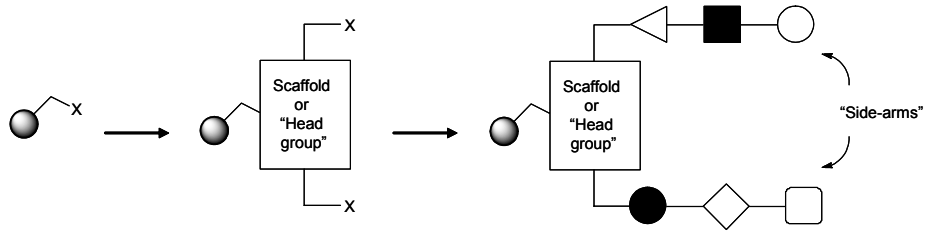

Fig 22.Combinatorial approach to tweezers receptors proceeds.

Combinatorial chemistry generates large libraries and detection method of the effective compound is therefore the major feature of this approach. A common strategy has been to attach fluorescent or color dyes to the receptor (or to the guest) in order to accelerate the detection process. Beads that show the greatest fluorescence or color are selected and decoded to identify the compound structure. This methodology has been successfully employed over the years for different kind of host-guest systems (an example is shown in Fig 23 with sulfonamide tweezers)[50]. High-throughput detection is indeed based on visual examination and is part of the rapid expansion of combinatorial approach for receptor chemistry.

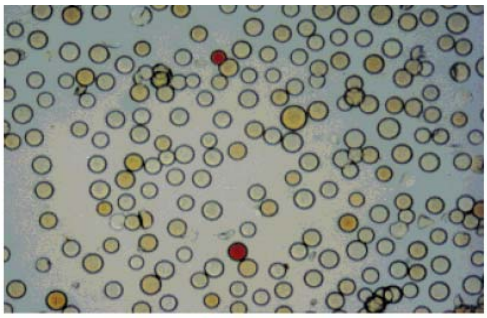

Fig 23. Photographs of a screening assay of tweezers receptors for binding to a bead-supported tripeptide library.

[50] Löwik, D. W. P M.; Weingarten, M. D.; Broekema, M.; Brouwer, A. J.; Still, W. C. Liskamp, R. M. J. *Angew. Chem. Int. Ed.* **1998**, *37*, 1846-1850**.**

Still and co-workers have successfully applied the chemosensor process to the sequence-selective peptide detection.[51] The peptide-binding receptors contain both a fluorophore (***F***) and a quencher (***Q***) (Fig 24). In the absence of binding, ***F*** is quenched intramolecularly by the second fluorophore ***Q***. When peptide analyte is bound in chloroform, the separation between ***F*** and ***Q*** increases causing the enhancement of fluorescence emission and can be visually detected. Besides, the fluorescence amplification was used to measure the binding constants between the selected receptors and tripeptides (by fluorescence-monitored titrations).

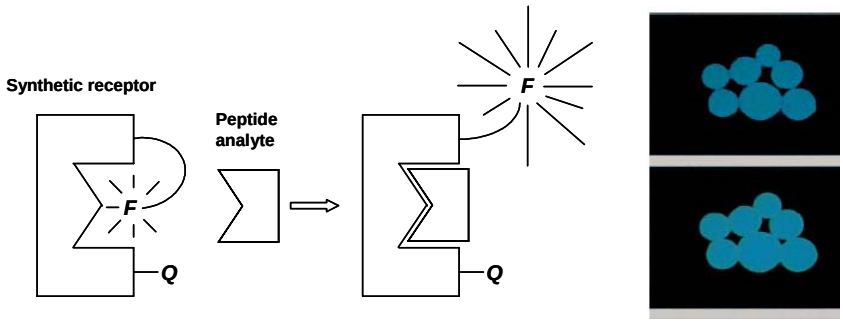

a) b)

Fig 24. a) *Analyte binding to the synthetic receptor increases the average separation between* ***F*** *and* ***Q****, resulting in enhanced fluorescence and b) fluorescence of the receptor with (bottom) or without (top) their peptide.*

3.3.1.2 Combinatorial Approach based on Guanidinium Receptors

In the process of designing combinatorial receptor, various functionalities have been incorporated in its scaffold depending on the target desired. A few research groups synthesized combinatorial libraries based on guanidinium receptors because of forming a good complement with a carboxylate terminus of peptides.

Kilburn and co-workers synthesized a library of symmetrical tweezers constituted by 2197 members incorporating a guanidinium scaffold and two tripeptide arms.[52] Screening of the library with the dye-labeled tripeptide Glu(O*t*Bu)-Ser(O*t*Bu)-

[51] Chen, C. T.; Wagner, H.; Still, W. C. *Science* **1998**, *279*, 851-853.

[52] Jensen, K. B.; Braxmeier, T. M.; Demarcus, M.; Frey, J. G.; Kilburn, J. D. *Chem. Eur. J.* **2002**, *8*, 1300-1309.

Val allows identification of a selective receptor in aqueous solvent (Fig 25a). The receptor was then synthesized by an independent way and binding constants, measured by UV titrations, confirmed its selectivity over the tripeptide enantiomer and the side chain deprotected tripeptide.

Kilburn has also recently reported the synthesis of an unsymmetrical 15625-membered library (Fig 25b).[53] Screening of the library with the bacteria wall cell precursor tripeptide *N*-Ac-Lys-D-Ala-D-Ala was achieved in order to identify a selective receptor. Binding study on solid state demonstrates its selectivity over the diastereoisomeric peptide *N*-Ac-Lys-L-Ala-L-Ala.

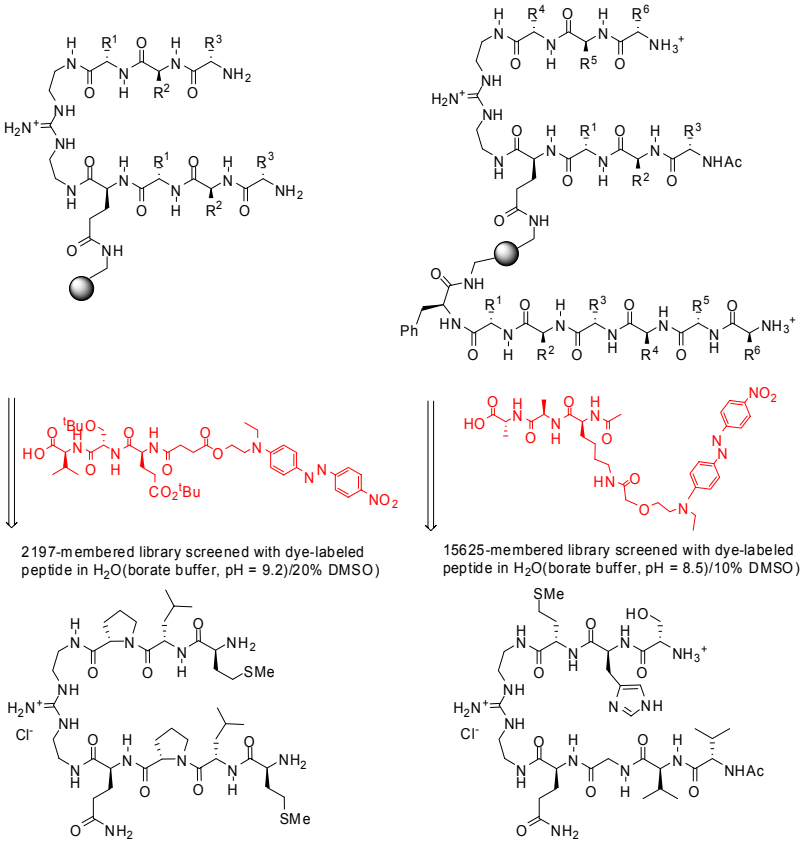

Fig 25. Two receptor libraries derived from a guanidinium scaffold: a) symmetrical and b) unsymmetrical tweezers.

[53] Sheperd, J.; Gale, T.; Jensen, K. B.; Kilburn, J. D. *Chem. Eur. J.* **2006**, *12*, 713-720.

Schmuck employs combinatorial receptor library in order to extend his guanidiniocarbonyl pyrrole scaffold (good complement for dipeptides) to larger substrates as tetrapeptides.[54] Particularly interesting is the introduction of a statistical method QSAR analysis (quantity structure-analysis relationship) in order to show that a nonhydrophobic tetrapetpide could be bound by a one-armed receptor in water without additional hydrophobic interaction or metal-ligand interactions.[55] Ion-pair formation in combination with hydrogen bonds is indeed the main driving force of the complex formation.

Recently, Schmuck and co-workers reported a remarkable stereoselectivity between D and L-Ala in a combinatorial library of 320 substrates (Fig 26). The stereoselectivity is only observed when the position of D/L-Ala exchange takes place is fixed at both sides by strong electrostatic interactions between the receptor and the substrate.[56]

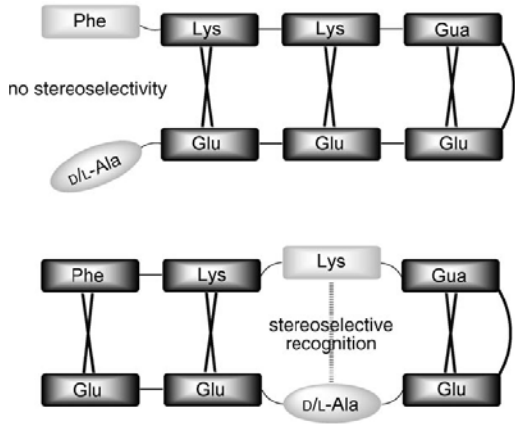

Fig 26. Stereoselectivity of receptor (top) depends on the sequence of the bound substrate (bottom).

As an alternative to produce a highly selective receptor, Anslyn introduced the concept of "differential" receptors, i.e. receptors that have different binding

[54] Schmuck, C. *Coord. Chem. Rev.* **2006**, *250*, 3053-3067 and references herein.

[55] Schmuck, C.; Heil, M.; Scheiber, J.; Baumann, K. *Angew. Chem. Int. Ed.* **2005**, *44*, 7208-7212.

[56] Schmuck, C.; Vich, P. *Angew. Chem.Int. Ed.* **2006**, *45*, 4277-4281.

characteristics but none of which is necessarily very specific or selective.[57] An array of sensors are generated and the composite signal evaluated by pattern-recognition protocols. Using this model, Anslyn and co-workers reported a sensing method utilizing a combinatorial library of receptors that can differentiate between structurally similar analytes, such as nucleotide phosphates (ATP, GTP and AMP) in water. The receptors possess guanidinium groups (known for their good affinity with nucleotide triphosphates) and two tripeptide arms for differential binding (Fig 27). A 4913-membered library was then generated and thirty beads were then selected and fluorescein was though introduced and bound to the receptor. On binding the analyte, the fluorescein is displaced and the beads lose the staining from the dye (the light emission was recorded and analyzed). This study demonstrates that each receptor responded differently to the three nucleotide phosphates.[58]

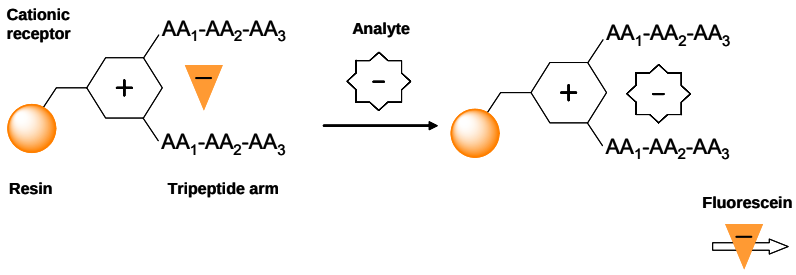

Fig 27. Signal transduction scheme used to detect nucleotide phosphates within the resin bound sensor.

3.3.1.3 Combinatorial Approach for Enantioselective Substrate

Combinatorial approach appears as an excellent alternative for the very demanding selective recognition of a single enantiomer.

[57] Lavigne, J. J.; Anslyn, E. V. *Angew. Chem. Int. Ed.* **2001**, *40*, 3118-3130.

[58] a) Schneider, S. E.; O'Neil, S. N.; Anslyn, E. V. *J. Am. Chem. Soc.* **2000**, 122, 542-543. b) McCleskey, S. C.; Griffin, M. J.; Schneider, S. E.; McDevitt, J. T.; Anslyn, E. V. *J. Am. Chem. Soc.* **2003**, 125, 1114-1115.

Still's research group reported a 60-membered library of receptors for enantiorecognition of proline derivatives.[59] Module A (15 D- and L-amino acids) carries the nucleophilic/basic amine, module B (*RR* or *SS* stereoisomers) links module A and C toward one another and Module C (*RRRR* or *SSSS*) provides the large functionalized surface (Fig 28). Screening with dye-labeled amino acid derivatives shows beads that turn blue (binding of the L configuration) or red (for the D-enantiomer). No enantiorecognition was concluded when brown color was obtained. Enantioselectivity excesses range from 39 to 81%.

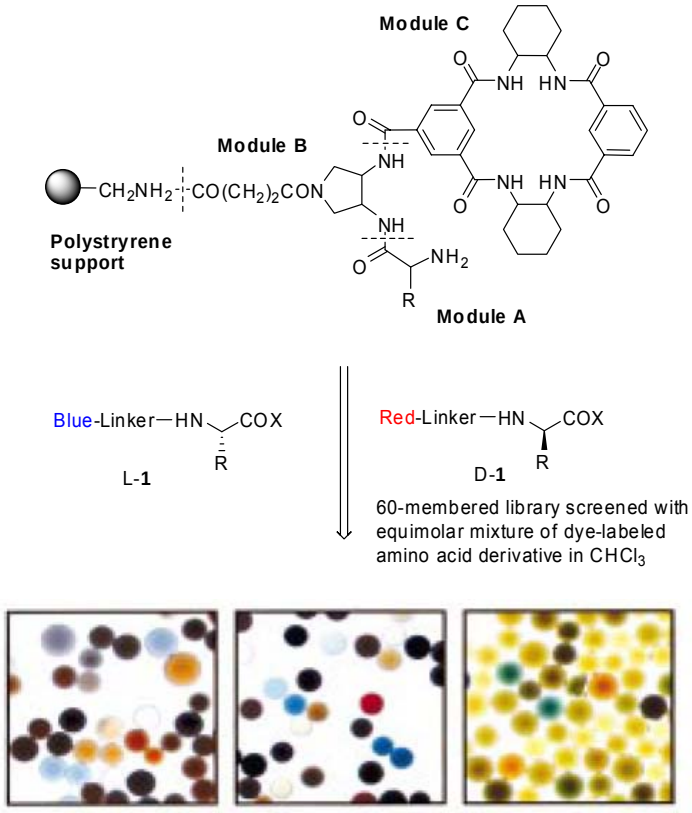

Fig 28. 60-membered library for enantiorecognition of proline derivatives.

[59] Weingarten, M. D.; Sekanina, K.; Still, W. C. *J. Am. Chem. Soc.* **1998**, 120, 9112-9113.

Fréchet and co-workers used combinatorial chemistry for developing highly selective chiral stationary phases (CSP) for HPLC. A first approach uses the principle of reciprocal association.[60] A single enantiomer of the target racemate is immobilized on a solid support and tested for separation of a 140-membered library of substituted dihydropyrimidines. The compound with the highest separation is synthesized and one enantiomer is attached to a solid support, thus the new CSP affords an effective medium for separation of the target. A second approach employs libraries of mixed chiral selectors immobilized on polymer beads.[61] The chiral phases are tested in the separation of racemic targets followed by deconvolution in order to obtain an optimized separation medium (Fig 29). In this context, only 11 different columns are necessary instead of 36 for a classical approach.

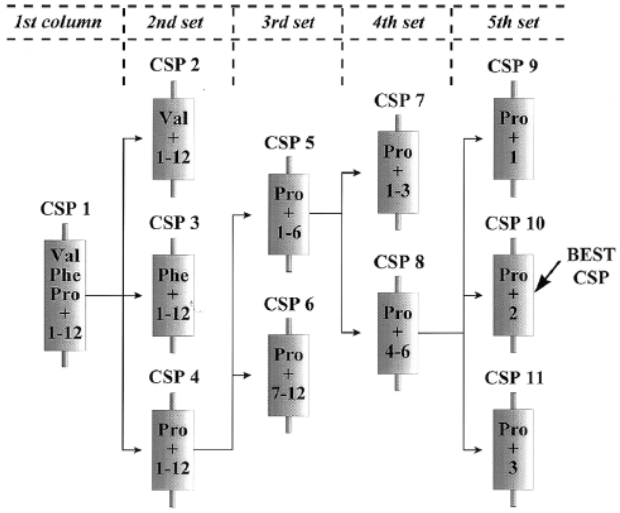

Fig 29. The mixed selector column approach by Fréchet et al.

Gagné et *al.* have recently reported the first use of a racemic dynamic combinatorial library (DCL) for enantiomeric recognition of (-)-adenosine.[62] Templating the racemic DCL with the enantiopure (-)-adenosine indeed amplifies the

[60] Lewandowski, K.; Murer, P.; Svec, F.; Fréchet, J. M. J. *Chem. Commun.* **1998**, 2237-2238.
[61] Murer, P.; Lewandowski, K.; Svec, F.; Fréchet, J. M. J. *Chem. Commun.* **1998**, 2559-2560.
[62] Voshell, S. M.; Lee, S. J.; Gagné, M. R. *J. Am. Chem. Soc.* **2006**, 128, 12422-12423.

most suitable host (Fig 30). Rac-**IX** is composed of a racemic proline and an achiral peptide. The addition of TFA deprotects the acetal and initiates reversible hydrazone exchange to form cyclic oligomers. Templating the racemic DCL amplified the dimer over higher order oligomers. Examining then the template effect of (-)-adenosine with (*S*)-**IX** and (*R*)-**IX** DCL showed the increased formation of dimer with (*S*)-DCL. Laser polarimetry allows indeed detection of the enantioselective peptide-like receptor (*S*,*S*)-**X.**

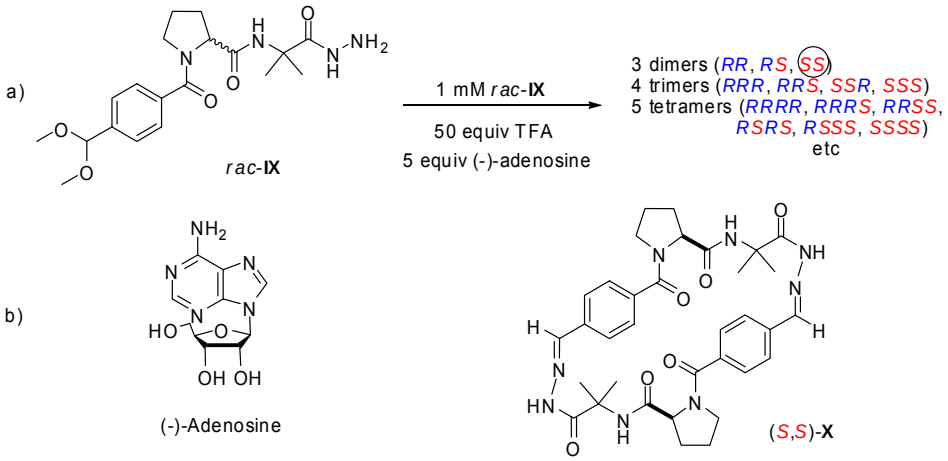

*Fig 30. a) Racemic DCL for (-)-adenosine;b) enantioselective receptor (S,S)-**X**.*

3.3.2 Combinatorial Approach to (*S*)-Naproxen Enantiorecognition

3.3.2.1 Previous Work

A receptor for enantiorecognition of (*S*)-Naproxen was previously synthesized in our group according to a strategy balanced between rational design and combinatorial approach.[63] One arm was designed to fix the complex by means of one additional hydrogen bond (amide NH) and π-interactions; the second arm was synthesized from the screening of a dipeptide library (Scheme 10a). 13 different amino acids were used for the dipeptide library creating 169 members. On the other hand, a red dye was attached to each enantiomer of Naproxen for the screening of the potential receptor. Some of these beads that colored on adding red-dyed (*S*)-Naproxen

[63] Pérez-Velasco, Alejandro **2002**, *DEA Universidad Autónoma de Madrid*.

but not with (*R*)-Naproxen were identified. The sequence Trp-Ser appeared three times and therefore a receptor containing this dipeptide was synthesized (Scheme 10b). Extraction was performed between racemic Naproxenate and the final receptor. However, ^{1}H-NMR as well as chiral HPLC pointed out the lack of selectivity of this receptor. Besides, two equivalents of guest were extracted whereas guanidinium receptors form only 1:1 complexes with the guest. Likely, a too low number of dyed beds were selected for screening, so the found consensus was simply an artifact. This was due to the deconvolution method employed, based on quite expensive Edman degradation sequences, that prevented a larger number of beads to be screened.

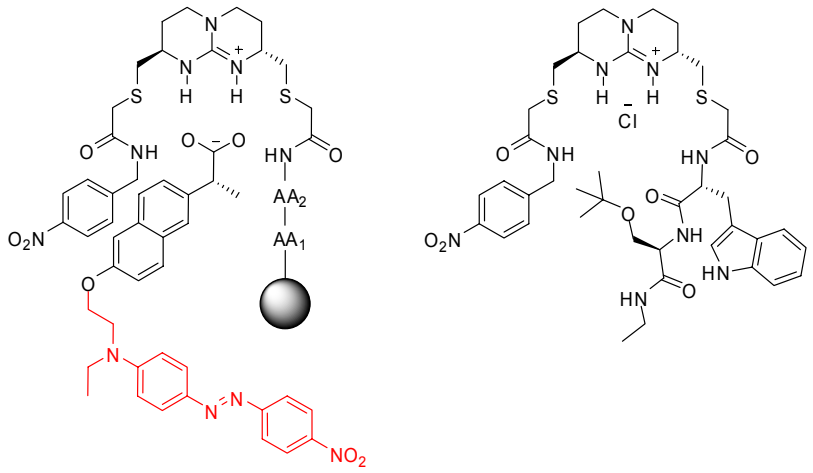

Scheme 10. a) Previous combinatorial approach to enantiorecognition of (S)-Naproxen and b) receptor synthesized.

3.3.2.2 New Approach

It appears essential to generate a peptide library because of the presence of the amino acid chiral center as well as the additional peptidic hydrogen bonds. Here, we aim at employing a larger peptide library using 8 different amino acids with 4 coupling steps: a library of 4096 members is therefore available.

In addition to the creation of a larger library, the combinatorial receptor was redesigned in order to get closer the peptide to the chiral center of the guest. Attaching the tetrapeptide directly to the receptor scaffold through an amine function located

three atoms away from the guanidinium moiety should better orient the discrimination of one enantiomer (Scheme 11a). A second proposal is based on an asymmetric receptor incorporating a urea function in one arm and the peptide library in the other (scheme 11b). The carboxylate part of the guest would bind to both guanidinium and urea NH getting a different orientation towards the peptide library. It was particularly attractive to compare screening results from these two receptors in order to look for the more effective one.

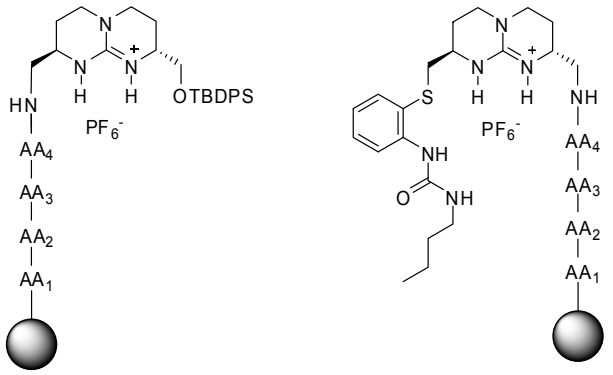

a) b)

Scheme 11. New tetrapeptidic guanidinium receptors.

Dye-labeled substrates are often giving misleading results due to false visual interpretations of the colored beads. A fluorescent probe appears to be a more reliable tool for screening. Moreover, its use has been successfully reported so far.[54] To do so the good chromophore Dansyl was attached to each enantiomer of the Naproxen through its methoxy group in order to not influence the chiral recognition process (scheme 12).

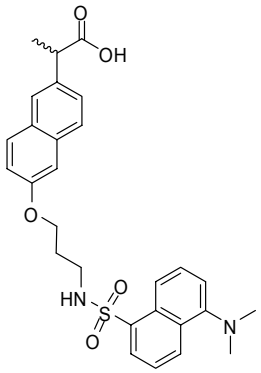

Scheme 12. Fluorescent Naproxen.

3.3.2.3 Synthesis of Guanidinium Receptors Libraries

Among the principal methods used in combinatorial chemistry, the *Split and Mix* one was employed for the synthesis of the tetrapeptide library.[64] At the end of the synthesis, one bead contains one single compound. An exemple of a Split and Mix method for three different amino acids with three coupling steps is shown in scheme 13. First, the resin is partionated in three different batches with the same amount of resin. After the amino acid coupling, a capping agent is added in a 15% yield in the resin periphery for tagging purposes. This agent will allow amino acid sequence identification by mass specrrometry, a more convenient and economic way than Edman degradation[65] sequencing. Batches are then mixed together followed by a deprotection step. Three different batches are then partionated again with the same amount of resine. The same procedure as previously described is performed: amino acid coupling, capping agent reaction, mixing, deprotection and division in three batches. This procedure is then repeated once again. For this example, with three different amino acids added each step, and three coupling steps, $3^3 = 27$ different beads are obtained corresponding to each single compound.

[64] The tetrapeptide library synthesis and the screening experiments were performed by Dr. Sandrine Peroche in collaboration with Jon Shepherd at Prof. Jeremy Kilburn's laboratory in Southampton, U.K..

[65] Edman, P.; Begg, G. *Eur. J. Biochem.* **1967**, *1*, 80-91.

The exact loading of the resin was determined by colorimetry with UV spectroscopy. The degree of substitution was established to be 0.215 mmol/g, in good agreement with theoretical value (0.21 mmol/g).

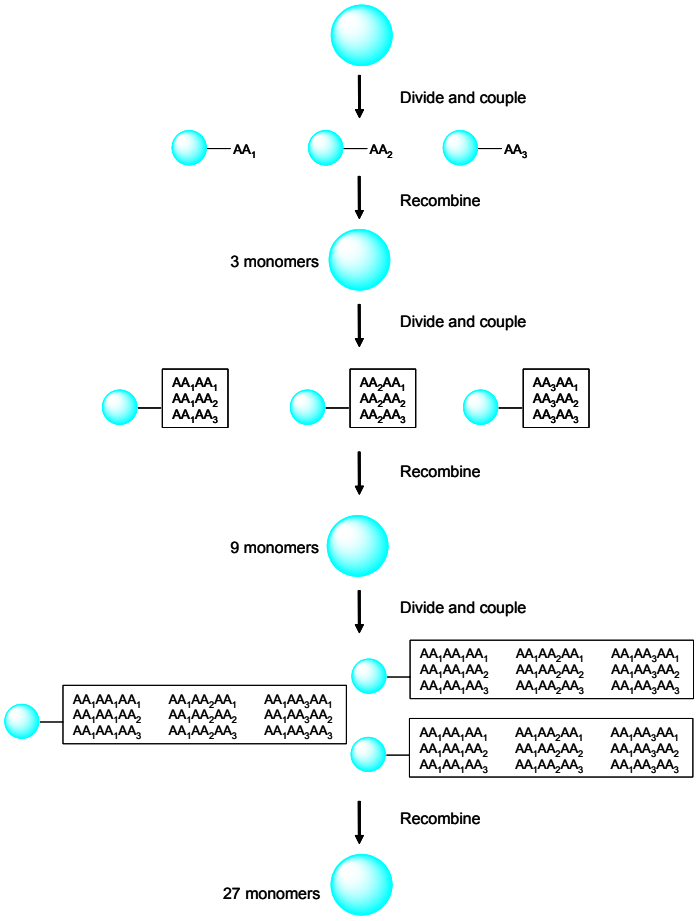

Scheme 13. Split and Mix method for three amino acids with three synthetic cycles.

The synthesis of our first combinatorial receptor **31** is described in scheme 14. Selective deprotection of the TBDMS group was followed by the activation as a methanosulfonate derivative **30** in a 98% yield. Incorporation of the tetrapeptide library was achieved with DIPEA in DMF on solid phase in order to afford receptor **31**.[64]

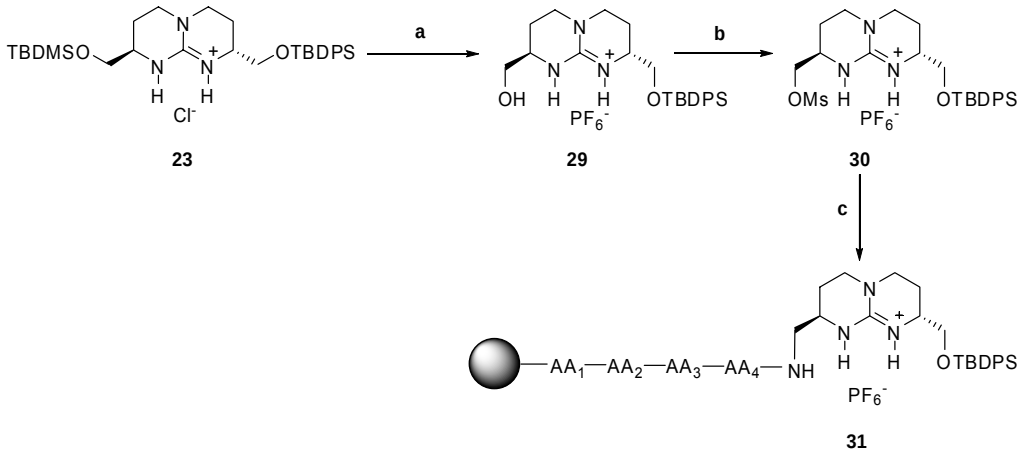

23 **29** **30** **31**

Reagents and conditions: **a**) H_2O-HOAc-THF (1:3:1), 24 H (98%). **b**) Ms_2O, NMM, THF (95%). **c**) DIPEA, DMF.

*Scheme 14. Synthesis of guanidinium receptor **31**.*

Scheme 15 describes the synthesis of the second combinatorial receptor **36**. Introduction of the 2-aminothiophenol group was achieved with Cs_2CO_3 in 70% yield followed by urea formation upon addition of butylisocyanate in dry CH_2Cl_2 in a sealed vessel in 75% yield. Deprotection of the second protecting group TBDPS by TBAF was again followed by activation as methansulfonate derivative **35** in 90% yield. Coupling with the tetrapeptide library was done with DIPEA in DMF in order to afford final receptor **36**.

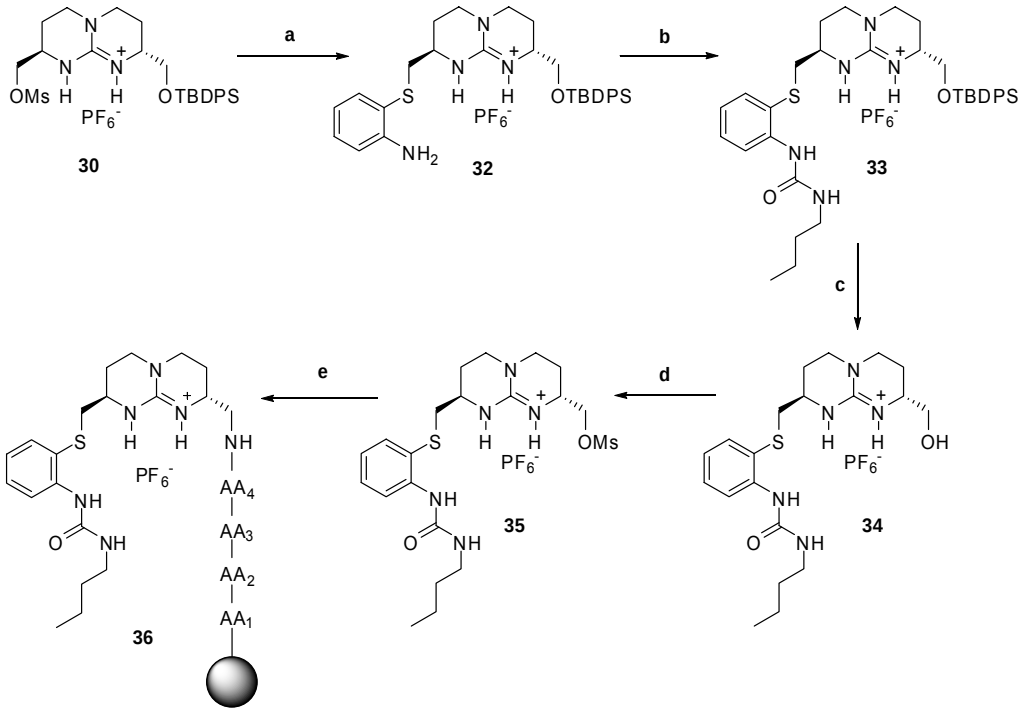

Reagents and conditions: **a**) 2-aminothiophenol, Cs_2CO_3, CH_2Cl_2 (70%). b) butylisocyanate, dry CH_2Cl_2 (75%). c) TBAF, dry THF (86%). d) Ms_2O, NMM, THF (90%). e) DIPEA, DMF.

*Scheme 15. Synthesis of guanidinium receptor **36**.*

3.3.2.4 Synthesis of a Fluorescent Naproxen

At first, fluorescein was chosen as the chromophore to be attached to the Naproxen. Fluorescein was previously employed by our research group and attached to a tetraguanidinium receptor.[66] The fluorescent (*R*) and (*S*)-Naproxen **37** was therefore synthesized (Scheme 16).[67]

Afterwards, screening experiments were performed on adding the fluorescent (*R*) or (*S*)-Naproxen **37** to the receptor library **31**. However, all beads turned out to be fluorescent and no selectivity was therefore noticed. The fluorescein carboxylate

[66] Fernández-Carneado, J.; Van Gool, M.; Martos, V.; Castel, S.; Prados, P.; de Mendoza, J.; Giralt, E. *J. Am. Chem. Soc.* **2005**, *127*, 869-874.

[67] (*R*) and (*S*)-**37** were synthesized by Dr. Sandrine Peroche, unpublished results.

moiety may act as a competitive function to the carboxylate part of the Naproxen and be responsible for the overall fluorescence.[64]

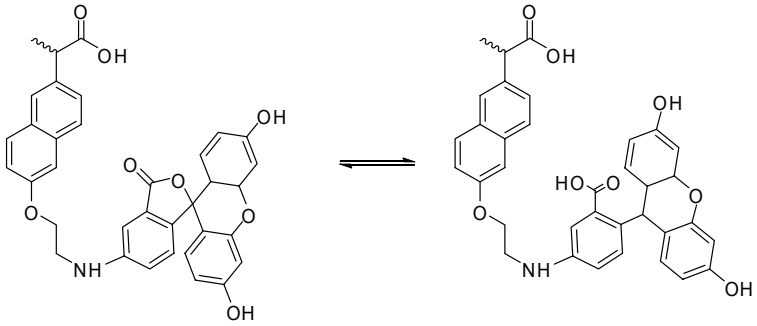

*Scheme 16. Fluorescent (R) and (S)-Naproxen **37**.*

As an alternative to fluorescein, the dansyl group was thus attached to the Naproxen. Demethylation of the naphthyl group of the Naproxen followed by the protection of the carboxylic acid function was the successful strategy to introduce the dansyl group (Scheme 17).[68] A chain large enough has to be introduced between the fluorophore and the Naproxen to avoid interaction with the host.

A Boc was preferred over a benzyl or methyl group as the protective group of the carboxylic acid function of the Naproxen during the synthesis. Alkylation of such compounds was indeed rather complicated and never afforded the desired product.

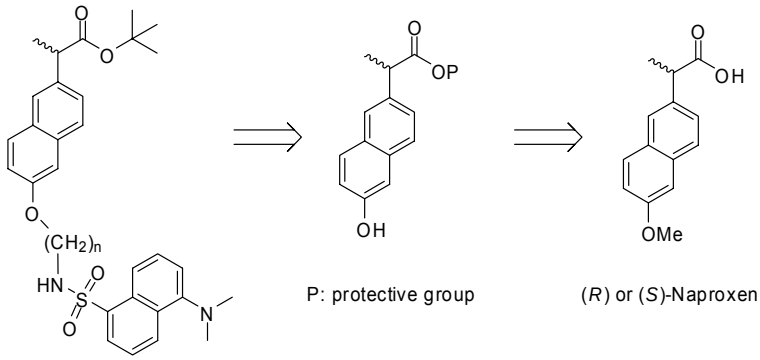

Scheme 17. Retrosynthetic pathway to the fluorescent dansyl-Naproxen.

[68] A similar strategy was previously used for the introduction of a dye: see ref. 63.

Demethylation of the naphthyl group was first achieved with BBr_3 in CH_2Cl_2 at 0ºC in quantitative yield. However, characterization of purified **38** by chiral HPLC (Whelk-01(*S*,*S*)) revealed a partial racemization of the compound. Almost 40% of (*R*)-**38** was formed starting from (*S*)-Naproxen. The procedure using BBr_3 was then replaced by HBr and eventually HCl at reflux giving the desired compound **38** without racemization (according to results reported by Dickinson *et al*.)[69]. The too harsh conditions of BBr_3 procedure may induce a proton transfer in α position of the carboxylic acid moiety through formation of the corresponding, easily enolizable acyl bromide.

Protection of the carboxylic acid function was then performed with trifluoroacetic anhydride and *tert*-butanol in dry CH_3CN in 87% yield.[70]

Starting from dansyl chloride, the derivatives **41** and **42** with respectively two different leaving groups MsO and Br were obtained in good yields. However, coupling the chromophore derivatives **41** or **42** with the protected Naproxen **39** never produced the desired compound. It seems that **41** or **42** degrades during the reaction prior to reacting. **39** was indeed recovered unchanged (Scheme 18).

[69] Lo, A.; Addison, R. S.; Hooper, W. D.; Dickinson, R. G. *Xenobiotica*, **2001**, *31*, 309-319.

[70] Optimization synthesis of **39** was performed by Dr. Sandrine Peroche.

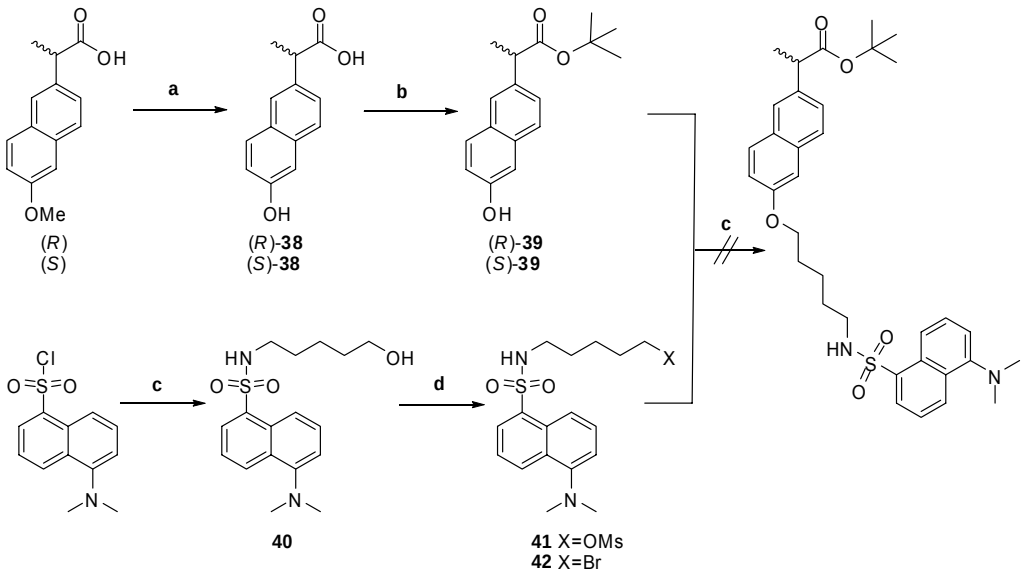

Reagents and conditions: **a**) HCl reflux (88%). **b**) $(CF_3CO)_2O$, ^tBuOH, dry THF (87%). **c**) Et_3N, THF (99%). **d**) for X = OMs : Ms_2O, NMM, THF (88%); for X = Br : CBr_4, PH_3P, CH_2Cl_2 (70%). **e**) K_2CO_3, THF.

Scheme 18. Synthesis attempt of fluorescent Dansyl-Naproxen.

A reverse strategy was then employed: alkylation of the naphthyl group followed by introduction of the dansyl part (Scheme 19). Alkylation of **39** by 1,3-dibromopropane was achieved in THF with K_2CO_3. Yield increased from 50 up to 75% as the number of 1,3-dibromopropane equivalents is increased from one to five (to prevent disubstitution).

Besides, dansyl amine **44** was obtained from dansyl chloride in 50 % yield.[71] Reaction between protected Naproxen **43** and dansyl amine **44** gives the desired compound **45** in a 90% yield. Deprotection of the Boc group in the presence of 30% TFA in dichloromethane and a catalytic amount of triethylsilane gives the final compound **46** in 95% yield.

[71] Jersey, J. A.; Choshen, E.; Jensen, J. N.; Johnson, J. D. *Environ. Sci. Technol.* **1990**, *24*, 1536-1541.

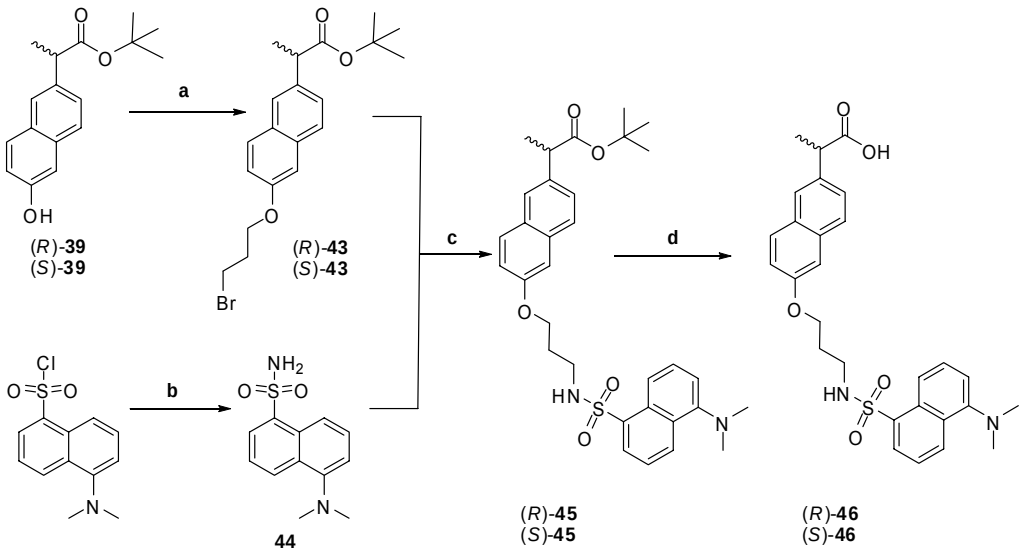

Reagents and conditions: **a**) 1,3-dibromopropane, K_2CO_3, THF (75%). **b**) NH_3 (30%), (50%). **c**) K_2CO_3, CH_3CN (90%). **d**) Et_3SiH, TFA, CH_2Cl_2 (95%).

*Scheme 19. Synthesis of fluorescent (R) and (S) Dansyl-Naproxen **46**.*

The chromatogram of final products (*R*) and (*S*)-**46** in chiral HPLC is shown in figure 29. A ratio of 90/10 was measured for each enantiomer. Some racemization occurs during the final step, however. Recrystallization was attempted in several solvents and mixed solvents without success. For this reason, purification at a small scale (just a few milligrams to perform the experiments) was achieved by analytical chiral HPLC (Fig. 29 bottom).

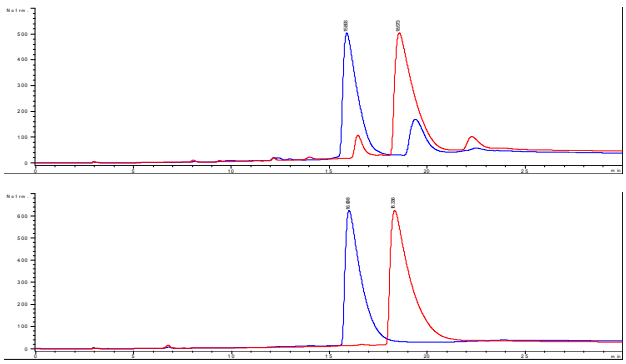

*Fig 31. HPLC spectrum of (R)-**46**(blue) and (S)-**46** (red) synthesized (top) and after chiral HPLC purification (Bottom).*

3.3.2.5 Screening Experiments

Screening experiments were carried out with library **31**, **36** as well as the free tetrapeptide **48** using the fluorescent guests (*S*) and (*R*)-**46.** Screening experiments were carried out in CH_3CN. A library sample was equilibrated in CH_3CN for one hour and the fluorescent guest (*S*)-**46** (as tetrabutylammonium salt) dissolved in CH_3CN is added. The selectivity in binding the receptor can be judged by observation of fluorescent beads, visualized under an optical microscope (Fig 32).

Control experiments with dansyl chloride showed that the observed fluorescence activity is indeed due to selective complexation by the receptor and not to the chromophore.

After selecting the most fluorescent beads (about 50 in each of the 3 cases), the beads were washed several times to remove the Naproxen derivative (*S*)-**46**. The same procedure was then carried out with (*R*)-**46**, but now the ones that did not form a complex with the *R* enantiomer were isolated. Indeed, the beads that can form a complex with the *S* enantiomer and not with the *R* one are likely containing the enantioselective receptors. Five beads were therefore selected for mass spectrometry analysis in each of the three receptor libraries.

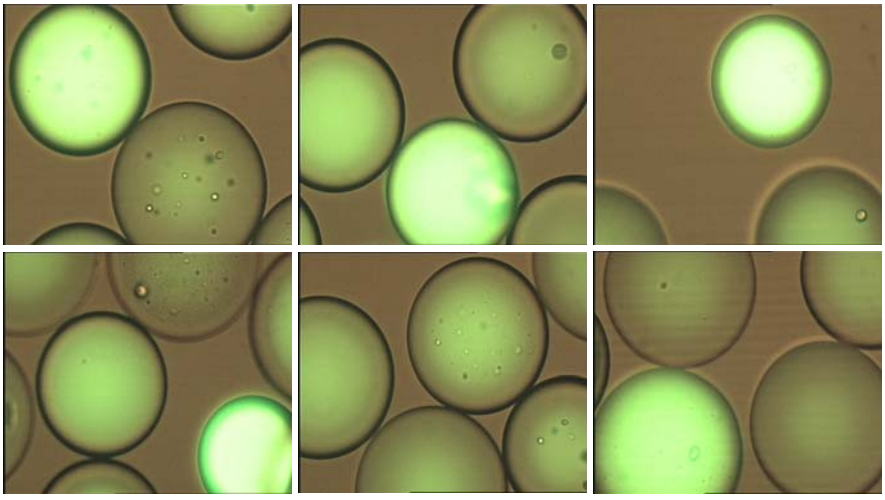

a) b) c)

Fig 32. Photographs of screening assay of receptors a) ***31****, b)* ***36*** *and c) the free tetrapeptide libraries for binding to (S)-****46****.*

As an alternative to the widely used Edman degradation for determination of the sequence of bead-based peptides, a new encoding methodology developed by Kilburn *et al*.[72] has been employed. Split and Mix peptide libraries have been indeed encoded by capping a cleavable sequence with *p*-bromobenzoic acid (Fig. 33). The resin **47** was thus prepared by sequential coupling of methionine, arginine (Pbf) and two aminohexanoic acid moieties on to a tentagel resin. Four rounds of Split and Mix synthesis using eight amino acids (Asp(O*t*Bu), Gln, Tyr(O*t*Bu), Trp(Boc), Thr(O*t*Bu), Val, Gly, Pro) followed each time by incorporation of the capping agent gave the encoded library **48**. The beads selected were cleaved and then analyzed by mass spectrometry (MALDI-TOF MS). The mass analysis of the single bead cleavage followed by processing the bromine isotopes gave the peptide sequence by calculating the mass difference of the amino acid residues (Fig 34). The complexity of the spectrum can be dramatically reduced by just plotting the peaks differing by two mass units (those containing bromine). This simplification allows an easy detection of the relevant masses.

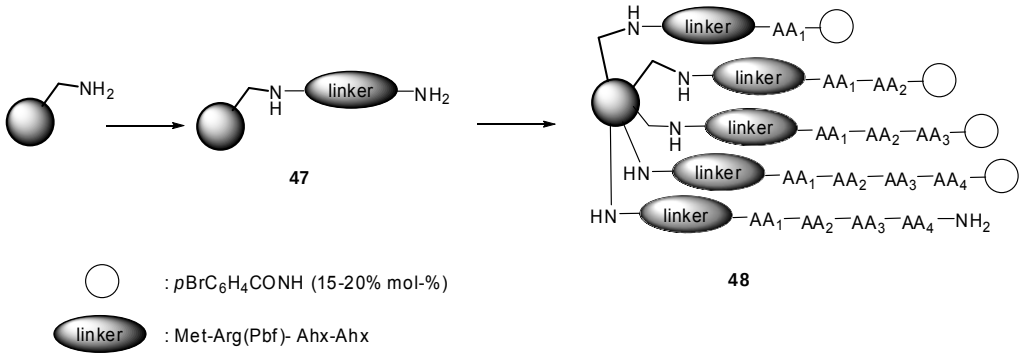

Fig. 33. Split and Mix tetrapeptide library encoded by a capping reaction with p-bromobenzoic acid (15-20 mol% of resin loading).

[72] Sheperd, J.; Langley, G. J.; Herniman, J. M.; Kilburn, J. D. *Eur. J. Org. Chem.* **2007**, 1345-1356.

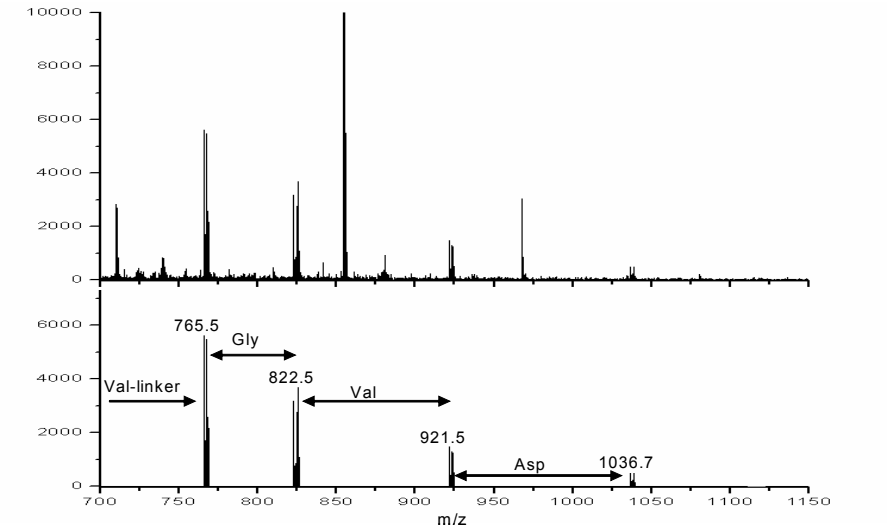

*Fig 34. Mass spectra of sample from a single cleaved bead of **36**, top: raw data, down: processed to identified Br-isotope patterns.*

Sequencing was unsuccessful for three beads isolated suggesting either unsuccessful coupling or a cleavage reaction (Table 8). On the other hand, four sequences could not be entirely determined because of the absence of bromine isotopes or too weak peaks in mass analysis. Tetrapeptide sequences of libraries **48** and **31** are probably too small and appear to lack enough consensus to conclude about any specific amino acid in each position. However, library **36** gave four entire sequences and one with only the first amino acid identified. Thus, Asp is present three times in position 4 as well as two times in position 2. Apart the presence of two Val in position 1, no other repeats were present in the sequences. Asp appears in four beads of **36** suggesting that it is an important amino acid for selectivity of the target.

The sequences identified do not show a specific agreement between the beads isolated even if the presence of certain amino acid (Asp) is recurrent. It is curious that no Trp was detected despite its tendency to form π-stacking interactions with the aromatic ring of Naproxen.

Bead	aa_1	aa_2	aa_3	aa_4
48				
1	Gly	-	-	-
2	Gln	-	-	-
3	Val	Asp	Asp	Tyr
4	Val	Asp	-	-
5	-	-	-	-
31				
1	Asp	Asp	-	-
2	Tyr	Thr	Gly	-
3	Val	Gln	Gln	-
4	-	-	-	-
5	-	-	-	-
36				
1	Val	Val	Asp	Asp
2	Asp	Asp	Gln	Asp
3	Pro	Asp	Tyr	Gly
4	Val	Gly	Val	Asp
5	Gln	-	-	-

*Table 8. Sequencing results for 5 beads identified from screening experiments of receptor libraries **48**, **31** and **36** with (S)-**46** and (R)-**46** in CH_3CN.*

3.4 Conclusions

In this chapter, flexible chiral guanidinium receptors as well as rigid macrocycles have been synthesized with none to rather low enantioselectivity towards Naproxen.

NOBIN-based macrocycles present however a modest discrimination (1.5:1). An X-ray solid state structure has been resolved for **21** (Cl^-) and showed an unprecedented intermolecular binding of the macrocycle.

Further studies with those macrocycles with other targets as for instance protected amino acid are currently ongoing.

A combinatorial approach was also attempted. A fluorescent (*S*) and (*R*)-**46** dansyl-Naproxen was synthesized. Two guanidinium libraries **31** and **36** bearing a tetrapeptide arm were synthesized. Screening experiments showed selectivity towards the substrate. Identification was then achieved but could not afford a reliable consensus of optimal amino acid sequence.

3.5 Experimental Section

3.5.1 General Procedures

Molecular modeling. MMFFs and OPLS-AA force fields were used for molecular mechanics in chloroform for all complexes (continuum solvent GB/SA ($CHCl_3$). MacroModel (Schrodinger Inc.) were used for conformational search in Mixed Mode MCMM (torsional angles)/LMCS (vibrational mode following). 20,000 MCMM/LMCS steps were run for L/D bound complex. MINTA computation was used for of $\Delta\Delta G_{S\text{-}R}$ (as an indication of relative ee´s).

3.5.2. Synthesis

General procedure for the synthesis of compounds **1**, **2**, **6**, **8-11**, **14-17**. The appropriate isocyanate (2 eq) was added, under nitrogen atmosphere, to a solution of **5** (1 eq) in dry CH_2Cl_2 (2 mL) in a sealed tube and the mixture was stirred at 45 ºC overnight. After evaporation of the solvent, the resulting solid was dissolved in CH_2Cl_2 and the organic layer was washed with 0.1M NH_4PF_6 solution, dried (Na_2SO_4), filtered over cotton and concentrated at reduced pressure. Purification of the crude was achieved by column chromatography on silica gel exept for (*R*,*R*)-**1** and (*R*,*S*)-**9** which do precipitate *in situ*, and were thus filtered over a Büchner funnel.

Compounds **8-11** were synthezised with both (*R*,*R*) and (*R*,*S*) stereochemistries, full characterisation (Mp, ^{1}H-NMR, ^{13}C-NMR and ESI-MS) is provided for only one stereochemistry [namely (*R*,*R*) one] for those compounds in order to avoid unecesssary duplications. Thus, unless otherwise stated, all guanidinium derivatives are of (*R,R*) configuration.

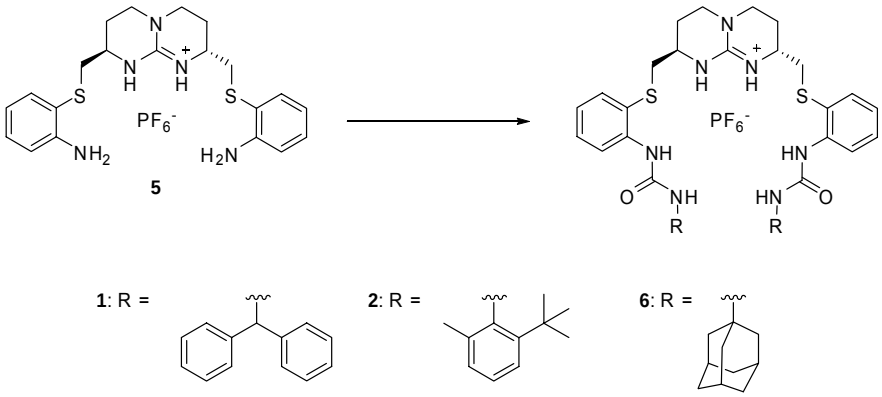

(2*R*,8*R*)-2,8-Bis-{[2-(3-benzhydrylureido)phenylthio]methyl}-2,3,4,6,7,8-hexahydro-2*H*-pyrimido[1,2-*a*]pyrimidin-9-ium hexafluorophosphate (1).
Prepared from diphenylmethyl isocyanate (0.04 mL, 0.19 mmol) and **5** (50 mg, 0.09 mmol). Purification by filtration over a Büchner funnel afforded **1** as a light yellow solid (75 mg, 86%). Mp 221-223ºC. $[\alpha]_D^{25}$ -94.46 (*c* = 1, CH_3CN). **^{1}H-NMR** (500 MHz, CD_3OD) δ 7.64 (d, *J* = 8.1 Hz, 2H, CH_{Ar}), 7.40 (d, *J* = 7.4 Hz, 2H, CH_{Ar}), 7.20 (m, 24H, NH_{guan}, CH_{Ar}), 6.96 (t, *J* = 7.8 Hz, 2H, CH_{Ar}), 6.88 (s, 2H, NH_{urea}), 6.58 (t, 2H, NH_{urea}), 5.95 (s, 2H, $CH(Ph)_2$), 3.05 (m, 6H, $CH_{2\gamma}$, CH_α), 2.90 (dd, *J* = 6.1, 13.9 Hz, 2H, CH_2S), 2.68 (dd, *J* = 7.8, 13.5 Hz, 2H, CH_2S), 1.85-1.65 (m, 4H, $CH_{2\beta}$). **^{13}C-NMR** (CD_3OD, 125 MHz) δ 155.6 (C_{urea}), 150.0 (C_{guan}), 141.3, 139.2, 138.4, 134.2, 129.5, 128.3, 126.4, 123.4, 122.1, 119.9, (CH_{Ar}, C_{Ar}), 55.6 ($CH(Ph)_2$), 47.9 (CH_α), 45.4 (CH_2S), 39.5 ($CH_{2\gamma}$), 25.6 ($CH_{2\beta}$). **ESI-MS** *m/z* 832.3 $(M\text{-}PF_6^-)^+$.

(2*R*,8*R*)-2,8-Bis-{[2-(3-(2-*tert*-butyl-6-methylphenyl)ureido)phenylthio] methyl}-2,3,4,6,7,8-hexahydro-2*H*-pyrimido[1,2-*a*]pyrimidin-9-ium hexafluorophosphate (2).
Prepared from 2-*tert*-butyl-6-methylphenyl isocyanate (35.5 mg, 0.19 mmol) and **5** (50 mg, 0.09 mmol). Purification by column chromatography on silica gel (CH_2Cl_2/MeOH, 98:2) afforded **2** as a light yellow solid (65 mg, 77%). Mp 210-212ºC. $[\alpha]_D^{25}$ -105.76 (*c* = 1, CH_3CN). **^{1}H-NMR** (500 MHz, CD_3CN) δ 7.60 (d, *J* = 7.9 Hz, 2H, CH_{Ar}), 7.40 (d, *J* = 7.5 Hz, 2H, CH_{Ar}), 7.20 (m, 8H, NH_{guan}, CH_{Ar}), 7.01 (m, 4H, CH_{Ar}), 6.94 (s, 2H, NH_{urea}), 6.60 (s, 2H, NH_{urea}), 3.09 (m, 6H, $CH_{2\gamma}$, CH_α), 2.90 (dd, *J* = 6.4, 13.5 Hz, 2H, CH_2S), 2.68 (dd, *J* = 7.5, 13.4 Hz, 2H, CH_2S), 2.12 (s, 6H, CH_3), 1.85-1.65 (m, 4H, $CH_{2\beta}$), 1.35 (s, 18H, $CH_{3t\text{-}Bu}$). **^{13}C-NMR** (CD_3CN, 125

MHz) δ 155.1 (C_{urea}), 150.1 (C_{guan}), 141.2, 139.2, 138.4, 134.2, 129.5, 128.3, 126.4, 124.5, 123.9, 123.4, 120.2, 118.3 (CH_{Ar}, C_{Ar}), 47.9 (CH_{α}), 45.1 (CH_2S), 39.5 ($CH_{2\gamma}$), 31.5 ($CH_{3t\text{-}Bu}$), 25.5 ($CH_{2\beta}$), 17.3 (CH_3). **ESI-MS** *m/z* 792.4 $(M\text{-}PF_6^-)^+$.

(2*R*,8*R*)-2,8-Bis-{[2-(3-adamantylureido)phenylthio]methyl}-2,3,4,6,7,8-hexahydro-2*H*-pyrimido[1,2-*a*]pyrimidin-9-ium hexafluorophosphate (6).
Prepared from 1-adamantyl isocyanate (32 mg, 0.19 mmol) and **5** (50 mg, 0.09 mmol). Purification by column chromatography on silica gel (CH_2Cl_2/MeOH, 98:2) afforded **6** as a light yellow solid (60 mg, 73%). Mp 232-234ºC. $[\alpha]_D^{25}$ -89.66 (*c* = 1, CH_3CN). **^{1}H-NMR** (500 MHz, CD_3CN) δ 7.77 (d, *J* = 7.2 Hz, 2H, CH_{Ar}), 7.46 (d, *J* = 7.8 Hz, 2H, CH_{Ar}), 7.21 (t, *J* = 7.5 Hz, 2H, CH_{Ar}), 7.16 (s, 2H, NH_{guan}), 7.06 (t, *J* = 7.4 Hz, 2H, CH_{Ar}), 6.69 (s, 2H, NH_{urea}), 5.54 (s, 2H, NH_{urea}), 3.31 (m, 6H, $CH_{2\gamma}$, CH_{α}), 2.99 (dd, *J* = 6.2, 13.5 Hz, 2H, CH_2S), 2.68 (dd, *J* = 7.1, 13.8 Hz, 2H, CH_2S), 2.06 (m, 12H, CH_2), 1.89 (m, 6H, CH), 1.84-1.70 (m, 10H, $CH_{2\beta}$, CH), 1.65 (m, 12H, CH). **^{13}C-NMR** (CD_3CN, 125 MHz) δ 155.6 (C_{urea}), 150.0 (C_{guan}), 138.4, 134.2 129.5, 122.1, 119.9, 117.5 (CH_{Ar}, C_{Ar}), 47.9 (CH_{α}), 45.4 (CH_2S), 40.8 (CH_2), 39.5 ($CH_{2\gamma}$), 38.6 (C), 36.4 (CH_2), 29.2 (CH), 25.6 ($CH_{2\beta}$). **ESI-MS** *m/z* 768.4 $(M\text{-}PF_6^-)^+$.

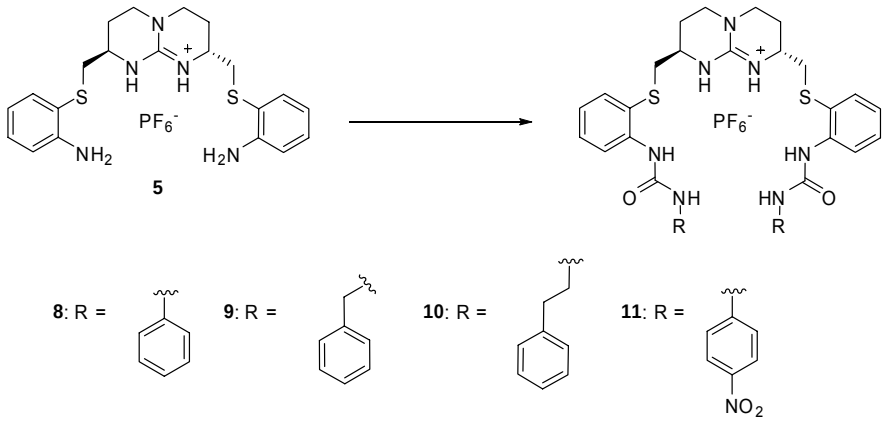

(2*R*,8*R*)-2,8-bis{[2-(3-phenylureido)phenylthio]methyl}-2,3,4,6,7,8-hexahydro-2*H*-pyrimido[1,2-*a*]pyrimidin-9-ium hexafluorophosphate [(*R*,*R*)-8].
Prepared from phenyl isocyanate (0.03 mL, 0.19 mmol) and **5** (50 mg, 0.09 mmol). Purification by column chromatography on silica gel (CH_2Cl_2/MeOH, 98:2) afforded **8** as a light yellow solid (60 mg, 84%). Mp 226-228ºC. $[\alpha]_D^{25}$ -106.15 (*c* = 1, CH_3CN).

^{1}H-NMR (500MHz, CD_3CN) δ 8.10 (s, 2H, NH_{guan}), 7.94 (d, J = 7.2 Hz, 2H, CH_{Ar}), 7.74 (s, 2H, NH_{urea}), 7.52 (d, J = 7.8 Hz, 2H, CH_{Ar}), 7.45 (d, J = 7.7 Hz, 4H, CH_{Ar}), 7.29 (m, 6H, CH_{Ar}), 7.09 (t, J = 7.4 Hz, 2H, CH_{Ar}), 7.04 (t, J = 7.3 Hz, 2H, CH_{Ar}), 6.72 (s, 2H, NH_{urea}), 3.25 (m, 6H, $CH_{2\gamma}$, CH_{α}), 3.00 (dd, J = 6.4, 13.8 Hz, 2H, CH_2S), 2.71 (dd, J = 7.0, 13.6 Hz, 2H, CH_2S), 1.92-1.78 (m, 4H, $CH_{2\beta}$). **^{13}C-NMR** (125 MHz, CD_3CN) δ 153.1 (C_{urea}), 150.1 (C_{guan}), 139.6, 138.9, 134.0, 128.9, 128.7, 124.1, 122.8, 119.2 (CH_{Ar}, C_{Ar}), 47.3 (CH_{α}), 44.4 (CH_2S), 38.8 ($CH_{2\gamma}$), 24.4 ($CH_{2\beta}$). **ESI-MS** *m/z* 652.2 $(M\text{-}PF_6^-)^+$.

(2*R*,8*S*)-2,8-bis{[2-(3-phenylureido)phenylthio]methyl}-2,3,4,6,7,8-hexahydro-2*H*-pyrimido[1,2-*a*]pyrimidin-9-ium hexafluorophosphate [(*R*,*S*)-8].
Prepared from phenyl isocyanate (0.03 mL, 0.19 mmol) and (*R*,*S*)-**5** (50 mg, 0.09 mmol). Purification by column chromatography on silica gel (CH_2Cl_2/MeOH, 98:2) afforded (*R*,*S*)-**8** as a light yellow solid (65 mg, 91%).

(2*R*,8*R*)-2,8-bis{[2-(3-benzylureido)phenylthio]methyl}-2,3,4,6,7,8-hexahydro-2*H*-pyrimido[1,2-*a*]pyrimidin-9-ium hexafluorophosphate [(*R*,*R*)-9].
Prepared from benzyl isocyanate (0.03 mL, 0.19 mmol) and **5** (50 mg, 0.09 mmol). Purification by column chromatography on silica gel (CH_2Cl_2/MeOH, 98:2) afforded **9** as a light yellow solid (55 mg, 75%). Mp 223-225ºC. $[\alpha]_D^{25}$ -81.35 (c = 1, CH_3CN). **^{1}H-NMR** (500MHz, CD_3CN) δ 7.68 (d, J = 7.3 Hz, 2H, CH_{Ar}), 7.50-7.30 (m, 16H, NH_{guan}, CH_{Ar}), 7.04 (t, J = 7.41 Hz, 2H, CH_{Ar}), 6.72 (s, 2H, NH_{urea}), 6.30 (t, 2H, NH_{urea}), 4.34 (m, 4H, CH_2), 3.12-3.00 (m, 8H, CH_{α}, $CH_{2\gamma}$, CH_2S) 2.63 (dd, J = 7.1, 13.5 Hz, 2H, CH_2S), 1.92-1.58 (m, 4H, $CH_{2\beta}$). **^{13}C-NMR** (125 MHz, CD_3CN) δ 156.3 (C_{urea}), 149.9 (C_{guan}), 139.5, 138.2, 133.3, 128.5, 128.1, 126.7, 124.7, 124.3, 119.8 (CH_{Ar}, C_{Ar}), 46.9 ($CH_{2\alpha}$), 44.2 (CH_2S), 43.0 (CH_2), 38.8 ($CH_{2\gamma}$), 24.6 ($CH_{2\beta}$). **ESI-MS** *m/z* 680.3 $(M\text{-}PF_6^-)^+$.

(2*R*,8*S*)-2,8-bis{[2-(3-benzylureido)phenylthio]methyl}-2,3,4,6,7,8-hexahydro-2*H*-pyrimido[1,2-*a*]pyrimidin-9-ium hexafluorophosphate [(*R*,*S*)-9].
Prepared from benzyl isocyanate (0.03 mL, 0.19 mmol) and (*R*,*S*)-**5** (50 mg, 0.09 mmol). Purification by filtration over a Büchner funnel afforded (*R*,*S*)-**9** (60 mg, 81 %) as a pure white solid.

(2*R*,8*R*)-2,8-bis{[2-(3-phenethylureido)phenylthio]methyl}-2,3,4,6,7,8-hexahydro-2*H*-pyrimido[1,2-*a*]pyrimidin-9-ium hexafluorophosphate [(*R*,*R*)-10].
Prepared from phenethyl isocyanate (0.03 mL, 0.19 mmol) and **5** (50 mg, 0.09 mmol). Purification by column chromatography on silica gel (CH_2Cl_2/MeOH, 98:2) afforded **10** as a light yellow solid (58 mg, 76%). Mp 218-220ºC. $[\alpha]_D^{25}$ -85.54 (*c* = 1, CH_3CN). **^{1}H-NMR** (500MHz, CD_3CN) δ 7.70 (d, *J* = 7.3 Hz, 2H, CH_{Ar}), 7.47 (d, *J* = 7.4 Hz, 2H, CH_{Ar}), 7.50-7.30 (m, 12H, NH_{guan}, CH_{Ar}), 7.09 (t, *J* = 7.2 Hz, 2H, CH_{Ar}), 6.90 (s, 2H, NH_{urea}), 5.84 (t, 2H, NH_{urea}), 3.43 (q, *J* = 7.6 Hz, 4H, CH_2), 3.28 (m, 6H, CH_{α}, $CH_{2\gamma}$), 3.13 (dd, *J* = 4.4, 14.5 Hz, 2H, CH_2S), (t, *J* = 6.8 Hz, 4H, CH_2), 2.71 (dd, *J* = 10.1, 12.4 Hz, 2H, CH_2S), 2.04-1.72 (m, 4H, $CH_{2\beta}$). **^{13}C-NMR** (125 MHz, CD_3CN) δ 157.6 (C_{urea}), 150.1 (C_{guan}), 139.5, 138.2, 134.4, 130.0, 129.6, 128.1, 126.6, 125.8, 120.5 (CH_{Ar}, C_{Ar}), 48.4 ($CH_{2\alpha}$), 45.8 (CH_2S), 44.6 (CH_2), 40.4 ($CH_{2\gamma}$), 26.7 ($CH_{2\beta}$). **ESI-MS** *m/z* 708.3 $(M\text{-}PF_6^-)^+$.

(2*R*,8*S*)-2,8-bis{[2-(3-phenethylureido)phenylthio]methyl}-2,3,4,6,7,8-hexahydro-2*H*-pyrimido[1,2-*a*]pyrimidin-9-ium hexafluorophosphate [(*R*,*S*)-10].
Prepared from phenethyl isocyanate (0.03 mL, 0.19 mmol) and (*R*,*S*)-**5** (50 mg, 0.09 mmol). Purification by column chromatography on silica gel (CH_2Cl_2/MeOH, 98:2) afforded (*R*, *S*)-**10** as a light yellow solid (65 mg, 85%).

(2*R*,8*R*)-2,8-Bis{[2-(3-(4-nitrophenyl)ureido)phenylthio]methyl}-2,3,4,6,7,8-hexahydro-2*H*-pyrimido[1,2-*a*]pyrimidin-9-ium hexafluorophosphate [(*R*,*R*)-11].
Prepared from *p*-nitrophenyl isocyanate (30 mg, 0.19 mmol) and **5** (50 mg, 0.09 mmol). Purification by column chromatography on silica gel (CH_2Cl_2/MeOH, 98:2) afforded **6** as a light yellow solid (57 mg, 72%). Mp 215-217ºC. $[\alpha]_D^{25}$ -109.58 (*c* = 1, CH_3CN).**^{1}H-NMR** (500MHz, CD_3CN) δ 8.62 (s, 2H, NH_{guan}), 8.12 (d, *J* = 7.1 Hz, 4H, CH_{Ar}), 8.00 (d, *J* = 7.2 Hz, 2H, CH_{Ar}), 7.87 (s, 2H, NH_{urea}),7.69 (d, 4H, *J* = 7.7 Hz, CH_{Ar}), 7.57 (d, *J* = 7.3 Hz, 2H, CH_{Ar}), 7.31 (t, *J* = 7.4 Hz, 2H, CH_{Ar}), 7.14 (t, *J* = 7.3 Hz, 2H, CH_{Ar}), 6.25 (s, 2H, NH_{urea}), 3.24-3.18 (m, 6H, $CH_{2\gamma}$, CH_{α}), 3.03 (dd, *J* = 5.7, 13.8 Hz, 2H, CH_2S), 2.72 (dd, *J* = 9, 14.9 Hz, 2H, CH_2S), 1.90-1.70 (m, 4H, $CH_{2\beta}$). **^{13}C-NMR** (125 MHz, CD_3CN) δ 153.1 (C_{urea}), 150.1 (C_{guan}), 139.6, 138.9 134.0, 128.9, 128.7, 124.1, 122.8, 119.2 (CH_{Ar}, C_{Ar}), 47.3 ($CH_{2\alpha}$), 44.4 (CH_2S), 38.8 ($CH_{2\gamma}$), 24.4 ($CH_{2\beta}$). **ESI-MS** *m/z* 742.2 $(M\text{-}PF_6^-)^+$.

(2*R*,8*S*)-2,8-Bis{[2-(3-(4-nitrophenyl)ureido)phenylthio]methyl}-2,3,4,6,7,8-hexahydro-2*H*-pyrimido[1,2-*a*]pyrimidin-9-ium hexafluorophosphate ((*R*, *S*)-11). Prepared from *p*-nitrophenyl isocyanate (30 mg, 0.19 mmol) and (*R*, *S*)-**5** (50 mg, 0.09 mmol). Purification by column chromatography on silica gel (CH_2Cl_2/MeOH, 98:2) afforded (*R*, *S*)-**11** as a light yellow solid (60 mg, 76%).

(2*R*,8*R*)-2,8-bis{[2-(3-(4-nitrobenzyl)ureido)phenylthio]methyl}-2,3,4,6,7,8-hexahydro-2*H*-pyrimido[1,2-*a*]pyrimidin-9-ium hexafluorophosphate [(*R*,*R*)-12].

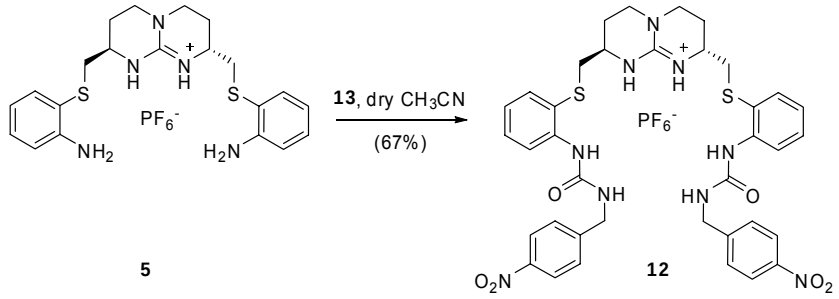

Procedure

A solution of guanidinium salt **5** (50 mg, 0.09 mmol) and **13** (66 mg, 0.27 mmol) in dry CH_3CN (2 mL) in a sealed tube was stirred overnight at 70ºC under nitrogen atmosphere. After removing the solvent, the resulting solid was dissolved in CH_2Cl_2, and the organic layer was washed with a 0.1M NH_4PF_6 solution, dried (Na_2SO_4), filtered over cotton and concentrated at reduced pressure. The crude was purified by column chromatography on silica gel (CH_2Cl_2/MeOH 98:2) to afford the pure compound as a yellow solid (55 mg, 67%). Mp 234-236ºC. $[\alpha]_D^{25}$ -108.63 (*c* = 1, CH_3CN). **^{1}H-NMR** (500MHz, CD_3CN) δ 8.13 (d, *J* = 7.4 Hz, 4H, CH_{Ar}), 7.65 (d, *J* = 7.3 Hz, 2H, CH_{Ar}), 7.51-7.42 (m, 8H, NH_{guan}, CH_{Ar}), 7.26 (t, *J* = 7.4 Hz, 2H, CH_{Ar}), 7.13 (t, *J* = 7.5 Hz, 2H, CH_{Ar}), 6.81 (s, 2H, NH_{urea}), 6.48 (t, *J* = 5.8 Hz, 2H, NH_{urea}), 4.46 (qd, *J* = 5.9, 16.9 Hz, 4H, CH_2), 3.20-3.11 (m, 8H, CH_α, $CH_{2\gamma}$, CH_2S), 2.58 (dd, *J* = 10.3, 13.7 Hz, 2H, CH_2S), 1.92-1.58 (m, 4H, $CH_{2\beta}$). **^{13}C-NMR** (125 MHz, CD_3CN) δ 156.3.1 (C_{urea}), 149.9 (C_{guan}), 139.5, 138.2, 133.3, 128.5, 128.1, 126.7, 124.7, 124.3, 120.3 (CH_{Ar}, C_{Ar}), 46.9 (CH_α), 44.2 (CH_2S), 43.0 (CH_2), 38.8 ($CH_{2\gamma}$), 24.6 ($CH_{2\beta}$). **ESI-MS** *m/z* 770.2 $(M\text{-}PF_6^-)^+$.

(2*R*,8*S*)-2,8-bis{[2-(3-(4-nitrobenzyl)ureido)phenylthio]methyl}-2,3,4,6,7,8-hexahydro-2*H*-pyrimido[1,2-*a*]pyrimidin-9-ium hexafluorophosphate [(*R*,*S*)-12]. Prepared from guanidinium salt (*R*,*S*)-**5** (50 mg, 0.09 mmol) and 13 (66 mg, 0.27). Purification by column chromatography on silica gel (CH_2Cl_2/MeOH, 98:2) afforded (*R*, *S*)-**11** as a light yellow solid (65 mg, 79%).

***N*-(4-nitrobenzyl)-1*H*-imidazole-1-carboxamide (13).**

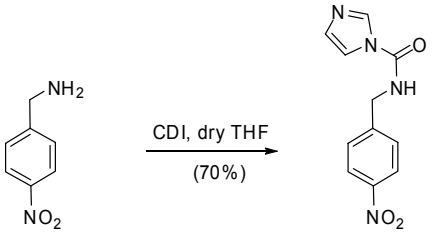

13

Procedure

A solution of 4-nitrophenylamine (360 mg, 2.359 mmol) and CDI (314 mg, 2.359 mmol) in dry THF was stirred during 1 hour. The solvent was removed and the crude was purified by column chromatography on silica gel (hexane/EtOAc 6:3) to afford **13** as a pure yellow solid (410 mg, 70%). Mp 158-159ºC. **^{1}H-NMR** (500 MHz, $CDCl_3$) δ 8.23 (d, J = 7.3 Hz, 2H, CH_{Ar}), 8.12 (s, 1H, CH_{Ar}), 7.63 (d, J = 7.7 Hz, 2H, CH_{Ar}), 7.51 (s, 1H, CH_{Ar}), 7.46 (s, 1H, NH), 7.05 (s, 1H, CH_{Ar}), 4.65 (d, J = 6.9 Hz, 2H, CH_2). **^{13}C-NMR** (125 MHz, $CDCl_3$) δ 160.0 (CO), 146.1, 136.1, 130.0, 128.3, 123.5, 117.3, 116.3 (CH_{Ar}, C_{Ar}), 43.4 (CH_2).

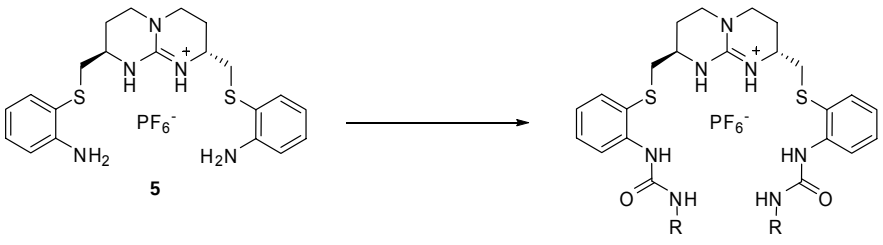

5

14: R = **15**: R = **16**: R = **17**: R =

(2*R*,8*R*)-2,8-bis{[2-(3-((*S*)-1-phenylethyl)ureido)phenylthio]methyl}-2,3,4,6,7,8-hexahydro-2*H*-pyrimido[1,2-*a*]pyrimidin-9-ium hexafluorophosphate [(*R*,*R*)-14]. Prepared from (*R*)-(−)-α-methylbenzyl isocyanate (0.03 mL, 0.19 mmol) and **5** (50 mg, 0.09 mmol). Purification by column chromatography on silica gel (CH_2Cl_2/MeOH, 98:2) afforded **14** as a light yellow solid (65 mg, 85%). Mp 195-197ºC. $[\alpha]_D^{25}$ -70.84 (*c* = 1, CH_3CN). **^{1}H-NMR** (500 MHz, CD_3CN) δ 7.79 (d, *J* = 6.8 Hz, 2H, CH_{Ar}), 7.68 (d, *J* = 7.6 Hz, 2H, CH_{Ar}), 7.40 (s, 2H, NH_{guan}),7.35-7.20 (m, 12H, CH_{Ar}), 7.10 (t, *J* = 7.4 Hz, 2H, CH_{Ar}), 6.55 (s, 2H, NH_{urea}), 6.26 (s, 2H, NH_{urea}), 4.84 (m, 2H, CH), 3.18 (m, 6H, CH_{α}, $CH_{2\gamma}$), 3.05 (dd, *J* = 5.1, 13.2 Hz, 2H, CH_2S), 2.67 (dd, *J* = 9.3, 13.0 Hz, 2H, CH_2S), 1.92-1.58 (m, 4H, $CH_{2\beta}$), 1.44 (d, *J* = 7.0 Hz, 6H, CH_3). **^{13}C-NMR** (125 MHz, CD_3CN) δ 156.3.1 (C_{urea}), 149.9 (C_{guan}), 139.5, 138.2, 133.3, 128.5, 128.1, 126.7, 124.7, 124.3, 119.8 (CH_{Ar}, C_{Ar}), 50.8 (CH), 46.9 (CH_{α}), 44.2 (CH_2S), 38.8 ($CH_{2\gamma}$), 24.6 ($CH_{2\beta}$), 21.2 (CH_3). **ESI-MS** *m/z* 708.3 $(M\text{-}PF_6^-)^+$.

(2*R*,8*S*)-2,8-bis{[2-(3-((*S*)-1-phenylethyl)ureido)phenylthio]methyl}-2,3,4,6,7,8-hexahydro-2*H*-pyrimido[1,2-*a*]pyrimidin-9-ium hexafluorophosphate [(*R*,*S*)-14]. Prepared from (*R*)-(−)-α-methylbenzyl isocyanate (0.03 mL, 0.19 mmol) and (*R*, *S*)-**5** (50 mg, 0.09 mmol). Purification by column chromatography on silica gel (CH_2Cl_2/MeOH, 98:2) afforded (*R*, *S*)-**14** as a light yellow solid (68 mg, 89%). Mp 195-197ºC. $[\alpha]_D^{25}$ -18.31 (*c* = 1, CH_3CN). **^{1}H-NMR** (500 MHz, CD_3CN) δ 7.89 (d, *J* = 9.1 Hz, 1H, CH_{Ar}), 7.63 (d, *J* = 8.1 Hz, 1H, CH_{Ar}), 7.52 (d, *J* = 7.6 Hz, 1H, CH_{Ar}), 7.48 (d, *J* = 7.6 Hz, 1H, CH_{Ar}), 7.32-7.19 (m, 14H, CH_{Ar}, NH_{guan}), 7.16 (t, *J* = 7.3 Hz, 1H, CH_{Ar}), 7.10 (t, *J* = 7.3 Hz, 1H, CH_{Ar}), 6.73 (s, 1H, NH_{urea}), 6.64 (s, 1H, NH_{urea}), 6.28 (m, 2H, NH_{urea}), 4.89 (m, 1H, CH), 4.81 (m, 1H, CH), 3.16 (m, 6H, CH_{α}, $CH_{2\gamma}$), 3.01-2.85 (m, 4H, CH_2S), 2.01-1.57 (m, 4H, $CH_{2\beta}$), 1.46 (d, *J* = 7.0 Hz, 3H, CH_3), 1.41 (d, *J* = 7.0 Hz, 3H, CH_3). **^{13}C-NMR** (125 MHz, CD_3CN) δ 155.2, 154.9 (C_{urea}), 150.3 (C_{guan}), 139.3, 138.2, 133.9, 133.6, 129.1, 128.7, 128.5, 128.3, 126.9, 126.8, 125.8, 125.6, 125.5, 125.0. 124.0, 122.9 (CH_{Ar}, C_{Ar}), 50.1, 49.8 (CH), 47.9, 47.4 (CH_{α}), 45.2, 44.9 (CH_2S), 39.7, 38.6 ($CH_{2\gamma}$), 25.1, 24.8 ($CH_{2\beta}$), 22.4, 22.3 (CH_3). **ESI-MS** *m/z* 708.3 $(M\text{-}PF_6^-)^+$.

(2*R*,8*R*)-2,8-bis{[2-(3-((*R*)-1-phenylethyl)ureido)phenylthio]methyl}-2,3,4,6,7,8-hexahydro-2*H*-pyrimido[1,2-*a*]pyrimidin-9-ium hexafluorophosphate [(*R*,*R*)-15].

Prepared from (*S*)-(+)-α-methylbenzyl isocyanate (0.03 mL, 0.19 mmol) and **5** (50 mg, 0.09 mmol). Purification by column chromatography on silica gel (CH_2Cl_2/MeOH, 98:2) afforded **15** as a light yellow solid (65 mg, 85%). $[\alpha]_D^{25}$ -96.30 (*c* = 1, CH_3CN).

(2*R*,8*S*)-2,8-bis{[2-(3-((*R*)-1-phenylethyl)ureido)phenylthio]methyl}-2,3,4,6,7,8-hexahydro-2*H*-pyrimido[1,2-*a*]pyrimidin-9-ium hexafluorophosphate [(*R*,*S*)-15].
Prepared from (*S*)-(+)-α-methylbenzyl isocyanate (0.03 mL, 0.19 mmol) and (*R*, *S*)-**5** (50 mg, 0.09 mmol). Purification by column chromatography on silica gel (CH_2Cl_2/MeOH, 98:2) afforded (*R*, *S*)-**15** as a light yellow solid (68 mg, 89%). $[\alpha]_D^{25}$ 41.52 (*c* = 1, CH_3CN).

(2*R*,8*R*)-2,8-bis{[2-(3-((*S*)-1-(naphthalen-1-yl)ethyl)ureido)phenylthio]methyl}-2,3,4,6,7,8-hexahydro-2*H*-pyrimido[1,2-*a*]pyrimidin-9-ium hexafluorophosphate [(*R*,*R*)-16].
Prepared from (*R*)-(−)-α-methylnaphthyl isocyanate (0.03 mL, 0.19 mmol) and **5** (50 mg, 0.09 mmol). Purification by column chromatography on silica gel (CH_2Cl_2/MeOH, 98:2) afforded **16** as a light yellow solid (75 mg, 88%). Mp 209-211ºC. $[\alpha]_D^{25}$ -61.04 (*c* = 1, CH_3CN). **^{1}H-NMR** (500 MHz, CD_3CN) δ 8.15 (d, *J* = 7.8 Hz, 2H, CH_{Ar}), 7.94 (d, *J* = 7.9 Hz, 2H, CH_{Ar}), 7.83 (d, *J* = 7.8 Hz, 2H, CH_{Ar}), 7.74 (d, *J* = 7.6 Hz, 2H, CH_{Ar}), 7.66 (d, *J* = 8.0 Hz, 2H, CH_{Ar}), 7.53 (m, 6H, CH_{Ar}), 7.42 (d, *J* = 7.8 Hz, 2H, CH_{Ar}), 7.36 (s, 2H, NH_{guan}), 7.24 (t, *J* = 7.5 Hz, 2H, CH_{Ar}), 7.08 (t, *J* = 7.4 Hz, 2H, CH_{Ar}), 6.44 (s, 2H, NH_{urea}), 6.36 (s, 2H, NH_{urea}), 5.64 (m, 2H, CH), 2.97 (m, 8H, CH_{α}, $CH_{2\gamma}$, CH_2S), 2.46 (m, 2H, CH_2S), 1.74 (m, 2H, $CH_{2\beta}$), 1.59 (d, *J* = 6.1 Hz, 6H, CH_3), 1.30 (m, 2H, $CH_{2\beta}$). **^{13}C-NMR** (CD_3CN, 125 MHz) δ 156.1 (C_{urea}), 150.2 (C_{guan}), 139.3, 138.9, 133.9, 129.1, 128.7, 128.5, 127.2, 126.8, 125.6, 124.0, 122.8 (CH_{Ar}, C_{Ar}), 47.7 (CH_{α}), 45.1 (CH_2S), 38.9 ($CH_{2\gamma}$), 25.6 ($CH_{2\beta}$), 21.8 (CH_3). **ESI-MS** *m/z* 808.3 $(M\text{-}PF_6^-)^+$.

(2*R*,8*S*)-2,8-bis{[2-(3-((*S*)-1-(naphthalen-1-yl)ethyl)ureido)phenylthio]methyl}-2,3,4,6,7,8-hexahydro-2*H*-pyrimido[1,2-*a*]pyrimidin-9-ium hexafluorophosphate [(*R*,*S*)-16].
Prepared from (*R*)-(−)-α-methylnaphthyl isocyanate (0.03 mL, 0.19 mmol) and (*R*,*S*)-**5** (50 mg, 0.09 mmol). Purification by column chromatography on silica gel (CH_2Cl_2/MeOH, 98:2) afforded (*R*,*S*)-**16** as a light yellow solid (75 mg, 88%). Mp

209-211ºC. $[\alpha]_D^{25}$ -20.32 (*c* = 1, CH_3CN). **^{1}H-NMR** (500 MHz, CD_3CN) δ 8.15 (d, *J* = 7.0 Hz, 1H, CH_{Ar}), 7.93 (m, 4H, CH_{Ar}), 7.83 (d, *J* = 7.5 Hz, 1H, CH_{Ar}), 7.80 (d, *J* = 7.3 Hz, 1H, CH_{Ar}), 7.69 (d, *J* = 6.9 Hz, 1H, CH_{Ar}), 7.66 (d, *J* = 7.0 Hz, 1H, CH_{Ar}), 7.46 (m, 9H, NH_{guan}, CH_{Ar}), 7.34 (s, 1H, NH_{guan}), 7.29 (t, *J* = 7.0 Hz, 1H, CH_{Ar}), 7.22 (t, *J* = 7.4 Hz, 1H, CH_{Ar}), 7.09 (m, 3H, CH_{Ar}), 6.68 (s, 1H, NH_{urea}), 6.44 (m, 2H, NH_{urea}), 6.29 (s, 1H, NH_{urea}), 5.68 (m, 1H, CH), 5.61 (m, 1H, CH), 3.13 (m, 1H, CH_2S), 2.89 (m, 6H, CH_α, $CH_{2\gamma}$, CH_2S), 2.66 (m, 1H, CH_α), 2.45 (m, 2H, CH_α, CH_2S), 1.79 (m, 1H, $CH_{2\beta}$), 1.64 (m, 1H, $CH_{2\beta}$), 1.58 (d, *J* = 6.0 Hz, 3H, CH_3), 1.55 (d, *J* = 6.0 Hz, 3H, CH_3), 1.43 (m, 1H, $CH_{2\beta}$). **^{13}C-NMR** (CD_3CN, 125 MHz) δ 156.1 (C_{urea}), 150.2 (C_{guan}), 139.3, 138.9, 133.9, 133.6, 129.1, 128.9, 128.7, 128.5, 128.3, 127.2, 127.0, 126.8, 125.8, 125.6, 125.5, 125.0, 124.3, 124.0, 122.9, 122.8 (CH_{Ar}, C_{Ar}), 48.1, 48.0 (CH_α), 45.3, 45.1 (CH_2S), 38.9, 38.6 ($CH_{2\gamma}$), 25.7, 25.6 ($CH_{2\beta}$), 21.8, 21.5 (CH_3).**ESI-MS** *m/z* 808.3 $(M\text{-}PF_6^-)^+$.

(2*R*,8*R*)-2,8-bis{[2-(3-((*R*)-1-(naphthalen-1-yl)ethyl)ureido)phenylthio]methyl}-2,3,4,6,7,8-hexahydro-2*H*-pyrimido[1,2-*a*]pyrimidin-9-ium hexafluorophosphate [(*R*,*R*)-17].

Prepared from (*S*)-(+)-α-methylnaphthyl isocyanate (0.03 mL, 0.19 mmol) and **5** (50 mg, 0.09 mmol). Purification by column chromatography on silica gel (CH_2Cl_2/MeOH, 98:2) afforded **17** as a light yellow solid (75 mg, 88%). $[\alpha]_D^{25}$ -134.06 (*c* = 1, CH_3CN).

(2*R*,8*S*)-2,8-bis{[2-(3-((*R*)-1-(naphthalen-1-yl)ethyl)ureido)phenylthio]methyl}-2,3,4,6,7,8-hexahydro-2*H*-pyrimido[1,2-*a*]pyrimidin-9-ium hexafluorophosphate [(*R*,*S*)-17].

Prepared from (*S*)-(+)-α-methylnaphthyl isocyanate (0.03 mL, 0.19 mmol) and (*R*,*S*)-**5** (50 mg, 0.09 mmol). Purification by column chromatography on silica gel (CH_2Cl_2/MeOH, 98:2) afforded (*R*,*S*)-**17** as a light yellow solid (75 mg, 88%). $[\alpha]_D^{25}$ 10.05 (*c* = 1, CH_3CN).

Macrocycle 19.

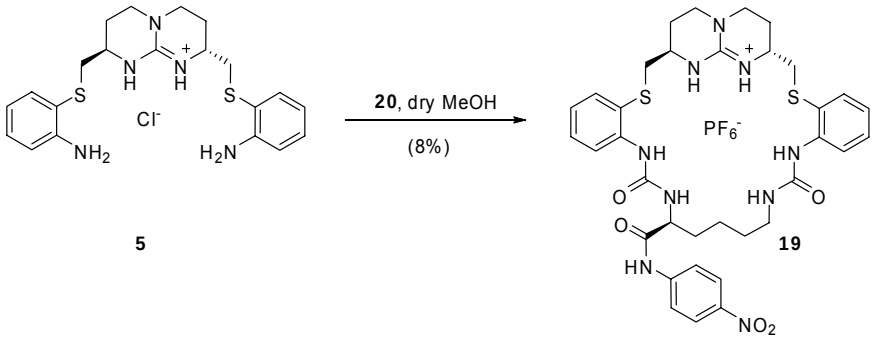

Procedure

A solution of guanidinium salt **5** (Cl^-) (90 mg, 0.20 mmol) and **20** (91 mg, 0.20 mmol) in dry MeOH (10 mL) in a sealed tube was stirred during two days at 80ºC under argon atmosphere. The solvent was removed and the residue purified by column chromatography on silica gel (CH_2Cl_2/ MeOH from 100:0 to 98:2). The residue was then purified by semi-preparative HPLC (Column: SunFire C18 5 µm, 4.6 x 100 mm, FM: ACN (0.1% TFA) / H_2O (0.1% TFA), Gradient: 10-100% ACN (0.1% TFA) in 30 min, Flow: 1 mL/min, ambient temperature) to afford **19** as pure white product. A solution of **19** in MeOH was then eluted through a Dowex resin (PF_6^-) column to homogenize the counterion as PF_6^- (13 mg, 8 %). Mp 231-233ºC. $[\alpha]_D^{25}$ -105.76 (*c* = 1, CH_3CN). **^{1}H-NMR** (500MHz, CD_3CN) δ 9.21 (s, 2H, NH_{guan}), 7.35 (dd, *J* = 1.5, 7.6 Hz, 2H, CH_{Ar}), 7.18 (m, 6H, NH_{urea}, CH_{Ar}), 7.09 (td, *J* = 1.3, 7.5 Hz, 2H, CH_{Ar}), 6.67 (dd, *J* = 1.2, 7.9 Hz, 2H, CH_{Ar}), 6.61 (td, *J* = 1.1, 7.3 Hz, 2H, CH_{Ar}), 3.40 (m, 2H, CH_α), 4.24 (m, 1H, CHN), 3.50-3.35 (m, 10H, CH_2, $CH_{2\gamma}$), 3.05-2.95 (m, 2H, CH_2S), 2.16-1.85 (m, 4H, $CH_{2\beta}$), 1.51 (m, 4H, CH_2). **ESI-MS** *m/z* 731.9 $(M\text{-}PF_6^-)^+$.

(*S*)-*N*,*N'*-[6-(4-nitrophenylamino)-6-oxohexane-1,5-diyl]bis(1H-imidazole-1-carboxamide) (20).

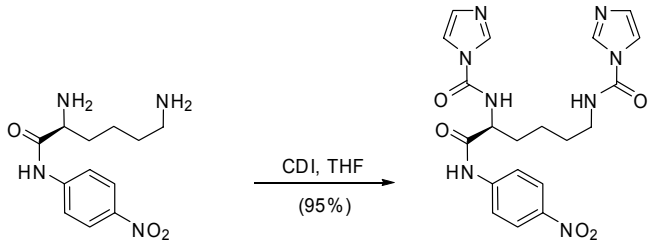

20

Procedure

To a solution of carbonyldiimidazol (476 mg, 2.98 mmol) in THF, L-lysine *p*-nitroanilide dihydrobromide (0.114 mL, 0.978 mmol) was added and the mixture stirred for 24 hours. The solvent was removed and the pure compound precipitates in ethyl acetate as a white solid (280 mg, 95%). Mp 154-157ºC. $[\alpha]_D^{25}$ -31.40 (*c* = 1, MeOH). **^{1}H-NMR** (500 MHz, CD_3OD) δ 8.37 (d, *J* = 9.6 Hz, 2H, CH_{Ar}), 8.27 (s, 1H, NH), 8.20 (s, 2H, CH_{Ar}), 7.77 (d, *J* = 9.2 Hz, 2H, CH_{Ar}), 7.63 (s, 1H, NH), 7.29 (s, 4H, CH_{Ar}), 7.07 (s, 1H, NH), 4.32 (dd, *J* = 4.1, 6.5 Hz, 1H, CH), 3.43 (t, *J* = 7.1 Hz, 2H, CH_2), 2.00 (m, 2H, CH_2), 1.73 (m, 2H, CH_2), 1.64 (m, 2H, CH_2). ^{13}C NMR (125 MHz, CD_3OD) δ 168.5, 150.8 (CO), 137.8, 136.0, 128.6, 126.3, 123.6, 120.3, 116.4 (CH_{Ar}, C_{Ar}), 56.7 (CH), 47.0 (CH_2), 40.0 (CH_2), 28.5 (CH_2), 21.6 (CH_2).

(2*R*,8*R*)-2,8-Bis-[(*S*)-2'-*tert*-butylcarbamate-1,1'-binaphthyl-2-oxymethyl]-3,4,6,7,8,9-hexahydro-2*H*-pyrimido[1,2-*a*]pyrimidin-1-ium chloride (26).

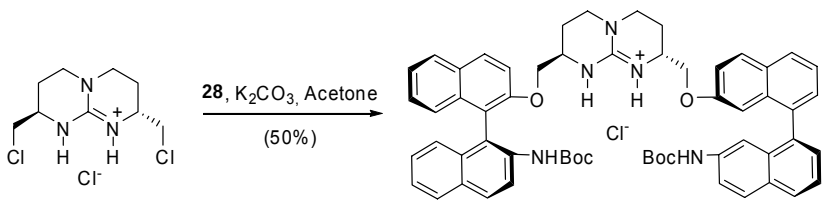

25 **26**

Procedure

To a solution of **25** (50 mg, 0.18 mmol) in acetone was added **28** (149 mg, 0.39 mmol) and K_2CO_3 (55 mg, 0.40 mmol) and the mixture was stirred for 24 hours. The mixture was concentrated *in vacuo*, the residue was dissolved in CH_2Cl_2 and washed with

water. The organic layer was dried (Na_2SO_4), filtered over cotton and concentrated at reduced pressure. Purification by column chromatography on silica gel (CH_2Cl_2/MeOH from 100:0 to 96:4) affords **26** (86 mg, 50%) as a pure brown solid. Mp 258-260ºC. $[\alpha]_D^{25}$ -125.69 (*c* = 1, MeOH). **^{1}H-NMR** (500 MHz, $CDCl_3$) δ 8.14 (d, *J* = 7.8 Hz, 2H, CH_{Ar}), 8.07 (d, *J* = 7.7 Hz, 2H, CH_{Ar}), 8.00 (d, *J* = 7.4 Hz, 2H, CH_{Ar}), 7.87 (d, *J* = 7.7 Hz, 2H, CH_{Ar}), 7.82 (d, *J* = 7.6 Hz, 2H, CH_{Ar}), 7.62 (s, 2H, NH_{guan}), 7.56 (d, *J* = 7.5 Hz, 2H, CH_{Ar}), 7.41 (td, *J* = 6.1, 7.8 Hz, 2H, CH_{Ar}), 7.29 (td, *J* = 5.4, 7.3 Hz, 2H, CH_{Ar}), 7.20 (td, *J* = 5.8, 7.9 Hz, 2H, CH_{Ar}), 6.99 (td, *J* = 5.8, 7.8 Hz, 2H, CH_{Ar}), 6.96 (d, *J* = 7.5 Hz, 2H, CH_{Ar}), 6.89 (d, *J* = 7.4 Hz, 2H, CH_{Ar}), 6.68 (s, 2H, NH_{Boc}), 3.99 (m, 4H, CH_2O), 3.19 (m, 2H, CH_α), 2.40-2.26 (m, 4H, $CH_{2\gamma}$), 1.36-1.20 (m, 4H, $CH_{2\beta}$), 1.18 (s, 18H, CH_3). **^{13}C-NMR** (125 MHz, $CDCl_3$) δ 154.2 (C_{Boc}), 150.1 (C_{guan}), 133.4, 130.7, 129.7, 128.3, 127.8, 127.1, 126.5, 125.1, 124.8, 124.3, 117.3, 115.0 (CH_{Ar}, C_{Ar}), 70.9 (CH_2O), 47.1 (CH_α), 43.9 ($CH_{2\gamma}$), 27.4 (CH_3), 21.7 ($CH_{2\beta}$). **ESI-MS** *m/z* 934.4 $(M\text{-}PF_6^-)^+$.

(2*R*,8*R*)-2,8-Bis-[(*S*)-2'-amino-1,1'-binaphthyl-2-oxymethyl]-3,4,6,7,8,9-hexahydro-2*H*-pyrimido[1,2-*a*]pyrimidin-1-ium hexafluorophosphate (28).

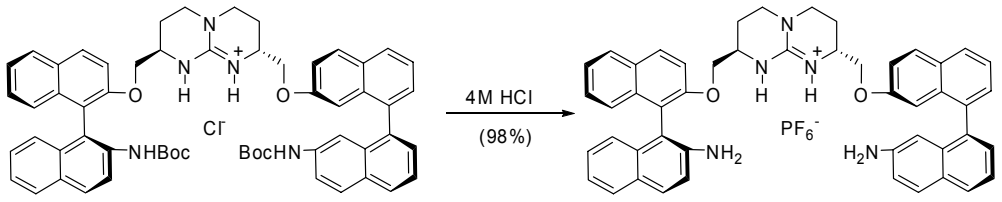

26 **28**

Procedure

A solution of **26** (120 mg, 0.12 mmol) in HCl (1 mL, 4M) in 1,4-dioxane was stirred overnight. The solvent was removed and the crude was dissolved in CH_2Cl_2, washed with water, then with a 0.1M NH_4PF_6 solution. The organic layer was dried (Na_2SO_4), filtered over cotton and concentrated at reduced pressure in order to give a pure maroon solid (106 mg, 98 %). Mp 253-255ºC. $[\alpha]_D^{25}$ -102.9 (*c* = 1, CH_3CN). **^{1}H-NMR** (500 MHz, $CDCl_3$) δ 8.14 (d, *J* = 7.8 Hz, 2H, CH_{Ar}), 8.17 (d, *J* = 7.7 Hz, 2H, CH_{Ar}), 8.03 (d, *J* = 7.6 Hz, 2H, CH_{Ar}), 7.64 (d, *J* = 7.5 Hz, 2H, CH_{Ar}), 7.58 (d, *J* = 7.3 Hz, 4H, CH_{Ar}), 7.45 (td, *J* = 6.5, 7.5 Hz, 2H, CH_{Ar}), 7.32 (td, *J* = 6.3, 7.2 Hz, 2H, CH_{Ar}), 7.04

(m, 6H, CH_{Ar}), 6.90 (td, *J* = 6.2, 7.8 Hz, 2H, CH_{Ar}), 6.72 (d, *J* = 7.5 Hz, 2H, CH_{Ar}), 6.05 (s, 2H, NH_{guan}), 4.26 (dd, *J* = 6.5, 7.9 Hz, 2H, CH_2O), 4.01 (s, 4H, NH_2), 3.93 (dd, *J* = 6.1, 7.8 Hz, 2H, CH_2O), 3.22 (m, 2H, CH_α), 2.81-2.69 (m, 4H, $CH_{2\gamma}$), 1.70-1.47 (m, 4H, $CH_{2\beta}$). **^{13}C-NMR** (125 MHz, $CDCl_3$) δ 150.2 (C_{guan}), 133.4, 130.7, 129.7, 128.3, 127.8, 127.1, 126.5, 125.1, 124.8, 124.3, 117.3, 115.0 (CH_{Ar}, C_{Ar}), 70.9 (CH_2O), 47.1 (CH_α), 43.9 ($CH_{2\gamma}$), 21.7 ($CH_{2\beta}$). **ESI-MS** *m/z* 734.3 $(M\text{-}PF_6^-)^+$.

Macrocycle 21.

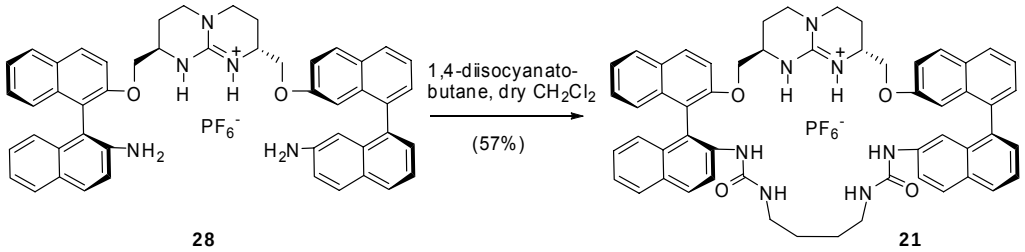

Procedure

To a solution of **28** (0.03 g, 0.04 mmol) in dry CH_2Cl_2 (5 mL) in a sealed tube was added under nitrogen atmosphere 1,4-diisocyanatobutane (0.004 mL, 0.04 mmol) and the mixture was stirred at 45ºC during 48 hours. After evaporation of the solvent, the resulting solid was dissolved in CH_2Cl_2 and the organic layer was washed with a 0.1M NH_4PF_6 solution, dried (Na_2SO_4), filtered over cotton and concentrated at reduced pressure. Purification of the crude by column chromatography on silica gel (CH_2Cl_2/MeOH 98:2) afforded **21** as a pure white solid (20 mg, 57 %). Mp 270-272ºC. $[\alpha]_D^{25}$ -177.45 (*c* = 1, CH_3CN). **^{1}H-NMR** (500 MHz, CD_3CN) δ 8.29 (d, *J* = 8.1 Hz, 2H, CH_{Ar}), 8.13 (m, 4H, CH_{Ar}), 8.05 (d, *J* = 7.6 Hz, 4H, CH_{Ar}), 7.71 (d, *J* = 7.5 Hz, 2H, CH_{Ar}), 7.48 (m, 4H, CH_{Ar}), 7.35 (m, 4H, CH_{Ar}, NH_{guan}), 7.28 (t, *J* = 7.5 Hz, 2H, CH_{Ar}), 7.04 (d, *J* = 7.6 Hz, 2H, CH_{Ar}), 7.00 (d, *J* = 7.8 Hz, 2H, CH_{Ar}), 6.52 (s, 2H, NH_{urea}), 5.37 (t, 2H, NH_{urea}), 3.90 (dd, *J* = 6.3, 7.9 Hz, 2H, CH_2O), 3.69 (m, 2H, CH_2O), 3.31 (m, 2H, CH_α), 3.09 (m, 6H, $CH_{2\gamma}$, CH_2), 2.89 (m, 2H, CH_2), 1.68-1.44 (m, 4H, $CH_{2\beta}$), 1.30 (m, 4H, CH_2). **^{13}C-NMR** (125 MHz, CD_3CN) δ 155.1 (CO), 150.2 (C_{guan}), 133.4, 130.7, 129.7, 128.3, 127.8, 127.1, 126.5, 125.1, 124.8, 124.3, 117.3,

115.0 (CH_{Ar}, C_{Ar}), 70.9 (CH_2O), 47.1 (CH_α), 43.9 ($CH_{2\gamma}$), 39.9 (CH_2), 26.2 (CH_2), 21.7 ($CH_{2\beta}$). **ESI-MS** *m/z* 874.4 $(M\text{-}PF_6^-)^+$.

Crystal data for **21** (Cl^-) at 100 K**:** $C_{55}H_{52}ClN_7O_4$, 909.38 $gmol^{-1}$, monoclinic, $P2_1$, a = 15.9831(14) Å, b = 15.2438(14) Å, c = 23.763(2) Å, $\alpha = 90°$, $\beta = 100.466(2)°$, $\gamma = 90º$, V = 5693.4(9) $Å^3$, Z = 2, ρ_{calcd} = 1.253 Mg/m^3, R1 = 0.1007, wR2 = 0.2510 for 87423 reflections with $I>2\sigma(I)$ (for 41035 reflections [R_{int}: 0.0908] with a total measured of 30934 reflections), goodness-of-fit on F^2 = 1.022, Flack: 0.01(2), largest diff. peak (hole) = 1.379 and -0.658 $e.Å^{-3}$.

Macrocycle 22.

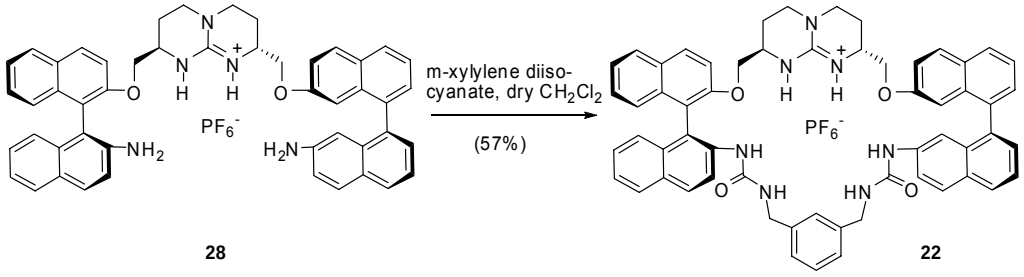

28 **22**

Procedure

To a solution of **28** (0.03 g, 0.04 mmol) in dry CH_2Cl_2 (5 mL) in a sealed tube was added under nitrogen atmosphere *m*-xylylene diisocyanate (0.004 mL, 0.04 mmol) and the mixture was stirred at 45ºC during 48 hours. After evaporation of the solvent, the resulting solid was dissolved in CH_2Cl_2 and the organic layer was washed with a 0.1M NH_4PF_6 solution, dried (Na_2SO_4), filtered over cotton and concentrated at reduced pressure. Purification of the crude by column chromatography on silica gel (CH_2Cl_2/MeOH 98:2) afforded **21** as a pure white solid (20 mg, 57 %). Mp 280-282ºC. $[\alpha]_D^{25}$ -309.84 (*c* = 1, CH_3CN). **^{1}H-NMR** (500 MHz, CD_3CN) δ 8.17 (d, *J* = 8.0 Hz, 2H, CH_{Ar}), 8.05 (d, *J* = 8.1 Hz, 2H, CH_{Ar}), 7.98 (m, 4H, CH_{Ar}), 7.65 (d, *J* = 7.6 Hz, 2H, CH_{Ar}), 7.48 (m, 10H, CH_{Ar}), 7.01 (m, 8H, $CH_{Ar,}$), 6.84 (s, 2H, NH_{guan}), 6.25 (s, 2H, NH_{urea}), 5.95 (t, 2H, NH_{urea}), 4.61 (dd, *J* = 6.5, 8.7 Hz, 2H, CH_2N), 3.95 (m, 6H, CH_2O, CH_2N), 3.05 (m, 6H, CH_α, $CH_{2\gamma}$), 1.70-1.40 (m, 4H, $CH_{2\beta}$).**^{13}C-NMR** (125 MHz, CD_3CN) δ 154.9 (CO), 150.2 (C_{guan}), 136.8, 133.4, 130.7, 129.7, 128.3, 127.8, 127.1, 126.5, 126.3, 125.1, 124.8, 124.3, 123.5, 123.2, 117.3(CH_{Ar}, C_{Ar}), 70.9 (CH_2O),

47.1 (CH_{α}),45.0 (CH_2N), 43.9 ($CH_{2\gamma}$), 39.9 (CH_2), 26.2 (CH_2), 21.7 ($CH_{2\beta}$). **ESI-MS** *m/z* 922.4 $(M\text{-}PF_6^-)^+$.

(*S*)-*tert*-butyl 2'-hydroxy-1,1'-binaphthyl-2-ylcarbamate (*S*)-(-)-(28).

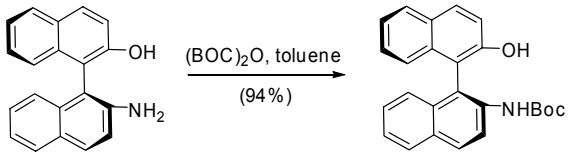

28

Procedure

$(BOC)_2O$ (220 mg, 0.94 mmol) was added to a stirred solution of (*S*)-NOBIN (300 mg, 1.05 mmol) in toluene (3 mL) and the stirring was continued for another 12 h at 80 ºC. The mixture was concentrated *in vacuo* and the residue was purified by flash-chromatography on silica gel (hexane/EtOAc 6:1) to afford **28** (380 mg, 94%). Mp 170-172ºC. $[\alpha]^{25}_D$ = -68.51 (*c* = 1.0, $CHCl_3$). **^{1}H-NMR** (500 MHz, $CDCl_3$) δ 8.52 (d, *J* = 7.6 Hz, 1H, CH_{Ar}), 8.04 (d, *J* = 7.4 Hz, 1H, CH_{Ar}), 7.99 (d, *J* = 7.7 Hz, 1H, CH_{Ar}), 7.91 (m, 2H, CH_{Ar}), 7.40 (m, 3H, CH_{Ar}), 7.30 (m, 2H, CH_{Ar}), 7.08 (d, *J* = 7.3 Hz, 1H, CH_{Ar}), 7.06 (d, *J* = 7.7 Hz, 1H, CH_{Ar}), 6.27 (s, 1H, NH_{Boc}), 5.03 (s, 1H, OH), 1.41 (s, 9H, CH_3). **^{13}C-NMR** (125 MHz, $CDCl_3$): δ 152.0 (CO), 136.6, 131.2, 130.8, 130.3, 129.7, 129.3, 128.3, 128.2, 127.3, 124.9, 124.4, 120.0, 118.0 (CH_{Ar}, C_{Ar}), 28.3 (CH_3).

(2*R*,8*R*)-2-(*tert*-butyldiphenylsilanyloxymethyl)-8-hydroxymethyl-3,4,6,7,8,9-hexahydro -2*H*-pyrimido[1,2-*a*]pyrimidin-1-ium methansulfonate (29).

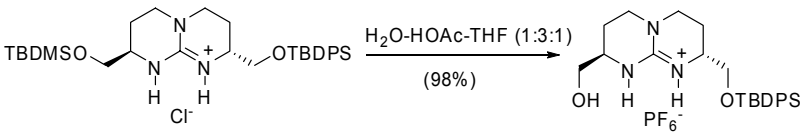

23 **29**

Procedure

A solution of **23** (6 g, 10.20 mmol) in a mixture of H_2O-HOAc-THF (1:3:1) was stirred at room temperature for 20 h. After removing the solvent, the crude product was dissolved in dichloromethane (150 mL) and washed subsequently with a sat solution of Na_2CO_3 (100 mL) and 2% (v/v) methanesulfonic acid (100 mL). The organic phase was dried over cotton and after evaporating the solvent, the remaining

oil was triturated with toluene/diethyl ether, yielding **29** (5.33 g, 98%) as a white solid. M.p. 130-132ºC. $[\alpha]^{25}_{D}$ -42.01 (*c* = 0.85, $CHCl_3$). **^{1}H-NMR** (500 MHz, $CDCl_3$) δ 9.23 (s, 1H, NH_{guan}), 7.78 (s, 1H, NH_{guan}), 7.67-7.63 (m, 4H, CH_{Ar}), 7.46-7.40 (m, 6H, CH_{Ar}), 3.83 (dd, *J* = 3.5, 14.5 Hz, 1H, CH_2OSi), 3.73 (dd, *J* = 12.5, 5.2 Hz, 1H, CH_2OSi), 3.63-3.47 (m, 4H, CH_2O, CH_α), 3.36-3.21 (m, 4H, $CH_{2\gamma}$), 2.13-1.86 (m, 5H, OH, $CH_{2\beta}$), 1.07 (s, 9H, $C(CH_3)_3$). **^{13}C-NMR** (125 MHz, $CDCl_3$) δ 151.2 (C_{guan}), 135.5, 135.4, 132.6, 129.8, 128.9, 127.8 (CH_{Ar}, C_{Ar}), 65.3, 63.7 (CH_2O), 50.6, 49.3 (CH_α), 45.6, 44.6 ($CH_{2\gamma}$), 26.7 ($C(CH_3)_3$), 22.7 ($CH_{2\beta}$), 19.1 ($C(CH_3)_3$). **ESI-MS** *m/z* 474.5 $[(M\text{-}PF_6^-)^+$.

(2*R*,8*R*)-2-(*tert*-butyldiphenylsilanyloxymethyl)-8-methansulfonyloxymethyl-3,4,6,7,8,9-hexahydro-2*H*-pyrimido[1,2-*a*]pyrimidin-1-ium hexafluorophosphate (30).

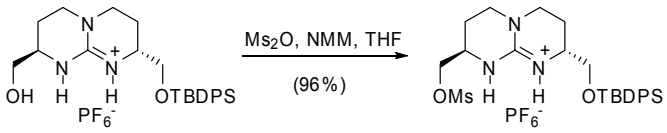

29 **30**

Procedure

To a solution of **29** (1.54 g, 2.89 mmol) in THF (50 mL) was added *N*-methylmorpholine (1.15 mL, 11.56 mmol) and methanesulfonic anhydride (1.14 g, 7.23 mmol) and the mixture was stirred at room temperature for 40 min. The solvent was removed at reduced pressure and the crude product dissolved in CH_2Cl_2. The organic phase was washed with a 0.1M NH_4PF_6 solution. The solvent was removed and the crude product was purified by column chromatography on silica gel (CH_2Cl_2/MeOH, 98:2), to afford **30** (1.82 g, 96%) as a white solid. M.p. 60-62ºC. $[\alpha]^{25}_{D}$ -43.51 (*c* = 0.5, MeOH). **^{1}H-NMR** (500 MHz, $CDCl_3$) δ 7.67-7.63 (m, 4H, CH_{Ar}), 7.46-7.40 (m, 6H, CH_{Ar}), 6.24 (s, 1H, NH_{guan}), 6.08 (s, 1H, NH_{guan}), 4.30 (m, 1H, CH_2OMs), 4.17 (m, 1H, CH_2OMs), 3.80 (m, 1H, CH_α), 3.66-3.63 (m, 2H, CH_2OSi), 3.57 (m, 1H, CH_α), 3.33 (m, 4H, $CH_{2\gamma}$), 3.08 (s, 3H, CH_3SO_3), 2.05-1.89 (m, 4H, $CH_{2\beta}$), 1.06 (s, 9H, $C(CH_3)_3$). **^{13}C-NMR** (125 MHz, $CDCl_3$) δ 150.6 (C_{guan}), 135.5, 132.5, 130.0, 128.9 (CH_{Ar}, C_{Ar}), 69.5 (CH_2OMs), 66.2 (CH_2OSi), 50.1, 47.7 (CH_α),

45.3, 44.9 ($CH_{2\gamma}$), 37.1 (CH_3SO_3), 26.7 ($C(CH_3)_3$), 22.4, 21.9 ($CH_{2\beta}$), 19.1 ($C(CH_3)_3$). **ESI-MS** *m/z* 516.2 $[(M\text{-}PF_6^-)^+$.

Compound 31.

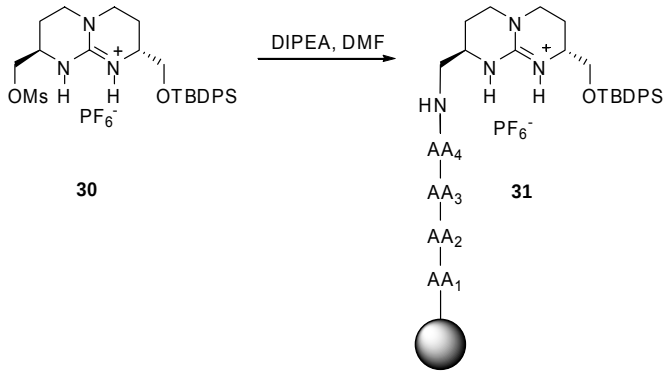

Procedure

To a suspension of resin (150 mg) in DMF, was added a solution of **30** (23 mg, 0.03 mmol) and DIPEA (3 drops) and the suspension was shaken during 2 days. Solvent was removed and the resin was subsquently washed with DMF and CH_2Cl_2. The ninhydrin test was negative (no free amine function NH_2 left).

(2*R*,8*R*)-2-(*tert*-butyldiphenylsilanyloxymethyl)-8-(2-aminobenzenethiolmethyl)-3,4,6,7,8,9-hexahydro-2*H*-pyrimido[1,2-*a*]pyrimidin-1-ium hexafluorophosphate (32).

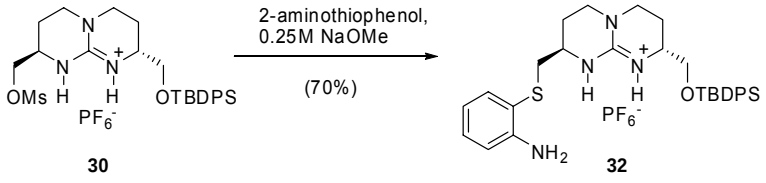

Procedure

A solution of **30** (200 mg, 0.30 mmol) and 2-aminothiophenol (0.096 mL, 0.91 mmol) in NaOMe (3.60 mL, 0.25M) was stirred overnight under argon atmosphere. The solvent was removed and the crude dissolved in CH_2Cl_2, washed with a 0.1M NH_4PF_6 solution, dried over Na_2SO_4 and concentrated *in vacuo*. The residue was purified by column chromatography on silica gel (CH_2Cl_2/ MeOH 96:4) to afford **32** as a pure maroon solid (145 mg, 70%). M.p. 165-167ºC. $[\alpha]^{25}_D$ -47.50 (*c* = 0.5, MeOH). **^{1}H-NMR** (500 MHz, $CDCl_3$) δ 7.65-7.60 (m, 4H, CH_{Ar}), 7.50-7.41 (m, 7H, CH_{Ar}), 7.13 (t,

J = 6.4 Hz, 1H, CH_{Ar}), 6.72 (m, 2H, CH_{Ar}), 6.67 (s, 1H, NH_{guan}), 6.07 (s, 1H, NH_{guan}), 4.43 (s, 2H, NH_2), 3.72 (m, 2H, CH_2S), 3.57 (m, 1H, CH_α), 3.35-3.26 (m, 5H, $CH_{2\gamma}$, CH_α), 2.95-2.79 (m, 2H, CH_2O), 2.12-1.85 (m, 4H, $CH_{2\beta}$), 1.00 (s, 9H, $C(CH_3)_3$). **^{13}C-NMR** (125 MHz, $CDCl_3$) δ 150.4 (C_{guan}), 148.5, 136.3, 135.6, 132.1, 130.6, 130.0, 127.9, 119.5, 116.2, 115.9 (CH_{Ar}, C_{Ar}), 65.2 (CH_2O), 49.9, 48.3 (CH_α), 45.6, 45.0 ($CH_{2\gamma}$), 40.0 (CH_2S), 26.8 (CH_3), 25.4, 22.4 ($CH_{2\beta}$), 19.4 ($C(CH_3)_3$). **ESI-MS** *m/z* 545.3 $[(M\text{-}PF_6^-)^+$.

(2*R*,8*R*)-2-(*tert*-butyldiphenylsilanyloxymethyl)-8-[1-butyl-3-(2-mercaptophenyl)ureamethyl]-3,4,6,7,8,9-hexahydro-2*H*-pyrimido[1,2-*a*]pyrimidin-1-ium hexafluorophosphate (33).

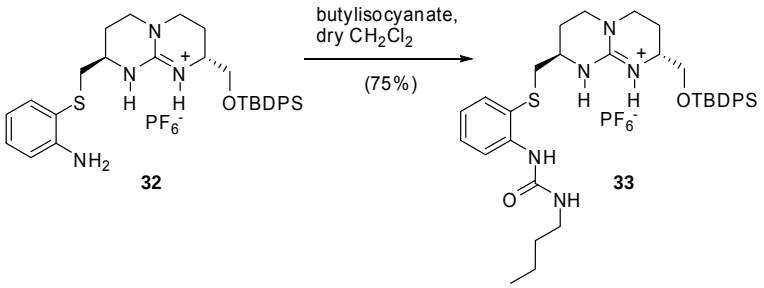

Procedure

To a solution of **32** (100 mg, 0.14 mmol) in dry CH_2Cl_2 (5 mL), butyl isocyanate (0.05 mL, 0.43 mmol) was added under argon atmosphere and the mixture was stirred overnight. The solvent was removed; the crude was then dissolved in CH_2Cl_2, washed with a 0.1 M NH_4PF_6 solution, dried (Na_2SO_4) and concentrated *in vacuo*. The residue was purified by column chromatography on silica gel (CH_2Cl_2/ MeOH 98:2) to afford **33** as a pure white solid (86 mg, 75 %). M.p. 116-118ºC. $[\alpha]^{25}_D$ -60.12 (c = 1, CH_3CN). **^{1}H-NMR** (500 MHz, CD_3CN) δ 7.65 (m, 4H, CH_{Ar}), 7.50 (m, 8H, CH_{Ar}), 7.24 (m, 4H, NH_{guan}, CH_{Ar}), 6.61 (s, 2H, NH_{urea}), 5.85 (s, 2H, NH_{urea}), 3.64 (m, 1H, CH_2), 3.24-2.84 (m, 12H, CH_α, $CH_{2\gamma}$, CH_2S, CH_2O), 1.92-1.78 (m, 4H, $CH_{2\beta}$), 1.58 (m, 4H, CH_2), 1.39 (m, 4H, CH_2), 1.06 (s, 9H, CH_3), 0.89 (t, 3H, CH_3). **^{13}C-NMR** (CD_3CN, 125 MHz) δ 155.6 (C_{urea}), 150.0 (C_{guan}), 135.6, 135.5, 129.9, 128.8, 127.9, 122.1, 120.4 (CH_{Ar}, C_{Ar}), 65.9 (CH_2O), 49.9, 47.9 (CH_α), 45.4 (CH_2S), 39.1 ($CH_{2\gamma}$), 32.1 (CH_2), 26.1 ($CH_{2\beta}$), 22.5 (CH_2), 19.9 (CH_3), 14.6 (CH_3). **ESI-MS** *m/z* 545.3 $[(M\text{-}PF_6^-)^+$.

(2*R*,8*R*)-2-hydroxymethyl-8-[1-butyl-3-(2-mercaptophenyl)ureamethyl]-3,4,6,7,8,9-hexahydro-2*H*-pyrimido[1,2-*a*]pyrimidin-1-ium hexafluorophosphate (34).

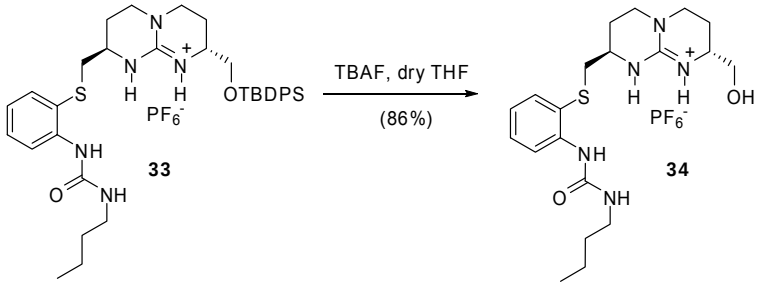

Procedure

A solution of **33** (250 mg, 0.32 mmol) and tetrabutylammonium fluoride (0.32 mL, 1M in THF) was stirring in dry THF overnight under argon atmosphere. The solvent was removed; the crude was then dissolved in CH_2Cl_2, washed with a 0.1 M NH_4PF_6 solution, dried (Na_2SO_4) and concentrated *in vacuo*. The residue was purified by column chromatography on silica gel (CH_2Cl_2/ MeOH 100 to 96:4) to afford **34** as a pure white solid (150 mg, 86%). M.p. 90-92ºC. $[\alpha]^{25}_D$ -50.21 (*c* = 1, CH_3CN). **^{1}H-NMR** (500 MHz, CD_3CN) δ 7.63 (d, *J* = 7.5 Hz, 1H, CH_{Ar}), 7.43 (d, *J* = 7.3 Hz, 1H, CH_{Ar}), 7.32 (t, *J* = 7.5 Hz, 1H, CH_{Ar}), 7.28 (s, 1H, NH_{guan}), 7.21 (m, 2H, NH_{guan}, CH_{Ar}), 6.55 (s, 1H, NH_{urea}), 3.44-3.15 (m, 11H, CH_2, CH_α, $CH_{2\gamma}$, CH_2S, CH_2O), 2.81 (dd, *J* = 6.9, 13.5 Hz, 1H, CH_2O), 1.92-1.84 (m, 4H, $CH_{2\beta}$), 1.56 (m, 4H, CH_2), 1.41 (m, 4H, CH_2), 0.91 (t, *J* = 7.8 Hz, 3H, CH_3). **^{13}C-NMR** (CD_3CN, 125 MHz) δ 155.6 (C_{urea}), 150.0 (C_{guan}), 135.6, 135.5, 129.9, 128.8, 127.9, 122.1, 120.4 (CH_{Ar}, C_{Ar}), 65.9 (CH_2O), 49.9, 47.9 (CH_α), 45.4 (CH_2S), 41.0 (CH_2) 39.1 ($CH_{2\gamma}$), 32.1 (CH_2), 26.1 ($CH_{2\beta}$), 22.5 (CH_2), 14.5 (CH_3). **ESI-MS** *m/z* 406.2 $[(M\text{-}PF_6^-)^+$.

(2*R*,8*R*)-2-methanesulfonyloxymethyl-8-[1-butyl-3-(2-mercaptophenyl)ureamethyl]-3,4,6,7,8,9-hexahydro-2*H*-pyrimido[1,2-*a*]pyrimidin-1-ium hexafluorophosphate (35).

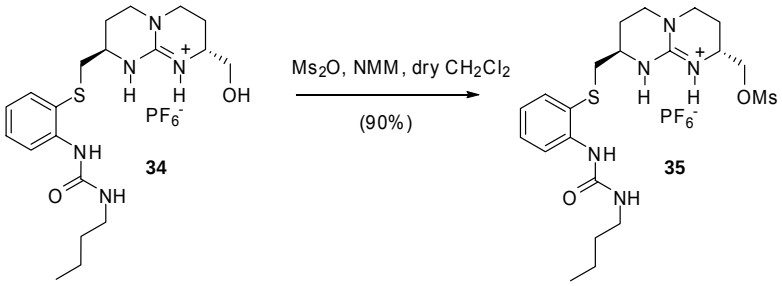

Procedure

To a solution of **34** (72 mg, 2.89 mmol) in dry CH_2Cl_2 (10 mL) was added *N*-methylmorpholine (0.06 mL, 0.52 mmol) and methanesulfonic anhydride (51 mg, 0.37 mmol) and the mixture was stirred at room temperature for 2 hours. The solvent was removed; the crude was then dissolved in CH_2Cl_2, washed with a 0.1 M NH_4PF_6 solution, dried (Na_2SO_4) and concentrated *in vacuo*. The residue was purified by column chromatography on silica gel (CH_2Cl_2/ MeOH 100 to 98:2) to afford **35** as a pure white solid (74 mg, 90%). M.p. 87-89ºC. $[\alpha]^{25}_D$ -47.25 (*c* = 1, CH_3CN). **^{1}H-NMR** (500 MHz, CD_3CN) δ 7.63 (d, *J* = 7.5 Hz, 1H, CH_{Ar}), 7.43 (d, *J* = 7.3 Hz, 1H, CH_{Ar}), 7.32 (t, *J* = 7.5 Hz, 1H, CH_{Ar}), 7.28 (s, 1H, NH_{guan}), 7.21 (m, 2H, NH_{guan}, CH_{Ar}), 6.55 (s, 1H, NH_{urea}), 5.57 (s, 1H, NH_{urea}), 3.44-3.15 (m, 14H, CH_2, CH_α, $CH_{2\gamma}$, CH_2S, CH_2O, CH_3), 2.81 (dd, *J* = 6.8, 13.7 Hz, 1H, CH_2O), 1.92-1.84 (m, 4H, $CH_{2\beta}$), 1.56 (m, 4H, CH_2), 1.41 (m, 4H, CH_2), (t, *J* = 7.8 Hz, 3H, CH_3). **^{13}C-NMR** (CD_3CN, 125 MHz) δ 155.6 (C_{urea}), 150.0 (C_{guan}), 135.6, 135.5, 129.9, 128.8, 127.9, 122.1, 120.4 (CH_{arom}, C_{Ar}), 65.9 (CH_2O), 49.9, 47.9 (CH_α), 45.4 (CH_2S), 39.9, 39.1 ($CH_{2\gamma}$), 37.1 (CH_3SO_3), 32.1 (CH_2), 26.1 ($CH_{2\beta}$), 22.5 (CH_2), 14.5 (CH_3). **ESI-MS** *m/z* 484.2 $[(M-PF_6^-)^+$.

Compound 36.

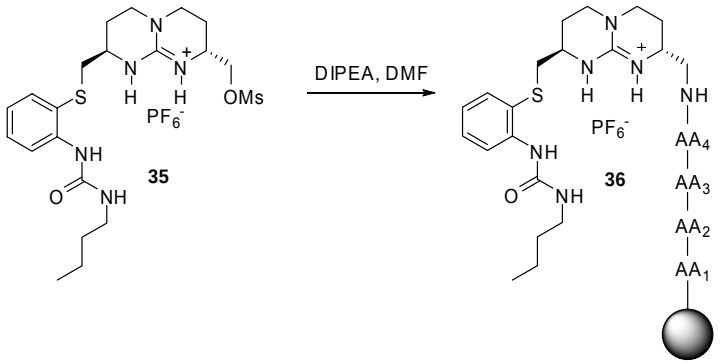

Procedure

To a suspension of resin (150 mg) in DMF, was added a solution of **35** (20 mg, 0.03 mmol) and DIPEA (3 drops) and the suspension was shaken during two days. Solvent was removed and the resin was subsquently washed with DMF and CH_2Cl_2. The ninhydrin test was negative (no free amine function NH_2 left).

(*R*)-2-(6-hydroxy-naphthalen-2-yl)-propionic acid (*R*)-38.

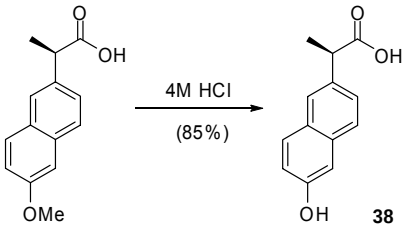

Procedure

A solution of (*R*)-Naproxen (1.0 g, 4.34 mmol) in a 4M HCl solution (5 ml) was stirred for 48 hours at reflux. The mixture was allowed to cool down to room temperature, filtered and the resulted solid was washed with very cold water to afford **(*R*)-38** as a pure white solid (0.80 g, 85 %). M.p. 144-146ºC. $[\alpha]^{25}_{D}$ -53.2 (*c* = 1.5, acetone). **^{1}H-NMR** (500 MHz, [D_6]-DMSO) δ9.65 (s, 1H, OH), 7.73 (d, *J* = 8.7 Hz, 1H, CH_{Ar}), 7.62 (m, 2H, CH_{Ar}), 7.32 (m, 1H, CH_{Ar}), 7.05 (m, 2H, CH_{Ar}), 3.75 (q, *J* = 7.1 Hz, 1H, CH), 1.42 (d, J = 7.1Hz, 3H, CH_3,). **^{13}C-NMR** (125 MHz, [D_6]-DMSO) δ 175.5 (CO), 155.1, 135.4, 133.5, 127.6, 126.2, 126.1, 125.5, 126.1, 118.8, 106.8 (CH_{Ar}, C_{Ar}), 44.6 (CH), 18.4 (CH_3).

(*S*)-2-(6-hydroxy-naphthalen-2-yl)-propionic acid (*S*)-38.

Prepared from (*S*)-Naproxen (3.0 g, 13.03 mmol) in a 4M HCl solution (15 ml) in order to afford **(*S*)-38** as a pure white solid (2.56 g, 91 %). $[\alpha]^{25}_{D}$ +54.7 (*c* = 1.5, acetone).

(*R*)-2-(6-Hydroxy-naphthalen-2-yl)-propionic acid *tert*-butyl ester (*R*)-39.

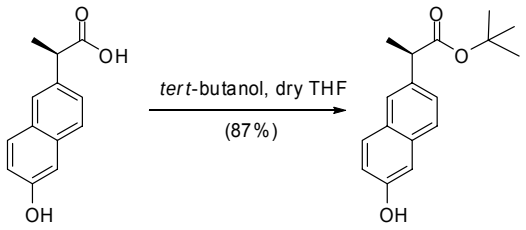

38 **39**

Procedure

The Naproxen derivative **(*R*)-38** (0.78 g, 3.39 mmol) was dissolved in dry THF (35 ml) under nitrogen atmosphere. The solution was cooled to 0 °C before trifluoroacetic anhydride (2.8 mL, 20.30 mmol) was added dropwise. The mixture was further stirred for 4 hours maintaining the temperature below 5 °C. *tert*-Butanol (8 ml) was added dropwise and the resulting mixture was then allowed to rise to room temperature and was vigorously stirred overnight. The reaction was cooled again to ice-bath temperature and NH_4OH (35 % in water, 3 mL) was added dropwise. After completing addition, the mixture was allowed to warm up to room temperature again and was eventually stirred for further 30 minutes before the volatiles were evaporated under vacuum. The residue was triturated with boiling CH_2Cl_2 and the crystalline solid formed was removed by filtration. The filtrate was washed with an aqueous $NaHCO_3$ saturated solution, dried ($MgSO_4$) and concentrated *in vacuo*. Purification by column chromatography on silica gel (Hexane / AcOEt 75:25) affords **(*R*)-39** as a white solid (775 mg, 87%). M.p. 160-162ºC. $[\alpha]^{25}_{D}$ -25.8 (*c* = 1.0, $CHCl_3$). **^{1}H-NMR** (500 MHz, $CDCl_3$) δ 7.69 (d, *J* = 8.7 Hz, 1H, CH_{Ar}), 7.63 (m, 2H, CH_{Ar}), 7.39 (dd, *J* = 1.8, 8.5 Hz, 1H, CH_{Ar}), 7.11-7.06 (m, 2 H, CH_{Ar}), 3.75 (q, *J* = 7.1 Hz, 3H, CH_3), 1.53 (d, *J* = 7.2 Hz, 1H, CH), 1.41 (s, 9H, $CH_{3t\text{-}Bu}$). **^{13}C-NMR** (125 MHz, $CDCl_3$) δ 175.2 (CO), 155.6, 136.0, 133.5, 129.8, 126.7, 126.6, 126.0, 125.3, 118.0, 109.4 (CH_{Ar}, C_{Ar}), 46.6 (CH), 28.1 ($C_{t\text{-}Bu}$), 18.4 (CH_3).

(*S*)-2-(6-Hydroxy-naphthalen-2-yl)-propionic acid *tert*-butyl ester (*S*)-39.

Prepared form **(*S*)-38** (2.5 g, 10.85 mmol) in dry THF (110 mL), trifluoroacetic anhydride (9.1 mL, 65.14 mmol), *tert*-butanol (26 mL), NH_4OH (35 % in water, 7.5 mL) in order to afford **(*S*)-39** as a white solid (2.46 g, 83%). $[\alpha]^{25}_D$ +27.2 (*c* = 1.0, $CHCl_3$).

(*R*)-2-(6-(3-bromopropoxy)naphthalen-2-yl)propionic acid *tert*-butyl ester (*R*)-43.

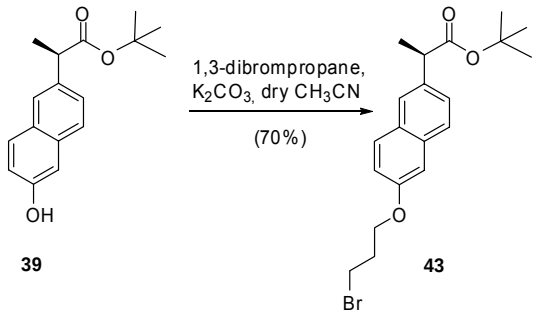

39 43

Procedure

To a solution of **(*R*)-39** (400 mg, 1.47 mmol) and K_2CO_3 (168 mg, 1.21 mmol) in dry CH_3CN (10 ml) under nitrogen atmosphere was added 1,3-dibromopropane (0.66 mL, 5.88 mmol) and the reaction mixture was stirred at 60ºC for 48 hours. After removing the solvent, the residue was dissolved in CH_2Cl_2, washed with water, dried ($MgSO_4$) and concentrated *in vacuo*. Purification by column chromatography on silica gel (hexane/AcOEt 9:1) afforded **(*R*)-43** as a pure colorless oil (400 mg, 70%). M.p. 158-160ºC. $[\alpha]^{25}_D$ -31.5 (*c* = 1, $CHCl_3$). **^{1}H-NMR** (500 MHz, $CDCl_3$) δ 7.72 (m, 3H, CH_{Ar}), 7.44 (dd, *J* = 1.6, 8.4 Hz, 1H, CH_{Ar}), 7.17 (m, 2 H, CH_{Ar}), 4. 24 (t, *J* = 5.8 Hz, 2H, CH_2O), 3.76 (q, *J* = 7.2 Hz, 1H, CH), 3.66 (t, *J* = 6.4 Hz, 2H, CH_2Br), 2.40 (q, *J* = 6.1 Hz, 2H, CH_2), 1.55 (d, *J* = 7.1 Hz, 3H, CH_3), 1.41 (s, 9H, $CH_{3t\text{-}Bu}$). **^{13}C-NMR** (125 MHz, $CDCl_3$) δ 174.0 (CO), 156.6 (CO), 136.7, 133.7, 129.5, 129.2, 127.2, 127.1, 126.6, 125.9, 119.0, 106.8 (CH_{Ar}, C_{Ar}), 80.6 ($C(CH_{3t\text{-}Bu})$), 65.5 (CH_2O), 46.6 (CH), 32.5 (CH_2Br), 30.1 (CH_2), 28.1 ($CH_{3t\text{-}Bu}$), 18.5 (CH_3).

(*S*)-2-[6-(3-bromopropoxy)naphthalen-2-yl]propionic acid *tert*-butyl ester (*S*)-43. Prepared from **(*S*)-39** (400 mg, 1.47 mmol), K_2CO_3 (168 mg, 1.21 mmol), dry CH_3CN (10 ml), 1,3-dibromopropane (0.66 mL, 5.88 mmol) in order to afford **(*S*)-43** as a pure colorless oil (400 mg, 70%). $[\alpha]^{25}_D$ +30.3 (*c* = 1, $CHCl_3$).

(*R*)-*tert*-Butyl-2-{6-[3-(5-(dimethylamino)naphthalene-1-sulfonamido)propoxy] naphthalen-2-yl}propanoate [(*R*)-45].

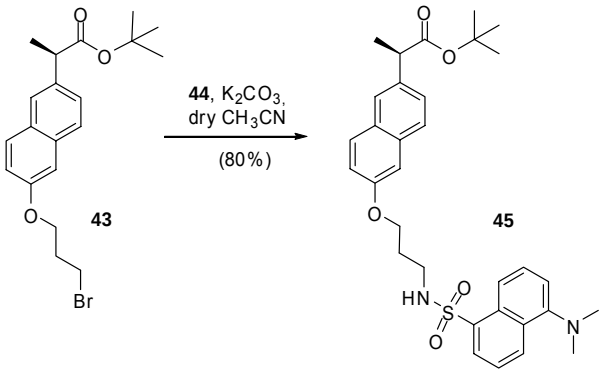

Procedure

A solution of **(*R*)-43** (35 mg, 0.09 mmol), **44** (33 mg, 0.14 mmol) and K_2CO_3 (18 mg, 0.14 mmol) in dry CH_3CN was stirred under nitrogen at 80ºC during 24 hours. After removing the solvent, the residue was dissolved in CH_2Cl_2, washed with water, dried ($MgSO_4$) and concentrated *in vacuo*. Purification by column chromatography on silica gel (from hexane/AcOEt 95:5 to CH_2Cl_2 95:5) afforded **(*R*)-45** as a pure yellow solid (40 mg, 80%). M.p. 192-194ºC. $[\alpha]^{25}_D$ -48.5 (*c* = 1, $CHCl_3$). **^{1}H-NMR** (500 MHz, $CDCl_3$) δ 8.50 (d, *J* = 8.5 Hz, 1H, CH_{Ar}), 8.29 (d, *J* = 8.6 Hz, 2H, CH_{Ar}), 7.66 (m, 3H, CH_{Ar}), 7.51 (m, 1H, CH_{Ar}), 7.43 (m, 2H, CH_{Ar}), 7.11 (d, *J* = 7.2 Hz, 1H, CH_{Ar}), 7.03 (d, *J* = 7.2 Hz, 1H, CH_{Ar}), 6.93 (m, 1H, CH_{Ar}), 5.09 (t, *J* = 5.8Hz, 1H, NH), 4.15 (q, *J* = 6.1 Hz, 2H, CH_2N), 3.98 (t, *J* = 5.8 Hz, 2H, CH_2O), 3.75 (q, *J* = 7.2 Hz, 1H, CH), 3.17 (q, *J* = 6.6 Hz, 2H, CH_2), 2.85 (s, 6H, CH_3), 1.55 (d, *J* = 7.1 Hz, 3H, CH_3), 1.42 (s, 9H, $CH_{3t\text{-}Bu}$). **^{13}C-NMR** (125 MHz, $CDCl_3$) δ 174.0 (CO), 156.6 (CO), 151.9, 136.8, 130.5, 129.8, 129.3, 128.4, 127.0, 126.4, 125.7, 123.2, 118.7, 118.5, 115.2, 106.5 (CH_{Ar}, C_{Ar}), 65.7 (CH_2O), 46.6 (CH), 45.4 ($C_{t\text{-}Bu}$), 41.2 (CH_2N), 28.9 (CH_2), 28.0 ($CH_{3t\text{-}Bu}$), 18.6 (CH_3).

(*S*)-*tert*-Butyl-2-{6-[3-(5-(dimethylamino)naphthalene-1-sulfonamido)propoxy] naphthalen-2-yl}propanoate [(*S*)-45].

Prepared from **(*S*)-43** (110 mg, 0.28 mmol), **44** (105 mg, 0.42 mmol) and K_2CO_3 (58 mg, 0.42 mmol) in order to afford **(*S*)-45** as a pure yellow solid (140 mg, 89%). $[\alpha]^{25}_D$ +50.0 (*c* = 1, $CHCl_3$).

(*R*)-2-{6-[3-(5-(dimethylamino)naphthalene-1-sulfonamido)propoxy]naphthalen-2-yl}propanoic acid [(*R*)-46].

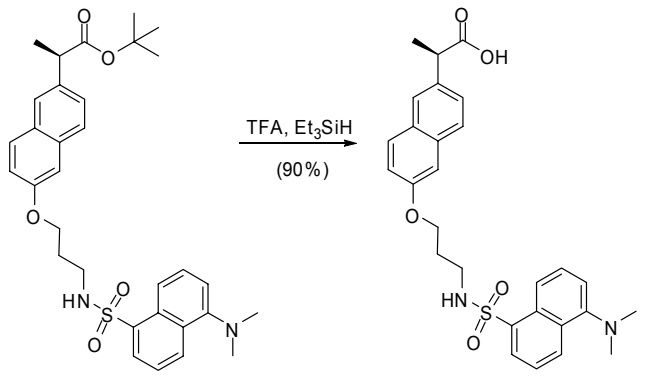

Procedure

A solution of **(*R*)-45** (32 mg, 0.06 mmol), TFA (0.5 mL) and Et_3SiH (0.2 mL) in CH_2Cl_2 was stirred during 24 hours. After removing the solvent, the residue was dissolved in CH_2Cl_2, washed with water, dried ($MgSO_4$) and concentrated *in vacuo*. Purification by column chromatography on silica gel (hexane/AcOEt 1:9) afforded **(*R*)-46** as a pure yellow solid (26 mg, 90%). M.p. 187-189ºC. $[\alpha]^{25}_D$ -41.3 (*c* = 1, $CHCl_3$). **^{1}H-NMR** (500 MHz, $CDCl_3$) δ 8.48 (d, *J* = 8.5 Hz, 1H, CH_{Ar}), 8.29 (m, 2H, CH_{Ar}), 7.68 (m, 3H, CH_{Ar}), 7.43 (m, 3H, CH_{Ar}), 7.07 (d, *J* = 7.2 Hz, 1H, CH_{Ar}), 7.01 (d, *J* = 7.1 Hz, 1H, CH_{Ar}), 6.89 (m, 1H, CH_{Ar}), 5.26 (s, 1H, NH), 3.98 (t, *J* = 5.8 Hz, 2H, CH_2O), 3.94 (m, 3H, CH, CH_2O), 3.18 (q, *J* = 6.1 Hz, 2H, CH_2), 2.82 (s, 6H, CH_3), 1.94 (m, 2H, CH_2), 1.62 (d, *J* = 7.1 Hz, 3H, CH_3). **^{13}C-NMR** (125 MHz, $CDCl_3$) δ 180.0 (CO), 156.5 (CO), 152.0, 135.1, 133.8, 130.5, 129.8, 129.7, 129.3, 128.9, 128.4, 127.4, 126.2, 126.1, 123.2, 118.9, 118.5, 115.2, 106.5 (CH_{Ar}, C_{Ar}), 65.5

(CH_2O), 45.5 (CH), 45.4 ($C_{t\text{-}Bu}$), 41.0 (CH_2N), 28.9 (CH_2), 18.2 (CH_3). **ESI-MS** *m/z* 506.1 $(M\text{-}PF_6^-)^+$.

(*S*)-2-{6-[3-(5-(dimethylamino)naphthalene-1-sulfonamido)propoxy]naphthalen-2-yl}propanoic acid [(*S*)-46].

Prepared from **(*S*)-45** (180 mg, 0.32 mmol), TFA (3.0 mL) and Et_3SiH (1.2 mL) in CH_2Cl_2 (10 mL) to afford **(*S*)-46** as a pure yellow solid (150 mg, 92%). $[\alpha]^{25}_D$ +43.4 (*c* = 1, $CHCl_3$).

5-dimethylamino-*N*-(5-hydroxypentyl)naphthalene-1-sulfonamide (40).

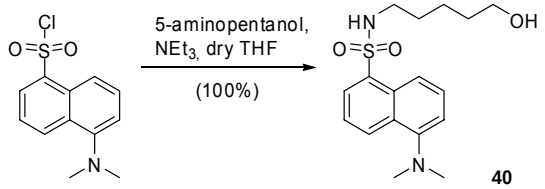

40

Procedure

A mixture of dansyl chloride (520 mg, 1.89 mmol), triethylamine (790 µl, 5.66 mmol) and 5-aminopentanol (195 mg, 2.00 mmol) was stirred in dry THF (40 ml) at room temperature during two days. The solvent was removed and the crude dissolved in CH_2Cl_2, washed twice with water and once with brine, dried on $MgSO_4$ and concentrated *in vacuo*. The residue was purified by column chromatography on silica gel (AcOEt / Hexane 8:2) to afford **40** as a pure yellow solid (530 mg, 100%). M.p. 75-77ºC. **^{1}H-NMR** (500 MHz, $CDCl_3$) δ 8.52 (d, J = 8.5 Hz, 1H, CH_{Ar}), 8.33 (d, J = 8.6 Hz, 1H, CH_{Ar}), 8.22 (d, J = 7.3 Hz, 1H, CH_{Ar}), 7.53 (m, 2H, CH_{Ar}), 7.16 (d, J = 7.2 Hz, 1H, CH_{Ar}), 5.44 (t, J = 6.1 Hz, 1H, NH), 3.46 (t, J = 6.4 Hz, 2H, CH_2O), 2.89 (m, 8H, CH_2N, CH_3), 1.37 (m, 4H, CH_2), 1.26 (m, 2H, CH_2). **^{13}C-NMR** (125 MHz, $CDCl_3$) δ 151.9, 134.9, 130.3, 129.9, 129.6, 129.5, 128.3, 123.3, 118.9, 115.2 (CH_{Ar}, C_{Ar}), 62.4 (CH_2O), 45.4 (CH_3), 43.0 (CH_2), 31.8 (CH_2), 29.1 (CH_2), 22.6 (CH_2).

5-[5-(dimethylamino)naphthalene-1-sulfonamido]pentyl methanesulfonate (41).

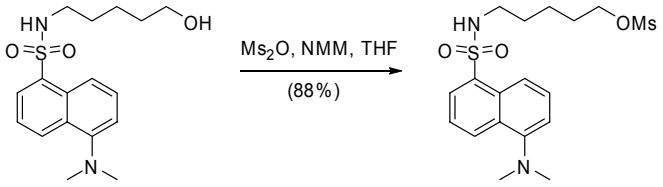

40 **41**

Procedure

To a solution of **40** (1.08 g, 3.35 mmol) and NMM (1.5 ml, 13.4 mmol) in dry THF (15 ml) was added a solution of Ms_2O (1.20 g, 6.70 mmol) in dry THF (5 ml) under nitrogen atmosphere at room temperature. The mixture was stirred overnight and the solvent was removed. The crude was dissolved in CH_2Cl_2 and washed twice with water and brine, dried over $MgSO_4$ and then concentrated *in vacuo*. The crude product was then purified by column chromatography on silica gel (AcOEt / Hexane 7:3) to afford **41** as a pure yellow solid (611 mg, 88%). M.p. 72-74ºC. **^{1}H-NMR** (500 MHz, $CDCl_3$) δ 8.56 (d, J = 8.5 Hz, 1H, CH_{Ar}), 8.33 (d, J = 8.6 Hz, 1H, CH_{Ar}), 8.22 (d, J = 7.3 Hz, 1H, CH_{Ar}), 7.53 (m, 2H, CH_{Ar}), 7.16 (d, J = 7.2 Hz, 1H, CH_{Ar}), 5.44 (t, J = 6.1 Hz, 1H, NH), 4.05 (t, J = 6.4 Hz, 2H, CH_2O), 2.98 (s, 3H, CH_3), 2.89 (m, 8H, CH_2N, CH_3), 1.55 (m, 2H, CH_2), 1.43 (m, 2H, CH_2), 1.31 (m, 2H, CH_2). **^{13}C-NMR** (125 MHz, $CDCl_3$) δ 152.4 (CN), 134.9, 130.5, 129.9, 129.8, 129.6, 128.4, 123.2, 118.7, 115.3 (CH_{Ar}, C_{Ar}), 69.7 (CH_2N), 45.5 (CH_3N), 42.9 (CH_2O), 37.3 (CH_3S), 28.9 (CH_2), 28.4 (CH_2), 22.3 (CH_2).

***N*-5-bromopentyl-5-(dimethylamino)naphthalene-1-sulfonamide (42).**

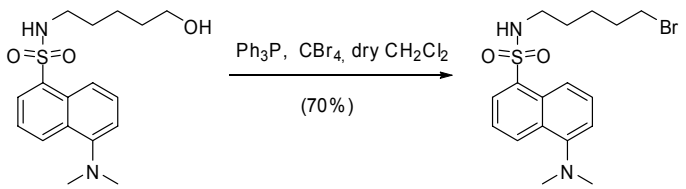

40 **42**

Procedure

A solution of 40 (50 mg, 0.15 mmol), Ph_3P (117 mg, 0.44 mmol) and CBr_4 (146 mg, 0.45 mmol) in dry CH_2Cl_2 (5 ml) was stirred overnight under nitrogen atmosphere at

room temperature. The solvent was removed and the residue was dissolved in CH_2Cl_2 and washed with brine, dried (Na_2SO_4) and then concentrated *in vacuo*. Purification by column chromatography on silica gel (AcOEt / Hexane 7:3) affords **42** as a pure yellow solid (40 mg, 70%). M.p. 80-82ºC. **^{1}H-NMR** (500 MHz, $CDCl_3$) δ 8.60 (d, J = 8.4 Hz, 1H, CH_{Ar}), 8.32 (d, J = 8.4 Hz, 1H, CH_{Ar}), 8.28 (d, J = 8.3 Hz, 1H, CH_{Ar}), 7.58 (m, 2H, CH_{Ar}), 7.16 (d, J = 7.2 Hz, 1H, CH_{Ar}), 4.82 (t, J = 5.9 Hz, 1H, NH), 3.35 (t, J = 6.4 Hz, 1H, CH_2Br), 3.25 (t, J = 6.3 Hz, 1H, CH_2Br), 2.89 (m, 8H, CH_2N, CH_3), 1.85-1.50 (m, 6H, CH_2). **^{13}C-NMR** (125 MHz, $CDCl_3$) δ 152.1 (CN), 134.8, 130.5, 129.9, 129.8, 129.6, 128.5, 123.2, 118.7, 115.2 (CH_{Ar}, C_{Ar}), 45.5 (CH_3N), 43.0 (CH_2) 31.8 (CH_2), 28.8 (CH_2), 24.9 (CH_2), 23.7 (CH_2).

5-(dimethylamino)naphthalene-1-sulfonamide (44).

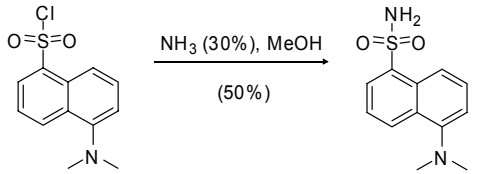

44

Procedure

Dansyl chloride was stirred in NH_3 (30%, 30 mL)/MeOH (10 mL) during 8 hours. The solvent was removed and the residue was purified by column chromatography on silica gel (Hexane/ AcOEt 1:1) to afford **44** as a pure white solid (230 mg, 50%). M.p. 60-62ºC. **^{1}H-NMR** (500 MHz, CD_3CN) δ 8.57 (d, J = 8.7 Hz, 1H, CH_{Ar}), 8.31 (d, J = 8.5 Hz, 1H, CH_{Ar}), 8.22 (d, J = 8.7 Hz, 1H, CH_{Ar}), 7.62 (q, J = 8.1 Hz, 2H, CH_{Ar}), 7.31 (d, J = 8.2 Hz, 1H, CH_{Ar}), 5.83 (s, 2H, NH_2), 2.91 (s, 6H, CH_3). **^{13}C-NMR** (125 MHz, CD_3CN) δ 152.1, 134.8, 130.5, 129.9, 129.8, 129.6, 128.5, 123.2, 118.7, 115.2 (CH_{Ar}, C_{Ar}), 45.5 (CH_3).

3.5.3 Library synthesis and Screening Experiments

Chloranil Test.[73]

To a small sample were added two drops of 2% acetaldehyde/DMF and two drops of 2% *p*-chloranil/DMF. The sample was allowed to stand for 5 minutes. Blue stained beads indicate the presence of secondary amines on the resin ("positive" result).

Resin Synthesis

The Tentagel NH_2 resin (1.0902, loading 0.51 mmol) was swelled in CH_2Cl_2. It was then washed several times with DMF. Met(Fmoc)OH (0.381 mg, 1.02 mmol), DIC (240 µL, 1.53 mmol) and HOBT (208 mg, 1.53 mmol) were dissolved in DMF (2ml) and added to the resin. A solution of DIPEA (262 µL, 1.53 mmol) in DMF was added. The funnel was degazed and DMF was added about for ¾ of the tube. The solution was stirred during two hours. The solvent was removed by filtration. DMF was added and filtered. The resin was washed with CH_2Cl_2 (three times), DMF (once). A qualitative ninhydrin test was negative. The Fmoc group was removed using treatment by 20% piperidine in DMF during 20 min and the resin washed with DMF and CH_2Cl_2. A qualitative ninhydrin test was positive.

A solution of FmocArg(Pbf)OH (0.663 mg, 1.02 mmol), DIC (240 µL, 1.53 mmol) and HOBT (208 mg, 1.53 mmol) in DMF (2 mL) was added to the resin, followed by DIPEA (262 µL, 1.53 mmol) and the suspension was shaken overnight. Solvent was removed and the resin was subsquently washed with DMF, CH_2Cl_2, DMF and CH_2Cl_2. The ninhydrin test was negative. Fmoc deprotection was achieved by 20% piperidine-DMF solution. A qualitative ninhydrin test was positive.

[73] Vojkovsky, T. *Pept. Res*., **1995**, *8*, 236-237.

Synthesis of FmocAhx.[74]

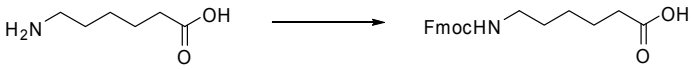

Ahx (1.167 g, 8.9 mmol) was dissolved in a H_2O/dioxane mixture (16:14 mL) and Na_2CO_3 (1.890 g, 17.8 mmol) was added. The mixture was cooled to 0°C. A solution of FmocCl (2.300 g, 8.9 mmol) in dioxane (14 mL) was added dropwise. The mixture was stirred for one hour at 0°C and then at room temperature for 16 hours. The reaction mixture was diluted with water (about 100 mL) and washed with Et_2O. The aqueous phase was acidified with concentrated HCl and extracted with AcOEt. The organic phase was then dried ($MgSO_4$) and evaporated to give the expected product as a white solid (2.95 g, 94%).

The resin was first washed with a 1:1 DIPEA-DMF solution three times. A solution of FmocAhx (0.360 mg, 1.02 mmol), DIC (240 µL, 1.53 mmol) and HOBT (208 mg, 1.53 mmol) in DMF (2 mL) was added to the resin, followed by DIPEA (262 µL, 1.53 mmol) and the suspension was shaken all night. Solvent was removed and the resin was subsquently washed with DMF, CH_2Cl_2, DMF and CH_2Cl_2. The ninhydrin test was negative Fmoc deprotection was achieved by 20% piperidine-DMF solution. A qualitative ninhydrin test was positive. This coupling was realized twice.

Determination of the exact loading of the resin.

To a known quantity (3-5 mg) of resin was added ninhydrin A solution (3 drops) and ninhydrin B solution (1 drop). A control was also prepared simply using the stains without the resin present. The three tests tubes (resin in double) were then heated in the hot block at 100°C for 5 minutes. Approx 2 ml of 60% EtOH aqueous solution was added to each test glass and then the solution was transferred to a 25 mL volumetric flask by pipetting through a glass wool plug-in pipette. The volume was then made up to 25 mL with 60% EtOH aqueous solution.

[74] Narasimhan, C.; Lai, C.-S.; Joseph, J. *Bioorg. Chem.* **1996**, *24*, 50-58.

UV absorbance is measured at 570 nm. Use the control as a blank, i.e. the background with it, then measure the absorbance of the resin sample.

Substitution (mmol/g) = $(A_{570}. V.10^3) / E.m$

Where m: mass (mg)

V: volume (mL)

$E = 1.5.10^4$ (M/cm)

Done four times: Substitution: 0.215 mmol/g: theoretical: 0.210 mmol/g

"Split and Mix" synthesis.

The peptide library was then prepared, using four cycles of "split and mix method". The resulting resin was divided in eight equal portions. To each resin portion one of the following Fmoc amino acids was added: L-Asp (O^tBu), L-Gln, L-Tyr(^tBu), L-Trp(BOC), L-Thr(^tBu), L-Val, L-Gly, L-Pro (0.72 mmol amino acid per resin portion), along with HOBt (16 mg, 1.1 mmol), EDCI (18 µL, 1.1 mmol), followed by DIPEA addition (2 drops) in DMF. The reaction mixture was shaken for 2 hours. Qualitative ninhydrin test was carried out to check that all the couplings were complete. The terminal Fmoc-groups were removed with 20% piperidine in DMF during 20 minutes.

Ninhydrin test was different for Pro (secondary amine): to a sample of resin were added 2 drops of 2% acetaldehyde in DMF and 2 drops of 2% *p*-chloranil/DMF. The sample was allowed to stand for 5 mn. Blue stained beads indicate the presence of the secondary amines of the resin (positive deprotection).

Capping agent coupling.

In order to know the amino acid sequence of a selected bead, a capping agent is coupled in 15% on the resin periphery. It is introduced by a classical coupling reaction. As the loading is proportional to the amount of resin (about 0.170 g of resin and 0.215 mmol/g), a stock solution of bomophenylacetic acid is prepared and added to the resin.

To be sure that the distribution will be in all the beads, the solution was stirred during 1 hour with the capping agent and then coupling reagents (HOBT, EDCI and

DIPEA) were added. The reagents were not weighted: they were added with a spatula and a pipette.
Stock solution : 0.05 mol/L of bromophenylacetic acid in DMF

For example:
Tube 1. 168.0 mg resin: 36.1 x 10^{-2} mmol: 15%: 5.42 x 10^{-3} mmol : 0.108 mL
Tube 2. 164.5 mg resin: 35.4 x 10^{-2} mmol: 15%: 5.30 x 10^{-3} mmol : 0.106 mL
Tube 3. 174.5 mg resin: 37.5 x 10^{-2} mmol: 15%: 5.63 x 10^{-3} mmol : 0.113 mL
Tube 4. 166.3 mg resin: 35.7 x 10^{-2} mmol: 15%: 5.36 x 10^{-3} mmol : 0.107 mL
Tube 5. 175.4 mg resin: 37.7 x 10^{-2} mmol: 15%: 5.66 x 10^{-3} mmol : 0.113 mL
Tube 6. 167.0 mg resin: 35.9 x 10^{-2} mmol: 15%: 5.40 x 10^{-3} mmol : 0.108 mL
Tube 7. 166.2 mg resin: 35.7 x 10^{-2} mmol: 15%: 5.35 x 10^{-3} mmol : 0.107 mL
Tube 8. 167.0 mg resin: 35.9 x 10^{-2} mmol: 15%: 5.38 x 10^{-3} mmol : 0.108 mL

Reactions were shaken for two days. The solvent was removed. The mixtures were individually washed with DMF- CH_2Cl_2 sequences washes. The different resins were mixed together and dried during one hour under vacuum. Resins were split again into eight equal portions and the procedure repeated three times to build up the receptor library.

	Second sequence		Third sequence		Fourth sequence	
	AA (mg)	CA (µl)	AA (mg)	CA (µl)	AA (mg)	CA(µl)
Tube 1. Asp:	42	119	38	108	42	104
Tube 2. Gln:	34	117	41	106	46	104
Tube 3. Tyr:	44	119	35	106	50	101
Tube 4. Trp:	58	119	39	105	39	104
Tube 5. Thr:	42	119	33	106	40	104
Tube 6. Val:	36	115	31	105	41	104
Tube 7. Gly:	34	119	43	110	57	106
Tube 8. Pro:	34	119	37	108	46	105

CA: capping agent

Screening Experiments

A sample of library **31** (25.0 mg) was equilibrated in CH_3CN (300 μL) for 24 h. A solution of guest (*S*)-**46** (20 μM, 500 μL) in CH_3CN was added to the library sample to give a 12.5 μM concentration in guest. Equilibration was continued for 24 h. Beads were analyzed in flat-bottomed glass pots under a Leica inverted DML microscope and fifty highly fluorescent beads were selected with tweezers and washed several times to remove the Naproxen derivative (*S*)-**46**. The same procedure was then carried out with (*R*)-**46**, but now the ones that did not form a complex with the *R* enantiomer were isolated.

In addition, screening experiments were achieved for library **36** as well as for the free tetrapeptide library **48** with both (*R*)-**46** and (*S*)-**46**.

As control experiments, a sample of the library **31** was equilibrated in CH_3CN for 24 h and a solution of Dansyl chloride was added to the equilibrated solution. The concentrations and conditions were the same as described above for the screening experiments. After 48 h (to allow for equilibration time) no selective staining was observed.

Deprotection and cleavage of material from the single resin beads

A single resin bead to be analyzed was placed in a glass insert using tweezers. For Pbf deprotection: the bead was treated with 50 μL of 50% TFA/CH_2Cl_2 for 1 hour. The solvent was then removed under vacuum.

Cleavage was performed by treatment of the bead with 20 μL of a solution of CNBr in 1:1 TFA/H_2O (concentration 50-80mg/mL) and incubation in the dark for 18 hours, sealed. The cleavage solution was evaporated from the sample tubes *in vacuo*. 20 μL of CH_3CN was then added to the tube. The samples were sonicated for 5 minutes. 1 μL of each sample was spotted onto MALDI-platen. 1 μL of a solution of matrix was then applied on top and the sample mixed on the platen surface. The spot was allowed to dry under a stream of air before analysis.

The α-cyanahydroxycinnamic acid matrix was prepared as a saturated solution in acetone for application as above.

Summary

This thesis reports the synthesis and design of guanidinium-based receptors as multiple hydrogen bond hosts for molecular recognition of anions with a special emphasis on small anions such as nitrate and the anti-inflammatory drug Naproxen.

The first chapter reviews the guanidinium-based artificial receptors for molecular recognition of oxoanions such as carboxylates as well as biologically relevant phosphates and sulfates in order to introduce the objectives of this work. Chiral recognition is also reported as catching a large interest in supramolecular chemistry focusing on the enantiorecognition of amino acids.

Despite its significant involvement in environmental pollution, little attention has been given to nitrate by supramolecular chemists. Chapter two reports the design of several macrocycles combining a guanidinium and two urea moieties for an optimal complement of size, charge and binding sites to nitrate. Synthesis of hosts of different sizes, rigidity and stereochemistry as well as quantification of their binding affinity towards small anions is reported. Although association constants evaluated for nitrate with one of the receptors described herein is one the highests reported so far for this anion, spherical chloride is the most suitable guest for stabilization of the complex. Both results in solution and in solid state are in good agreement to show encapsulation of nitrate, chloride and acetate guest inside the host cavities.

Chapter tree presents two different approaches for Naproxen enantiorecognition, such as a rational design and a combinatorial chemistry approach. Naproxen is the only Non-Steroidal Anti-Inflammatory drug (NSAID) marketed as a pure enantiomer. The industrial preparation of the drug involves the synthesis of the racemic acid followed by a resolution process to afford the desired compound (resolution accounts for two thirds of the production costs). Here, we propose as an alternative the use of a physical separation method (liquid-liquid extraction) employing a chiral receptor.

Various guanidinium receptors have been synthesized based on concepts of steric hindrance, tweezers and pre-organization. None to small enantioselectivity was observed by this approach.

A tetrapeptide library was synthesized by solid phase synthesis and attached to two guanidinium receptors. On the other hand, a fluorescent derivative of Naproxen was prepared for the screening of the libraries highlighting the selectivity of the receptors by enhancement of fluorescence of several beads. Identification of receptors was then achieved by mass spectrometry analysis but could not afford a reliable consensus of optimal amino acid sequence.

Introducción general y resultados

Más allá de la química de los enlaces covalentes, que unen los átomos para formar moléculas, la química supramolecular[1] es la química de las interacciones débiles: una disciplina que agrupa el concepto de reconocimiento de las moléculas entre sí mismas hacia una mayor estabilidad. En esta memoria se trata una parte específica de dicho campo: el reconocimiento de aniones cuyo desarrollo, en comparación al de los cationes, está mucho menos avanzado. Los receptores descritos en este trabajo llevan una unidad de guanidinio como esqueleto principal. De hecho, la naturaleza utiliza frecuentemente grupos guanidinio, como por ejemplo en la cadena lateral del aminoácido arginina, que permite establecer pares iónicos fuertes con grupos carboxilatos o fosfatos de sistemas biológicos.

En el primer Capítulo se revisa la importancia de la interacción guanidinio-oxoaniones a través de la bibliografía, con ejemplos característicos de reconocimiento de carboxilatos así como de fosfatos y sulfatos.[2] Se pone especial énfasis en el reconocimiento quiral de moléculas de relevancia biológica, como los aminoácidos. Tras la introducción, los objetivos de la tesis se presentan de forma resumida: el reconocimiento del anión nitrato y el reconocimiento quiral del fármaco Naproxeno.

Uno de los problemas más importantes del nitrato es su presencia en el agua procedente de la filtración de pesticidas utilizados por los agricultores. Una vez ingerido, el nitrato es reducido por el organismo a nitrito, y éste es responsable de diversas enfermedades infantiles. Las técnicas utilizadas para eliminar los nitratos del agua son esencialmente el intercambio de aniones, la osmosis inversa y la electrodiálisis. Una alternativa sería el uso de un receptor capaz de extraer el anión de una fase acuosa a otra mediante extracciones en paralelo o transporte a través de membranas liquidas. Este concepto ha sido ya descrito por nuestro grupo de investigación en relación con los aminoácidos.[3]

---

[1] Lehn, J.-M. *Science* 1985, *227*, 849-851.

[2] Blondeau, P.; Segura, M.; Pérez-Fernández, R.; de Mendoza, J. *Chem. Soc. Rev.* 2007, *36*, 198-210.

[3] Breccia, P.; Van Gool, M.; Pérez-Fernández, R.; Martin-Santamaria, S.; Gago, F.; Prados, P.;

A continuación, en el Capítulo 2, se describe el diseño de macrociclos con una subunidad de guanidinio y dos de urea para complementar el nitrato de forma ideal en cuanto a tamaño, carga y centros de unión. Se describe la síntesis de macrociclos de diferente tamaño, rigidez y estereoquímica para alcanzar la mejor estabilización del complejo con el anión. Por calorimetría isotérmica, las constantes de asociación han sido medidas, extrayéndose conclusiones sobre la selectividad de cada compuesto. Se ha conseguido así una de las asociaciones con el nitrato más altas descritas hasta ahora.[4] Sin embargo, los compuestos presentan mejores constantes de complejación con el esférico anión cloruro. Estructuras resueltas por difracción de rayos X muestran el tipo de interacciones presentes entre el receptor y el anión. Tanto los resultados en disolución como los obtenidos en estado sólido ponen en evidencia la inclusión de nitrato, acetato y cloruro en el interior de la cavidad del macrociclo.

Cada año, el porcentaje de fármacos enantioméricamente puros que salen al mercado aumenta, hasta superar un 30% en el año 2000. El Naproxeno es el único fármaco anti-inflamatorio no esteroídico vendido como un único enantiómero. La forma (*S*) es de hecho 28 veces más efectiva que la (*R*). Tras la síntesis de la mezcla racémica se lleva a cabo la resolución del acido para obtener el enantiómero deseado (más de 66% de los costes de la producción provienen de esta última etapa de resolución). Así pues, nos proponemos emplear métodos de separación física (como extracción líquido-líquido) mediante un receptor quiral para reconocer un enantiómero del Naproxeno. Ninguna molécula ha sido descrita con la capacidad de extraer enantioselectivamente este fármaco hasta ahora. El Capítulo 3 muestra dos estrategias complementarias utilizadas para alcanzar dicho objetivo: el diseño *de novo* y la química combinatoria.

Además de incorporar una unidad de guanidinio y dos de urea, los receptores requieren de otras interacciones, además de centros de quiralidad adicionales, para alcanzar la selectividad entre ambos enantiómeros. Unos grupos voluminosos o superficies aromáticas se incorporan en primer lugar sobre receptores abiertos, sin que se produzca ninguna discriminación. Receptores con más pre-organizados han sido

---

de Mendoza, J. *J. Am. Chem. Soc.* **2003**, *125*, 8270-8284.

[4] Blondeau, P.; Benet-Buchholz, J.; de Mendoza, J. *New J. Chem.* **2007,** in press, DOI: 10.1039/b616409a.

sintetizados a continuación, mediante la introducción de un derivado del aminoácido lisina o del ligando de catálisis NOBIN, con poca selectividad en este último caso.

El secundo método implica el uso de química combinatoria como medio para sintetizar un gran conjunto de receptores para luego identificar el más selectivo. Una librería de tetrapéptidos ha sido sintetizada en fase sólida y luego incorporada a la unidad de guanidinio. Al Naproxeno se le ha incorporado un grupo fluorescente para realizar los experimentos de selectividad. Las partículas poliméricas se tornan fluorescentes cuando la interacción con el Naproxeno es fuerte y se pueden identificar por espectrometría de masas. Las secuencias identificadas no presentan suficiente consenso como para llevar a una conclusión definida respeto a una secuencia optima de aminoácidos.